A. Baklanov · S. Grimmond
A. Mahura · M. Athanassiadou
(Eds.)

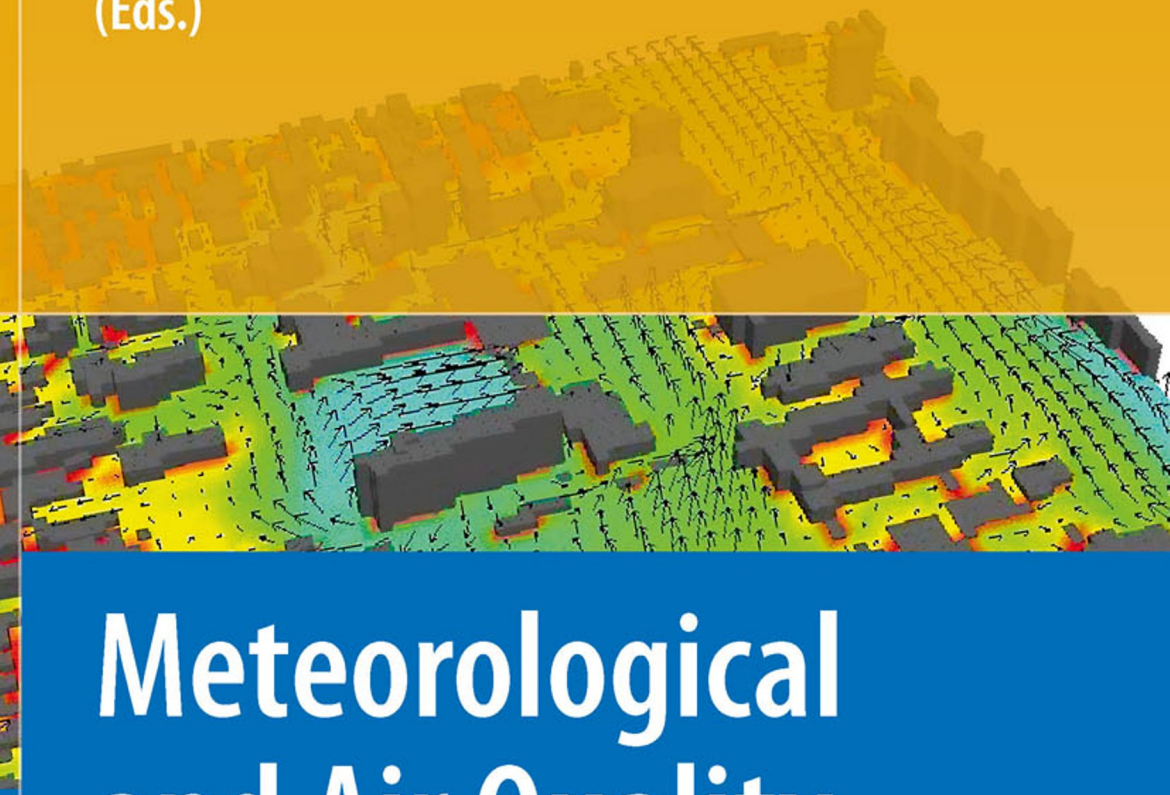

Meteorological and Air Quality Models for Urban Areas

Springer

Meteorological and Air Quality Models for Urban Areas

Alexander Baklanov · CSB Grimmond ·
Mahura Alexander · Maria Athanassiadou
Editors

Meteorological and Air Quality Models for Urban Areas

Springer

Editors
Alexander Baklanov
Danish Meteorological Institute
Lyngbyvej 100
2100 Copenhagen
Denmark
alb@dmi.dk

Mahura Alexander
Danish Meteorological Institute
Lyngbyvej 100
2100 Copenhagen
Denmark
ama@dmi.dk

CSB Grimmond
King's College London
Dept. Geography Strand
London
United Kingdom WC2R 2LS
Sue.Grimmond@kcl.ac.uk

Maria Athanassiadou
Met Office
FitzRoy Road,
Exeter EXI 3PB
United Kingdom
maria.athanassiadou@metoffice.gov.uk

ISBN 978-3-642-00297-7 e-ISBN 978-3-642-00298-4
DOI 10.1007/978-3-642-00298-4
Springer Dordrecht Heidelberg London New York

Library of Congress Control Number: 2009927000

Cover design: Bauer, Thomas

Printed on acid-free paper

Springer is part of Springer Science+Business Media (www.springer.com)

Introduction to the Problem and Aims

Alexander Baklanov

Urban features essentially influence atmospheric flow and microclimate, strongly enhance atmospheric turbulence, and modify turbulent transport, dispersion, and deposition of atmospheric pollutants (e.g., Piringer et al., 2007). Increased resolution in numerical weather prediction (NWP) models allows for a more realistic reproduction of urban air flows and air pollution processes, however most of the operational models still do not consider, or consider very poorly, the urban effects. This has triggered new interest in model development and investigation of processes specific to urban areas. Recent developments performed as part of the European project FUMAPEX on integrated systems for forecasting urban meteorology and air pollution (Baklanov et al., 2002, 2005), the US EPA and NCAR communities for MM5 (Dupont et al., 2004; Bornstein et al., 2006; Taha 2008), WRF models (Chen et al., 2006), and other relevant studies (see e.g. Baklanov and Grisogono, 2007) have shown many opportunities in the "urbanization" of weather forecasting and atmospheric pollution dispersion models.

Atmospheric models for urban areas have different requirements (e.g. relative importance of the urban boundary layer (UBL) and urban surface sublayer (USL) structure) depending on:

(i) the scale of the models (global, regional, city, local, micro, etc.);
(ii) the functional type of the model, e.g.:

- Forecasting or assessment type of models,
- Urban or regional climate models,
- Research meso-meteorological models,
- Numerical weather prediction models,
- Atmospheric pollution models (city-scale),
- Emergency preparedness models,
- Meteo-preprocessors (or post-processors).

A wide range of approaches have been taken to incorporating urban characteristics. In addition there are a wide range of processes which includes: characteristics of the urban canopy sublayer, components of urban surface energy balance (net radiation, sensible and latent heat fluxes, storage heat flux, etc.), and water

transport. This results in a wide range of models (e.g., Brown and Williams, 1998; Oke et al., 1999; Grimmond and Oke, 1999; Kusaka et al., 2001; Masson, 2000; Dupont, 2001; Martilli et al., 2002). Most urban NWP or meso-meteorological models modify the existing non-urban approaches (e.g., the Monin-Obukhov similarity theory, MOST) for urban areas by parameterisation or finding proper values for the effective roughness lengths, displacement height, and heat fluxes, including the anthropogenic heat flux, heat storage capacity, albedo and emissivity change, etc. The main limitation is when there is a need to resolve meteorological profiles within the urban canopy, where the MOST assumption of a constant flux surface layer is invalid. This is obviously important as it is a layer into which pollutants are emitted and in which people live. The sophistication of urbanization within research mesoscale models has increased during the last 10 years, starting with the work of Brown and Williams (1998), which included urban effects in their TKE scheme. Masson (2000) then included a detailed canyon energy balance scheme into his surface energy balance equation. Martilli et al. (2002) expanded on the work of these two studies to include effects from canyon walls, roofs, and streets in each prognostic PBL equation. A similar, but less complex urbanization scheme has been developed by Kusaka et al. (2001). A drawback to these advanced urbanization schemes is that they require detailed (i.e., on scale of a few 10 s of meters) urban morphological data, including land use and land cover, surface roughness, building thermal characteristics, and anthropogenic heat fluxes.

The urban canopy models, modules and parameterisations which are available are very different in terms of the sophistication of process descriptions, computing resources required and in the associated difficulties in implementing in numerical meso-scale models. Many publications consider separate aspects of urban features but none provide a complete picture of the necessary algorithms and steps required. Proceeding from the above, the *main aim* of the COST Action 728 (http://cost728.org) workshop on "Urbanisation of meteorological and air quality models" (May 3–4, 2007, UK Met Office, Exeter, UK) was to discuss and make recommendations on the best practice and strategy for urbanisation of different types of meteorological and air quality models.

International organising committee of the workshop included: Maria Athanassiadou (UK Met Office, responsible local organiser), Alexander Baklanov (Danish Meteorological Institute, responsible for scientific program), Bob Bornstein (San Jose State University, USA), Peter Clark (UK Met Office), Stefano Galmarini (Joint Research Centre, Italy), Sven-Erik Gryning (Risø NL, Denmark), Alberto Martilli (CIEMAT, Spain), Ranjeet Sokhi (University of Hertfordshire, UK), Sergej Zilitinkevich (Helsinki University, Finland). The workshop program and list of participants are listed in Appendices 1 and 2.

This workshop is a logical continuation of the Sessions and Round Table Discussion entitled "Urban sub-layer parameterisations in meteorological, climate and environmental models" of the 6th International Conference on Urban Climate (ICUC6) in Göteborg, Sweden, June 12th–16th 2006 (ICUC, 2006). The main focuses of the Section, which included 22 oral presentations, were:

– Urban physiographic data classification and utilisation of surface satellite data,
– Parameterisations and models of urban soil/heat, roughness sublayer and internal boundary layers,
– Urbanisation of meso-meteorological and numerical weather prediction models,
– Urban sublayer models, parameterisations and meteo-preprocessors for urban air quality and emergency preparedness models,
– The incorporation of urban effects into regional climate models.

An outcome from the Round Table was to build a world-wide working group on "Model urbanization strategy" and to organise a workshop associated with COST 728. The Round Table discussions were summarised by A. Baklanov, J. Ching, A. Martilli and V. Masson and published in the COST 728 "Model urbanisation" report (COST728, 2007). With increasing numbers of users simulating at the meso-scale (or higher resolution) it becomes increasingly necessary to include some urban characteristics and therefore parameterisations in their models.

This volume, based on the presentations given at this workshop, is concerned with the following *main topics*:

1. Urban morphology and databases,
2. Parameterisations of urban canopy,
3. Strategy for urbanization of different types of models,
4. Evaluation and city case studies/field studies.

The workshop was oriented towards NWP and air quality modelling. Presentations were concerned with dynamic (on wind and turbulent) and thermal effects (on temperature and energy in general). Most of the papers presented at the workshop are published in this volume. However the following were not available for this volume but PowerPoint presentations are also available at the workshop web-site (http://www.cost728wg1.org.uk):

- Dirk Schuttemeyer "The present setup for the urban experiment in Bonn, Germany";
- Omduth Coceal "Turbulence statistics from DNS and LES – implications for urban canopy models" (Coceal and Belcher, 2004; Coceal et al., 2006, 2007);
- Valery Masson "CAPITOUL experiment: first experimental results and parameterization" (Hidalgo et al., 2008; Masson et al., 2008);
- Fei Chen "Advancing the multi-scale urban modelling in the community mesoscale WRF model: current status and future plan" (Chen et al., 2004, 2006; Lo et al., 2006);
- Bob Bornstein "Urbanization of US meso-scale models" (Otte et al., 2004; Bornstein et al., 2006).

The final chapter of this volume summarizes the discussion and conclusions from the four main topics and provides recommendations and future requirements.

Cutting across the main topics, issues of concern and major interest arise:

- Which variables do we need to model (and to what degree of precision) for which applications (air quality, emergency response, urban climatology, weather forecast, etc.). For example,

  - Do we need values within the canopy or only whole surface fluxes?
  - Do we need good turbulence fluxes?
  - For dispersion applications, do we need mean concentrations or also the variances?

- What is the best way to evaluate the capability of the parameterizations to model the relevant variables i.e.,

  1. urban measurement campaigns,
  2. wind tunnel experiments,
  3. role of the CFD/LES models.

- What ways could the parameterizations improved (if needed):

  - For dynamics: porosity models, dispersive stress, role of CFD/LES models,
  - For energy: need for building energy models.

References

Baklanov, A., S. Joffre, and S. Galmarini (Eds.), 2005: "Urban Meteorology and Atmospheric Pollution (EMS-FUMAPEX)". *Atmos. Chem. Phys.*, Special Issue 24. http://www.atmos-chem-phys.net/special_issue24.html

Baklanov, A., A. Rasmussen, B. Fay, E. Berge, and S. Finardi, 2002: Potential and shortcomings of numerical weather prediction models in providing meteorological data for urban air pollution forecasting. *Water, Air Soil Poll.: Focus*, 2 (5–6): 43–60.

Bornstein, R., R. Balmori, H. Taha, D. Byun, B. Cheng, J. Nielsen-Gammon, S. Burian, S. Stetson, M. Estes, D. Nowak, and P. Smith, 2006: Modeling the effects of land-use land cover modifications on the urban heat island phenomena in Houston, Texas. SJSU Final Report to Houston Advanced Research Center for Project No. R-04-0055, 127 pp.

Brown, M. and M. Wiliams, 1998: An Urban canopy parameterization for Mesoscale Meteorological Models. AMS 2nd Urban Environment Symposium, Albuquerque, NM USA.

Chen, F., H. Kusaka, M. Tewari, J.-W. Bao, and H. Hirakuchi, 2004: "Utilizing the coupled WRF/LSM/urban modeling system with detailed urban classification to simulate the urban heat island phenomenon over the greater Houston area", Paper 9.11, American Meteorological Society Fifth Symposium on the Urban Environment, 23–27 August 2004, Vancouver, British Columbia.

Chen, F., M. Tewari, H. Kusaka, and T.L. Warner, 2006: Current status of urban modeling in the community Weather Research and Forecast (WRF) model. Sixth AMS Symposium on the Urban Environment, Atlanta GA, January 2006.

Coceal, O. and Belcher, S.E., 2004: A canopy model of mean winds through urban areas. *Q. J. Roy. Meteor. Soc*. 130: 1349–1372.

Coceal, O., A. Dobre, and T.G. Thomas, 2007: Unsteady dynamics and organized structures from DNS over a building canopy. *Int. J. Climatol*. 27: 1943–1953.

Coceal, O., T.G. Thomas, I.P. Castro, and S.E. Belcher, 2006: Mean flow and turbulence statistics over groups of urban-like cubical obstacles. *Bound.-Layer Meteorol*. 121: 491–519.

COST728, 2007: Overview of the urban sublayer/exchange parameterizations in meso-meteorological and air pollution models. Report of the WG1 COST728, available from: http://cost728.org

Dupont, S., 2001: Modelisation Dynamique et Thermodynamique de la Canopee Urbaine: Realisation du Modele de Sols Urbains pour SUBMESO, Doctoral thesis, Universite de Nantes, France.

Dupont, S., T.L. Otte, and J.K.S. Ching, 2004: Simulation of meteorological fields within and above urban and rural canopies with a Mesoscale Model (MM5). *Bound.-Layer Meteorol*., 113: 111–158.

Grimmond, C.S.B. and Oke, T.R., 1999: Heat storage in urban areas: observations and evaluation of a simple model. *J. Appl. Meteorol*., 38: 922–940.

Hidalgo, J., G. Pigeon, and V. Masson, 2008: Urban-breeze circulation during the CAPITOUL experiment: Observational data analysis approach, *Meteorol. Atmos. Phys.*, 102(3–4): 223–241.

ICUC, 2006: 6th International Conference on Urban Climate, June 12–16, 2006, Goteborg, Sweden, Proceedings. ISBN-10:91-613-9000-1.

Kusaka, H., H. Kondo, Y. Kikegawa, and F. Kimura, 2001: A simple single-layer urban canopy model for atmospheric models: Comparison with multi-layer and SLAB models. *Bound.-Layer Meteorol*. 101: 329–358.

Lo, J., A.K.H. Lau, J.C.H. Fung, and F, Chen, 2006: Investigation of enhanced cross-city transport and trapping of air pollutants by coastal and urban land-sea breeze circulations. *J. Geophys. Res*., 111, D14104, doi:10.1029/2005JD006837.

Martilli, A., A. Clappier, and M.W. Rotach, 2002: An urban surface exchange parameterisation for mesoscale models. *Bound.-Layer Meteorol*. 104: 261–304.

Masson, V., 2000: A physically-based scheme for the urban energy budget in atmospheric models. *Bound.-Layer Meteorol*. 98: 357–397.

Masson, V., L. Gomes, G. Pigeon, C. Liousse, V. Pont, J.-P. Lagouarde, J. Voogt, J. Salmond, T. Oke, J. Hidalgo, D. Legain, O. Garrouste, C. Lac, O. Connan, X. Briottet, and S. Lachérade, 2008: The Canopy and Aerosol Particles Interactions in TOulouse Urban Layer (CAPITOUL) experiment. *Meteorol. Atmos. Phys.*, 102(3–4): 135–157.

Oke, T.R., R. Spronken-Smith, E. Jauregui, and C.S.B. Grimmond, 1999: Recent energy balance observations in Mexico City. *Atmos. Environ*., 33: 3919–3930.

Otte, T.L., A. Lacser, S. Dupont, and J.K.S. Ching, 2004: Implementation of an urban canopy parameterization in a mesoscale meteorological model. *J. Appl. Meteor*., 43: 1648–1665.

Baklanov and Grisogono (eds.), 2007: Atmospheric boundary layers: nature, theory and applications to environmental modelling and security. Springer Publishers, 241, doi:10.1007/978-0-387-74321-9.

Piringer, M., S. Joffre, A. Baklanov, A. Christen, M. Deserti, K. De Ridder, S. Emeis, P. Mestayer, M. Tombrou, D. Middleton, K. Baumannstanzer, A. Dandou, A. Karppinen, and J. Burzynski, 2007: The surface energy balance and the mixing height in urban areas – activities and recommendations of COST Action 715. *Bound.-Layer Meteorol*. 124: 3–24.

Taha, H., 2008: Sensitivity of the urbanized MM5 (uMM5) to perturbations in surface properties in Houston Texas. *Bound.-Layer Meteorol*., 127: 193–218.

Contents

Part I Urban Morphology and Databases

1 Facilitating Advanced Urban Meteorology and Air Quality Modelling Capabilities with High Resolution Urban Database and Access Portal Tools 3
Jason Ching, Adel Hanna, Fei Chen, Steven Burian, and Torrin Hultgren

2 Relating Small-Scale Emission and Concentration Variability in Air Quality Models 11
Stefano Galmarini, Jean-François Vinuesa, and Alberto Martilli

3 Performance of Different Sub-Grid-Scale Surface Flux Parameterizations for Urban and Rural Areas 21
Sylvia Bohnenstengel and Heinke Schlünzen

Part II Parameterizations of Urban Canopy

4 How to Use Computational Fluid Dynamics Models for Urban Canopy Parameterizations 31
Alberto Martilli and Jose Luis Santiago

5 Review of Japanese Urban Models and a Scale Model Experiment 39
Manabu Kanda

6 Urban Soil-Canopy-Atmosphere Exchanges at Submesoscales: Learning from Model Development, Evaluation, and Coupling with LES 47
Isabelle Calmet and Patrice Mestayer

7 The Effect of Stratification on the Aerodynamic Roughness Length 59
Sergej Zilitinkevich, Ivan Mammarella, Alexander Baklanov, and Sylvain Joffre

Part III Strategy for Urbanization of Different Types of Models

8 FUMAPEX Experience of Model Urbanisation 69
Alexander Baklanov and FUMAPEX Team

9 Evolution of Urban Surface Exchange in the UK Met Office's Unified Model 77
Peter Clark, Martin Best, and Aurore Porson

10 Sensitivity Tests in the Dynamical and Thermal Part of the MRF-Urban PBL Scheme in the MM5 Model 87
Aggeliki Dandou and Maria Tombrou

Part IV Evaluation and Case Studies/Observations

11 Urban Surface Energy Balance Models: Model Characteristics and Methodology for a Comparison Study 97
CSB Grimmond, Martin Best, Janet Barlow, A. J. Arnfield, J.-J. Baik, A. Baklanov, S. Belcher, M. Bruse, I. Calmet, F. Chen, P. Clark, A. Dandou, E. Erell, K. Fortuniak, R. Hamdi, M. Kanda, T. Kawai, H. Kondo, S. Krayenhoff, S. H. Lee, S.-B. Limor, A. Martilli, V. Masson, S. Miao, G. Mills, R. Moriwaki, K. Oleson, A. Porson, U. Sievers, M. Tombrou, J. Voogt, and T. Williamson

12 Measuring Meteorology in Urban Areas – Some Progress and Many Problems 125
Sven-Erik Gryning and Ekaterina Batchvarova

13 Derivation of Vertical Wind and Turbulence Profiles, the Mixing-Layer Height, and the Vertical Turbulent Exchange Coefficient from Sodar and Ceilometer Soundings in Urban Measurement Campaigns 133
Stefan Emeis

14 Verification and Case Studies for Urban Effects in HIRLAM Numerical Weather Forecasting 143
Alexander Mahura, Alexander Baklanov, Claus Petersen, Niels W. Nielsen, and Bjarne Amstrup

15 Model Urbanization Strategy: Summaries, Recommendations and Requirements 151
Alexander Baklanov, Jason Ching, CSB Grimmond, and Alberto Martilli

Appendix 1: Program of the COST 728 Workshop on Model Urbanization Strategy, UK Met Office, Exeter, UK, 3–4 May 2007 163

Appendix 2: List of Workshop Participants 167

Colour Plate 171
Index 179

Contributors

Bjarne Amstrup Danish Meteorological Institute, DMI, Lyngbyvej 100, DK-2100, Copenhagen, Denmark, bja@dmi.dk

John Arnfield Department of Geography, The Ohio State University, Columbus, 43210, OH, USA, aja@osu.edu

Jong-Jin Baik School of Earth and Environmental Sciences, Seoul National University, Seoul 151-742, Korea, jjbaik@snu.ac.kr

Alexander Baklanov Danish Meteorological Institute, DMI, Lyngbyvej 100, DK-2100, Copenhagen, Denmark, alb@dmi.dk

Janet Barlow Department of Meteorology, University of Reading, Earley Gate, PO Box 243, Reading, RG6 6BB, UK, j.f.barlow@reading.ac.uk

Ekaterina Batchvarova National Institute of Meteorology and Hydrology, 66 Tzarigradsko Chaussee Sofia 1784, Bulgaria, ekaterina.batchvarova@meteo.bg

Stephen Belcher Department of Meteorology, University of Reading, Earley Gate, PO Box 243, Reading, RG6 6BB, UK, s.e.belcher@reading.ac.uk

Martin Best Met Office, Hadley Centre for Climate Prediction and Research, London Road, Bracknell, Berkshire, RG12 2SY UK, martin.best@metoffice.com

Sylvia Bohnenstengel Department of Meteorology, University of Reading, Earley Gate, PO Box 243, Reading, RG6 6BB, UK, s.i.l.d.bohnenstengel@reading.ac.uk

Michael Bruse Institute of Geography, Johannes-Gutenberg University of Mainz, Johann-Joachim-Becher Weg 21, D-55099 Mainz, Germany, m.bruse@geo.uni-mainz.de

Steven Burian Department of Civil and Environmental Engineering, University of Utah, 122 S Central Campus Drive, Suite 104, Salt Lake City, UT 84112, USA, burian@eng.utah.edu

Isabelle Calmet Laboratoire de Mécanique des Fluides, Ecole Centrale de Nantes (ECN), UMR 6598 CNRS, BP 92101, F-44321 Nantes Cedex 3, France, Isabelle.Calmet@ec-nantes.fr

Fei Chen Research Applications Laboratory, National Center for Atmospheric Research (NCAR), P.O. Box 3000, Boulder, CO 80307-3000, USA, feichen@ucar.edu

Jason Ching Atmospheric Modeling and Analysis Division, US Environmental Protection Agency (EPA), 109 T W Alexander Drive, Research Triangle Park, NC 27711, USA, Ching.Jason@epamail.epa.gov

Peter Clark Met Office, Joint Centre for Mesoscale Meteorology (JCMM), Earley Gate PO Box 243, Reading, RG6 6BB, UK, peter.clark@metoffice.gov.uk

Aggeliki Dandou Department of Environmental Physics and Meteorology, National and Kapodistrian University of Athens, 15784, Athens, Greece, mtombrou@phys.uoa.gr

Stefan Emeis Institute for Meteorology and Climate Research, Atmospheric Environmental Research, Kreuzeckbahnstraße 19, 82467, Garmisch-Partenkirchen, Germany, stefan.emeis@imk.fzk.de

Evyatar Erell Ben Gurion University of the Negev, Jacob Blaustein Institute for Desert Research, Sede-Boqer Campus Midreshet, Ben-Gurion 84990, Israel, erell@bgu.ac.il

Krzysztof Fortuniak Department of Meteorology and Climatology, University of Lodz, Narutowicza Str. 88, 90-139 Lodz, Poland, kfortun@uni.lodz.pl

Stefano Galmarini European Commission – DG Joint Research Centre (JRC), Institute for Environment and Sustainability, TP 441, 21020 Ispra, Italy, stefano.galmarini@jrc.it

CSB Grimmond King's College London (KCL), Strand, London WC2R 2LS, UK, Sue.Grimmond@kcl.ac.uk

Sven-Erik Gryning Risø National Laboratory for Sustainable Energy, Technical University of Denmark, DK-4000, sven-erik.gryning@risoe.dk

Rafiq Hamdi Royal Meteorological Institute, Avenue Circulaire, 3, B-1180 Brussels, Belgium, rafiq.hamdi@oma.be

Adel Hanna Institute for the Environment, The University of North Carolina, Chapel Hill, 27599-6116 NC, USA, ahanna@unc.edu

Torrin Hultgren National Computing Center, US Environmental Protection Agency (EPA), 79 Alexander Drive, Research Tiangle Park, NC 27709, USA, hultgren.torrin@epa.gov

Sylvain Joffre Finnish Meteorological Institute, P.O. Box 503, FIN-00101, Helsinki, Finland, sylvain.joffre@fmi.fi

Manabu Kanda Tokyo Institute of Technology, 2-12-1, Ookayama, Meguro-ku, Tokyo 152-8552, Japan, kanda@ide.titech.ac.jp

T. Kawai Tokyo Institute of Technology, 2-12-1, Ookayama, Meguro-ku, Tokyo 152-8552, Japan, tkawai@geo.titech.ac.jp

H. Kondo National Institute of Advanced Industrial Science and Technology, 1-1-1 Umezono Tsukuba, Ibaraki 305-8568 Japan, kondo-hrk@aist.go.jp

Scott Krayenhoff Department of Geography, University of British Columbia, Vancouver, BC V6T 1Z2, Canada, skrayenh@gmail.com

S.H. Lee School of Earth and Environmental Sciences, Seoul National University, Seoul 151-742, Korea, nihil93@snu.ac.kr

S.-B. Limor Ben-Gurion University of the Negev, P.O.B. 653, Beer-Sheva 84105 Israel, shashual@bgu.ac.il

Alexander Mahura Danish Meteorological Institute (DMI), Lyngbyvej 100, DK-2100, Copenhagen, Denmark, ama@dmi.dk

Ivan Mammarella Division of Atmospheric Sciences, University of Helsinki, P.O. Box 64, FIN-00014; Finnish Meteorological Institute, Box 503, FIN-00102, Helsinki, Finland

Alberto Martilli Centro de Investigaciones Energéticas, Medioambientales y Tecnológicas (CIEMAT), Avenida Complutense 22, 28040, Madrid, Spain, alberto.martilli@ciemat.es

Valery Masson Centre National de Recherches. Météorologiques, Meteo-France, 42 av Coriolis, 31057 Toulouse Cedex France, valery.masson@meteo.fr

Patrice Mestayer Laboratoire de Mécanique des Fluides, Ecole Centrale de Nantes (ECN), UMR 6598 CNRS, BP 92101, F-44321 Nantes Cedex 3, France, Patrice.Mestayer@ec-nantes.fr

S. Miao Institute of Urban Meteorology, No.55 Beiwaxili, Haidian District, Beijing, P.R. China, 100089, sgmiao@ium.cn

Gerald Mills School of Geography, Planning & Environmental Policy, University College, Newman Building, Belfield, Dublin 4, Ireland, gerald.mills@ucd.ie

R. Moriwaki Department of Civil Engineering, Tokyo Institute of Technology, Ookayama Campus 2-12-1 Ookayama, Meguro-ku, Tokyo 152-8550, Japan

Niels Nielsen Danish Meteorological Institute (DMI), Lyngbyvej 100, DK-2100, Copenhagen, Denmark, nwn@dmi.dk

Keith Oleson National Center for Atmospheric Research (NCAR), P.O. Box 3000, Boulder, Colorado 80307-3000, USA, oleson@ucar.edu

Claus Petersen Danish Meteorological Institute (DMI), Lyngbyvej 100, DK-2100, Copenhagen, Denmark, cp@dmi.dk

Aurore Porson Department of Meteorology, University of Reading, Earley Gate, P.O. Box 243, Reading, RG6 6BB UK, a.n.f.porson@reading.ac.uk

Jose Luis Santiago Centro de Investigaciones Energéticas, Medioambientales y Tecnológicas (CIEMAT), Avenida Complutense 22, 28040, Madrid, Spain, joseluis@ciemat.es

Heinke Schlünzen Max-Planck-Institut for Meteorologie, ZMAW, Bundesstr. 53, 20146 Hamburg, Germany, heinke.schluenzen@zmaw.de

Uwe Sievers Deutscher Wetterdienst, Stefan-Meier-Str. 4, D-79104 Freiburg, Germany, uwe.sievers@dwd.de

Maria Tombrou Department of Environmental Physics and Meteorology, National and Kapodistrian University of Athens, 15784, Athens, Greece, mtombro@phys.uoa.gr

Jean-François Vinuesa European Commission – DG Joint Research Centre (JRC), Institute for Environment and Sustainability, TP 441, 21020 Ispra, Italy, jeff.vinuesa@jrc.it

James Voogt Department of Geography, University of Western Ontario, 1151 Richmond Street, London, Ontario, N6A 5C2, Canada, javoogt@uwo.ca

Terence Williamson University of Adelaide, Australia, terence.williamson@adelaide.edu.au

Sergej Zilitinkevich Division of Atmospheric Sciences, University of Helsinki, FIN-00014, Helsinki, Finland, sergej.zilitinkevich@fmi.fi

Chapter 1
Facilitating Advanced Urban Meteorology and Air Quality Modelling Capabilities with High Resolution Urban Database and Access Portal Tools

Jason Ching, Adel Hanna, Fei Chen, Steven Burian, and Torrin Hultgren

Abstract Information on urban morphological features at high resolution is needed to properly model and characterize the meteorological and air quality fields in urban areas. Here a project called National Urban Database with Access Portal Tool (NUDAPT) that addresses this need is described. NUDAPT is designed to produce gridded fields of urban canopy parameters to improve urban meteorological simulations. It makes use of the availability of high-resolution urban buildings and land use data. An important core-design feature is the utilization of Portal technology to enable NUDAPT to be a "Community" based system. Sensitivity studies showing air quality simulations driven with outputs from urban meteorology preprocessors using advanced urban descriptions are described.

1.1 Introduction

Current data and modelling tools are limited in their capability to perform accurate air quality assessments in urban areas that contain highest and most vulnerable population densities. Advanced treatments of high resolution urban morphological features for meteorological, air quality and human exposure modelling systems will be needed for future urban applications (OFCM 2005). In response, a project called National Urban Database with Access Portal Tool (NUDAPT) was launched. The initial NUDAPT prototype is sponsored by the United States Environmental Protection Agency (US EPA) and involves collaboration and contributions from many federal and state agencies, and from private and academic institutions. NUDAPT will produce gridded outputs of urban parameters required for current (Otte et al., 2004; Ching et al., 2004; Dupont et al., 2004; Chen et al., 2006) and future advanced urban

J. Ching (✉)
Atmospheric Modeling and Analysis Division, NERL/ORD/USEPA
e-mail: Ching.Jason@epamail.epa.gov

This material was prepared for the Sixth International Urban Air Quality Conference, 27–29 March 2007, Cyprus.

A. Baklanov et al. (eds.), *Meteorological and Air Quality Models for Urban Areas*,
DOI 10.1007/978-3-642-00298-4_1,

meteorological and air quality models. Additionally, ancillary information such as gridded population, energy usage and traffic will be incorporated to encourage and facilitate linkages to air quality and human exposure models. An important core-design feature is the portal technology to enable NUDAPT to be a "Community" based system. Web-based portal technology will facilitate data retrievals and handling based on data federation concepts. Houston, Texas is the NUDAPT's initial prototype. Advanced urban canopy implementations of the MM5 and WRF are used to demonstrate the NUDAPT features, including scope of the data and processing methodologies for an eventual extensibility to all other cities.

1.2 Approach

In this paper, we describe a prototype of an operational template that can be extended to provide an eventual nation-wide capability that will serve a broad user community engaged to develop and drive powerful new and advanced atmospheric transport and dispersion and air quality modelling tools. Already, the value of using high resolution urban data in meteorological and air quality simulations has been demonstrated from sensitivity studies based on mesoscale modelling system that incorporate urban canopy parameters (Ching et al., 2004; Dupont et al., 2004; Chen et al., 2006). This will provide a strategic implementation to both the modelling and decision support communities requiring appropriate modelling tools to support the assessments and applications required to reduce the health risks associated with exposure to air of poor quality. Further, it addresses homeland security in regard to transport and dispersion of toxic releases.

Houston, the fourth largest city in the USA, was selected to serve as the initial prototype to demonstrate the NUDAPT features. For this city there are lidar-derived building data with unrestricted use (Fig. 1.1) and air quality data from major

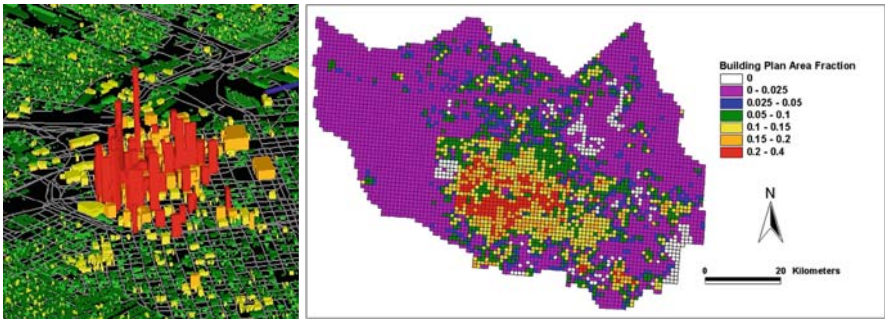

(a) (b)

Fig. 1.1 **(a)** 3D building data derived from airborne lidar platform for 1 × 1 km section of downtown Houston. **(b)** Building plan area density, an example of a UCP for Harris County (Houston Metropolitan area) (cf. Table 1.1) (See also Colour Plate 1 on page 171)

intensive field studies are available. Houston has active emissions management programs to address its poor air quality and associated health effects. The NUDAPT prototype includes:

(1) primary data sets such as (a) 3D building and geo-morphological data, roads and their linkages; (b) activity data including census data, traffic, and industrial outputs; (c) land surface characteristics data;
(2) derived daughter products including model specific urban canopy parameters (UCPs), diurnal population data (which accounts for human activities and therefore changing location), anthropogenic energy inputs and traffic emissions; and
(3) examples of model outputs and analyses to demonstrate a range of applications possible.

1.3 Features of Nudapt

1.3.1 Morphology Databases and Urban Canopy Parameters (UCP)

An important feature of NUDAPT is the provision to incorporate urban structure data and derived urban parameters. For example, the urbanized version of MM5 (Ching et al., 2004) makes use of UCPs introduced to building and vegetation influences on the drag, the partitioning of the surface energy budget components, and the generation of turbulence of the flow in the surface boundary layer. The set of UCPs in Table 1.1 (eight of which vary with height) used in the Dupont's modelling system (Dupont et al., 2004) are calculated for each grid in the modelling domain (Burian et al., 2004).

Geospatial databases, similar to that used in Houston, consisting of detailed building and other urban morphological structures imagery information (resolution: order 1 m) are being acquired for 133 USA urban centres. This is in response to

Table 1.1 Gridded UCPs from lidar-derived building and vegetation data for urbanized MM5 model

Canopy UCPs	Building UCPs	Vegetation, other UCPs
Mean canopy height	Mean building height	Mean vegetation height
Canopy plan area density	Standard deviation of building height	Vegetation plan area density
Canopy top area density	Building height histograms	Vegetation top area density
Canopy frontal area density	Building wall-to-plan area ratio	Vegetation frontal area density
Roughness length	Building height-to-width ratio	Mean orientation of streets
Displacement height	Building plan area density	Plan area fraction surface covers
Sky view factor	Building rooftop area density	Percent directly connected impervious area
	Building frontal area density	Building material fraction

the Homeland Security Infrastructure Program (HSIP); the Nunn-Lugar-Dominici Act (Defense Against Weapons of Mass Destruction Act of 1996) established a project by which the Department of Defence was tasked to help respond to chemical, biological and nuclear (CBN) incidences in the these urban centres. These data (together with the National Map Project of the US Geological Survey) provide the foundation for a national database. Of course, even higher resolution descriptions of building data exist. In principle, the NUDAPT can incorporate such data if it can be made available.

The primary data are from an airborne LiDAR system which collects data for Digital Elevation Model (DEM) and Digital Terrain Model (DTM). Differencing the DEM and DTM signals provides information regarding the buildings and trees (see example, Fig. 1.1a). High altitude aircraft and municipal property data provide information to complement the LiDAR database. Such data and the derived UCPs (example, Fig. 1.1b) are incorporated in the Houston Prototype.

1.3.2 Relevant Ancillary Data

Data obtained from NUDAPT are expected to improve meteorological fields for air quality, homeland security, and planning purposes. NUDAPT will also provide a service which links to other sources of data that we anticipate will be of high utility. Such information will include various activities and land-use data such as roads and their linkages, and activity data including census data, traffic, industrial outputs, and land surface characteristics data from which gridded products useful for models will be derived. In addition, NUDAPT will include gridded population data for the USA, e.g., day-night populations, indoor-outdoor populations, sensitive population groups and population mobility matrix. Such data are being generated for the prototype at latitude-longitude coordinates with a spatial resolution of 250 m. Other derived daughter products include model specific urban canopy parameters, gridded anthropogenic energy inputs and gridded traffic emissions. Selected illustrative examples of model outputs and analyses will be also available to demonstrate a range of applications possible.

1.3.3 NUDAPT Design Concept

NUDAPT will become a two level framework, in the form of a web-enabled database that provides ready access to the various datasets, both primary or source data and processed data to users. The first level, primary data, includes the high resolution building data. Access to this level will be granted for those interested in creating new or modified UCP datasets. The second level provides unrestricted access; users can query the database for relevant data, retrieve data in a form that can be readily assimilated into models such as MM5, and submit model results for further analysis. The database is federated, i.e., will act as a repository for multiple, heterogeneous datasets that all adhere to a consistent format and metadata specification.

This framework allows for analysis by the scientific community by providing an efficient means of sharing observed and modelled data. The community provides the means for detailed analysis and knowledge integration. The data-sharing concept in NUDAPT can facilitate research efforts to improve models of the urban environment. For example, if a researcher wishes to compare their model results with another simulation that used a different set of UCPs. This is easily accomplished by querying the database, retrieving the model run of interest, and analysing the results at the user end. Once researchers utilize these UCPs in their modelling, more knowledge integration will occur through enhanced model evaluations leading to improved models.

Datasets will either reside on the NUDAPT portal server or, where available for public download elsewhere, the portal will provide a link to facilitate the appropriate download. Because the site is expected to act as a data repository rather than an active transaction-heavy database, there does not appear to be a need to utilize database software to manage the datasets in question. Instead the datasets will exist as stand-alone files in the file system. The initial Prototype will use the ArcGIS 9.2 server that provides the desired functionality needed to handle both vector and raster data formats.

1.4 Discussion and Summary

Initial sensitivity studies of air quality (and other) applications using outputs of advanced meteorological models that incorporate NUDAPT type data are being performed. Figure 1.2 contrasts the mixed layer simulations from MM5 with and without UCP. The urban area of Houston is categorized with one urban land use category in the standard version of MM5. Figure 1.3 illustrates the sensitivity of the Community Multiscale Air Quality (CMAQ) modelling system to MM5 versions with and without detailed urban canopy features. In this instance, significant differences are seen, serving as a motivation for advancements in urban modelling.

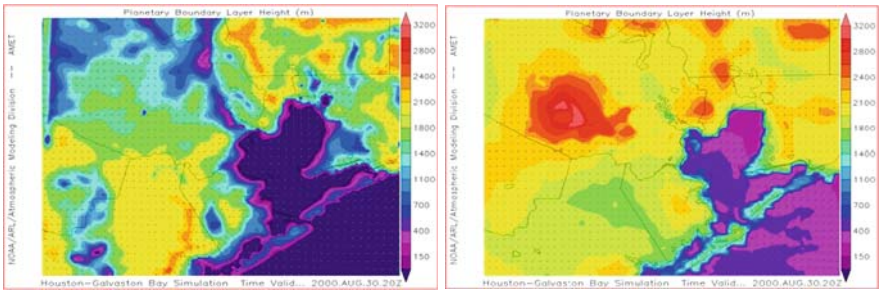

(a) (b)

Fig. 1.2 Simulations of mixed layer heights size for 2100 GMT on August 30, 2000 using MM5 with **(a)** UCP and **(b)** standard version of MM5 at 1 km grid (See also Colour Plate 2 on page 171)

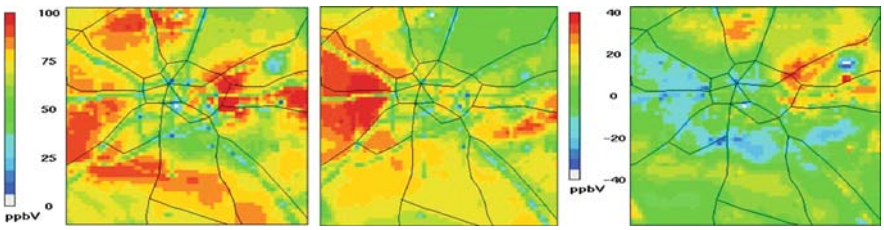

(a) (b) (c)

Fig. 1.3 Simulations of surface ozone using CMAQ driven by UCP **(a)** and No-UCP **(b)** versions of MM5 (see Fig. 1.2) and **(c)** differences between simulations (at 2100 GMT on August 30, 2000) (See also Colour Plate 3 on page 172)

The development of NUDAPT represents a promising resource to stimulate the addressing of many of the emerging problems in urban areas. NUDAPT provides a platform for accessing and developing data and for sharing information with the user community. Primary data in NUDAPT will include physical and morphological data prepared and collected under various conventional and unconventional systems. The preparation of NUDAPT daughter products which are closely directed to urban gridded modelling applications will need to consider various map projections that are used in typical meteorological and air quality modelling applications. Due to the multiple scales of applications that will potentially be used in various studies, it is important that the NUDAPT include methodologies for re-projecting and re-gridding these daughter products in a way that conserves their properties for generalized applications. Currently, a database for Houston is serving as the NUDAPT prototype. Eventually, the goal for NUDAPT is to be extended to all major urban areas within the United States; ultimately, there is nothing to preclude this concept to extend beyond the USA.

Disclaimer: *The research presented here was performed under the Memorandum of Understanding between the U.S. Environmental Protection Agency (EPA) and the U.S. Department of Commerce's National Oceanic and Atmospheric Administration (NOAA) and under agreement number* DW13921548. *This work constitutes a contribution to the NOAA Air Quality Program. Although it has been reviewed by EPA and NOAA and approved for publication, it does not necessarily reflect their policies or views.*

References

Burian, S. J., S. W. Stetson, W. Han, J. Ching, and D. Byun (2004). High-resolution dataset of urban canopy parameters for Houston, Texas. Preprint proceedings, Fifth Symposium on the Urban Environment, AMS, 23–26 August, Vancouver, BC, Canada, 9 pp.

Chen, F., M. Tewari, H. Kusaka, and T. L. Warner (2006). Current status of urban modeling in the community Weather Research and Forecast (WRF) model. Sixth AMS Symposium on the Urban Environment, Atlanta GA, January 2006.

Ching, J. K. S., S. Dupont, R. Gilliam, S. Burian, and R. Tang (2004). Neighborhood scale air quality modeling in Houston using urban canopy parameters in MM5 and CMAQ with improved characterization of mesoscale lake-land breeze circulation. Fifth Symposium on the Urban Environment, Vancouver BC, Canada, 23–26 August. American Meteorological Society, Boston, Paper 9.2.

Dupont, S., T. L. Otte, and J. K. S. Ching, 2004: Simulation of meteorological fields within and above urban and rural canopies with a mesoscale model (MM5) Boundary Layer Meteor., 113, 111–158.

Office of the Federal Coordinator for Meteorology (2005): Proceedings from the Forum on Urban Meteorology. www.ofcm.gov/homepage/text/pub.htm

Otte, T. L., A. Lacser, S. Dupont, and J. K. S. Ching (2004). Implementation of an urban canopy parameterization in a mesoscale meteorological model. J. Appl. Meteor., 43, 1648–1665.

Chapter 2
Relating Small-Scale Emission and Concentration Variability in Air Quality Models

Stefano Galmarini, Jean-François Vinuesa, and Alberto Martilli

Abstract A novel approach to account for the spatial variability of the small-scale emission in air quality models is proposed. This approach includes a formulation for the sub-grid variability of pollutant concentrations and relates it to the spatial heterogeneity of the emissions. The parameterization is implemented in a 3D transport model and tested against large eddy simulations of convective atmospheric boundary layers.

2.1 Introduction

The atmospheric motion, evolution and scalar concentrations can be described by a system of non-linear partial differential equations. These equations are derived from thermodynamics and fluid mechanics (Navier-Stokes equations). They describe the characteristics of a given air mass and are the base of all geophysical models. They link large and small scale motions due to the wide range of temporal and spatial scales of geophysical processes and the energy feedback from smaller scales into the larger scale motions. Since the equations are simply too complicated to be exactly solved for any practical atmospheric modelling, statistical representations of the complete physical description is required. Currently, the Navier-Stokes equations are resolved by performing scale decomposition. Geophysical models are in fact an adaptation of these equations to a spatial grid and discrete steps in time. It is therefore important to realize that features smaller than the dimension of one grid cell cannot be resolved by the model. These are referred to as subgrid scale processes.

Urban and suburban environments are characterized by heterogeneous emissions. These are not reflected in emission inventories except as an average value and so this is not accounted for in meso/limited area air quality models. The emissions are

S. Galmarini (✉)
European Commission – DG Joint Research Centre, Institute for Environment and Sustainability, TP 441, 21020 Ispra, Italy
e-mail: stefano.galmarini@jrc.it

A. Baklanov et al. (eds.), *Meteorological and Air Quality Models for Urban Areas*,
DOI 10.1007/978-3-642-00298-4_2,

averaged over the grid cell where the emission source is located. The source can be linear (e.g. roads), areal (fields or urban areas) or point (factory) but after the averaging procedure, it is considered as a surface source with the same extent as the grid cell. This means that not only is the surface heterogeneity lost in terms of its level of variability but also it will not be accounted for in the upper atmospheric levels and the impact of the spatial distribution of emissions on the spatial distribution of concentrations, is lost. This can represent a serious issue in the case of passive as well as chemically reactive species, or for the estimation of long- or short-term exposures.

Since this crucial component can be at smaller scales than the grid size, it could be accounted for through a sub-grid parameterization. In this paper, we propose a novel approach to this parameterization, including a formulation for the sub-grid variability of pollutant concentrations that takes into account the spatial heterogeneity of the emissions. The formulation that can be used in mesoscale models relies on the resolution of a prognostic equation for the sub-grid concentration variance, i.e. the quantity that accounts for the distribution of concentration within a grid-cell of a mesoscale model, by using a 1.5 order closure. The parameterization is implemented in a 3D transport model and tested against large eddy simulations of convective atmospheric boundary layers.

2.2 Formulation

We propose a parameterization to account for the concentration variability ($\overline{c'^2}$) that is based the conservation equation of the concentration variance. The latter reads:

$$\underbrace{\frac{\partial \overline{c'^2}}{\partial t}}_{S} + \underbrace{\overline{u_i}\frac{\partial \overline{c'^2}}{\partial x_i}}_{A} = \underbrace{-2\overline{c'u'}_i \frac{\partial \overline{c}}{\partial x_i}}_{G} \underbrace{-\overline{\frac{\partial u_i' c'^2}{\partial x_i}}}_{T} \underbrace{-\varepsilon_c}_{D} + \underbrace{2\overline{c'E'}}_{E}, \tag{2.1}$$

where u_i, c, E represent the wind components, the concentration and the emission. Equation (2.1) accounts for the time evolution of concentration variance (S) created by turbulent motion (T) and transported in 3D (A and G) space while it is dissipated (D). It contains an extra term that accounts for the contribution to the variance production originating from the surface spatial variability of the emissions. In order to solve (2.1) for the variance we need to close some of the terms. While terms G, T and D can be closed conventionally by using well assessed parameterizations (see Appendix), for the term E we propose the following expression,

$$\overline{c'E'} = r\left(\overline{c'^2}\right)^{1/2}\left(\overline{E'^2}\right)^{1/2}, \tag{2.2}$$

where r is the correlation coefficient between the concentration and the emission variances.

2.3 Methodology

Our method is based on using two models with different physical assumptions:

(1) A Reynold Averaged Navier-Stokes (RANS) equation model that assumes an instantaneous and homogeneous mixing i.e. does not solve turbulence; and
(2) a 3D Large Eddy Simulation (LES) model that explicitly solves the heterogeneity of mixing by the turbulent characteristics of the atmosphere.

The RANS model hosts the parameterization developed to account for the sub-grid emission variability and the concentration variance. We use for this purpose the Finite Volume Model (FVM) developed by Martilli (2002) Martilli et al. (2002). The LES code (Cuijpers and Duynkerke, 1993) generates all the control runs used to test the parameterization. When the 3D results of a LES are averaged according to the x and y directions and time they can be reduced to a vertical profile that coincides with a solely 1D-column of the 3D-RANS model.

With the LES code, we simulate a dry convective boundary layer over a domain of $10 \times 10 \times 1.5$ km^3 with vertical and horizontal resolutions of 25 and 100 m, respectively, leading to $100 \times 100 \times 60$ grid-points simulation. For the wind and the potential temperature, periodic lateral boundary conditions are assumed. The maximal time step used is 0.5 s. The surface sensible heat flux is 0.05 K m s^{-1}. The geostrophic wind is set equal to 5 m s^{-1}, and the initial potential temperature profile has a constant value of 288 K below 662.5 m and increases by 0.6 K every hundred meters above this height.

The domain is divided into 4 sub-domains of 5×5 km^2, in which statistics is calculated at each time step. In one of these sub-domains we have two centred emission scenarios where the surface of the emission is equal to 64 and 16% of the sub-domain area. The sources have different surface dimensions but emit the same quantity of mass (see Fig. 2.1).

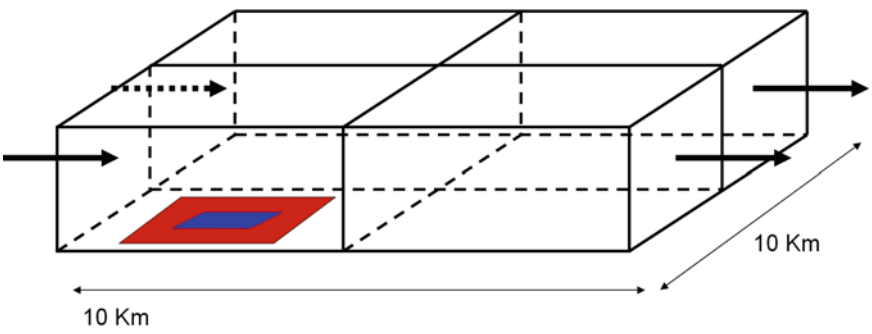

Fig. 2.1 Schematic representation of the modelling set-up. The *red* and *blue* areas represent the emitting surfaces of the two emission scenarios

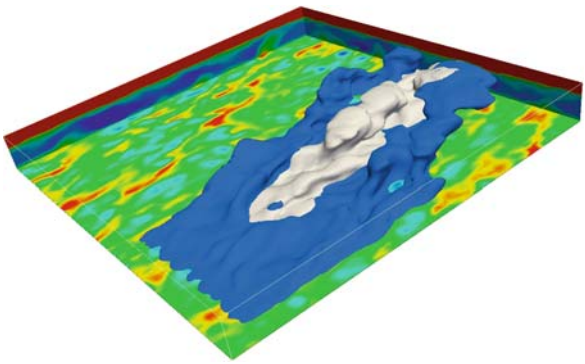

Fig. 2.2 Instantaneous contour plot of the concentration fields for the two emission scenarios (64% in *blue* and 16% in *grey*) after two hours of simulation and with a threshold of 0.1 ppb. The potential temperature is also shown as coloured surfaces (See also Colour Plate 4 on page 172)

An instantaneous contour plot of the concentration fields for the two emission scenarios after two hours of simulation is shown in Fig. 2.2. The two plumes generated by the two emission patterns can be distinguished (blue and grey contours). The contours show clearly the squared shape of the emission pattern and its advection to the right of the domain.

The simulation runs for 2 h after a pre-run of 1 h for the dynamics only. The scalars have no initial concentrations in the atmospheric boundary layer (ABL). They are emitted from the surface with an emission rate of 0.1 ppb s^{-1}. Statistics are calculated for the last hour.

Using FVM we simulate the same ABL over the same domain, but using a horizontal mesh of 2×2 grid cells. The code is initialized with the results of the pre-run of 1 h performed by LES.

Let us assume that within a RANS grid cell of 5×5 km^2 (coinciding with the LES sub-domain size with a resolution of 100 m $\times$ 100 m) we have a source with finite dimensions. The normal practice would be to average the emission from the source over the grid cell size and to use it as source term to solve the average concentration equation in order to account for the atmospheric dispersion. In our case, we take into account the variability of the source by including (2.2) into (2.1) and solving (2.1). The emission variances are calculated from the high-resolution emission inventory (used for the LES simulation); the parameter from r is deduced from the LES simulation and the concentration variance is calculated in a straight-forward manner.

2.4 Results

Figure 2.3 shows the result of the comparison between the LES variance and the RANS model variance for the 64% Emission Surface/Grid-Cell scenario in the four sub-domains. The agreement in the sub-domain where the emission takes place is excellent. However, results deteriorate for the other cells where the variances are

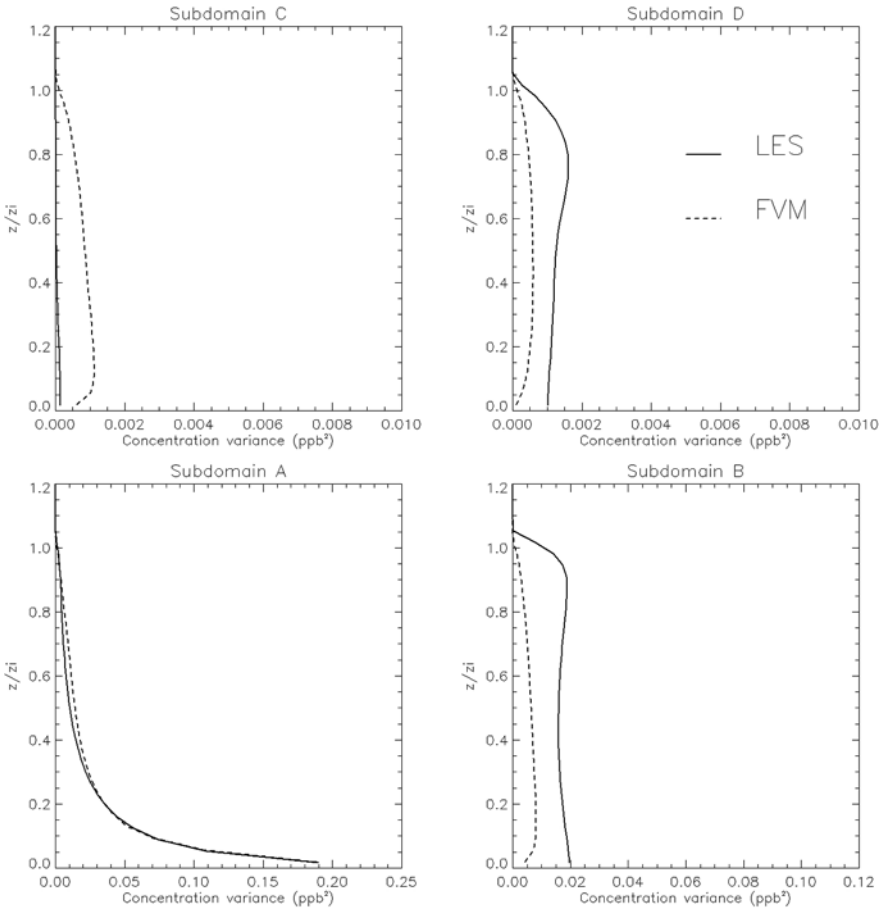

Fig. 2.3 Comparison of LES results with the RANS model (for different subdomains A–D) for the concentration of the 64% Emission Surface/Grid-Cell Surface scenario

only transported and dissipated. This is likely to be due to the lack of resolution in advection schemes since only a few grid points are considered.

From the beginning, we assumed that the LES represented true atmospheric motion due to its high resolution and accuracy in simulating atmospheric flow and dispersion. Within the LES domain we introduce 10 virtual measuring locations (Fig. 2.4) to investigate how the use of the emission variance parameterization will improve 3D RANS model results when compared with instantaneous measurements collected at 10 points (1–10) in Fig. 2.4.

Figure 2.5 shows the time evolution of concentration sampled at 12.5 m for the two emission patterns at 10 locations. The data are instantaneous concentration values produced by the LES with a 5 minute frequency. The thick black lines are the concentrations obtained from the 3D model whereas the shading is correspond

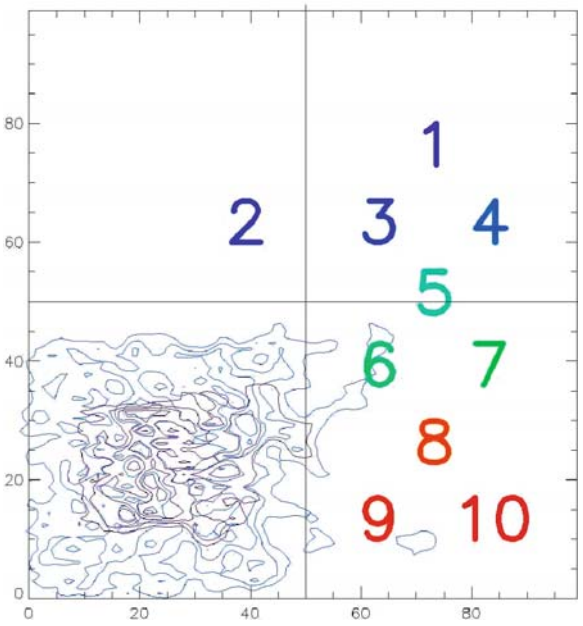

Fig. 2.4 Position of ten virtual sampling locations where time profiles of the concentrations for the two emission cases have been extracted

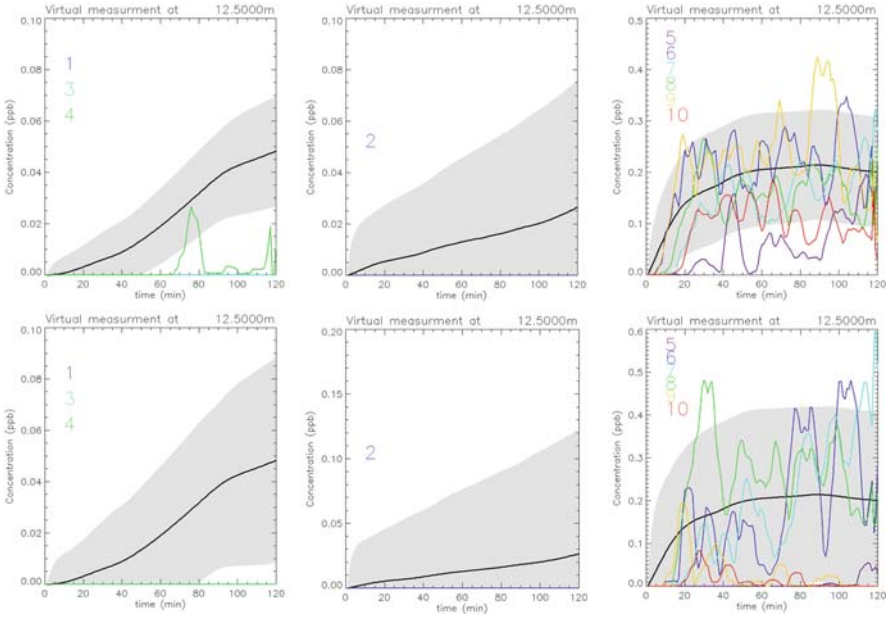

Fig. 2.5 Time profiles of the instantaneous concentrations sampled at 12.5 m and at the 10 locations (Fig. 2.4). The *thick black lines* show the average concentration obtained by the FVM model. The *shading* is the variance calculated with the new formulation. (*Upper*) 64% Emission Surface/Grid-Cell Surface case. (*Lower*) 16% Emission Surface/Grid-Cell Surface scenario (See also Colour Plate 5 on page 173)

to ±1 standard deviation (note, values below 0 have been discard as meaningless). As seen the 3D model results can be better compared with those of the LES, despite differences in the modelling approaches. Even with the extreme case of comparing instantaneous equations with Reynolds Averaged ones, when we consider the spatial variability of the emissions we can generalize the results of the RANS model.

2.5 Conclusions

A simple method to account for variability of emission has been proposed. The RANS model results compared to LES model are very encouraging. The parameterization will allow error bars to be added to model results. The next step will consider the analysis of different and more complex emission patterns and the refinement of information on the spatial variability.

Appendix: Other Closures Used for Prognostic Equation for the Variance of Pollutant Concentration

A description of the other closures used to solve the prognostic equation for the variance of pollutant concentration is given.

The turbulent fluxes of (G) (2.1) are calculated for the eddy covariance ($\overline{w'c'}$)

$$\overline{w'c'} = -\frac{K_z}{\mathrm{Pr}}\frac{\partial \overline{c}}{\partial z} \tag{2.3}$$

where the turbulent coefficient K_z is estimated using a K-l closure (Bougeault and Lacarrère, 1989; Bélair et al., 1999), w is the vertical velocity, and Pr is the Prandtl number. In this closure a prognostic equation for the turbulent kinetic energy (TKE) e is solved, and turbulent coefficients and TKE dissipation are derived using length scales as follows:

$$K_z = c_k l_k e^{1/2} \tag{2.4}$$

$$\varepsilon_e = c_\varepsilon \frac{e^{3/2}}{l_\varepsilon} \tag{2.5}$$

The lengths l_k and l_ε are calculated at a particular level from the possible upward and downward displacements (l_{up} and l_{down}) that air parcels with kinetic energy e originating from the level z could accomplish before being stopped by buoyancy. In the following β is the buoyancy coefficient.

$$\int_z^{z+l_{up}} \beta\left(\theta(z) - \theta(z')\right)dz' = e(z) \tag{2.6}$$

$$\int_{z-l_{down}}^{z} \beta \left(\theta(z') - \theta(z)\right) dz' = e(z) \tag{2.7}$$

Therry and Lacarrère (1983) proposed a relation between l_k and l_ε

$$l_k = \left(1 + \frac{g}{\theta} \frac{\overline{w'\theta'}}{c_\varepsilon e^{3/2}} l_\varepsilon\right) l_\varepsilon \tag{2.8}$$

Bélair et al. (1999) used the budget equation for the TKE to derive the relation neglecting the turbulent transport contribution and assuming steady-state. This leads to

$$l_k = \left(1 + \frac{B_e}{D_e}\right) l_\varepsilon \tag{2.9}$$

or

$$l_k = \left(\frac{2B_e + G_e}{B_e + G_e}\right) l_\varepsilon \tag{2.10}$$

where B_e, D_e and G_e are the buoyancy, the dissipation and the gradient terms of the TKE budget equation. l_k is determined as the minimum between l_{up} and l_{down} (Bougeault and Lacarrère, 1989).

The turbulent transport T of (2.1) can be written as

$$\frac{\partial \overline{u_i' c'^2}}{\partial x_i} = -\frac{\partial}{\partial z}\left(\frac{K_z}{\mathrm{Pr}} \frac{\partial \overline{c'^2}}{\partial z}\right) \tag{2.11}$$

The dissipation D of (2.1) can be written as

$$\varepsilon_{\overline{c'^2}} = \frac{\overline{c'^2}}{\tau_{\overline{c'^2}}} \tag{2.12}$$

Verver et al. (1997) used the TKE dissipation timescale divided by 2.5 as variance dissipation timescale to be inserted in the expression of the scalar variance dissipation. Using this expression with (2.5) leads to

$$\varepsilon_{\overline{c'^2}} = 2.5 c_\varepsilon \frac{e^{3/2}}{l_\varepsilon} \overline{c'^2} \tag{2.13}$$

C_ε and C_k are set to 0.125 and 0.7 and the Prandtl number Pr is 1/1.3. Boundary conditions for the TKE and the variances are calculated assuming no gradients across the surface.

References

Bélair, S., Mailhot, J., Strapp, J.W., and MacPherson, J.I.: An examination of local versus nonlocal aspects of a TKE-based boundary-layer scheme in clear convective conditions. Journal of Applied Meteorology, 38, 1499–1518, 1999.

Bougeault, P., and Lacarrère, P.: Parameterization of orography-induced turbulence in a mesobeta-scale model. Monthly Weather Review, 117, 1872–1890, 1989.

Cuijpers, J.W.M., and Duynkerke, P.G.: Large eddy simulations of trade wind with cumulus clouds. Journal of the Atmospheric Sciences, 50, 3894–3908, 1993.

Martilli, A.: Numerical study of urban impact on boundary layer structure: sensitivity to wind speed, urban morphology, and rural soil moisture. Journal of Applied Meteorology, 41, 1247–1266, 2002.

Martilli, A., Clappier, A., and Rotach, M.: An urban surface exchange parameterisation for mesoscale models. Boundary-Layer Meteorology, 104(2), 261–304, 2002.

Therry, G., and Lacarrére, P.: Improving the eddy kinetic energy model for planetary boundary layer description. Boundary-Layer Meteorology, 25, 63–88, 1983.

Verver, G.H.L., Van Dop, H., and Holtslag, A.A.M.: Turbulent mixing of reactive gases in the convective boundary layer. Boundary-Layer Meteorology, 85, 197–222, 1997.

Chapter 3
Performance of Different Sub-Grid-Scale Surface Flux Parameterizations for Urban and Rural Areas

Sylvia Bohnenstengel and Heinke Schlünzen

Abstract With increasing computing power resolutions of mesoscale atmospheric models increase. However, this does not necessarily improve model performance as evaluations show. Especially, in very heterogeneous areas like urban areas, where densely built areas with sealed surfaces and irrigated gardens and parks occur within the same grid box the aggregation effect impacts model performance. To ensure a good forecast of pollutant concentrations an accurate prediction of the flow field and the vertical mixing is essential. Two schemes to parameterize sub-grid-scale surface fluxes are applied to the area around Berlin for different meteorological situations and grid resolutions. Parameter averaging and a flux aggregation method with blending height concept are validated for grid resolutions 4, 8 and 16 km. Model performance is determined by calculating hit rates from the German Weather Service (DWD) routine data.

3.1 Introduction

The parameterization of surface fluxes with inclusion of sub-grid-scale land-use becomes substantially important in very heterogeneous areas like urban ones. The so-called "aggregation effect" (Giorgi and Avissar, 1997) affects the representativeness of the grid box averaged fluxes, since the system acts highly non-linear. In urban areas different land-use types, which are highly varying in their surface characteristics, occur within one grid box. A good forecast of concentration does not only depend on emissions and chemical reactions, but also on the flow field. The latter is investigated for the area of Berlin. Like other urban areas the urban geometry results in lower wind speeds leading to a less intense vertical mixing in contrast to suburban or rural areas. In the densely built areas the latent heat flux is lower than in suburban and rural areas resulting in high Bowen ratios. Thus,

S. Bohnenstengel (✉)
Max-Planck-Institut for Meteorologie, ZMAW, Bundesstr. 53, 20146 Hamburg, Germany
e-mail: sylvia.bohnenstengel@zmaw.de

A. Baklanov et al. (eds.), *Meteorological and Air Quality Models for Urban Areas*,
DOI 10.1007/978-3-642-00298-4_3,

heat release is dependent on the intensity of the sensible heat flux and more heat is stored in the urban layer compared to rural areas leading to higher temperatures. However, within a grid box irrigated gardens or parks may result in a low Bowen ratio with an intense heat release due to the latent heat flux. Both extremes may occur in the same grid box. The contrary fluxes have to be represented by some kind of grid box averaged fluxes. Vertical exchange and flow field react sensitive to the parameterization applied for sub-grid-scale surface fluxes of heat and momentum. In addition, model performance depends on the resolution applied (Schlünzen and Katzfey, 2003).

3.2 Methodology

Two different parameterization schemes, flux aggregation with a blending height approach and parameter averaging, are applied to represent sub-grid-scale surface fluxes. They are evaluated for urban and rural areas. The resolutions of 4, 8 and 16 km are applied for different meteorological situations and compared to DWD routine measurements of the basic variables like temperature, dew point, wind speed and direction. Five meteorological situations investigated differ in the influence of surface characteristics on the flow.

3.2.1 Model Set-Up

The 3D simulations were conducted for a very heterogeneous and flat area in Northern Germany (Fig. 3.1), which has the advantage that orographically induced effects are of minor relevance. In the centre of the region is Berlin, with four urban measurement sites. Details on the model can be found in Schlünzen (1990), Dierer et al. (2005), and Schröder et al. (2006). Here we focus on the parameterizations relevant for properly calculating surface fluxes. The vertical exchange coefficients are calculated with a mixing length approach for stable, neutral and slightly unstable stratification. A counter gradient scheme is used for convective situations (Lüpkes and Schlünzen, 1996) to correct turbulent heat flux in convective conditions, where large-eddy turbulent motion can produce a heat flux counter to the direction of the local temperature gradient (Holtslag and Moeng, 1991). Two parameterization schemes are alternatively applied to calculate surface fluxes: (1) a parameter averaging scheme; and (2) a flux aggregation method with blending height approach (von Salzen et al., 1996). Both can be applied to calculate area averages of the scaling values friction velocity (u^*), free convection velocity (w^*) and the scaling values for the virtual potential temperature ($\theta_v{}^*$) and for specific humidity (q^*). The heterogeneous sub-grid-scale land-cover is incorporated as fractions f_i for 10 land-cover classes (Fig. 3.1) per grid cell.

When using parameter averaging, surface properties like u^*,w^*, $\theta_v{}^*$ and q^* are not calculated separately for each sub-grid-scale land-cover class (i), but are derived

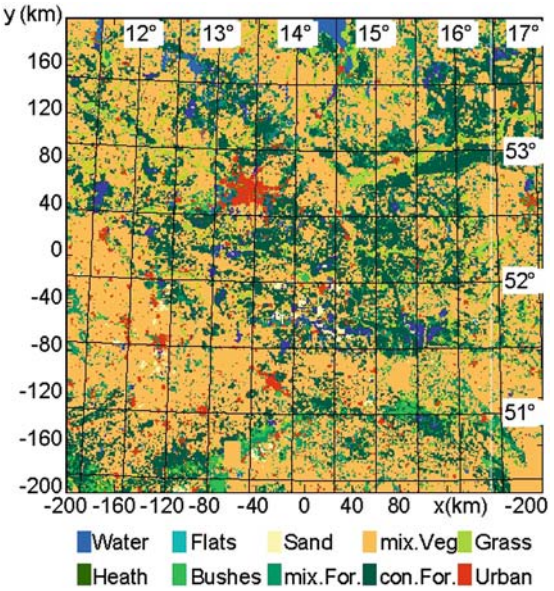

Fig. 3.1 Land use in the model domain (See also Colour Plate 6 on page 173)

using e.g. an effective roughness length z_0. This z_0 is an artificial homogeneous roughness length representative for each grid box.

$$z_0 = \sum_{i=1}^{n} f_i z_{0i} \tag{3.1}$$

The same averaging is applied for the other surface characteristics. This method has the advantage of being very cost-efficient and it performs well as long as the surface characteristics are not too distinct. Problems may arise when an area with a large fractional coverage connected with a marginal flux is next to a small area with a large flux. In these cases, the grid box flux based on averaged parameters might be overestimated or have a direction counter the area-averaged vertical temperature gradient.

This problem should be solved when applying the more expensive flux aggregation method using a blending height concept (von Salzen et al., 1996). Here the sub-grid-scale surface fluxes are calculated for each land-use class i based on the class specific roughness lengths for momentum z_{0i}, temperature and humidity (z_{0qi}). As an example the latent heat flux is given:

$$\begin{aligned} \rho\, l_{21} q_* u_* &= \rho\, l_{21} \sum_{i=1}^{n} f_i\, q_{*_i}\, u_{*_i} \\ &= \rho\, l_{21} \kappa^2 U(z_1) \\ \cdot \sum_{i=1}^{n} f_i \cdot \left(q(z_1) - q(z_{0qi})\right) \cdot &\left[\left(\ln\left(\frac{z_1}{z_{0i}}\right) - \psi_m\left(\frac{z_1}{L_i}\right)\right) \cdot \left(\ln\left(\frac{z_1}{z_{0qi}}\right) - \psi_q\left(\frac{z_1}{L_i}\right)\right)\right]^{-1} \end{aligned} \tag{3.2}$$

Where ρ is density of air, q is specific humidity, $U(z_1)$ is the main flow in x-direction at height z_1, ψ_m and ψ_q are the stability functions for momentum and humidity (Dyer, 1974), L_i is the Obukhov stability length for land use class i, κ is the von Kárman constant (0.4) and l_{21} the latent heat of vaporisation of water. The sub-grid-scale surface fluxes are then averaged to a box averaged flux at the blending height, which is the height, where the influence of the individual surface characteristics is blended out.

3.2.2 Simulated Situations

The 3D version of the atmospheric MEsoscale TRAnsport and Stream (METRAS) model (Schlünzen, 1990) is initialized with 1D background profiles assuming horizontal homogeneity. The simulations are nested in European wide observational data based on soundings and surface observations using a nudging approach (e.g. Dierer et al., 2005). Table 3.1 summarizes the situations simulated. The selected situations differ by the influence of surface fluxes. This is characterized by the locality index (I_{lt}), a measure for the locality of the meteorological situation, which describes how relevant local influences might be for the selected day. It is a measure for the strength of the turbulent transport from the surface and is mainly a function of the friction velocity and the free convection velocity.

Table 3.1 Situations simulated

Date	Grid sizes [km]	I_{lt}	Comment on situation
21.07.1974	18, 4	0	very dry
04.03.2003	16, 8, 4	10	humid
04.01.2003	16, 8, 4	20	humid
10.03.2003	16, 8, 4	30	very dry
03.06.2003	16, 8, 4	40	very dry

3.2.3 Result Evaluation

The model performance is evaluated by calculating hit rates from routine data of four DWD stations in the Berlin area (10381, 10382, 10384, and 10389).

The model results of air temperature, dew point, wind speed and direction are interpolated into the locations of the DWD stations at 2 m height above the surface. The hit rates are calculated following Eq. (3.3):

$$H = \frac{100}{m}\sum_{i=1}^{m} n_i, \quad \text{with} \begin{cases} 1 \text{ for } |\text{difference (measurement, model)}| < A \\ 0 \text{ for } |\text{difference (measurement, model)}| \geq A \end{cases} \tag{3.3}$$

The desired accuracy, A, for the air temperature and dew point is set to ±2ºC, for wind speed ±1 ms^{-1}, for wind direction ±30° and for pressure ±1.7 hPa.

3.3 Results and Discussion

In general, the flux aggregation method with blending height concept performs better than the parameter averaging method in nearly all cases, for all resolutions and parameters as shown by Figs. 3.2 and 3.3. Increasing the resolution for each of both parameterization methods mostly pays back for the less well performing parameter averaging method, since sub-grid scale surface characteristics are resolved more explicitly by higher resolutions. This leads to more realistic averaged surface characteristics. In contrast, for the flux aggregation method with blending height concept differences in hit rates due to changes in resolution are mostly within 5%, which can be considered as negligible. Exceptions are found for some of the urban measurement sites, e.g. the wind direction in the Berlin area for an index of 30 was not simulated well with the 16 km resolution and is improved with higher resolutions.

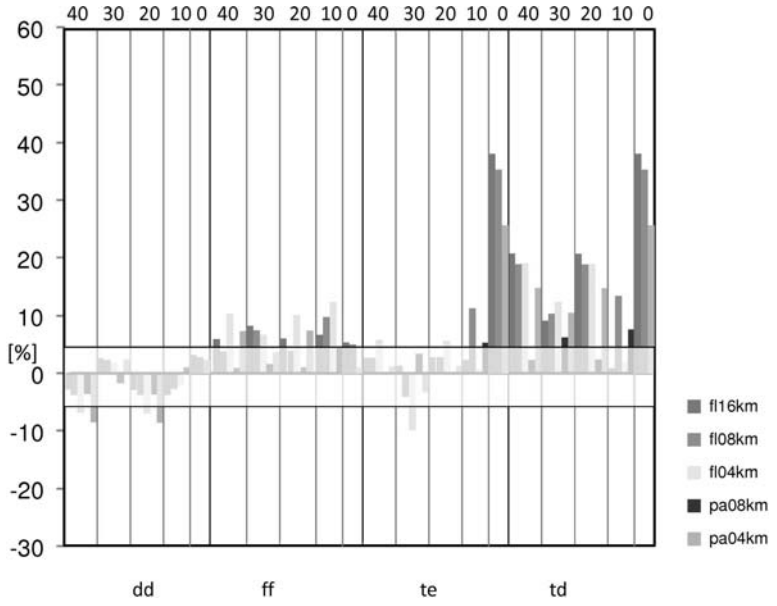

Fig. 3.2 Differences in hit rates for rural areas for all simulations with flux aggregation with blending height concept (fl16 and fl08) and parameter averaging (pa08 and pa04) compared to the theoretically worst case (parameter averaging with 16 km resolution). The results are grouped into changes in hit rates for wind direction (dd), wind speed (ff), temperature (te) and dew point temperature (td) and for all I_{lt} cases. The uncertainty of calculated hit rates is ±5%; changes in hit rates within this range are covered by a white transparent rectangle

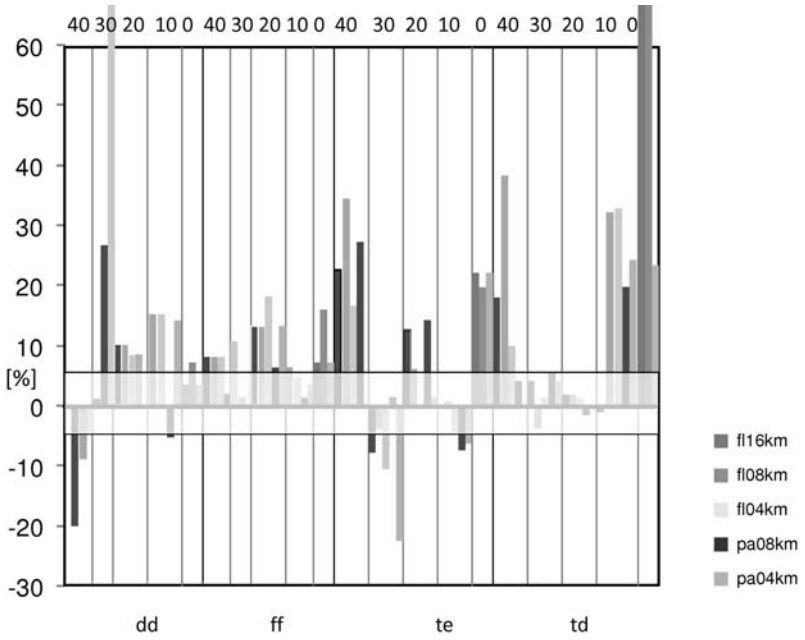

Fig. 3.3 Like Fig. 3.2 but for urban area measurement sites in Berlin

Increasing the resolution in this case results in a better agreement with the measurements, since the urban area is resolved more detailed. Even though the $I_{lt} = 40$ case shows a worsening of performance for wind direction in urban areas compared to the 16 km parameter averaging case, the pattern of improvement of performance by increasing the resolution is similarly found as for the $I_{lt} = 30$ case. Further significant differences occur for temperature and dew point temperature in urban areas for the very locally driven meteorological situation with a locality index of 40.

Overall, the thermodynamical values are more sensitive to the parameterization and resolution applied than the dynamical values in rural as well as in urban areas, since they are directly affected by the sensible and latent heat fluxes. The dynamical values show a smaller dependence on resolution for rural and urban areas for parameter averaging than for the flux aggregation approach. When comparing the hit rates between the rural areas and Berlin for all parameters it is found that METRAS performs better for rural than for urban areas, although METRAS captures some of the urban phenomenon's associated with an urban heat island like the enhanced dryness for example.

A dependence on the meteorological situation described by the locality index I_{lt} could not be found so far. The current results suggest that the humidity in the lower boundary layer might play a significant role in the model performance and should be accounted for when classifying meteorological situation.

3.4 Conclusions

In this study, five case scenarios were simulated for different model resolutions to determine the performance of two parameterization schemes (flux aggregation with a blending height concept and parameter averaging) for sub-grid-scale surface fluxes. In general, the performance differs between these two parameterisation schemes: better performance of the flux aggregation compared to the parameter averaging is the general outcome. In addition, results are better for rural than for urban sites. Improved performance for urban sites was found when the flux aggregation was applied. Both methods seem to be resolution dependent, although the flux aggregation is less so than the parameter averaging. However, the best parameterization for each situation could not be determined, as dynamic and thermodynamic parameters perform differently for the same case. A number of additional factors influence the evaluation, such as the forcing values that are used in the model via a nudging technique and the interpolation of the model results to the routine observation stations. To derive a conclusion that is independent of these shortcomings more case studies are necessary.

Acknowledgments This work is partly funded by the German Science Foundation under SCHL 499/1-1 and is a contribution to COST728.

References

Dierer, S., Schlünzen, K.H., Birnbaum, G., Brümmer, B., Müller, G., 2005. Atmosphere-sea ice interactions during cyclone passage investigated by using model simulations and measurements. Month. Wea. Rev., 133(12), 3678−3692.

Dyer, A., 1974. A review of flux-profile relationship. Boundary Layer Meteorol., 7, 362–372.

Giorgi, F., Avissar, R., 1997. Representation of heterogeneity effects in earth system modeling: experience from land surface modeling. Rev. Geophys., 35(4), 413–438.

Holtslag, A.A.M., Moeng, C.H., 1991. Eddy diffusivity and countergradient transport in the convective atmospheric boundary layer. J. Atmos. Sci., 48, 1690–1698.

Lüpkes, C., Schlünzen, K.H., 1996. Modelling the Arctic convective boundary-layer with different turbulence parameterizations. Boundary-Layer Meteorol., 79, 107–130.

Schlünzen, K.H., 1990. Numerical studies on the inland penetration of sea breeze fronts at a coastline with tidally flooded mudflats. Beitr. Phys. Atmos., 63, 243–256.

Schlünzen, K.H., Katzfey, J.J., 2003. Relevance of sub-grid-scale land-use effects for mesoscale models. Tellus, 55A, 232–246.

Schröder, G., Schlünzen, K.H., Schimmel, F., 2006. Use of (weighted) essentially non-oscillating advection shemes in the mesoscale model. Q. J. Roy. Met. Soc., 132, 1509–1526.

von Salzen, K., Claussen, M., Schlünzen, K.H., 1996. Application of the concept of blending height to the calculation of surface fluxes in a mesoscale model. Meteorol. Zeitschrift NF 5, 60–66.

Chapter 4
How to Use Computational Fluid Dynamics Models for Urban Canopy Parameterizations

Alberto Martilli and Jose Luis Santiago

Abstract The highest spatial resolution of today's mesoscale models is few hundreds of meters. However, in urban areas important atmospheric features occur at the scale of the hetereogenity (few tenths of meters). Mesoscale models can not resolve these features, and their effect must be parameterized. In this contribution, starting from the basic averaging schemes used in mesoscale models, it is explained why Computational Fluid Dynamics models can be used to test and derive such parameterizations. An example of the technique is presented based on simulations over an array of cubes.

4.1 Introduction

The spatial resolution of mesoscale atmospheric models is the result of a balance between three factors:

- the size of the mesoscale circulations object of investigation, which should be contained within the model domain;
- the scale of the surface heterogeneities, which should be resolved at best by model resolution;
- the computational time needed, that should be kept reasonable (few hours).

In general these factors fix, for today's computer, the spatial resolution for mesoscale models at few kilometres (or several hundreds of meters at best). This means that only atmospheric structures larger than the model grid cell can be resolved (a more rigorous estimate may fix the smallest size of resolvable structures to, at least, twice, or $2\Delta x$, the size of the grid cell, but for simplicity thereafter we will always refer to the grid cell size as lower limit).

A. Martilli (✉)
CIEMAT, Centro de Investigaciones Energéticas, Medioambientales y Tecnológicas, Madrid, Spain
e-mail: alberto.martilli@ciemat.es

A. Baklanov et al. (eds.), *Meteorological and Air Quality Models for Urban Areas*,
DOI 10.1007/978-3-642-00298-4_4,

Unfortunately such resolution is 2–3 orders of magnitude larger than the spatial scale of heterogeneities in urban areas (the size of the streets or buildings can be considered of the order of 1–10 m). Even if the computer power is increasing very quickly, the gap to bridge is quite significant, before we will be able to run a mesoscale model with a spatial resolution of few meters over a typical mesoscale domain. A quick estimation can be done. Let assume that the spatial resolution must be increased by a factor 10^{2-3} in both horizontal direction, and a factor 10 in the vertical. The total number of point will increase by a factor 10^{5-7}. Moreover, an increase of resolution will imply a reduction of the time step by the same amount to fulfil the CFL (Courant Friedich Levy) condition. It can be estimated that the time step will need to be decreased by a factor 100. In total, so, we can expect that the CPU time of the simulation will increase by factor 10^{7-9} compared to the CPU time of a standard today's mesoscale simulation. Assuming that the computational power will keep increasing by a factor of ten every five years, (as it has happened in the last decades, Foster, 1994), it is possible that 35–45 years will be needed before to reach enough CPU power to run a mesoscale model with a resolution of few meters. Even in the case of a reduction of model domain size (for example to the city size), still we can expect that 20–25 years will be needed. Moreover, the increased CPU time may be used not only to increase the resolution, but also for other needs, for example, to make:

- longer runs (multi-year);
- multiple runs with different input parameters, to span their uncertainty (ensemble approaches);
- using of more complex and sophisticated physical parameterizations;
- coupling of the model with other models (hydrological, building energy, etc.).

Due to these considerations, it seems reasonable to make an effort to improve the techniques used to parameterize urban impact on the spatially averaged variables computed by mesoscale models (Urban Canopy Parameterizations, UCP).

4.2 Averaging Schemes in Mesoscale Models

There are two ways to define the averaging operators used in mesoscale models.

The first (Pielke, 1984) is to consider the averaging operator as a simple spatial average over the grid cell and time average over the time step, or:

$$\langle \psi \rangle = \frac{\int_{x-\Delta x/2}^{x+\Delta x/2} \int_{y-\Delta y/2}^{y+\Delta y/2} \int_{z-\Delta z/2}^{z+\Delta z/2} \int_{t}^{t+\Delta t} \psi(x,y,z,t) dx dy dz dt}{\Delta x \Delta y \Delta z \Delta t} \tag{4.1}$$

With this approach all the features smaller than the grid cell (no matter if turbulent or not) are parameterized, and all the features larger than the grid cell (no matter

if turbulent or not) are resolved. The advantage of this approach is that it is relatively easy to understand. The disadvantage is that the turbulence closures should depend on the resolution. Moreover, when the resolution reaches few hundreds of meters, the largest turbulent eddies may be explicitly resolved by the model. If part of the turbulent motions is resolved explicitly, due to their stochastic nature, only one of the many possible realizations is represented by model's solution. In such situations, a time average of the results may be needed in order to recover some useful statistical information (Calmet et al., 2007). However, the determination of the averaging time, in particular, in complex situations as urban areas, is not always easy to identify.

A second approach consists in performing at first a Reynolds decomposition of the atmospheric variables in mean (deterministic) and turbulent (stochastic) parts, where the mean can be defined using a probability density function *f*.

$$\begin{aligned} \overline{\psi} &= \int_{-\infty}^{\infty} \psi f(\psi) d\psi \\ \psi' &= \psi - \overline{\psi} \end{aligned} \tag{4.2}$$

With this method all the turbulent features are not resolved and need to be parameterized, while only the mean deterministic fields are explicitly resolved. Then, due to the spatial resolution of the mesoscale model a spatial average over the volume of the cell V is needed:

$$\left\langle \overline{\psi} \right\rangle = \frac{\int_V \overline{\psi} dV}{V} \tag{4.3}$$

The consequences of this procedure are in the arising of an extra term in the conservation equation (dispersive flux), representing the flux due to mean deterministic structures smaller than the grid cell. This term is usually neglected in mesoscale models, but it may be important over heterogeneous surface as urban areas. The advantage of this approach is that the model outputs are mean values, which is useful information in many applications. Note, also, that, despite in the majority of publications on model formulations the definition (1) is used for the averaging operator, the turbulence closures adopted in the models are largely based on definition (2) (or ensemble averaging; see, for example, Mellor and Yamada's papers).

In any case, no matter which definition is chosen, it is clear that model results are spatial averages, and should be compared with spatially averaged variables. The problem is that in urban areas the heterogeneity is so important that a point measurement cannot be representative of a spatial average. The ergodic assumption, in fact, usually done over flat and homogeneous surfaces, saying that the spatial average is equal to a time average in one point, is clearly not valid in urban areas, in particular within the urban canopy. One solution could be to have a measurement network very dense in order to be able performing such spatial averaging. This can be technically difficult and very costly. Another option is to use CFD models.

4.3 The Role of CFD Models

With the term Computational Fluid Dynamics (CFD) models we usually indicate numerical models that solves the Navier-Stokes equations over small domains (few hundreds of meters at maximum), at high resolution (meters or less), and explicitly resolve the buildings. There are two main types of such models:

1. Large Eddy Simulations (LES) models explicitly resolve the largest eddies, and parameterize the effect of the sub grid features. Such models resolve time dependent, spatially filtered Navier-Stokes equations. They may be quite heavy computationally, in particular when a time average is needed to derive statistical information.
2. Reynolds Averaged Navier Stokes (RANS) models that parameterize all the turbulence, and resolve only the mean motions. Very often these models are solved in a stationary state. Although in general such models are less computational time demanding than LES, but they are less precise.

The ability of CFD models to reproduce microscale (e. g. building scale) airflow behaviour in urban areas has been tested extensively in the last years, in particular over simplified geometries (wind tunnel cases, for example), with encouraging results.

The procedure we propose to use CFD models is the following:

1. Validate CFD model results, by comparison with point measurements. Since the spatial resolution of the models is of the order of meters, a comparison with point measurements is meaningful. Measurements can come both from wind tunnel experiment (where the conditions are controlled) and field campaigns. Such model intercomparison is useful to define the degree of confidence in the CFD model results that we can expect.
2. Perform spatial averages of the CFD model results in order to derive averaged variables comparable with those of the mesoscale models.

The spatially averaged variables can be used to test urban parameterization, or to improve them (for example, deriving values for some constant needed in the parameterization, as it is the case of the drag coefficient), or to investigate the importance of different physical mechanisms (e.g. dispersive stress). Moreover, CFD results can be used to derive parameterizations of the subgrid spatial distributions of mean pollutant concentration or of the variability due to turbulence. Information, that can be both useful for exposure studies, for example.

The choice of the CFD approach to use (RANS vs. LES) can be influenced by several factors: (1) the type of ‘averaging’ operator chosen in the mesoscale model. If the definition (1) is used, for example, LES may give more useful information, while if (2) is chosen, RANS results are probably enough. (2) The CPU time needed. In order to do a parameter study with CFD, for example, RANS may be preferable, since it allows performing more simulations over different configurations in a

shorter time than LES. It may also be considered to use time averaged LES results in order to improve the turbulence closures used in RANS models.

4.4 An Example

In the following we will briefly describe an example of how CFD-RANS models can be used to derive spatially averaged information. The example is taken from Santiago et al. (2007) and Martilli and Santiago (2007). Only the points relevant for the scope of this article are presented here. For more details we refer to the publications.

The CFD-RANS model used in this study is FLUENT (Fluent Inc., 2005), with the κ–ε standard turbulence closure. It has been run over an aligned array of cubes, with the distance between the cubes equal to the cube's side. This is the same configuration used in a wind tunnel study at Los Alamos National Laboratory (Brown et al., 2001). The first step of the study, then, is to validate model results against wind tunnel measurements. This has been done using a hit rate methodology proposed by Schlünzen et al. (2004).

$$q = \frac{N}{n} = \frac{1}{n}\sum_{i=1}^{n} N_i \text{ with } N_i = \begin{cases} 1 \; if \; \left|\frac{P_i - O_i}{O_i}\right| \leq RD \;\; or \;\; |P_i - O_i| \leq AD \\ 0 \; else \end{cases}$$

where, q is the hit rate, n is the total number of points compared, O_i and P_i are wind tunnel data and model results, respectively. RD and AD represent a relative deviation and an absolute deviation of model results from reference data, respectively. Results are satisfactory and fulfil the criteria proposed by Schlünzen et al. (2004) which fix the limit for validation at $q > 66\%$ in the case of the reference data are wind tunnel measurements. This step gives, then the confidence that the model is able to capture the most important features of the urban boundary layer.

The second step consists of performing horizontal spatial averaging over horizontal slabs, with an extension equal to the cube's unit (Fig. 4.1).

This spatial average has been done for the six cubes' units and for the whole array. The values obtained are, then, spatial averages that can be considered similar to mesoscale models variables (e.g. variables of a non-building resolving model).

With this methodology it is possible, for example, to evaluate the importance of the dispersive stress (vertical flux of momentum due to mean motions smaller than the cube's unit), and compare it against the spatially averaged Reynolds stress (momentum flux due to the turbulent motions), as can be seen in Fig. 4.2.

Such results show that the dispersive stress may play a significant role in the vertical transfer of momentum within the urban canopy. Other important information is derived also for the formulations of the drag term in the momentum equation, and the value of the drag coefficients. We refer to the publications for more details on this topic.

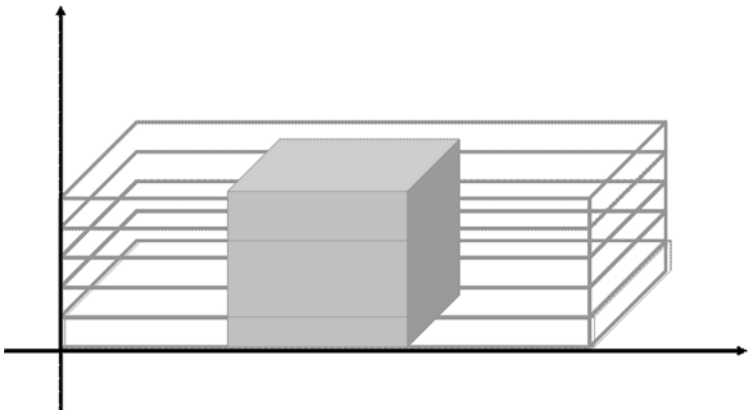

Fig. 4.1 Horizontal slabs where the spatial averages are computed

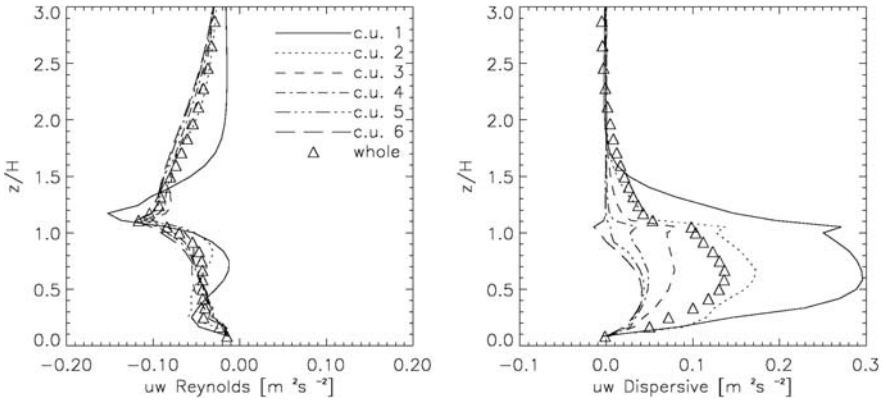

Fig. 4.2 Vertical profiles of **(a)** spatially averaged Reynolds stress and **(b)** dispersive stress

4.5 Conclusions

It is impossible to run an atmospheric model over an entire city and the surrounding (in order to capture the mesoscale circulations) with spatial resolution of few meters, needed to resolve explicitly the urban heterogeneity (buildings, roads, etc.). The best resolution that can be achieved with today's computer is few hundreds of meters. There is a need, then to develop and improve urban parameterizations for models that do not resolve the buildings explicitely. In this contribution, we claim that CFD micro scale models can play a very important role in the testing and development of such parameterization, because they allow performing the needed spatial average,

which are impossible to do with point measurements. An example about how to use such model has been given by Santiago et al. (2007) and Martilli and Santiago (2007).

References

Brown MJ, Lawson RE, DeCroix DS, Lee RL (2001). Comparison of centerline velocity measurements obtained around 2D and 3D buildings arrays in a wind tunnel, Report LA-UR-01-4138, Los Alamos National Laboratory, Los Alamos, 7p.

Calmet I, Leroyer S, Mestayer PG (2007). High-resolution simulations of the urban atmosphere in sea-breeze conditions, 7th Symposium on the Urban Environment, September 10–13, San Diego, CA.

Fluent Inc (2005). FLUENT 6.2 user's guide, volumes 1–3, Fluent Inc., Lebanon, p. 2216.

Foster I (1994). Designing and Building Parallel Programs. Addison-Wesley.

Martilli A, Santiago JL (2007). CFD simulation of airflow over a regular array of cubes. Part II: analysis of spatial average properties. Boundary-Layer Meteorol 122:635–654.

Pielke RA (1984). Mesoscale Meteorological Modeling. Academic Press, 612p.

Santiago JL, Martilli A, Martin F (2007). CFD simulation of airflow over a regular arra of cubes. Part I: Three-dimensional simulation of the flow and validation with wind-tunnel measurements. Boundary-Layer Meteorol 122:609–634.

Schlünzen KH, Bächlin W, Brünger H, Eichhorn J, Grawe D, Schenk R, Winkler C (2004). An evaluation guideline for prognostic microscale wind field models. In: 9th international conference on harmonization within atmospheric dispersion modelling for regulatory purposes, Garmisch-Partenkirchen, June 1–4, Germany, 4p.

Chapter 5
Review of Japanese Urban Models and a Scale Model Experiment

Manabu Kanda

Abstract Numerical models including simple urban canopy models and computational fluid dynamic technologies developed in Japan and the Comprehensive Outdoor Scale MOdel (COSMO) experiment are reviewed.

5.1 Urban Models Developed in Japan

5.1.1 Simple Urban Canopy Models in Japan

Simple urban canopy models in Japan can be classified into two categories: (1) resistance network analogy (Kusaka et al., 2001; Kanda et al., 2005a) and (2) addition of sink/source terms to the basic equations (Uno et al., 1989; Ashie et al., 1999; Vu et al., 1999, 2002; Tanimoto et al., 2004; Kondo et al., 2005). The basic concepts were derived from similar vegetation models. However, vertically 1D approximations used in the parameterization of momentum and energy absorptions within the vegetation canopies are no longer valid for urban canopies. Special treatment of the 3D surface geometry is required instead. Urban radiation schemes typically include complicated sunlit and shade distributions with 2D (Kusaka et al., 2001) or 3D geometry (Ashie et al., 1999; Kanda et al., 2005b; Kondo et al., 2005). Parameterization of local transfer coefficients for momentum and scalars between surfaces (e.g., roof, street, walls) and a reference height requires more than a 1D approximation. However, a compilation of experimental data suggests that such coefficients largely differ case by case and thus are difficult to arrange in a simple formulation (see review Hagishima et al., 2005).

Implementation of simple urban canopy models into mesoscale weather forecast systems is a realistic way to generate routine predictions without excessive computational load. Several numerical studies have included mesoscale simulations

M. Kanda (✉)
Tokyo Institute of Technology, 2-12-1, Ookayama, Meguro-ku, Tokyo 152-8552, Japan
e-mai: kanda@ide.titech.ac.jp

A. Baklanov et al. (eds.), *Meteorological and Air Quality Models for Urban Areas*,
DOI 10.1007/978-3-642-00298-4_5,

that incorporate simple urban canopy models for investigating the urban heat island (UHI) (Kondo and Kikegawa, 2003; Kusaka and Kimura, 2004a, b; Tokairin et al., 2006; Kusaka and Hayami, 2006; Ohashi et al., 2007). A distinct improvement commonly observed in simulations that include a simple urban scheme is a better reproduction of the nocturnal urban temperature field because of the predicted large fraction of heat storage. Increased urban heat storage is a crucial process that must be considered. However, it is currently not clear what level of complexity to the representation of the urban surface is necessary for mesoscale simulations. Model comparison will be useful to identify the dominant physical processes and the most suitable representation for urban mesoscale simulations (e.g. Best, 2006).

5.1.2 Computational Fluid Dynamics Models in Japan

An alternative approach is to explicitly resolve the urban infrastructure using computational fluid dynamics (CFD) technology. Murakami et al. (1999) suggested the use of CFD analysis winds from human to urban scales. CFD methods have been used to examine flows around a single building (e.g., Murakami et al., 1990; Kogaki et al., 1997; Sada and Sato, 2002). Murakami et al. (1996) reviewed the strengths and weaknesses of various modelling approaches, including Reynolds-Averaged Navier–Stokes (RANS) models and Large Eddy Simulations (LES). Several numerical investigations have considered single street canyon flows (see review Li et al., 2006).

Limitations of computational resources, however, have so far restricted CFD applications to simple cases such as turbulent flows within and above a group of buildings. Turbulent flows within and above regular obstacle arrays have been investigated by direct numerical simulations (Miyake et al., 2001; Nagano et al., 2004) and LES (Kanda et al., 2004; Kanda, 2006a). Results from LES applications (Kanda et al., 2004; Kanda, 2006a) suggest there are some important physical aspects that are currently not emphasized in simpler CFD simulations i.e., large dispersive momentum flux within the urban canopy layer due to a mean stream such as recirculation; intermittent urban canyon flow; non-persistent stream patterns; and longitudinally elongated streaks of low speed over building arrays with a scale an order of magnitude larger than individual buildings. Dispersive flux contributions should be included in sink/source term approaches (e.g., Lien and Yee, 2005). Coupling of very large turbulent eddy motions and street canyon flows should be considered in the physical interpretation of turbulent flows within single street canyons.

Application of CFD technologies to real cities is a promising breakthrough in studies of urban meteorology (Fig. 5.1). CFD technologies do not require the concept of roughness, the Monin-Obukhov Similarity Theory (MOST), or simplified representative buildings, but instead explicitly include turbulent flows at multiple scales from individual buildings to the boundary layer, thereby representing more realistic effects of cities onto the atmosphere. Such applications are currently still in the trial stage because of difficulties in the boundary conditions and limitations in computational resources (e.g., Tamura et al., 2002; Ashie et al., 2005; Ashie and

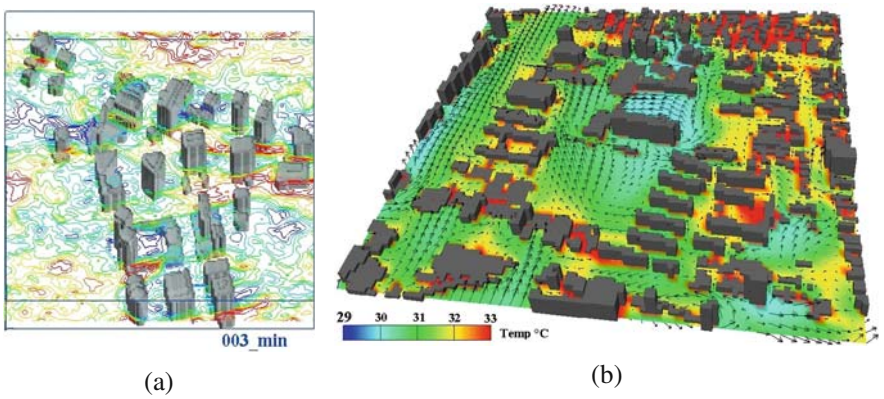

Fig. 5.1 Examples of CFD application to realistic urban geometries. **(a)** Contour map of instantaneous surface wind in Sinjuku (from Kanda, 2006c), and **(b)** contour map of instantaneous surface temperature field and surface wind vector at a coastal area in Tokyo (from Ashie et al., 2005). The area is 500 m × 500 m for **(a)** and **(b)** (See also Colour Plate 7 on page 174)

Kono 2006; Kanda, 2006c; Yamada, 2006). Calculation of multi-reflective radiation processes within real urban canopies requires tremendous computational loads, and LES require unrealistic quasi-cyclic conditions for lateral boundaries.

5.2 Scale Model Experiments

5.2.1 Brief Review of Reduced Scale Model Experiments for Urban Climate

In real cities, field data acquired using towers, aircrafts, and satellites yield a range of valuable information but have not yet resulted in a comprehensive understanding of the complex physics involved in the urban meteorology. Most of the difficulties arise from the heterogeneity and diversity in cities. Reduced-scale physical models provide an alternative and powerful method to study urban climates, free of site-specific diversities, although such models are often highly simplified. Indoor experiments that use arrays of urban-like flow obstacles or roughness elements including cubes, blocks, and cylinders have already contributed to the understanding of neutral-flow structures (see review Kanda, 2006b). Outdoor experiments are a promising way to systematically investigate relations between surface structures and physical processes within and above the roughness sublayer (RSL) under realistic synoptic conditions. Results from such models can be used to detect the physical parameters needed to construct numerical models. Pioneering outdoor experiments using large-scale obstacles (e.g., ~1 m) such as MUST (Yee et al., 2004) and Kit FOX (Hanna and Chang, 2001) focused on dispersion processes and did not consider energy balance. Pearlmutter et al. (2005) evaluated urban surface energy fluxes using an open-air scale model.

5.2.2 Comprehensive Outdoor Scale Model – COSMO – Experiments for Urban Climate

In September 2004, the Japanese Urban Climate Group of the Core Research for Evolutional Science and Technology (CREST) started the Comprehensive Outdoor Scale Model experiments for urban climate (hereafter, COSMO) at scales of 1/5 and 1/50 of real world. The purpose of COSMO is to obtain a comprehensive dataset including (1) energy balance, (2) land surface parameters, and (3) turbulent structures. The 1/5 model surface geometry consisted of concrete cubes 1.5-m on a side with 0.1-m thick walls. The blocks were distributed in an array on concrete pavement that has a total area of 100×50 m^2. The smaller 1/50 scale model was used to investigate the scale effect, which had the same surface geometry and material as the larger model. The models are located next to each other. In addition to the conventional turbulent flux estimate using the eddy covariance method, the direct measurement of the heat storage using thin heat plates allowed us to precisely estimate the surface energy balance closure. It is equipped with 60 thermocouples and 15 compact sonic anemometers aligned in lateral direction at 2H (H is the cube height) to detect the multiple scales of turbulent organized structures.

The roughness length for heat is a very important surface parameter but there are little empirical data. COSMO data were used successfully to develop a theoretical relation between the logarithmic ratio of roughness length for momentum to heat (κB^{-1}) and the roughness Reynolds number (Re*). Values of κB^{-1} associated

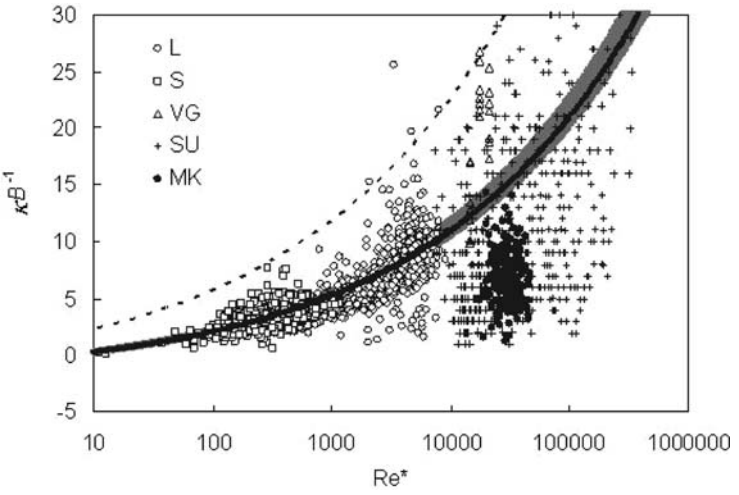

Fig. 5.2 κB^{-1} versus Re* (from Kanda et al., 2007). *Open circles*: large-scale model (L); *open squares*: small-scale model (S). *Open triangles* (VG: light industrial area, Vancouver), *crosses* (SU: business district, Tokyo), and *filled circles* (MK: dense residential area, Tokyo) correspond to urban data. *Lines* are from the theoretical relationship. The *dotted line* is from Brutsaert (1982). The *solid line* is from scale model data

with Re* for three different urban sites from previous field experiments were intercompared. Surprisingly, even though surface geometry differed from site to site, the regressed function agreed with data from the three urban sites as well as with the COSMO data. Field data showed that κB^{-1} values decreased as the areal fraction of vegetation increased (Fig. 5.2).

The surface energy balance data obtained from COSMO for one year is useful to interpret the observed values in real cities. It is surprising that the heat storage

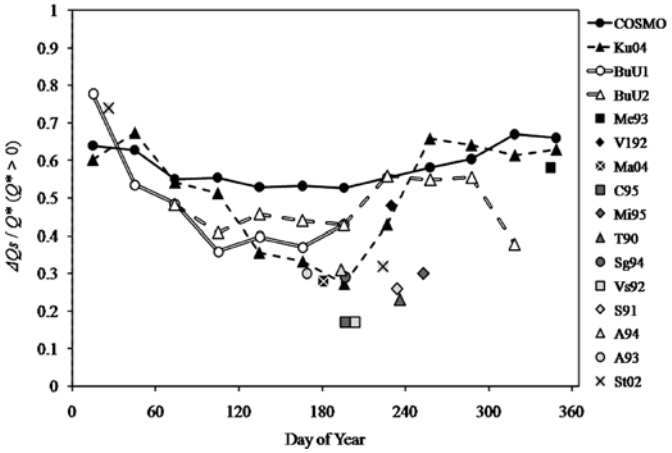

Fig. 5.3 The seasonal trend of dQ_s / Q_*. The values of COSMO and various cities are plotted together

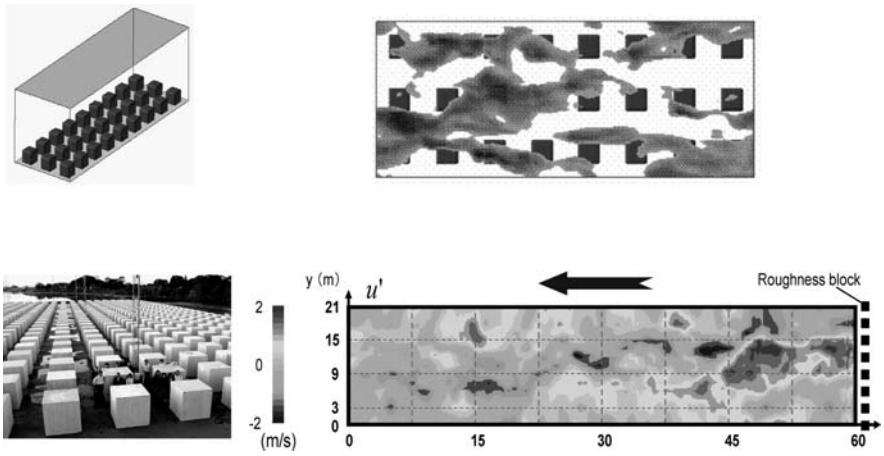

Fig. 5.4 Turbulent organized structures **(a)** simulated by LES (from Kanda, 2006a) and **(b)** observed in COSMO (from Inagaki and Kanda, 2006). *Grey region* are so called low speed streaks defined as the region where horizontal velocity fluctuation from the horizontal mean is negative

dQ_s normalized by net radiation Q_* has a common seasonality irrespective of the difference of surface geometry, land use and latitude among the cities (Fig. 5.3). Moreover, the values of dQ_s / Q_* in COSMO and real fields show a significant wind dependency. The large turbulent motions and corresponding multiple structure of turbulent eddies were also observed in COSMO (Fig. 5.4).

References

Ashie, Y. and T. Kono, 2006: Numerical simulation of urban thermal environment of the waterfront area in Tokyo by using a five meter horizontal mesh resolution. Proc. 6th international conference on urban climate. Goteborg, Sweden, 615–618.

Ashie, Y., T. Kono, and K. Takahashi, 2005: Development of numerical simulation model of urban heat island, Annual report of the earth simulator center, April 2004–March 2005, The earth simulator center, 85–88.

Ashie, Y., C. Vu Thanh, and T. Asaeda, 1999r: Building canopy model for the analysis of urban climate. J. Wind Eng. Ind. Aero., 81, 237–248.

Best, M., 2006: Progress towards better weather forecasts for city dwellers: from short range to climate change. Theor. Appl. Climatol., 84, 47–55.

Brutsaert, W., 1982: Evaporation into the Atmosphere. D. Reidel, Dordrecht, 299 p.

Hagishima, A., J. Tanimoto, and K. Narita, 2005: Intercomparisons of experimental convective heat transfer coefficients and mass transfer coefficients of urban surfaces. Bound. Layer Meteor., 117, 551–576.

Hanna S.R., and Chang J.C., 2001: Use of the kit fox field data to analyze dense gas dispersion modeling issues. Atmos. Environ., 35, 2231–2242.

Inagaki, A. and M. Kanda, 2006: Turbulent organized structure over a reduced urban scale model, Sixth Symposium on the Urban Environment, American Meterological Society, 29 January–2 February 2006, Atlanta, GA.

Kanda, M., 2006a: Large eddy simulations on the effects of surface geometry of building arrays on turbulent organized structures. Bound. Layer Meteor., 118, 151–168.

Kanda, M., 2006b: Progress in the scale modeling of urban climate: Review. Theor. Appl. Climatol., 84, 23–33

Kanda, M., 2006c: Atmospheric boundary layer and scalar dispersion with explicitly resolved urban geometries using Large eddy simulation for city. Sixth Symposium on the Urban Environment, American Meteorological Society, 29 January–2 February 2006, Atlanta, GA.

Kanda, M., R. Moriwaki, and F. Kasamatsu, 2004: Large eddy simulation of turbulent organized structure within and above explicitly resolved cubic arrays. Bound. Layer Meteor., 112, 343–368.

Kanda, M., T. Kawai, and K. Nakagawa, 2005a: A simple theoretical radiation scheme for regular building arrays. Bound. Layer Meteor., 114, 71–90.

Kanda, M., T. Kawai, M. Kanega, R. Moriwaki, K. Narita, and A. Hagishima, 2005b: A simple energy balance model for regular building arrays. Bound. Layer Meteor., 116, 423–443.

Kanda, M., M. Kanega, T. Kawai, R. Moriwaki, and H. Sugawara, 2007: Roughness lengths for momentum and heat derived from outdoor urban scale models. J. Appl. Meteor. Cimatol., 46, 1067–1079.

Kogaki, T., T. Kobayashi, and N. Taniguchi, 1997: Large eddy simulation of flow around a rectangular cylinder. Fluid Dyn. Res., 20, 11–24.

Kondo, H. and Y. Kikegawa, 2003: Temperature variation in the urban canopy with anthropogenic energy use. Pure Appl. Geophys., 160, 317–324.

Kondo, H., Y. Genchi, Y. Kikegawa, Y. Ohashi, H. Yoshikado, and H. Komiyama, 2005: Development of a multi-layer urban canopy model for the analysis of energy consumption

in a big city: Structure of the urban canopy model and its basic performance. Bound. Layer Meteor., 116, 395–421.

Kusaka, H. and F. Kimura, 2004a: Coupling a single-layer urban canopy model with a simple atmospheric model: Impact on urban heat island simulation for an idealized case. J. Meteor. Soc. Japan, 82, 67–80.

Kusaka, H. and F. Kimura, 2004b: Thermal effects of urban canyon structure on the nocturnal heat island: Numerical experiment using a mesoscale model coupled with an urban canopy model. J. Appl. Meteor., 43, 1899–1910.

Kusaka, H. and H. Hayami, 2006: Numerical simulation of local weather for a high photochemical oxidant event using the WRF model. J. Meteor. Soc. Japan, Int. J. Series B- Fluids and Thermal Eng., 49, 72–77.

Kusaka, H., H. Kondo, Y. Kikegawa, and F. Kimura, 2001: A simple single-layer urban canopy model for atmospheric models: Comparison with multi-layer and slab models. Bound. Layer Meteor., 101, 329–358.

Li, X.-X., C.-H. Liu, D.Y.C. Leung, and K.M. Lam, 2006: Recent progress in CFD modelling of wind field and pollutant transport in street canyons. Atmos. Environ., 40, 5640–5658.

Lien, F.-S. and E. Yee, 2005: Numerical modeling of the turbulent flow developing within and over a 3-D building array, Part III: A distributed drag force approach, its implementation and application, Bound. Layer Meteor., 114, 287–313.

Miyake, Y., K. Tsujimot, and M. Nakaji, 2001: Direct numerical simulation of rough-wall heat transfer in a turbulent channel flow. Int. J. Heat Fluid Flow, 22, 237–244.

Murakami, S., A. Mochida, and Y. Hayashi, 1990: Examining the k-ϵ model by means of a wind tunnel test and large-eddy simulation of the turbulence structure around a cube. J. Wind Eng. Indust. Aero., 35, 87–100.

Murakami, S., A. Mochida, R. Ooka, S. Kato, and S. Iizuka, 1996: Numerical prediction of flow around a building with various turbulence models: comparison of k-e EVM, ASM, DSM and LES with wind tunnel tests. ASHRAE Trans., AT-96-10-1.

Murakami, S., R. Ooka, A. Mochida, S. Yoshida, and S. Kim, 1999: CFD analysis of wind climate from human scale to urban scale. J. Wind Eng. Indust. Aero., 81, 57–81.

Nagano, Y., H. Hattori, and T. Houra, 2004: DNS of velocity and thermal fields in turbulent channel flow with transverse-rib roughness. Int. J. Heat Fluid Flow, 25, 393–403.

Ohashi, Y., Y. Genchi, H. Kondo, Y. Kikegawa, and Y. Hirano, 2007: Influence of air-conditioning waste heat on air temperature in Tokyo during summer: Numerical experiments using an urban canopy model coupled with a building energy model. J. Appl. Meteor., 46, 66–81.

Pearlmutter, D., P. Berliner, and E. Shaviv, 2005: Evaluation of urban surface energy fluxes using an open-air scale model. J. Appl. Meteor., 44, 532–545.

Sada, K. and A. Sato, 2002: Numerical calculation of flow and stack-gas concentration fluctuation around a cubical building. Atmos. Environ., 36, 5527–5534.

Tamura, T., O. Ohno, S. Cao, Y. Okuda, and H. Okada, 2002: LES analysis on wind profile over complex roughened ground surface in urban area. Proc. 15th Symposium on Boundary Layers and Turbulence, Wageningen, The Netherlands, 299–300.

Tanimoto, J., A. Hagishima, and P. Chimklai, 2004: An approach for coupled simulation of building thermal effects and urban climatology. Energy and Buildings, 36, 781–793.

Tokairin, T., H. Kondo, H. Yoshikado, Y. Genchi, T. Ihara, Y. Kikegawa, Y. Hirano, and K. Asahi, 2006: Numerical study on the effect of buildings on temperature variation in urban and suburban areas in Tokyo. J. Meteor. Soc. Japan, 84, 921–937.

Uno, I., H. Ueda, and S. Wakamatsu, 1989: Numerical modeling of the nocturnal urban boundary layer. Bound. Layer Meteor., 49, 77–98.

Vu Thanh, C., T. Asaeda, and Y. Ashie, 1999: Development of a numerical model for the evaluation of the urban thermal environment. J. Wind Eng. Indust. Aero., 81, 181–196.

Vu Thanh, C., Y. Ashie, and T. Asaeda, 2002: A k–ε turbulence closure model for the atmospheric boundary layer including urban canopy. Bound. Layer Meteor., 102, 459–490.

Yamada, T., 2006: Numerical simulations of urban heat islands and transport and dispersion of airborne materials around building clusters. Sixth Symposium on the Urban Environment, American Meteorological Society, 29 January–2 February 2006, Atlanta, GA.

Yee, E., A. Christopher, and C.A. Biltoft, 2004: Concentration fluctuation measurements in a plume dispersing through a regular array of obstacles. Bound. Layer Meteor., 111, 363–415.

Chapter 6
Urban Soil-Canopy-Atmosphere Exchanges at Submesoscales: Learning from Model Development, Evaluation, and Coupling with LES

Isabelle Calmet and Patrice Mestayer

Abstract The Soil Model for Sub-Mesoscales Urban version (SM2U) can be used as a stand-alone urban climatology model or as a boundary conditioning model in atmospheric codes. It is presented here by pointing out the specific parameterizations which make it differ from classical surface energy budget models. This paper relates the experience gained by performing validation exercises in documented meteorological situations for both the hydric and the thermal parts of the model, and sensitivity studies aimed at disclosing the relative efficiency of the different parameterizations (wall conduction, radiative trapping. . .). The SM2U model is then shown a very useful tool for small-scale climatology mainly due to the coupled computation of water and energy budgets. The atmospheric response to the SM2U ground forcing is also evaluated when coupled with a LES model, for different description modes of a coastal city. The heterogeneity of the districts and a fine description of the city are shown very important in the realistic assessment of the atmospheric lower layers, even in very complex situations including orography and sea influences.

6.1 Introduction

The Soil Model for Sub-Mesoscales Urban version (SM2U) has been developed as a surface flux processor for high resolution atmospheric boundary layer (ABL) model simulations over urbanized areas, and as a stand-alone model to simulate canopy exchanges at spatial resolutions ranging from 100 to 1000 m. The initial of the force-restore mesoscale two-layer soil model developed from Noilhan and Planton (1989) ISBA model for partially vegetated natural soils skeleton is Pleim and Xiu's (1995) version. A third reservoir layer (Noilhan and Mahfouf, 1996) is included in the model which computes in parallel the surface temperature and specific humidity

I. Calmet (✉)
Laboratoire de Mécanique des Fluides, UMR CNRS 6598, Ecole Centrale de Nantes,
BP 92101, 44321 Nantes cedex 3, France
e-mail: Isabelle.Calmet@ec-nantes.fr

A. Baklanov et al. (eds.), *Meteorological and Air Quality Models for Urban Areas*,
DOI 10.1007/978-3-642-00298-4_6,

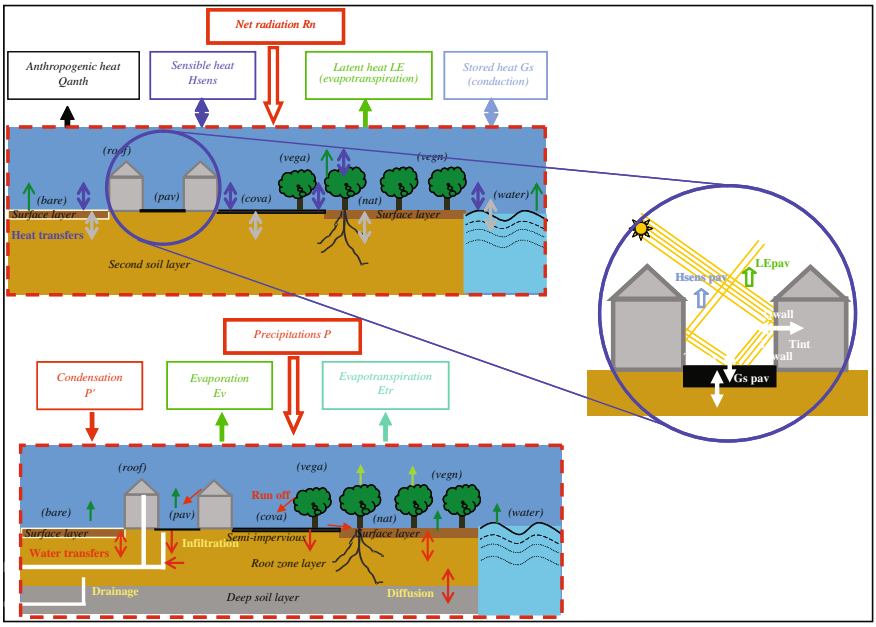

Fig. 6.1 Schematic representation of SM2U: the *upper box* shows the processes modelled in the energy budget part, with a zoom on the in-street radiation and heat storage processes due to building walls; the *lower box* shows the modelled water transfer processes. The *black brackets* indicate the different possible tiles within one grid mesh. Precipitation is a model input while the net radiation is computed by the model from the incoming global and atmospheric radiation inputs (See also Colour Plate 8 on page 174)

by means of force-restore equations. The heat and water fluxes through the surface layer are calculated from the surface energy and water balances resulting from the exchanges with the atmosphere and the underlying soil layer (Fig. 6.1). The advantage of computing in parallel the energy and water transfer processes is threefold: (i) the partition between sensible and latent heat fluxes is based on the moisture actually available due to long- and short-term water storage processes, (ii) the heat conduction into the ground depends on the actual soil humidity, and (iii) the available humidity in the canopy layer depends on the actual vegetation evapotranspiration.

6.2 Model Development

The SM2U development consisted of replacing the integrated approach by a tiling approach. In ISBA the vegetation fraction is an additional layer partially covering the unique surface soil layer whereas for the tiling approach the surface energy and water budgets are computed separately for the vegetation and bare soil fractions. The underlying soil layer under all surface layers and the overlying air layers are unique. The surface fluxes are averaged for the cell.

The first urbanization development consisted of:

– extending the tiling approach by adding in each cell the separate computation of surface budgets for each typical urban surface cover mode, pavement with or without trees, grounds with dispersed vegetation, and building roofs, considering the (semi-)impervious surfaces as water reservoirs with run-off to the neighbouring tiles and/or to the drainage network (Guilloteau, 1999);
– introducing Guilloteau's (1998) non-iterative algorithm to compute the fluxes with non-equal momentum and heat roughness lengths;
– Bottema's models to compute roughness length from the building morphological parameters (Bottema, 1996, 1997; Bottema and Mestayer, 1998; Mestayer and Bottema, 2002).

In this initial "flat canopy" approach, only the (quasi-)horizontal surfaces were modelled. Guilloteau and Dupont (2000) demonstrated that this was not sufficient to simulate correctly the diurnal cycle of the urban surface energy components, which requires the inclusion of the thermo-radiative influence of building walls. The second stage consisted in adding model equations for :

– energy transfer processes for walls and roads including storage,
– shadowing and radiation trapping between neighbouring buildings, with geometry-dependent "effective" albedo and emissivity of streets (Dupont, 2001), and
– influence of canopy shape in the heat transfer through the canopy layer (Piringer et al., 2002) by means of Zilitinkevich's (1995) heat roughness length formula.

The most recent development consisted in adding a scheme for computing the energy budget of the (coastal) sea surface, based on the LKB model (Liu et al., 1979) and Smith's (1988) formula for the momentum roughness length (Leroyer, 2006).

6.3 Model Validation and Implementation

The UBL-Escompte campaign over Marseille urban area (Mestayer et al., 2005) provided with observational data sets for evaluating urban surface energy budget (SEB) schemes. SM2U was tested and validated against the data obtained at the city centre (Grimmond et al., 2004) (Figs. 6.2 and 6.3).

The model allows evaluation of the role of the relative influences of the cover types. Figure 6.4 shows the phase shift between components, with the slow rise of the turbulent sensible heat flux in the morning due to the heat storage in the materials. After 3 pm and during the night the heat stored is released. At night this is nearly equivalent to the radiation loss. This behaviour is not apparent in the vegetation fraction fluxes ("natural" surfaces), where the available energy is about equally-partitioned between the sensible and latent heat fluxes with little heat storage and a small nocturnal negative radiation flux compensated by the sensible heat flux. For

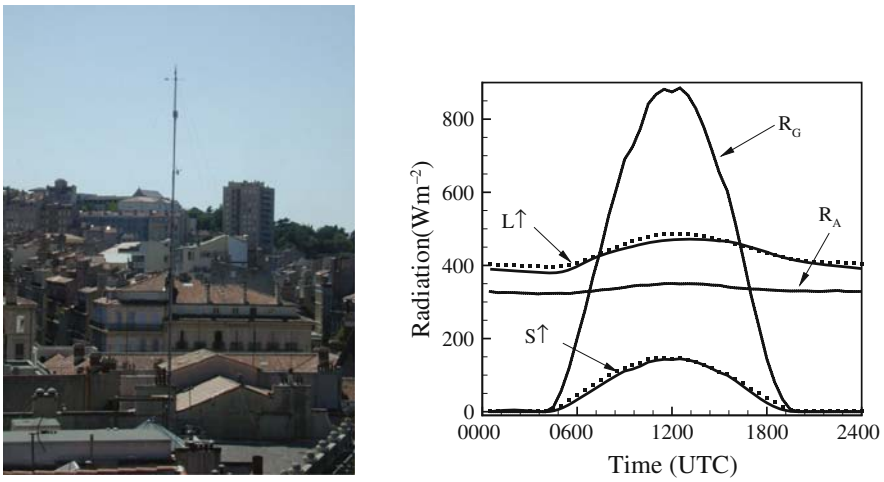

Fig. 6.2 Validation tests of SM2U with Marseille city centre measurements during the CLU-ESCOMPTE campaign; (**a**) view of the central meteorology/flux measurement site (photo, CSB Grimmond); (**b**) mean diurnal cycle of the radiation budget components (averaged over 21 days): the measured incoming shortwave (R_G) and longwave (R_A) radiations are the inputs of the model; the simulated shortwave (S↑) and longwave (L↑) outgoing radiations (*solid lines*) are compared to the observations (*dots*)

roofs the heat storage is small and remains positive to 5 pm and is also equivalent to the radiative loss during the night. The diurnal cycle of the streets, which includes street floors and building walls, demonstrates that the phase shift is essentially due to the wall behaviour: up to 8 am all the solar energy is transformed into heat by the wall vertical surfaces and stored into the materials, reaching a maximum at 10 am. Moreover, the released energy flux after 5 pm and during the night is so large that it compensates both the radiation loss and a positive sensible heat flux into the atmosphere. During daytime the sensible heat flux is relatively small (compared to that of the roofs) due to both the high canopy resistance to the aerodynamic transfers and the high heat capacity of building materials.

Detailed modelling of the heat transfer through walls appears necessary when rapid changes in canopy temperatures must be obtained over small time scales, e.g. at sunrise and during morning hours (Dupont and Mestayer, 2006). Alternative simulations (Fig. 6.5) demonstrate that modelling with two layers, at least, is needed to render both the rapid changes in surface radiation-heat conversion and the actual limits of wall heat capacity. Curiously Fig. 6.5b shows that, for this city centre, the radiation trapping does not significantly influence the sensible heat flux. It is also shown that a flat canopy approach could be sufficient if only the general behaviour without fine scale details is studied (Fig. 6.5b and d).

Evaluation with observational data for the Rezé suburban site (Fig. 6.6) demonstrated that the evapotranspiration scheme is key in the water budget at short time

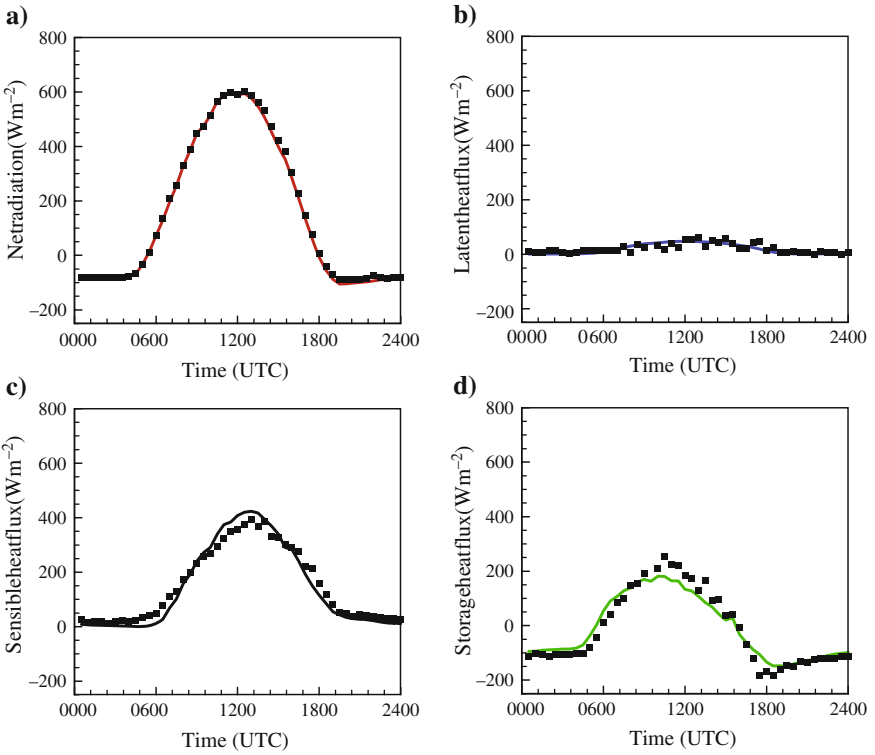

Fig. 6.3 Evaluation of SM2U with Marseille city centre measurements. Mean diurnal cycle of observed (*dots*) and simulated (*solid lines*) net radiation (**a**), turbulent latent heat flux (**b**), turbulent sensible heat flux (**c**), and (storage) heat flux by conduction into wall/roof/soil materials, estimated as the imbalance of the measured/simulated energy budgets (**d**). Net radiation and conduction fluxes are positive downwards, while turbulent heat fluxes are positive upwards

scales (Berthier et al., 2006). For long time scales water removal from the deep soil layer reservoir by infiltration in the draining network is important (Dupont et al., 2006). Alternate simulations demonstrated the potentially large influence of surface layout or management on the canopy microclimatology, especially in dry summer conditions (Fig. 6.7): a small watering of a day ground may reduce the daytime peak by several degrees, as well as the reduction of paved fraction. The difference between the top and bottom curves in Fig. 6.7 is what may be observed in two similar housing estates when the common surfaces are either kept as natural as possible or all paved and connected to the draining network.

Coupling the SEB model with an ABL model requires SM2U input parameters, averaged over each computational grid mesh. These parameters include canopy morphology descriptors and surface/material radiative and thermodynamic properties. In a first step the urban land use and morphological parameters are extracted from statistical analyses of urban databases by the DFmap pre-processor; in a second step a semi-automatic classification is operated with the k-means method to identify the urban districts, allowing to further identify the surface materials, hence their

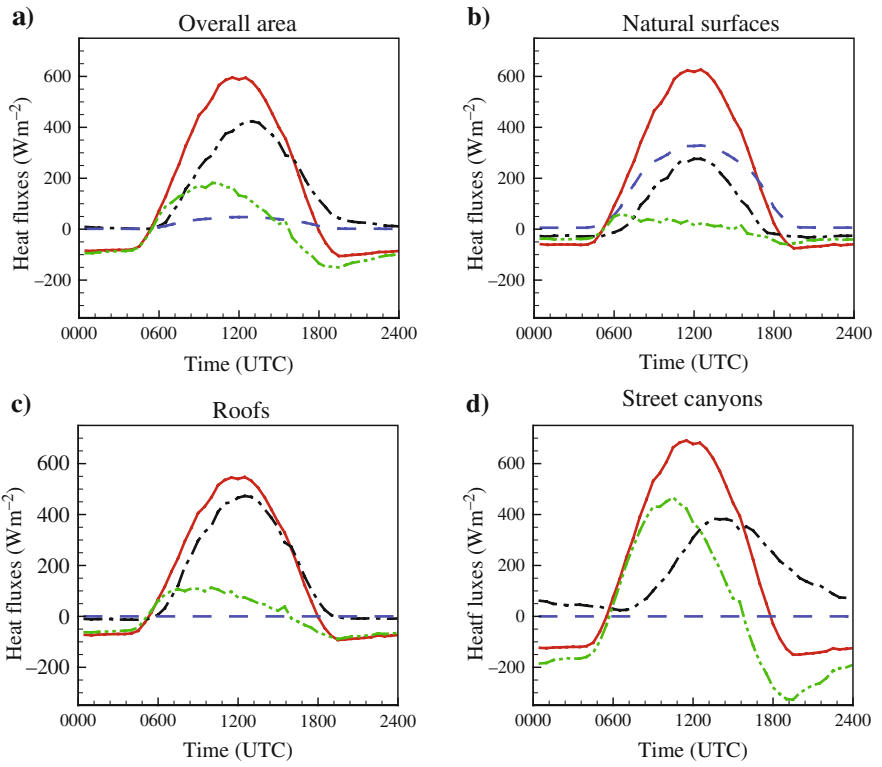

Fig. 6.4 Average simulated energy budget components of Marseille city center, for the overall footprint (**a**), the natural surfaces (**b**), the roofs (**c**), and the paved surfaces (**d**) *solid line*, net radiation flux; *dashed line*, latent heat flux; *dash–dot line*, sensible heat flux; *dash–dot–dot line*, (storage) conduction heat flux

thermodynamic properties (Long, 2003; Long and Kergomard, 2005). The method has been made available to the FUMAPEX participants (Mestayer et al., 2004, 2006; Baklanov and Mestayer, 2004; Baklanov et al., 2005, 2008).

SM2U has been coupled with the atmospheric model MM5 by Dupont et al. (2004) to simulate Philadelphia. This urbanized version of MM5 is freely available at the US EPA, has been used by, at least, the groups from ARL/NOAA (J. Ching), NCAR (F. Chen) and CORIA (A. Coppalle), and further developed by Bornstein et al. (2006). It has also been coupled with ARPS/SUBMESO (Leroyer, 2006), with HIRLAM for the Copenhagen area (Mahura et al., 2005), and with WRF (Chen et al., 2006).

Leroyer et al. (2006, 2009) used the Large Eddy Simulation model ARPS/SUBMESO with SM2U to study the dynamic structure of the boundary layer in the case of a coastal city, where the urban, coastal, and orographic influences are in competition. This study included simulations of simplified configurations and a further analysis of the data obtained in Marseille during a UBL-ESCOMPTE

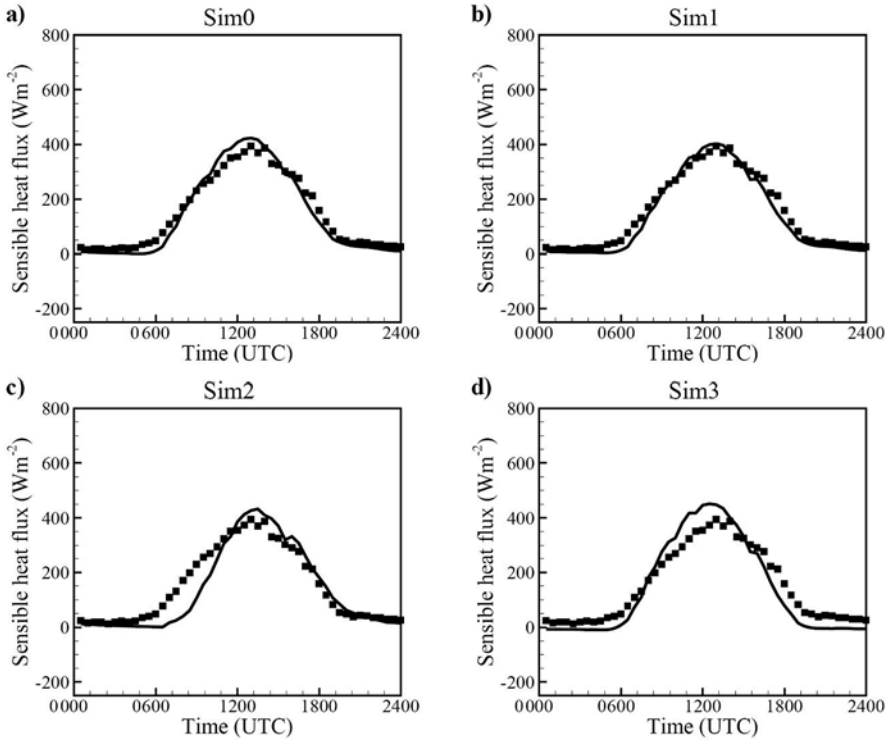

Fig. 6.5 Modelling influence of the radiative trapping and the heat conduction in the walls for the canopy sensible heat flux: Sim0 is the reference simulation (see Figs. 6.2, 6.3 and 6.4); in Sim1 the effective albedo and emissivity are replaced by the pavement counterparts; in Sim2 the wall/pavement two layers are replaced by one average layer; in Sim3 the walls are not accounted for in street heat transfer and storage

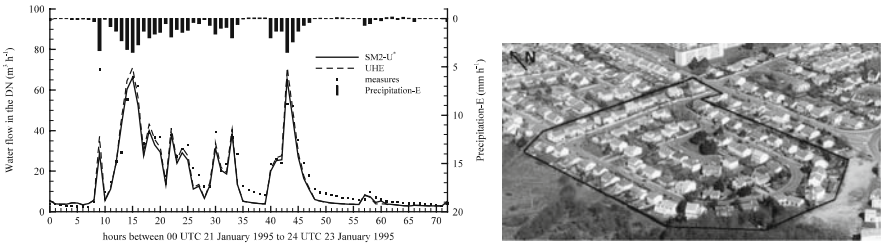

(a) (b)

Fig. 6.6 SM2U and measurements from the Rezé suburban site (**a**) precipitation (minus evaporation) and water flow in the catchment drainage network outlet during the stormy event of 21–23 Jan 1995, comparison of measurements (*dots*) with SM2U and UHE simulation (*solid and dashed lines*, respectively – the SM2U* symbol indicates that simulations were driven with an additional forcing rendering the water infiltration from the soil into the drainage network pipes). (**b**) view of the catchment

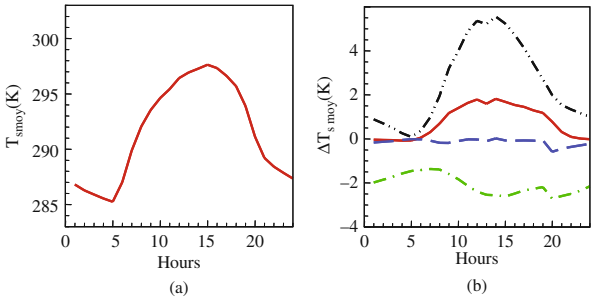

Fig. 6.7 Layout influence on local climatology the Rezé site for July 1996: (**a**) mean surface temperature diurnal cycle (**b**) surface temperature increment if July had been dry, for the same layout (*continuous line*), with vegetation watering one hour per evening (*dashed line*), with pavement replaced by grass (*dash-dot line*), with natural grounds replaced by pavement (*dash-dot-dot line*)

intensive observation period. The simulations for the actual situation and for an alternate situation without the city are compared (Figs. 6.9, 6.10 and 6.11) for midday June 25th 2001. The simulations were performed on the three nested domains (Fig. 6.8) with physiography from IGN (French national geographical institute) urban data base BDTopo for the G2 domain and from the Corine Land Cover outside. In the alternate situation, the urban area is replaced with the natural "garrigue", a low, sparse and dry vegetation.

The main differences between the simulations are observed in the first hundred metres above ground over the most urbanised areas, i.e. located on the west side of the west-east cross-section and at the centre of the south-north one (Figs. 6.9 and 6.10). The cold air carried by the south-west sea breeze is lifted by the urban thermals and roughness, while it penetrates further inland in the alternate simulation, showing the competition between large scale flow and local cover influence. As a consequence, in sea breeze conditions midday is characterized by a temperature increase from the coast to the land (Figs. 6.9 and 6.10) with a higher gradient in the

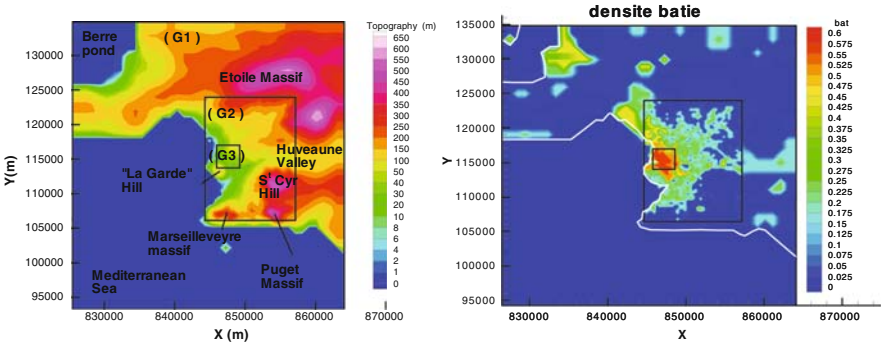

Fig. 6.8 Marseille area (**a**) topography and (**b**) building density. Black rectangles indicate the three computational grid limits, G1 (990 m mesh), G2 (330 m) over the urban area and G3 (110 m) over the city centre (See also Colour Plate 9 on page 175)

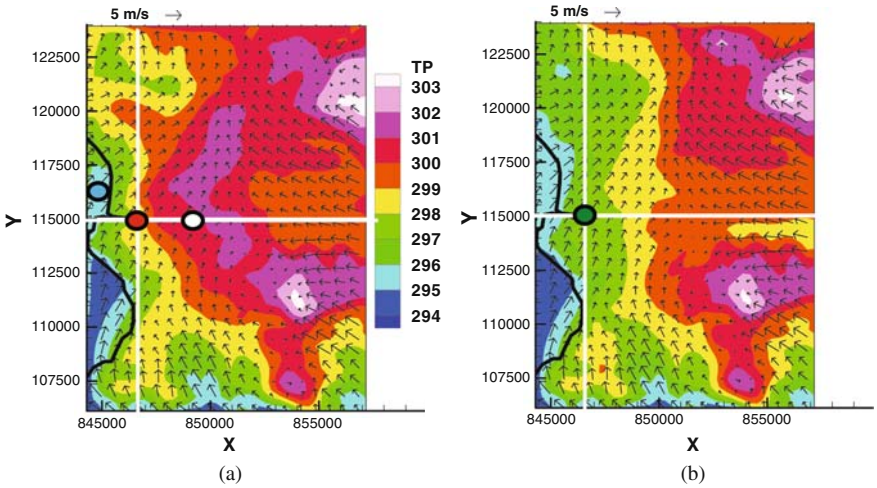

Fig. 6.9 City influence on the low level fields: (**a**) potential temperature (colours) and wind (vectors) at 1300 UTC (June 25, 2001) at 7.5 m above ground level (G2 domain), actual situation; (**b**) alternate simulation without the city (see text) – the white lines indicate the positions of Fig. 6.10 vertical cross-sections and the numbers indicate those of Fig. 6.11 vertical profiles (See also Colour Plate 10 on page 175)

actual situation, coupled with the thermal internal boundary layer development. At the same location, the atmosphere is clearly convective with the city, but slightly stable without (Fig. 6.11), showing the importance of city characteristics in numerical simulations.

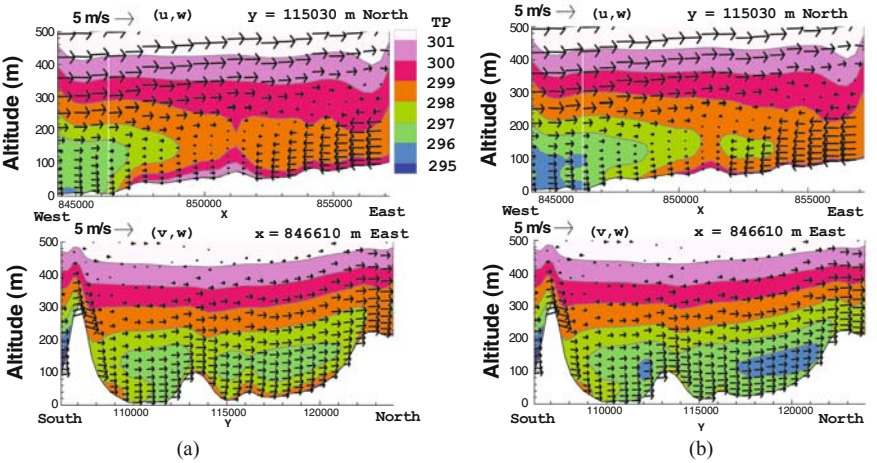

Fig. 6.10 (**a**) Vertical W-E (*top*) and S-N (*bottom*) cross-sections of the atmospheric boundary layer potential temperature and wind fields – same situation as Fig. 6.9, actual situation; (**b**) alternate simulation without the city. The white lines indicate the position of Fig. 6.11 city centre vertical profiles (2 and 4) (See also Colour Plate 11 on page 175)

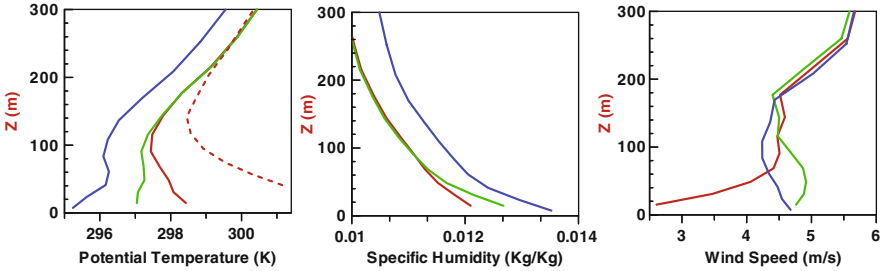

Fig. 6.11 Vertical profiles for the (**a**) potential temperature, (**b**) specific humidity, and (**c**) wind speed off the coast (*line 1*), at the city centre (*line 2*) and over the peri-centre (*line 3*) (see locations on Fig. 6.9) - same situation as Fig. 6.9. The profiles obtained at the city centre location in the alternate simulation without city are also shown (*line 4*)

6.4 Conclusion

The experience gained from development, evaluation, implementation into ABL numerical models, and the application of SM2U allows the following conclusions:

- a "flat canopy" approach may be sufficient only when the city influence at large temporal and spatial scales is evaluated;
- building walls and small scale heterogeneities diurnal cycle of the fluxes and other micro-climatological variables;
- the role of walls materials in radiation and heat conduction during the day and night need to be finely modelled to obtain the actual turbulent heat fluxes;
- radiative trapping may be of less important due to self mitigation, although it may be crucial for obtaining the canopy temperature. When the wind is very weak and the air-wall temperature difference is very large, Sini et al. (1996) showed that the aerodynamic transfer processes in the canopy layer may be significantly altered;
- computing in parallel the energy and water budgets is very important in microclimatology simulations due to the strong interdependence at both small and large temporal scales and the strong influence of the available humidity on the surface and canopy temperatures. This is true even in the city centre where vegetation and natural ground surfaces are limited because of the strong differences in air humidity, and the specific behaviour of soil moisture, associated with heterogeneous soil coverage.

References

Baklanov, A. and P. Mestayer (eds.), 2004: Improved parameterisations of urban atmospheric sublayer and urban physiographic data classification. / A. Baklanov, E. Batchvarova, I. Calmet, A. Clappier, J.V. Chordá, J.J. Diéguez, S. Dupont, B. Fay, E. Fragkou, R. Hamdi, N. Kitwiroon, S. Leroyer, N. Long, A. Mahura, P. Mestayer, N.W. Nielsen, J.L. Palau, G. Pérez-Landa,

T. Penelon, M. Rantamäki, G. Schayes and R.S. Sokhi. D4.1, 4.2 and 4.5 FUMAPEX Report, April 2004, Copenhagen, DMI, Denmark. DMI Scientific Report: #04-05, ISBN nr. 87-7478-506-0.

Baklanov, A. (ed.), B. Amstrup, A. Belivier, N. Bjergene, I. Calmet, A. Clappier, A. Coppalle, S. Dupont, R. Hamdi, B. Fay, S. Leroyer, N. Long, A. Mahura, P. Mestayer, L. Neunhäuserer, N.W. Nielsen, V. Ødegaard, J.-L. Palau, G. Pérez-Land, C. Petersen, C. Philippe, M. Rotach, K. Sattler, G. Schayes, R. Sokhi, Y. Yu, and S. Zilitinkevich, 2005: Integrated and validated NWP systems incorporating urban improvements. FUMAPEX M4.4 Report. DMI Sci. Report. 124 p.

Baklanov, A., P.G. Mestayer, A. Clappier, S. Zilitinkevich, S. Joffre, A. Mahura, and N.W. Nielsen, 2008: Towards improving the simulation of meteorological fields in urban areas through updated/advanced surface fluxes description, *Atmos. Chem. Phys*., **8**, 523–543.

Berthier, E., S. Dupont, P.G. Mestayer, and H. Andrieu, 2006: Comparison of two evapotranspiration schemes on a sub-urban site. *J. of Hydrol.* **328**, 635–646.

Bornstein, R., R. Balmori, H. Taha, D. Byun, B. Cheng, J. Nielsen-Gammon, S. Burian, S. Stetson, M. Estes, D. Nowak, and P. Smith, 2006: Modeling the effects of land-use land-cover modifications on the urban heat island phenomena in Houston, Texas. SJSU Final Report to Houston Advanced Research Center for Project No. R-04-0055, 127 pp.

Bottema, M., 1996: Roughness parameters over regular rough surfaces: Experimental requirements and model validation. *J. Wind Eng.* ***Ind. Aerodyn***., **64**, 249–265.

Bottema, M., 1997: Urban roughness modelling in relation to pollutant dispersion, *Atmos. Environ.*, **31**, 3059–3075.

Bottema, M. and P.G. Mestayer, 1998: Urban roughness mapping – validation techniques and some first results, *J. Wind Eng. Ind. Aerodyn.*, **74–76**, 163–173.

Chen, F., M. Tewari, H. Kusaka, and T.L. Warner, 2006: Current status of urban modeling in the community Weather Research and Forecast (WRF) model. Sixth AMS Symposium on the Urban Environment, Atlanta GA, January 2006.

Dupont, S., 2001: Modélisation dynamique et thermodynamique de la canopée urbaine: réalisation du modèle de sols urbains pour Submeso, Doctoral thesis, University of Nantes, France.

Dupont, S. and P.G. Mestayer, 2006: Parameterisation of the urban energy budget with the submesoscale soil model, *J. Appl. Meteorol. Climatol.*, **45**(12), 1744–1765.

Dupont, S., T.L. Otte, and J.K.S. Ching, 2004: Simulation of meteorological fields within and above urban and rural canopies with a mesoscale model (MM5), *Bound. Layer Meteorol.*, **113**, 111–158.

Dupont, S., P.G. Mestayer, E. Guilloteau, E. Berthier and H. Andrieu, 2006: Parameterisation of the urban water budget with the submesoscale soil model, *J. Appl. Meteorol. Climatol.*, **45**(4), 624–648.

Grimmond C.S.B, J.A Salmond, T.R. Oke, B. Offerle, and A. Lemonsu, 2004: Flux and turbulence measurements at a dense urban site in Marseille: heat, mass (water, carbon dioxide) and Momentum. JGR Atmospheres, 109, D24, D24101, 19 pp. DOI:10.1029/2004JD004936

Guilloteau, E., 1998: Optimized computation of transfer coefficients in surface layer with different momentum and heat roughness lengths, *Bound. Layer Meteorol.*, **87**, 147–160.

Guilloteau, E., 1999: Modélisation des sols urbains pour les simulations de l'atmosphère aux échelles sub-meso. Doctoral thesis, University of Nantes and Ecole Centrale de Nantes, France.

Guilloteau, E., and S. Dupont, 2000: A new modeling of heat exchanges between urban soil and atmosphere, *Surface energy balance in urban areas, COST Action 715 Expert meeting*, 12 April 2000, Antwerp, Belgium. Proceedings EUR 19447, M. Piringer edit., European Commission DG Environnement, Bruxelles, Belgium, pp. 76–91, 2000.

Leroyer, S., 2006: Simulations numériques de l'atmosphère urbaine avec le modèle SUBMESO: application à la campagne CLU-Escompte sur l'agglomération de Marseille. Doctoral thesis, Ecole Centrale de Nantes and University of Nantes, France.

Leroyer, S., I. Calmet, and P. Mestayer, 2009: Urban boundary layer simulations of sea-breeze over Marseille during the ESCOMPTE experiment, Int. J. Environment and Pollution (to appear).

Leroyer, S., I. Calmet, and P. Mestayer, 2006: Airflow analysis over the city of Marseille: Breezes interactions and impact of the city representation in the models, *Proc. 6th International Conference on the Urban Climatology ICUC 6*, Göteborg, Sweden, 12–16 June. pp. 148–151.

Liu, W.T., K.B. Katsaros, and J.A. Businger, 1979: Bulk parameterization of Air-Sea exchanges of heat and water vapor including the molecular constraints at the interface, *J. Atmos. Sci.*, **36**, 1722–1734.

Long, N., 2003: Analyses morphologiques et aérodynamiques du tissu urbain: application à la micro climatologie de Marseille pendant la campagne Escompte, Doctoral thesis, University of Sciences and Technics of Lille, France.

Long, N. and C. Kergomard, 2005: Classification morphologique du tissus urbain pour des applications climatologiques; Cas de Marseille, *Revue Internationale de Géomatique*, **15**, 487-512.

Mahura, A., S. Leroyer, P. Mestayer, I. Calmet, S. Dupont, N. Long, A. Baklanov, C. Petersen, K. Sattler, and N.W. Nielsen, 2005: Large eddy simulation of urban features for Copenhagen metropolitan area, *Atmos. Chem. Phys. Discuss.*, **5**, 11183–11213.

Mestayer, P.G. and M. Bottema, 2002: Parameterisation for roughness parameters in urban areas. In: Rotach M., Fisher B., Piringer M. (Eds.), COST Action 715 Workshop on Urban Boundary Layer Parameterisations (Zurich, 24–25 May 2001). Office for Official Publications of the European Communities, EUR 20355, pp. 51–61.

Mestayer, P., N. Long, and A. Mahura, 2004: Parameterizations for roughness parameters in urban areas. In: Baklanov A. (Ed.), Improved Models for Computing the Roughness Parameters of Urban Areas,. D4.4 FUMAPEX Report, DMI Scientific Report, ISBN: 87-7478-495-1, 11–22.

Mestayer, P.G., P. Durand, P. Augustin, S. Bastin, J.-M. Bonnefond, B. Bénech, B. Campistron, A. Coppalle, H. Delbarre, B. Dousset, P. Drobinski, A. Druilhet, E. Fréjafon, S. Grimmond, D. Groleau, M. Irvine, C. Kergomard, S. Kermadi, J.-P. Lagouarde, A. Lemonsu, F. Lohou, N. Long, V. Masson, C. Moppert, J. Noilhan, B. Offerle, T. Oke, G. Pigeon, V. Puygrenier, S. Roberts, J.-M. Rosant, F. Saïd, J. Salmond, M. Talbaut, and J. Voogt, 2005: The Urban Boundary Layer Field Campaign in Marseille (UBL/CLU-ESCOMPTE): set-up and first results, *Bound. Layer Meteorol.*, **114**, 315–365.

Mestayer, P.G., I. Calmet, S. Leroyer, A. Mahura, N. Long, 2006: Urban soil models for NWP models, In: Integrated Systems for Forecasting Urban Meteorology, Air Pollution and Population Exposure, Final Project Scientific Report; Volume III: CONTRIBUTION REPORTS BY THE PARTNERS, A. Bakalnov editor FUMAPEX contract EVK4-CT-2002-00097, Janvier 2006, pp. 53–59.

Noilhan, J., and S. Planton, 1989: A simple parametrization of land surface processes for meteorological models, *Mon. Wea. Rev.*, **117**, 536–549.

Noilhan, J., and J.-F. Mahfouf, 1996: The ISBA land surface parameterisation scheme. *Global Planet. Change*, **13**, 145–159.

Piringer, M., C.S.B. Grimmond, S.M. Joffre, P. Mestayer, D.R. Middleton, M.W. Rotach, A. Baklanov, K. De Ridder, J. Ferreira, E. Guilloteau, A. Karpinnen, A. Martilli, V. Masson, and M. Tombrou, 2002: Investigating the surface energy balance in urban areas – Recent advances and futur needs, *J. Water, Air, Soil Pollut: Focus*, **2**, N° 5–6, 1–16.

Pleim, J.E., and A. Xiu, 1995: Development and testing of a surface flux and planetary boundary layer model for application in mesoscale models. *J. Appl. Meteor.*, **34**, 16–32.

Sini, J.-F., S. Anquetin, and P.G. Mestayer, 1996: Pollutant dispersion and thermal effects in urban street canyons, *Atmos. Environ.*, **30**, 2659–2677.

Smith, S.D., 1988: Coefficients for sea surface wind stress, heat flux and wind profiles as a function of wind speed and temperature, *J. Geophys. Res.*, **93**, 15467–15474.

Zilitinkevich, S.S., 1995: Non-local turbulent transport: pollution dispersion aspects of coherent structure of convective flows. In: Power H., Moussiopoulos N., Brebbia C.A. (Eds.), Air Pollution Theory and Simulation, Vol. 1, Air Pollution III, Computational Mechanics Publications, 53–60.

Chapter 7
The Effect of Stratification on the Aerodynamic Roughness Length

Sergej Zilitinkevich, Ivan Mammarella, Alexander Baklanov, and Sylvain Joffre

Abstract The roughness length, z_{0u}, is a fundamental concept presented in every textbook on fluid mechanics. It characterizes the friction exerted by the roughness elements on turbulent flows and provides conventional boundary condition for a wide range of turbulent-flow problems. Classical lab experiments and theories treated z_{0u} as a "geometric" parameter independent of the properties of the flow. This conclusion has been taken as granted in environmental physics. In this paper we disclose a strong dependence of z_{0u} on hydrostatic stability, develop the relevant theory, validate it against experimental data and recommend it for use in meteorology, oceanography and hydrology.

7.1 Introduction

The concept of roughness length, z_{0u}, was introduced in the early thirties by classics, Ludwig Prandtl (1875–1953) and Theodore von Karman (1881–1963), to parameterize the transfer of momentum from turbulent flows to aerodynamically rough surfaces, i.e. those with the typical roughness-element height, h_0, larger than the viscous layer height, ν/u_* (where ν is the molecular viscosity and u_* is the friction velocity). Classical laboratory experiments with neutrally stratified boundary-layer flows have shown that z_{0u} does not depend on properties of the flow and factually represents a geometric characteristic of the surface. This conclusion was universally accepted in dynamic meteorology and physical oceanography without any modification and even discussion. The question whether or not z_{0u} depends on stratification did not attract attention, although the crucial role of stratification in atmospheric and oceanic flows was already understood.

S. Zilitinkevich (✉)
Division of Atmospheric Sciences, University of Helsinki, FIN-00014, Finland; Finnish Meteorological Institute, FIN-00102, Helsinki, Finland; Nansen Environmental and Remote Sensing Centre, Thormohlensgt. 47, 5006 Bergen, Norway
e-mail: sergej.zilitinkevich@fmi.fi

A. Baklanov et al. (eds.), *Meteorological and Air Quality Models for Urban Areas*,
DOI 10.1007/978-3-642-00298-4_7,

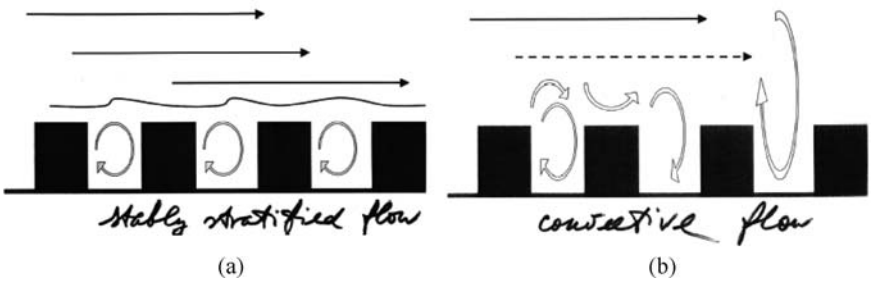

Fig. 7.1 Schematic demonstration of the stability dependence of the roughness length: (**a**) for stably stratified flows (**b**) for convective flows

In this paper this silence is broken with a proposal of a new z_{0u}-model which accounts for the effect of stratification (7–9). The model is evaluated (Figs. 7.1, 7.2 and 7.3) and the effect and practical importance demonstrated (Fig. 7.1). Recommendations are given on how to accurately determine z_{0u} and thus improve the formulation of an essential boundary condition in a range of applications such as numerical weather forecasting, climate and air pollution modelling, or gas exchange between the Earth's surface and the atmosphere.

To illustrate the physical background of the classical concept and its applicability to environmental problems, consider a neutrally stratified atmospheric boundary layer (ABL) over a horizontally homogeneous surface covered with obstacles (roughness elements) of standard shape, separated by standard distances and having standard heights, h_0. At heights, z, much larger than h_0 but much smaller than the ABL height, h, the locally generated turbulence does not depend on h, h_0, and other properties of the surface and, therefore, is fully characterized by z (that serves as the vertical turbulent length scale: $l_T \sim z$) and the vertical flux of momentum per unit

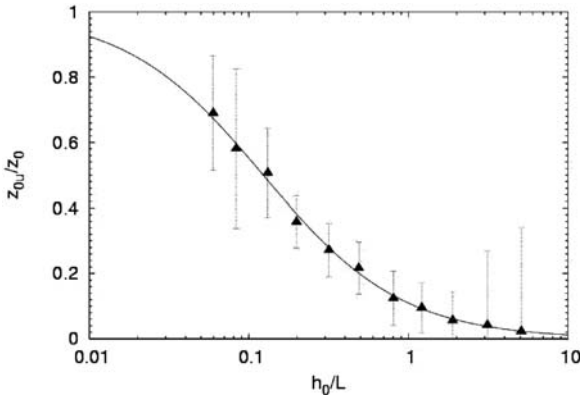

Fig. 7.2 Stable stratification: Bin-average values of z_{0u}/z_0 (the actual roughness length, z_{0u}, over its neutral-stability value, z_0) versus the roughness-layer stratification parameter, h_0/L, based on the Monin-Obukhov turbulent length scale, L, for boreal forest with the typical height of pine trees $h_0 = 13.5$ m ($z_0 = 1.1$m). The bars show standard errors. The theoretical curve is $z_{0u}/z_0 = (1 + 8.13h_0/L)^{-1}$

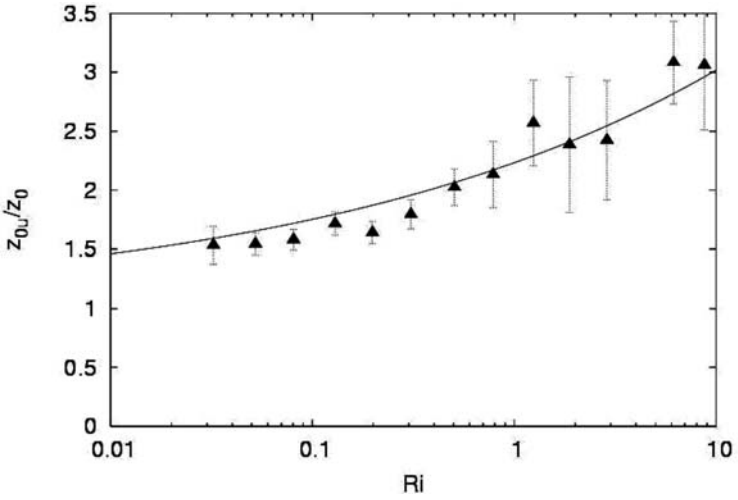

Fig. 7.3 Unstable stratification: Bin-average values of z_{0u}/z_0 versus empirical stratification parameter $\mathrm{Ri} = (g/\Theta_{32})(\Theta_{18}-\Theta_{32})h_0/U_{32}^2$, for the city of Basel with the typical height of buildings $h_0 \sim 14.6$ m and the neutral-stability roughness length $z_0 \approx 1.2 \pm 0.4$. The bars are standard errors. The curve is $z_{0u}/z_0 = 1 + 1.23\ \mathrm{Ri}^{3/14}$, which corresponds to the theoretical 1/3 power-law dependence: $z_{0u}/z_0 = 1 + 1.24(-h_0/L)^{1/3}$

mass, τ. As z increases, τ decreases; but in the "surface layer" ($5h_0 < z < 10^{-1}\ h$) it can be taken height-constant: $\tau \approx \tau|_{z=5h_0} \equiv u_*^2$, whereas u_* serves as a turbulent velocity scale: $u_T \sim u_*$.

Given l_T and u_T, the eddy viscosity, $K_\mathrm{M} \sim u_T l_T$ and the velocity gradient, $\partial U/\partial z$, become

$$K_M = k u_* z, \tag{7.1a}$$

$$\partial U/\partial z = \tau/K_M = u_*/kz, \tag{7.1b}$$

where $k \approx 0.4$ is the von Karman constant. Then integrating (7.1b) involves an integration constant: $U = k^{-1}u_* \ln z + \text{constant}$, or equivalently

$$U = \frac{u_*}{k} \ln \frac{z}{z_{0u}}, \tag{7.2}$$

where z_{0u} (redefined constant of integration) is just the "roughness length".[1] The above analysis is not justified in the "roughness layer" ($0 < z < 5h_0$) and not consistent with the non-slip boundary condition: $U = 0$ at $z = 0$. However, if z_{0u} is known,

[1] To achieve better accuracy, (7.2) is often modified by displacing the vertical axis: $U = k^{-1}u_* \ln\left[(z - d_{u0})/z_{u0}\right]$, where d_{0u} is a fitting parameter called "displacement height". Our analyses did not disclose pronounced effect of stratification on d_{0u} and basically confirmed the traditional estimate $d_{0u} \approx h_0$.

(7.2) realistically describes the velocity profile in the surface layer and allows calculating $u_T \sim u_*$ through $U(z)$ measured or modelled at any height z between 5 h_0 and 10^{-1} h.

Over very rough surfaces, the downward transfer of momentum is performed by pressure forces caused by flow-obstacle interactions, and characterized by h_0 and the maximal velocity in the roughness layer: $U_R \sim u_*$. Assuming that z_{0u} depends only on these two parameters yields $z_{0u} \sim h_0$ (u_* drops out for dimensionality reasons). Classical experiments with the sand roughness confirmed this conclusion and gave $z_{0u} \approx \frac{1}{30} h_0$ (Monin and Yaglom, 1971). For actual land surfaces, z_{0u}/h_0 varies from 1/10 to 1/30 and exhibits dependences on the shape of and the distance between the roughness elements, but no systematic dependence on u_*. Accordingly, land surfaces are traditionally characterized by their roughness lengths considered as constant parameters independent on the wind speed and stratification.

A few authors did observe that z_{0u} could depend on stratification (Arya, 1975; Joffre, 1982; Wood and Mason, 1991; Hasager et al., 2003; Grachev et al., 1997) or discuss a possibility of increases in z_{0u} due to convective plumes developing between warm roughness elements (Coelho and Hunt, 1989; Zilitinkevich et al., 2006a,b). Nevertheless the traditional consensus was not shaken and, to the best of the authors' knowledge, neither theoretical models nor systematic empirical analyses of the stratification effects on z_{0u} have been developed.

To analyze stratified atmospheric flows over rough land surfaces we, in the regular way, employ the Monin-Obukhov length scale (Monin and Obukhov, 1954):

$$L = -u_*^3 F_b^{-1}, \tag{7.3}$$

Where F_b is the vertical turbulent flux of buoyancy (defined as $b = g\rho/\rho_0$, ρ is fluid density, ρ_0 is its reference value, and g is the acceleration of gravity). In the atmosphere, $F_b \approx (g/T)F_\theta$, where T is a reference value of the absolute temperature and F_θ is the flux of potential temperature, Θ. As a general rule, the role of stratification is negligible at $z << L$; but becomes crucial as $z \sim L$ or larger (Monin and Yaglom, 1971). Especially for urban and woodland canopies with $h_0 \sim$ 20–50 m, comparable values of L are quite often observed, so that one can expect a pronounced effect of stratification upon z_{0u}.

We emphasize that physically z_{0u} is not a geometric feature of the surface but a measure of the depth of a sub-layer within the roughness layer with, say, 90% of the velocity drop from its maximal value, $U_R \sim u_*$, approached at $z \sim h_0$. Given the roughness-layer eddy viscosity scale (K_{M0}) the above definition allows estimation of z_{0u} from the conventional formula $\tau = K_{M0}\partial U/\partial z$ taking $\tau \sim u_*^2$ and $\partial U/\partial z \sim U_R/z_{0u} \sim u_*/z_{0u}$, which gives[2]

[2] Equation (7.4) is principally similar to the familiar "smooth-surface roughness length" formulation: $z_{0u} \sim \nu/u_*$, with the only difference that K_{M0} is substituted to ν.

$$z_{0u} \sim K_{M0} u_*^{-1}. \tag{7.4}$$

In turn, K_{M0} can be estimated by matching the roughness layer with the surface layer. In neutral stratification, (7.1a) provides an estimate for $K_{M0} \sim u_* h_0$, and (7.4) reduces to the classical formula:

$$z_{0u} \sim h_0. \tag{7.5}$$

In stable stratification (SS), the familiar formulation for K_M in the surface layer is $K_M = k u_* z (1 + C_u z/L)^{-1}$, where $C_u \approx 2{-}3$ is an empirical dimensionless constant (Zilitinkevich and Esau, 2007). It corresponds to the log-linear velocity profile (used below in data analysis) and gives $K_M \sim u_* L$ at $z > L$. Hence, when h_0 exceeds L, the roughness-layer eddy viscosity scale becomes $K_{M0} \sim u_* L$, so that (7.4) gives

$$z_{0u} \sim L. \tag{7.6}$$

To cover neutral and stable regimes, we interpolate between (7.5) and (7.6) taking the sum of reciprocals: $z_{0u}^{-1} = (C' h_0)^{-1} + (C'' L)^{-1}$, where C' and C'' are dimensionless coefficients (to give priority to the smaller limit: h_0 or L). Then, designating the roughness length in neutral stratification as $z_{0u} (= C' h_0)$, the interpolation formula becomes

$$\frac{z_{0u}}{z_0} = \frac{1}{1 + C_{SS} h_0 / L}, \tag{7.7}$$

where $C_{SS} = C'/C''$ is an empirical dimensionless coefficient.

In unstable stratification (US), $K_M = k u_* z + C_U^{-1} F_b^{1/3} z^{4/3}$, where $C_U \approx 1.7$ (Kader and Yaglom, 1990; Zilitinkevich, 2006). In strongly unstable stratification $z > -L$ this reduces to $K_M \sim F_b^{1/3} z^{4/3}$ (which corresponds to the $z^{1/3}$ velocity profile used below in data analysis). Then the roughness-layer eddy viscosity scale becomes $K_{M0} \sim F_b^{1/3} h_0^{4/3}$, and (7.4) gives

$$z_{0u} \sim h_0 (-h_0/L)^{1/3}, \tag{7.8}$$

so that z_{0u} increases with increasing instability (as predicted in Coelho and Hunt, 1989; Zilitinkevich et al., 2006a,b).

A reasonable interpolation formula linking the neutral and the strongly unstable regimes is just the sum of the right hand sides of (7.5) and (7.8):

$$\frac{z_{0u}}{z_0} = 1 + C_{US} \left(\frac{h_0}{-L} \right)^{1/3}, \tag{7.9}$$

where C_{US} is one more empirical dimensionless coefficient.

The suggested theory is evaluated with data measured over very rough surfaces including vegetation and urban canopy (Table 7.1). For the stable stratification data

Table 7.1 The near-neutral estimation of aerodynamic roughness length and displacement height for Sodankylä and Basel-Sperrtrasse

		Present values		Literature values	
Site	$\lvert z_3/L\rvert$	z_{oo}(m)	d_{oo}(m)	z_{oo}(m)	d_{oo}(m)
Sodankylä	<0.125	1.1±0.3	9.8±3.2	0.8 (Zilitinkevich et al., 2001) 1.4 (Joffre et al., 2001)	–
Basel-Sperrtrasse 280°–360° wind sector.	<0.3	1.2±0.4	11.8±3.6	∼ 1.7 (Christen, 2005)	∼ 12 (Christen, 2005)

collected by the Finnish Meteorological Institute in an area typical of the sub-arctic Northern Finland with Scots pine forests are used. The Sodankylä Meteorological Observatory (67° 22′ N, 26° 38′ E, 180 m) is located in Finnish Lapland, 100 km north of the arctic polar circle (Gryning et al., 2001; Joffre et al., 2001). For the convective regime an urban canopy dataset collected in the Basel Urban Boundary Layer Experiment (BUBBLE) between summer 2001 and summer 2002, are used (Rotach et al., 2005). For this analysis, wind and average turbulence data from the main urban tower "Basel-Sperrstrasse" (32 m high) located in a heavily build-up area in the city centre.

Figure 7.2 compares (7.7) with data for stable stratification from the mean-profile and turbulence measurements [providing $U(z)$ and u_*] at a 48 m tower during July 2003–June 2004 over a boreal forest at the Sodankylä Observatory. To determine z_{0u} the log-linear velocity profile was employed (Monin and Obukhov, 1954):

$$U(z) = k^{-1}u_* \left[\ln\left(z/z_{0u}\right) + C_u z/L\right].$$

Using data from three levels (23, 25, 47 m) z_{0u} and C_u were determined for each profile. This analysis confirms (7.7) with confidence and allows determination of $C_{SS} = 8.13 \pm 0.21$ (a side product was a reasonable estimate of $C_u = 3 \pm 0.05$).

For unstable stratification, using data of a similar kind measurements at three levels (17.9, 22.4, 31.7 m) at the "Basel-Sperrstrasse" meteorological tower, To achieve a pronounced effect, only cases of strong convection ($-h_0/L > 0.5$) when U and Θ profiles in the entire surface layer followed the $-1/3$ power law are used (Fig. 7.3):

$$U(z) = 3C_U u_* \left[(-z_{0u}/L)^{-1/3} - (-z/L)^{-1/3}\right], \tag{7.10a}$$

$$\Theta(z_2) - \Theta(z_1) = 3C_\Theta(-F_\Theta/u_*)\left[(-z_1/L)^{-1/3} - (-z_2/L)^{-1/3}\right], \tag{7.10b}$$

where $C_U = 1.7$ and $C_\Theta = 1.1$ (Kader and Yaglom, 1990; Zilitinkevich, 2006a).

Resolving (7.10a) allows determining z_{0u} from measured U and u_*. Unfortunately z_{0u} appears in this algorithm in the combination z_{0u}/L. Because L is

relatively inaccurate, displaying z_{0u}/z_0 versus h_0/L would display strong artificial self-correlation (the uncertain term L, would explicitly appear in the abscissa and, implicitly, in the ordinate). To overcome this problem, in Fig. 7.3 we present z_{0u}/z_0 as dependent on a dimensionless stratification parameter (a kind of Richardson number): $\mathrm{Ri} = (g/\Theta_{32})(\Theta_{18}-\Theta_{32})h_0/U_{32}^2$, where the subscripts refer to the measurement heights. Our (7.8) in combination with (7.10) yields $\mathrm{Ri} \sim (h_0/L)^{14/9}$. Then (7.9) rewritten in terms of Ri becomes $z_{0u}/z_0 = 1 + C_*\mathrm{Ri}^{3/14}$. Data in Fig. 7.3 are consistent with this power law and give $C_* = 1.23 \pm 0.05$. Eventually, this allows the estimation of the constant in (7.9): $C_{US} = C_*^{7/6}\left\{3^{-1}C_\Theta C_U^2 (h_0/z_0)^{2/3}\left[(h_0/z_1)^{1/3} - (h_0/z_3)^{1/3}\right]\right\}^{1/4} = 1.24 \pm 0.05$.

In contrast to the traditional assumption of a constant roughness length fully characterized by the geometric properties of the surface, we have demonstrated its essential dependence on the hydrostatic stability. Figure 7.4 shows z_{0u}/z_0 versus h_0/L after (7.7) and (7.9) with our empirical constants ($C_{SS} = 8.13$, $C_{US} = 1.24$). It follows that z_{0u} monotonically decreases with increasing stability and, in the "meteorological interval" $-10 < h_0/L < 10$, varies over more than two orders of magnitude from 4 z_0 to $10^{-2}z_0$. Much stronger stability dependence under stable compared to unstable conditions, revealed in Fig. 7.3, corroborates previous empirical evidence (Arya, 1975; Joffre, 1982).

Recall that the currently used roughness length formulation neglects this dependence, resulting in strong, systematic overestimations of the surface resistance in stable stratification. The proposed model makes up for this drawback. It can be immediately implemented in urban and forest meteorology, largely to improve modelling of the most harmful air pollution episodes typical of very stable stratification in cities.

Furthermore, in the light of our results, it would be relevant to check whether the inherent scatter in empirical determinations of the so-called universal constants of turbulent flows in the past could be reduced once this roughness-stability dependence is taken into account. Besides meteorology the new roughness length model is applicable to oceanographic and engineering problems which deal with stratified flows.

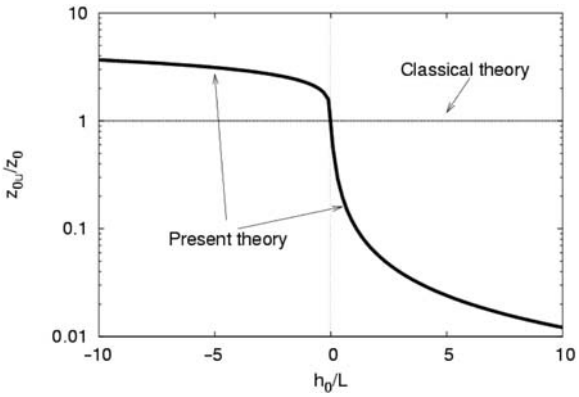

Fig. 7.4 Comparison of the new and traditional formulations of the roughness length: the solid line shows z_{0u}/z_0 versus h_0/L in the "meteorological interval" $-10 < h_0/L < 10$ after our Eqs. (7.7) and (7.9) with the empirical coefficients: $C_{SS} = 8.13$ and $C_{US} = 1.24$. The dashed line show the classical formulation: $z_{0u}/z_0 = 1$

Acknowledgments This work has been supported by EU Marie Curie Chair Project MEXC-CT-2003-509742, EU Project FUMAPEX EVK4-CT-2002-00097, ARO Project W911NF-05-1-0055, and EU Training Network Project WINDENG HPRN-CT-2002-00215.

References

Arya SPS (1975) Buoyancy effects in a horizontal flat-plate boundary layer. J. Fluid Mech. 68: 321–343.

Coelho SLV, Hunt JCR (1989) Vorticity dynamics of the near field of strong jets in cross flows. J. Fluid Mech. 200: 411–445.

Christen A (2005) Atmospheric turbulence and surface energy exchange in urban environments. PhD Dissertation, University of Basel.

Grachev AA, Fairall CW, Zilitinkevich SS (1997) Surface-layer scaling for the convection-induced stress regime. Bound. Layer Meteorol. 83: 423–439.

Gryning SE, Batchvarova E, De Bruin HAR (2001) Energy balance of a sparse coniferous high-latitude forest under winter conditions. Bound. Layer Meteorol. 99: 465–488.

Hasager CB, Nielsen NW, Boegh E, Jensen NO, Christensen JH, Dellwik E, Soegaard H (2003) Effective roughness calculated from satellite-derived land cover maps and hedge information and used in a weather forecasting model. Bound. Layer Meteorol. 109: 227–254.

Joffre SM (1982) Momentum and heat transfers in the surface layer over a frozen sea. Bound. Layer Meteorol. 24: 211–229.

Joffre SM, Kangas M, Heikinheimo M, Kitaigorodskii SA (2001) Variability of the stable and unstable atmospheric boundary-layer height and its scales over a boreal forest. Bound. Layer Meteorol. 99: 429–450.

Kader BA, Yaglom AM (1990) Mean fields and fluctuation moments in unstably stratified turbulent boundary layers. J. Fluid Mech. 212: 637–662.

Monin AS, Obukhov AM (1954) Basic laws of turbulence mixing in the surface layer of the atmosphere. Trudy Geofiz. Inst. AN SSSR 24 (151): 163–187.

Monin AS, Yaglom AM (1971) Statistical Fluid Mechanics, Vol. 1. MIT Press, Cambridge, Massachusetts, and London, England (Chapters 3 and 4).

Rotach MW, Vogt R, Bernhofer C, Batchvarova E, Christen A, Clappier A, Feddersen B, Gryning SE, Martucci G, Mayer H, Mitev V, Oke TR, Parlow E, Richner H, Roth M, Roulet YA, Ruffieux D, Salmond JA, Schatzmann M, Voogt JA (2005) BUBBLE – an Urban Boundary Layer Meteorology Project. Theor. Appl. Climatol. 81: 231–261.

Wood N, Mason P (1991) The Influence of static stability on the effective roughness lengths for momentum and heat transfer. Quart. J. Roy. Met. Soc. 117: 1025–1056.

Zilitinkevich SS, Esau IN (2007) Similarity theory and calculation of turbulent fluxes at the surface for the stably stratified atmospheric boundary layers. Bound. Layer Meteorol., 125: 193–206.

Zilitinkevich S, Perov VL, King JC (2001) Calculation Techniques of near-surface turbulent fluxes in stable stratification for numerical weather prediction models, Technical Report.

Zilitinkevich SS, Hunt JCR, Grachev AA, Esau IN, Lalas DP, Akylas E, Tombrou M, Fairall CW, Fernando HJS, Baklanov A, Joffre SM (2006a) The influence of large convective eddies on the surface layer turbulence. Quart. J. Roy. Met. Soc. 132: 1423–1456.

Zilitinkevich SS, Baklanov AA, Mammarella I, Joffre SM (2006b) The effect of stratification on the surface resistance for very rough vegetated and urban surfaces. In: 6th International Conference on Urban Climate, June 12–16, 2006, Goteborg, Sweden, ISBN-10:91-613-9000-1, pp. 415–418.

Chapter 8
FUMAPEX Experience of Model Urbanisation

Alexander Baklanov and FUMAPEX Team*

Abstract The increased resolution of numerical weather prediction models allows us to address more specifically, urban meteorology and air pollution processes and forecasts. This has triggered new interests in modelling the specific features and processes of urban areas. Recent developments and results performed within the EU-funded project FUMAPEX on integrated systems for forecasting urban meteorology and air pollution are reported. Several approaches, including the effective roughness and flux modifications, source and sink terms in the momentum, energy and turbulent kinetic energy equations due building effects, urban soil models, etc., are considered as applied to different meteorological models. Issues of optimum resolution, parameterisation of the urban roughness sublayer, surface exchange fluxes and the role of the urban soil layers are addressed with advanced meso- or submeso meteorological and numerical weather prediction models. Recommendations, especially with respect to advanced urban air quality forecasting and information systems are given, together with an assessment of the further research required.

8.1 Introduction

During the last decade, substantial progress in both meso-meteorological and numerical weather prediction (NWP) modelling and in the description of urban atmospheric processes, have been achieved. For instance, state-of-the-art nested NWP models have been developed which utilise land-use databases down to 1 km

A. Baklanov (✉)
Meteorological Institute, DMI, Copenhagen, Denmark
e-mail: alb@dmi.dk

*FUMAPEX Team: A. Clappier (EPFL), P. Mestayer (ECN), S. Zilinkevich (UH), S. Joffre (FMI), A. Mahura, C. Petersen (DMI), B. Fay (DWD), R. Hamdi (UCN), etc., see http://fumapex.dmi.dk

A. Baklanov et al. (eds.), *Meteorological and Air Quality Models for Urban Areas*,
DOI 10.1007/978-3-642-00298-4_8,

resolution or finer, enabling the provision of high quality urban meteorological data. Thus, NWP models are now approaching the necessary horizontal and vertical resolution to provide weather forecasts for the urban scale (e.g. Baklanov et al., 2002, 2008).

Many urban features can influence the atmospheric flow, its turbulence regime, the microclimate, and, accordingly modify the transport, dispersion, and deposition of atmospheric pollutants within urban areas, namely:

- Local-scale non-homogeneities, such as sharp changes of roughness and heat fluxes;
- Sheltering effects of buildings on wind;
- Redistribution of eddies, from large to small, due to buildings;
- Trapping of radiation in street canyons;
- Effects on urban soil structure;
- Differing diffusivities of heat and water vapour in the canopy layer;
- Anthropogenic heat fluxes;
- The so-called urban heat island;
- Urban internal boundary layers and the urban mixing height;
- Effects of pollutants (including aerosols) on urban meteorology and climate;
- Urban effects on clouds and precipitation.

Despite the increased resolution and various improvements, current operational NWP models still have several shortcomings with respect to urban areas including:

- Urban areas are mostly described by the same sub-surface, surface, and boundary layer formulations as rural areas.
- These formulations do not account for specific urban dynamics and energetics or for their impacts on the simulation of the atmospheric urban boundary layer (UBL) and its intrinsic characteristics (e.g. internal boundary layers, urban heat islands, precipitation patterns).
- NWP models have not been primarily developed for air pollution and emergency modelling and as such, their outputs need to be designed as suitable input for such urban-scale models.

Apart from Urban Air Quality Information and Forecasting Systems (UAQIFS) *per se*, improved urban meteorological forecasts will also provide information to city managers regarding additional hazardous urban climate features (e.g. urban runoff and flooding, ice and snow accumulation, high urban winds or gusts, heat or cold stress in growing cities and/or a warming climate). Moreover, the availability of reliable urban scale weather forecasts might be relevant in assisting the emergency management of fires, accidental toxic emissions, potential terrorist actions, etc.

8.2 Methodology for Urbanization of City-Scale Meteorological Models

8.2.1 FUMAPEX Strategy to Improve NWP and Meso-Scale Meteorological Models for Urban Areas

The FUMAPEX (FUMAPEX, 2005; Baklanov et al., 2005) strategy to improve NWP and meso-scale meteorological models includes the following aspects for the urbanisation of relevant submodels or processes:

(i) Model down-scaling, including increasing vertical and horizontal resolution and nesting techniques (one- and two-way nesting);
(ii) Modification of high-resolution urban land-use classifications, parameterizations and algorithms for roughness parameters in urban areas, based on the morphometric method;
(iii) Specific parameterization of the urban fluxes in meso-scale models;
(iv) Modelling/parameterization of meteorological fields in the urban sublayer;
(v) Calculation of the urban mixing height based on prognostic approaches.

The following meso-meteorological and NWP models were used for urban conditions or for different variants of the "urbanisation" scheme (user/developer teams are in brackets, cf. www.fumapex.dmi.dk): 1. DMI-HIRLAM (DMI); 2. Local Model LM (DWD, MeteoSwiss, EPA Emilia-Romagna); 3. MM5 (CORIA, met.no, UH); 4. RAMS (CEAM, Arianet); 5. Topographic Vorticity-Mode (TVM) Mesoscale Model (UCL); 6. Finite Volume Model FVM (EPFL); 7. SUBMESO model (ECN).

8.2.2 Urban Fluxes and Sublayer Parameterisation

Two main approaches to simulate urban canopy effects are considered :

1. Modifying existing non-urban approaches (e.g., the Monin-Obukhov similarity theory,) for urban areas by finding appropriate values for the effective roughness lengths, displacement height, and heat fluxes (adding anthropogenic heat flux, heat storage capacity and albedo change). In this case, the lowest model level is close to the top of the urban canopy (displacement height), and a new analytical model is suggested for the urban roughness sublayer which is the critical region where pollutants are emitted and where people live (Zilitinkevich and Baklanov, 2004).
2. Alternatively, source and sink terms are added in the momentum, energy and turbulent kinetic energy equations to represent the effects of buildings. Different parameterizations (Masson, 2000; Martilli et al., 2002) have been developed to estimate the radiation balance (shading and trapping effect of the buildings), the

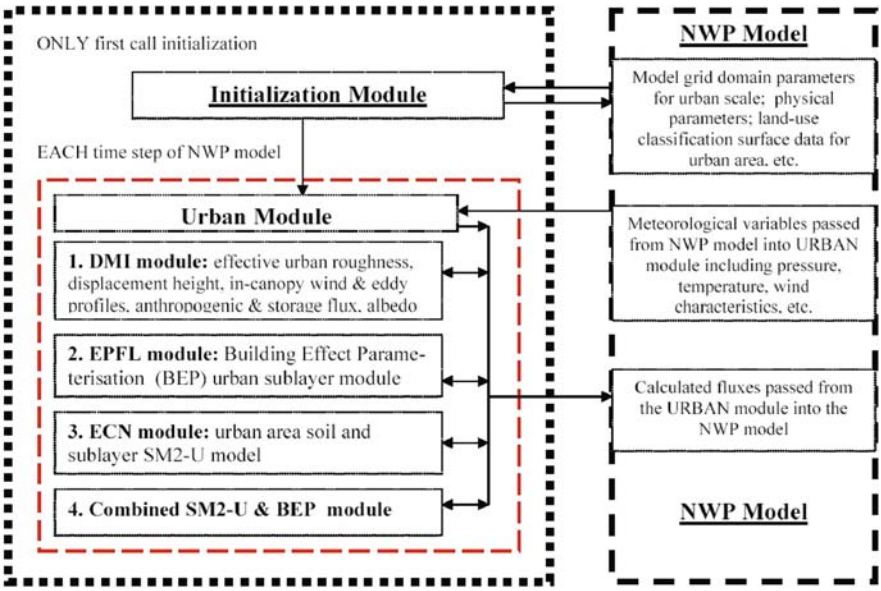

Fig. 8.1 General scheme of the FUMAPEX urban module for NWP models

heat, the momentum and the turbulent fluxes inside the urban canopy, considering a simple geometry of buildings and streets (3 surface types: roof, wall and road).

Several options for the integrated FUMAPEX urban module which can be used with NWP models have been suggested. In the first stage, four modules for model urbanisation (Fig. 8.1) were developed for further testing and for implementation in NWP models or their post-processors. It included the following modules:

1. DMI module: Based on the first approach, this includes a new diagnostic analytical parameterisation of the wind profile in the urban canopy layer (Zilitinkevich and Baklanov, 2004; Baklanov, 2008) and corrections to the surface roughness (with the incorporation of displacement height) for urban areas, and heat fluxes (adding anthropogenic heat fluxes, e.g., via heat/energy production/use in the city, heat storage capacity and albedo change) within existing physical parameterisations of the surface layer in NWP models, but with higher resolutions and improved land-use classification. This is applied in the city-scale version of the DMI-HIRLAM model.
2. EPFL module of the Building Effect Parameterisation (BEP): Based on the second approach and an improved urban surface exchange parameterisation submodel (Martilli et al., 2002; Hamdi, 2005). First this was tested in the research models FVM and TVM and then considered for inclusion in the DMI-HIRLAM and LM NWP models.

3. ECN module: Based on the detailed urban area soil and sublayer SM2-U model (Dupont and Mestayer, 2004; Dupont et al., 2004). First it was first tested with the large eddy simulation SUBMESO research model and then considered for incorporation into the DMI-HIRLAM NWP model.
4. Combined module: This includes all non-overlapping mechanisms from the SM2-U and BEP models. It was used in MM5 (Dupont et al., 2004) and applied to Paris by CORIA.

8.3 Results and Recommendations

8.3.1 Experience of Model Urbanisation

The range of improvement made by the FUMAPEX participants is summarized in Table 8.1. Many of the parameterisations were evaluated using data sets collected as part of the BUBBLE and ESCOMPTE projects. Implementation of the urban modules significantly improved the forecasted meteorological fields for urban areas. The first module, the cheapest way to "urbanise", can be easily implemented into operational NWP models as well as into Regional Climate Models. The second module, although more expensive (≈5–10% computational time increase), provides the possibility to consider the energy budget fluxes inside the urban canopy. However, this approach is sensitive to the vertical resolution of NWP models and is not very effective if the first model level is greater than 30 m. Therefore, an increase in the vertical resolution of current NWP models is required. The third module is considerably more expensive computationally than the first two. It provides the possibility to accurately study the urban soil and canopy energy exchange including the water budget. Consequently, the second and third modules are recommended for use in advanced urban-scale NWP and meso-meteorological research models. This will be demonstrated for NWP models in a forthcoming paper. The third module may be very useful for implementation into research submeso-scale or micrometeorological models (e.g., SUBMESO) for large eddy simulation or assessment (non-prognostic) studies. The first and second modules can be also used as urban interfaces or post-processors of NWP data for UAQ models.

Simulation results with these urban modules show that the radiation budget does not differ significantly for urban compared to rural surfaces, as the increased loss of a net longwave radiation is partly compensated by a gain in net shortwave radiation due to a lower albedo. The turbulent fluxes of sensible and latent heat, as well as their ratio, are variable and dependent in particular, on the amount of rainfall during the preceding period. The storage heat flux is usually significantly higher in urban areas compared to densely vegetated surfaces. This cannot be explained entirely by a higher thermal inertia, as this quantity is only slightly higher for urban than rural environments. Other factors of importance are the reduced moisture availability and the extremely low roughness length for heat fluxes. The anthropogenic heat flux, a typical urban energy flux, is absent in rural or natural areas.

Table 8.1 Overview of the improvements made by the FUMAPEX partners *(FUMAPEX, 2005)*

Models	Partner	Resolution	Urb. LUC	Roug. appr.	Urb. fluxes	BEP	SM2-U	UMH	Cities applied
Research:									
Sub-Meso	ECN	1 km	4(9)				+		Copenhagen, Marseilles
FVM	EPFL	1 km	1(un to 10)			+			Basel
TVM	ECL	1 km	1+ char.			+			Basel, Marseilles
MM5-SM2U	ECN, CORIA	3 km	1 uc + 4 sc	+		+	+		Paris
NWP:									
HIRLAM	DMI	1.4 km	1 + 4	+ (+USL)	+	+	+	+	Copenhagen, Malmø
Lokalmodell	DWD	1.1 km	1	+	+			+	Helsinki, Bologna, etc.
aLMo	EPFL/MetSwiss	7 km	1 + char.	+		+			Basel
MM5	UH	1 km	1	+	+				London
RAMS	CEAM	1.5 km	1(imp. LUC)						Valencia/Castellon
MM5+MIRLAM	Met. no	1 km	1	+				+	Oslo, Bergen, etc.
RAMS	ARIANET	1 km	1	+	+			+	Torino
LAMI	ARPA	1.1 km	1	+				+	Bologna

A sophisticated way to simulate the storage heat flux is using the BEP or SM2-U modules. One goal is to simplify the parameterisation of the storage heat flux in NWP model simulations for the main types of urban area and concentrations of urban elements. Use of these modules may provide the possibility to develop a simplified method for urban classes used in NWP models.

8.3.2 Further Improvements in NWP and UAQ Forecasting Systems

The next step should be the comparison of urban modules within the operational NWP models and their verification with respect to urban meteorological forecasts. It is also suggested to develop stand alone urban canopy models for uses as an interface or post processor module. These also need to be tested (module 2 has been successfully tested, FUMAPEX, 2005). These will be run with readily available NWP data as a first approximation and will improve meteorological fields of higher resolution that are near or within the urban canopy. This type of approach does not improve the meteorological forecast for the urban area and does not allow feedbacks. It does have the advantage that it does not require any modifications to an operational NWP model (which is usually very difficult and time consuming). This approach thus considers the urban sublayer models (together with several upper layers and surrounded areas) as interface modules between the NWP and UAQ models.

The current versions of the considered urban modules have several shortcomings which need to be further improved. For the first approach (module 1), the analytical model for wind velocity and diffusivity profiles inside the urban canopy (Zilitinkevich and Baklanov, 2004; Baklanov, 2008) has to be tested with different NWP models and meteorological pre-processors, and carefully evaluated using experimental data for different regimes. Additionally, it would be advisable to extend this for temperature and humidity profiles. The current version of the second module (BEP) does not consider the moisture and latent heat fluxes and does not completely incorporate the anthropogenic heat flux. Therefore, these should be included into a new version of the BEP module. Recalculation of accessible meteorological fields (e.g. wind prifiles) in the lowest sub-layers (not only on the NWP main vertical levels) is necessary. The third module (SM2-U) needs to consider the building drag effect (it will be realised in module 4), and snow and ice need to be included for NWP during winter periods, especially for high latitude areas. The existing version is computationally too expensive for operational NWP models, so it needs to be optimised to make calculations only for the urban cells.

Obviously these developments require more evaluation with appropriate data. Data availability, would also lead to addition development and initialisation improvements for NWP or meso-meteorological models simulations. This includes a need to conduct future urban field campaigns to provide data from which insights may be gained to help devise simpler models/parameterizations for complex models. The existing measurements have limitations which arise due to inescapable constraints on field programmes in cities.

References

Baklanov, A., 2008: Urban meteorological preprocessor for ARGOS. DMI Scientific Report 08-04. ISBN: 978-87-7478-569-9, ISSN: 1399–1949, 38 p.

Baklanov, A., A. Rasmussen, B. Fay, E. Berge, and S. Finardi, 2002: Potential and shortcomings of numerical weather prediction models in providing meteorological data for urban air pollution forecasting. *Water, Air and Soil Poll.: Focus*, 2, 43–60.

Baklanov, A., P.G. Mestayer, A. Clappier, S. Zilitinkevich, S. Joffre, A. Mahura, and N.W. Nielsen, 2008: Towards improving the simulation of meteorological fields in urban areas through updated/advanced surface fluxes description. *Atmos. Chem. Phys*., 8, 523–543.

Baklanov, A., S. Joffre, and S. Galmarini (Eds.), 2005: Urban Meteorology and Atmospheric Pollution (EMS-FUMAPEX). Special Issue of Atmospheric Chemistry & Physics Journal, 24, http://www.atmos-chem-phys.net/special_issue24.html

Dupont, S. and P.G. Mestayer, 2004: Evaluation of the urban soil model SM2-U on the city center of Marseille (France), *Fifth Symposium on the Urban Environment*, Vancouver, BC, Canada, AMS Proceeding CD (9.14).

Dupont, S., T.L. Otte, and S. Ching, 2004: Simulation of Meteorological Fields within and above Urban and Rural Canopies with a Mesoscale Model (MM5), *Boundary-Layer Meteorol*. 113, 111–158.

FUMAPEX, 2005: *EU project FUMAPEX: Integrated Systems for Forecasting Urban Meteorology, Air Pollution and Population Exposure*. Final project and WP4 Reports, available from web-site: http://fumapex.dmi.dk

Hamdi, R., 2005: On the study of the atmospheric boundary layer over urban areas with the urbanized version of TVM. Université catolique de Louvain, Belgium. PhD dissertation.

Martilli, A., A. Clappier, and M.W. Rotach, 2002: An urban surface exchange parameterisation for mesoscale models. *Boundary-Layer Meteorol*., 104, 261–304.

Masson, V., 2000: A physically-based scheme for the urban energy budget in atmospheric models, *Boundary-Layer Meteorol.*, 98, 357–397.

Zilitinkevich, S., A. Baklanov, 2004: An analytical model of the mean-wind and the momentum flux profiles in the urban roughness layer. *Ch. 3 in DMI Scientific Report* #04-08, ISBN: 87-7478-510-9, pp. 42–46.

Chapter 9
Evolution of Urban Surface Exchange in the UK Met Office's Unified Model

Peter Clark, Martin Best, and Aurore Porson

Abstract The UK Met Office model the Unifed Model (UM) has undergone a series of refinement to introduce urban characteristics in the surface scheme over the last decade. As these have been used operationally the philosophy is to retain simplicity and computational cheapness while capturing as much as possible the behaviour of urban areas in modifying surface fluxes. The different steps that have been taken and their performance are outlined.

9.1 Basic Approach

The resolution of practical numerical weather prediction (NWP) models has increased substantially in recent years, especially in regional models. As recently as 1998, the Met Office's Unified Model (UM) included no treatment of urban areas in its 3D operational configurations, beyond an artificial inclusion of enhanced roughness over London in the 12 km resolution version. This was justified because the true resolution of numerical models is several grid boxes (typically 5), so few, if any, cities are resolved. However, models with grid lengths of only a few km (or finer) are becoming available, necessitating the treatment of urban fluxes.

The current UM surface exchange scheme is designed for NWP use, and hence, to determine the effect of urban areas on the atmosphere (and so on the evolution of flow), and not vice versa. The implication of this is that the details of the urban canopy are regarded as unimportant and only the surface-layer fluxes are computed. In doing so, we assume that a surface layer exists and that standard Monin-Obukhov Similarity Theory (MOST) applies. This obviously has limitations. At present, the finest resolution used in the UM is typically $\approx$1 km, though higher resolution has been used for research purposes.

P. Clark (✉)
Met Office, Joint Centre for Mesoscale Meteorology, JCMM, UK
e-mail: peter.clark@metoffice.gov.uk

A. Baklanov et al. (eds.), *Meteorological and Air Quality Models for Urban Areas*,
DOI 10.1007/978-3-642-00298-4_9,

It is recognised that, in principle, at least, a diagnostic approach to deriving profiles etc. in the canopy layer is needed for practical outputs such as temperatures at street level and winds in the canopy. A certain amount of modification to raw profiles is used when UM output is the input for the off-line Nuclear Accident ModEl (NAME) transport and dispersion model, but further work is needed to improve the internal representation of the canopy.

9.2 Heterogeneity

The UM surface exchange scheme (MOSES II; Essery et al. 2001, 2003) uses a tiled approach to surface heterogeneity. This assumes independent, 1D vertical fluxes from different surfaces. The approach, based upon the concept of a blending height for fluxes (Mason, 1988), is based upon the mathematical approach of matched asymptotic expansions though more simple, heuristic arguments also exist.

We assume that, very close to a locally homogeneous surface 'patch', fluxes are in equilibrium with the local surface. However, sufficiently far away from the surface, fluxes are in equilibrium with a uniform, effective surface representing the aggregated effect of the whole surface. This approach, formulated for a given characteristic length-scale of heterogeneity, in this case a height (scale) exists below which local equilibrium and above which aggregated equilibrium may be assumed. This is the blending height. Since different surface patches may have different stabilities, in principle the blending height is stability dependent, and should be derived iteratively (the blending height depends on the overall stability and vice versa). An iterative solution has been implemented. However, in practice provided the first model layer is within the surface layer, use of the first model level works equally well. Under extremely stable conditions, the approach probably has some difficulties. Note the blending height differs from the diffusion height (the height at which all horizontal heterogeneity has dissipated). This is roughly an order of magnitude higher than the blending height.

In practice, the blending height approach cannot be applied to very small-scale heterogeneities because it is to close to the surface. Mason (1988) gives a rule of thumb of L/200 as a rough estimate of blending height, where L is the length scale of heterogeneity. This implies patches of different surfaces are at least, 100–200 m across. In an urban area this may stretch the concept. It may be reasonable for parkland but not necessarily for urban gardens etc. The assumption is that the patches are sufficiently large that the error incurred by ignoring the transition region from one patch to the other is negligible. An essential assumption is that tiles act independently (it does not matter how they are distributed in a grid mesh) and that local homogeneity can be assumed so that MOST can be used to compute exchange coefficients. However, see the Sect. 9.3 on the 2-tile approach.

The current scheme uses nine tiles of which one is urban. The characteristics of the urban tile can vary from point to point in principle, though in practice, at coarse resolution, fixed urban characteristics tend to be used. The urban tile fraction has been determined from IGBP (AVHRR-based) land-use (Brown et al., 2003), which

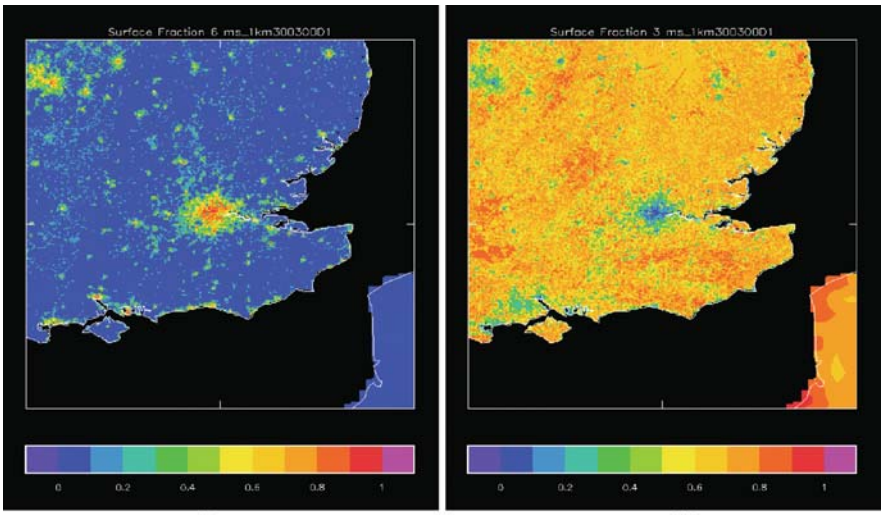

Fig. 9.1 Land-use fraction at 1 km resolution over SE England (centred on London) derived from CEH data **(a)** urban **(b)** C3 grass (i.e. grass and crops) (See also Colour Plate 12 on page 176)

provides single category data at ≈1 km resolution except over Great Britain, where CEH (Landsat-based) data are used (http://www.ceh.ac.uk/). The latter has 25 m resolution with two urban categories (urban and dense urban). Figure 9.1 shows an example from a 1 km configuration of the UM.

9.3 The Urban Tile, Thermal Canopy, Roughness Lengths for Heat and Anthropogenic Heat Flux

The urban tile was originally implemented simply through modification of tile properties such as albedo, roughness, drainage, canopy capacity, etc. This might be termed the 'rough concrete' approach, in that no explicit account is taken of the morphology of urban areas. This approach to urbanization has been taken in a number of models historically, as it requires no structural change to the model, only parameter changes. The approach has positive impacts, in that reduced wind speeds and enhanced surface fluxes with enhanced turbulence being reproduced, but the approach still leads to significant errors in the thermal response to the diurnal cycle, especially in the evening transition period. This is, in part, due to difficulties in reproducing the thermal behaviour of the surface. The UM has a further issue because, while the surface is tiled, the sub-surface ('soil') is not (yet). Even if a 'concrete soil' worked well, this could not be combined with the vegetation tiles within the same grid box.

Some of these problems have been overcome by including a 'thermal canopy' in the surface energy balance (SEB) (Best, 2005) which mimics, in a very simple way,

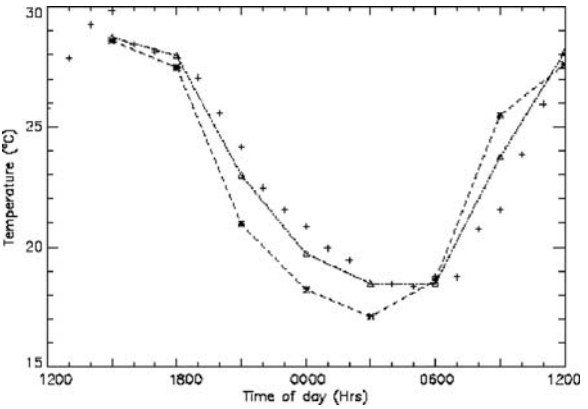

Fig. 9.2 Screen-level temperature for London from 12 UTC on 30 July to 12 UTC on 31 July 1999. Crosses: synoptic observations for the London Weather Centre; dashed line: traditional soil scheme for representing urban areas; and dashed dot line: canopy scheme for representing urban areas (Fig. 9 from Best, 2005)

the impact of phase lags introduced by storage within building materials. In essence, the traditional surface energy balance is split. The SEB drives the change of temperature of a homogeneous block, intended to represent the thermal inertia of building materials. This block is then radiatively coupled to the soil surface. This is a small change structurally but has a significant beneficial impact Figure 9.2 (Fig. 9 from

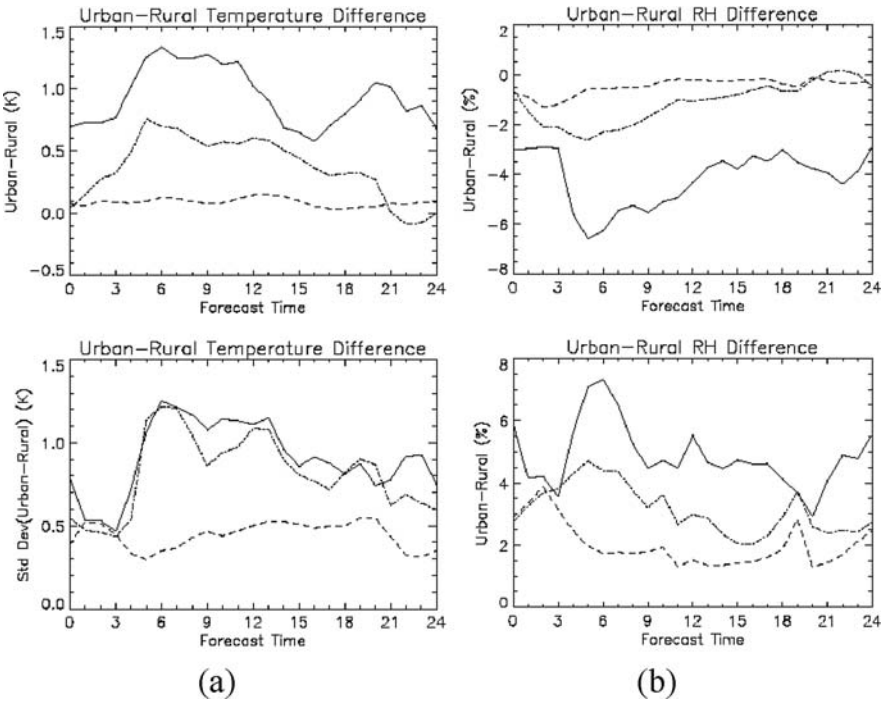

Fig. 9.3 Mean and standard deviation of **(a)** temperature and **(b)** relative humidity difference between Heathrow (largely urban) and Beaufort Park (largely rural). Observed (*solid*), Mesoscale model (*dashed*), SSFM (*dot-dashed*) over all 12 UTC forecasts from November and December 1997 and January 1998

Best, 2005) shows the improvement in nocturnal temperature forecast for a typical radiation night. A significant improvement was produced even in the operational forecast model (12 km) for urban areas, though errors in the diurnal cycle response were still evident. The approach has some similarities with the force-restore method of treating building thermal properties.

The thermal canopy was first implemented operationally within the "Site Specific Forecast Model", a 1D form of the UM driven from the 12 km model (Clark, 1998). Figure 9.3 shows results from a 3 month autumn/winter trial comparing the forecasts for two sites about 20 km apart, one largely rural, the other largely urban. For reference, the then-operational 12 km model is also compared – this contained essentially no urbanization. The variability of the temperature difference is well reproduced, and the bias roughly halved. Some impact is also evident on relative humidity, but clearly not enough.

Figure 9.4 shows the forecast vs observed urban heat island. The intensity of the urban heat island is somewhat under-estimated using this approach (typically a factor of two) – this was also observed after implementation of the scheme in the 12 km forecast model. Some improvement has been achieved through the addition of an anthropogenic heat source to the recently-implemented 4 km forecast model.

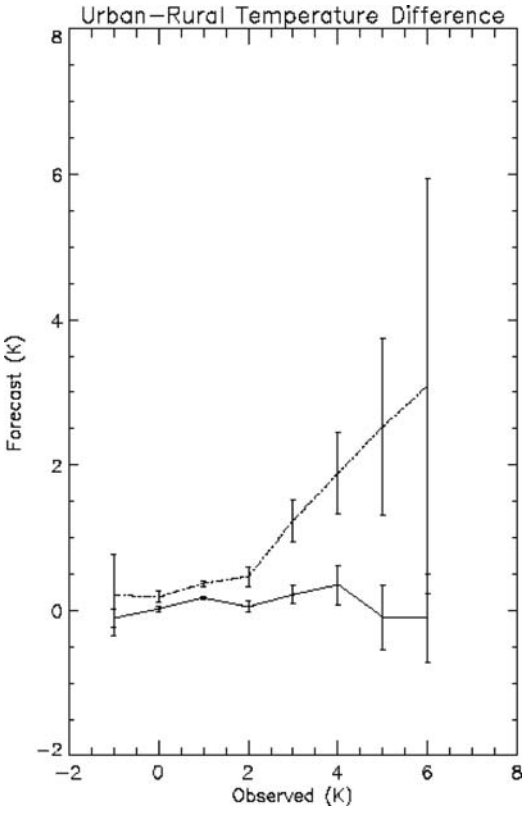

Fig. 9.4 Average forecast vs. observed temperature difference between Heathrow (largely urban) and Beaufort Park (largely rural). Mesoscale model (*solid*), SSFM (*dashed*) over all 06 UTC forecasts (T+7–T+24, i.e. 13 UTC-06UTC) from Nov–Dec 1997 and Jan 1998. Error bars denote two standard deviations from the mean

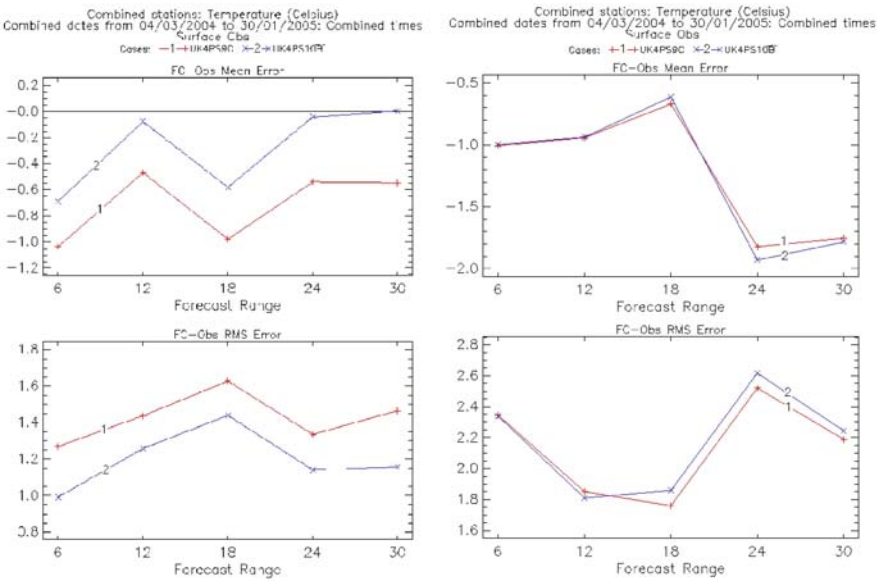

Fig. 9.5 Impact on forecasts of 'screen' temperature over 21 cases of including anthropogenic heat source in the operational 4 km UM **(a)** at a dense urban site (London Weather Centre) and **(b)** a very remote rural site. *line 1* is without, *line 2* with the heat source, *top* frames are bias, *bottom* RMS error

This source is deliberately conservative. It ignores the contribution of transport and is based on national energy use statistics, distributed uniformly over the urban land-use. Figure 9.5 shows the results from a trial over 21 representative cases of incorporating the anthropogenic heat source. A substantial improvement in bias and RMS error in screen temperature forecasts were produced at the few urban sites that are routinely monitored.

The system does a reasonable job of predicting UHIs, substantially better than the simple 'rough concrete' approach (Best et al., 2006). However, extensive testing against surface data from various cities has revealed limitations. The first is the specification of the roughness length for heat. Figure 9.6 (Fig. 3 from Best et al. 2006) shows the sensitivity to changes in z0t/z0m. This is usually set to 0.1 over vegetated terrain. The smaller value in urban areas arises because of the large contribution of bluff body pressure forces to the momentum flux. This contributes to the amplitude of turbulence but not to the surface scalar flux. This arises naturally out of more fundamental approaches based on canopies or canyons, but has to be specified in the simpler approaches adopted here. It is evident from Fig. 9.6 (and other results in Best et al., 2006) that, while the model can be adjusted to give sensible magnitudes of the terms in the SEB, it is difficult to produce good phase behaviour, especially for the sensible heat flux around dusk and (to a lesser extent) dawn.

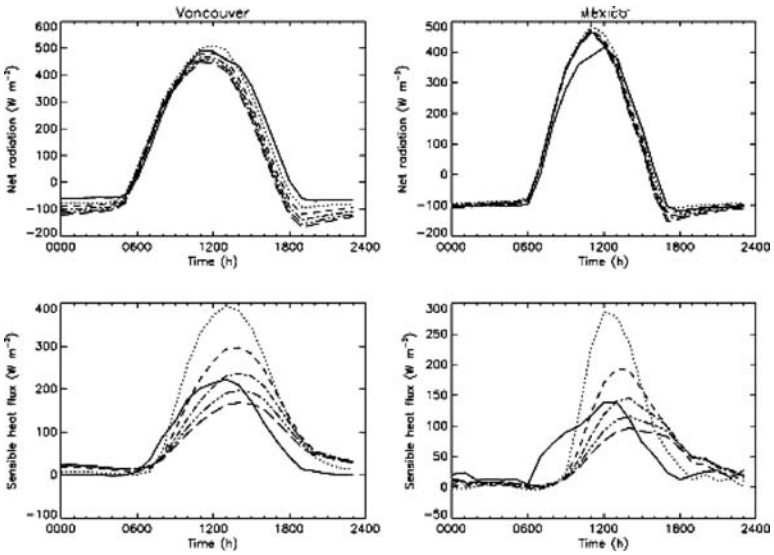

Fig. 9.6 Sensitivity test to changes in roughness length for heat (m). *Solid line*: observed ux, *dotted line*: $z_{0t}/z_{0m} = 10^{-1}$, *short dashed line*: $z_{0t}/z_{0m} = 10^{-3}$, *dashed dot line*: $z_{0t}/z_{0m} = 10^{-5}$, *dashed treble dot line*: $z_{0t}/z_{0m} = 10^{-7}$, *long dashed line* $z_{0t}/z_{0m} = 10^{-9}$ (Fig. 3 from Best et al., 2006)

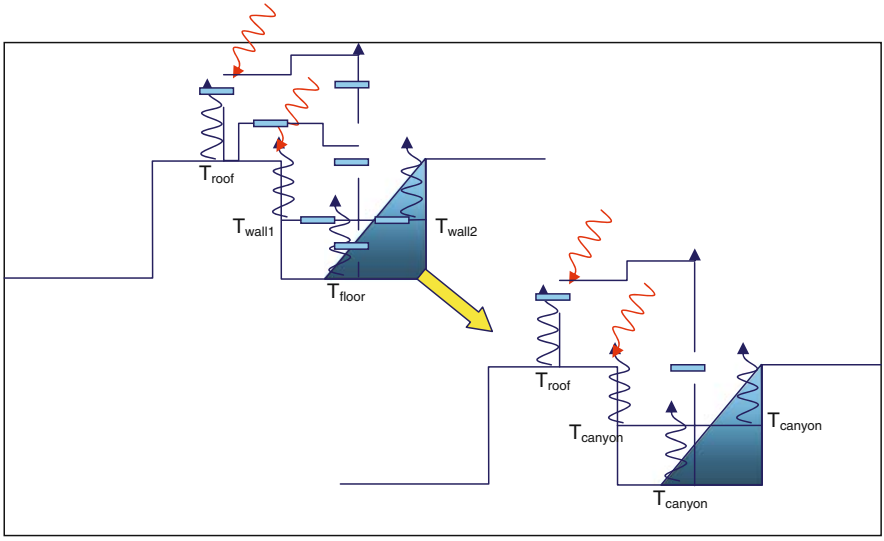

Fig. 9.7 Simplification of a four-facet canyon model to a two-tile (roof and canyon) model

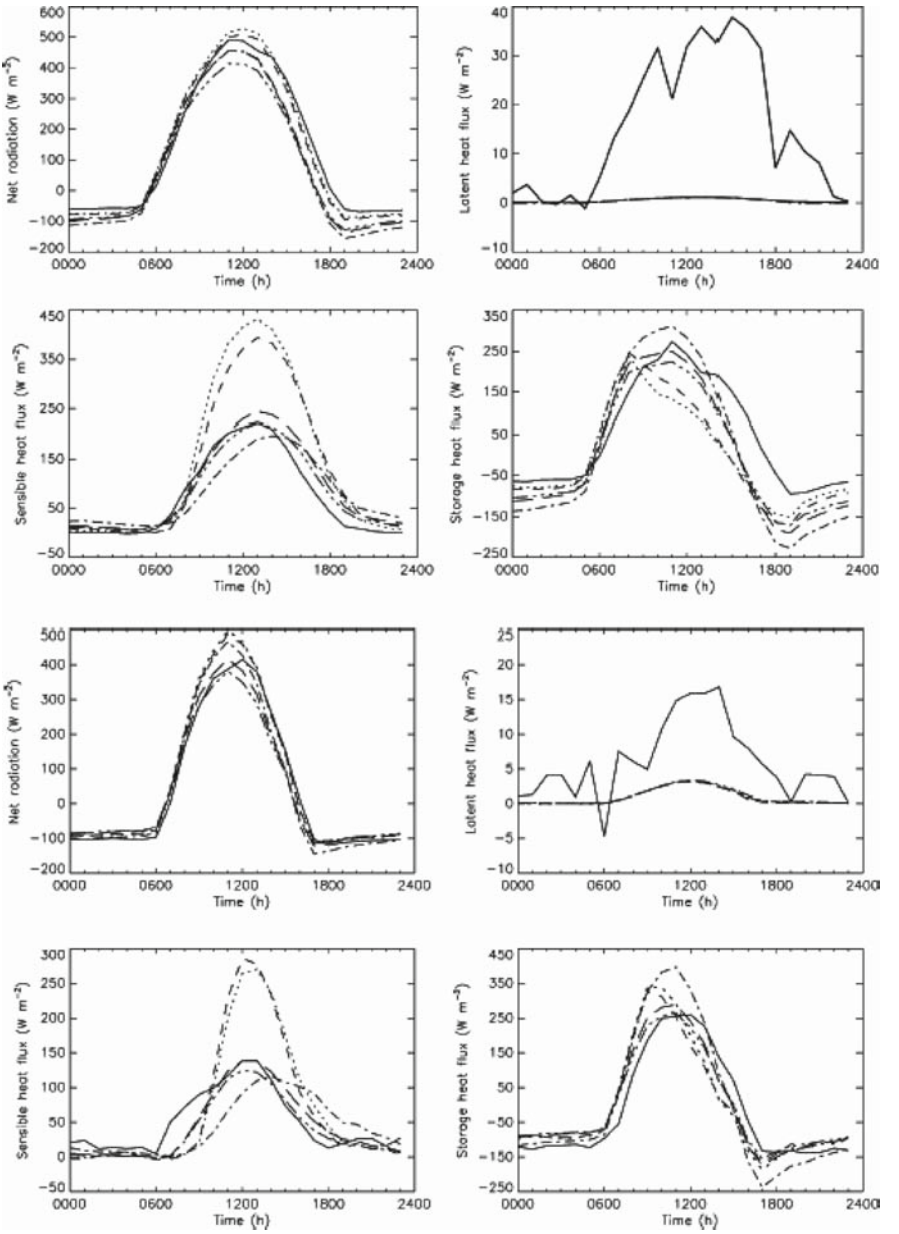

Fig. 9.8 Summary of model results. *Solid line*: observed ux; *dotted line*: default model parameters; *short dashed line*: observed values for model parameters; *dashed dot line*: $z_{0t}/z_{0m} = 10^{-7}$; *dashed treble dot line*: roof and canyon tiles with default albedos; *long dashed line*: roof and canyon tiles with albedos depending on urban geometry. **(a)** Vancouver; **(b)** Mexico City (Fig. 8 from Best et al., 2006)

9.4 The Two-Tile Approach

The 'rough-concrete' approach, with or without canopy, does not properly account for the fact that different parts of the building environment have different SEBs due to different radiation balance, turbulent exchange, materials, etc. Use of a single surface temperature brings problems. A detailed, multi-faceted approach of Masson (2000) addresses this problem. Harman (2003) developed a similar scheme for a 2D street canyon system, which included models of the scalar exchange coefficients with each facet which agreed well with observations (Barlow and Belcher, 2002), and also demonstrated two important simplifications. More information on the radition and heat exchange within the canyon can be found in Harman et al. (2004b) respectively.

The first simplification is that, to a very good approximation, the walls and floor of the canyon can be assumed to have the same temperature. This means that the canyon can be treated as one surface with very reasonable results. While the accuracy of the assumption may depend somewhat on the material properties of the walls and floor, it arises primarily because of the strong coupling between walls and floor (via radiation and turbulence) and the impact of sky-view factor when compared with the roof tile. Secondly, the measurements of exchange coefficients with the various facets show that the roof and canyon are not directly coupled.[1] This means that the assumption of independent surfaces associated with the tile scheme, is valid in spite of their proximity (though the same effective roughness for momentum must apply to each when coupled to the surface layer). The two approximations together leaded to a 'two-tile' approach, where the tiles are being the roof and canyon (Fig. 9.7).

A simple version of this was evaluated against surface flux data from various cities (see Fig. 9.8). This implemented a basic two-tile approach and a simple (albeit sufficient) treatment of effective albedo, but not the treatment of exchange coefficients and effective albedo and emissivity developed by Harman (2003). A more complete implementation is now underway in the UM but has yet to be fully evaluated.

9.5 Summary

In summary, there has been a steady refinement of the 'urbanization' of the UM over the last decade. The philosophy is to retain simplicity and hence computational cheapness while capturing as much as possible the behaviour of urban areas in modifying surface fluxes. The two-tile approach represents a scientifically sound simplification of more complex, multi-facet approaches, and appears to be an appropriate level of sophistication for computing fluxes at the mesoscale. It does not, however, directly produce useful within-canopy profiles, and is also likely to break down (like

[1] Work in progress.

any effective roughness approach) in areas with a wide variety of buildings. It is not yet clear how in-canopy vegetation should best be treated.

References

Barlow, J.F., Belcher, S.E., 2002, A wind tunnel model for quantifying fluxes in the urban boundary layer, *Boundary-Layer Meteorol.*, **104**, 131–150.

Best, M.J., 2005, Representing urban areas within operational numerical weather prediction models, *Boundary-Layer Meteorol.*, **114**, 91–109.

Best, M.J., Grimmond, C.S.B., Villani, M.G., 2006, Evaluation of the urban tile in MOSES with flux data, *Boundary Layer Meteorol.,* 118, 503–525, DOI: 10.1007/s10546-005-9025-5.

Brown, J., Loveland, T., Ohlen, D., Zhu, Z., 2003, LBA Regional Land Cover from AVHRR, 1-km, Version 1.2 (IGBP). Available on-line [http://www.daac.ornl.gov] from Oak Ridge National Laboratory Distributed Active Archive Center, Oak Ridge, Tennessee, USA.

Clark, P.A., 1998, The Implementation And Performance Of A 1D Model Coupled To NWP Forcing for Low-Cost Site-Specific Forecasting. AMS 2nd Urban Symposium, Albuquerque, NM, Nov 1998.

Essery, R., Best, M., Cox, P., 2001, MOSES 2.2 Technical Documentation, Hadley Centre Technical Report No. 30, Met Office Hadley Centre.

Essery, R.L.H., Best, M.J., Betts, R.A., Cox, P.M., 2003, Explicit Representation of Subgrid Heterogeneity in a GCM Land Surface Scheme, *J. Hydrometeorol.*, **4**, 530–543.

Harman, I.N., 2003, The energy balance of urban areas, Reading University PhD thesis.

Harman, I.N., Best, M.J., Belcher, S.E., 2004a, Radiative exchange in an urban street canyon, *Boundary-Layer Meteorol.*, **110**, 301–316.

Harman, I.N., Barlow, J.F., Belcher, S.E., 2004b, Scalar fluxes from urban street canyons, Part II: Model. *Boundary-Layer Meteorol.*, **113**, 387–410.

Mason, P.J., 1988, The formation of areally-averaged roughness lengths, *Q. J. R. Meteorol. Soc*., **114**, 399–420.

Masson, V., 2000, A physically-based scheme for the urban energy budget in atmospheric models. *Boundary-Layer Meteorol*., **94,** 357–397.

Chapter 10
Sensitivity Tests in the Dynamical and Thermal Part of the MRF-Urban PBL Scheme in the MM5 Model

Aggeliki Dandou and Maria Tombrou

Abstract In the present study, sensitivity tests were carried out in the 'dynamical' and 'thermal' part of a meteorological model in urban environment. The numerical simulations were performed by the PSU/NCAR Mesoscale Model (MM5), by applying the non-local Medium-Range Forecast (MRF) Planetary Boundary Layer (PBL) parameterisation scheme, plus the MRF-urban scheme, whereby urban features are considered. An unrealistic run was also performed by the MRF scheme, where the city of Athens was replaced by dry cropland and pasture surface, as in the surrounding area. The model results were compared with sonic anemometer measurements of turbulence and routine meteorological data. Modifications in both the 'dynamical' and 'thermal' parts seem to play an important role and improve the model's results. In addition, a delay in the sea breeze front was found, and a reasonable frictional retard concerning its penetration, as well as an inland displacement of the heat island, as the air moved over the city of Athens.

10.1 Introduction

Urbanization leads to the replacement of natural surfaces with buildings and paved surfaces. This change in surface characteristics together with human activities in urban environments alters heat, moisture and momentum exchange processes in the atmospheric boundary layer (ABL) and distinguishes the urban climate from that of surrounding rural areas (Fan and Sailor, 2005). Land-surface parameterizations in nearly all advanced meteorological models are built around a prognostic energy budget equation for the earth's surface temperature and they may include a prognostic equation for soil moisture, as well (Seaman, 2000). The urban areas usually appear as bare soil with different classifications of surface characteristics

A. Dandou (✉)
Department of Environmental Physics and Meteorology, National and Kapodistrian University of Athens, Greece
e-mail: mtombrou@phys.uoa.gr

A. Baklanov et al. (eds.), *Meteorological and Air Quality Models for Urban Areas*,
DOI 10.1007/978-3-642-00298-4_10,

and physical parameters, such as roughness length, albedo etc., while neither the anthropogenic heat nor the heat storage are included.

Recently, several efforts have been made in order to improve the representation of urban surface characteristics in mesoscale models (Brown, 2000). Attempts have been made to improve either the 'dynamic' part (impact on the wind field and the turbulent kinetic energy) or the 'thermal' part (impact on the heat fluxes) (Martilli et al., 2002). In the present study, sensitivity tests were carried out in the 'dynamic' and 'thermal' parts of MRF-urban planetary boundary layer (PBL) scheme (Dandou et al., 2005) in the meteorological PSU/NCAR Mesoscale Model (MM5) (Grell et al., 1994). The impact of both modifications seems to be important and improves the model's results. An attempt is also made in order to examine the interaction of the sea-breeze front with the heavily urbanized city of Athens, in terms of the surface drag in combination with the urban heat island (Dandou, et al., 2009).

10.2 Methodology

The numerical simulations were performed by the MM5 model version V3-6-1 (Grell et al., 1994). In particular, the high resolution non-local MRF PBL parameterisation scheme (Hong and Pan, 1996) was applied based on the Troen and Mahrt's (1986) representation for counter-gradients and K-profiles in the well-mixed convective boundary layer. The sensitivity tests refer to the 'dynamical' and 'thermal' part of the MRF-urban PBL scheme (Dandou et al., 2005), a modified version of the MRF PBL scheme, whereby urban features are considered. In particular, with respect to the 'thermal' part, the urban surface energy balance was modified by taking into account the anthropogenic heat and the urban heat storage term to produce for urban/building mass effect, including hysteresis (the Objective Hysteresis Model, Grimmond et al., 1991). The surface stress and fluxes of heat and momentum were also modified in the 'dynamical' part, following recent advantages in ABL over rough surfaces under unstable conditions (Akylas et al., 2003; Akylas and Tombrou, 2005) and stable conditions (King et al., 2001). It should be mentioned that the whole process was supplemented by detailed information on land use cover, derived from satellite image analysis (spatial resolution 30 m). Moreover, in order to examine topographic influences on air motions in the city, an unrealistic 'no-city' run was also performed by the MRF PBL scheme, where the city of Athens was replaced by dry cropland and pasture surface, as in the surrounding area (Dandou, et al., 2009).

The numerical simulations were performed by applying two-way nesting. The coarse domain covers the extended area of Greece, with spatial resolution 6×6 km, and the second domain is centred on the Attiki Peninsula, with spatial resolution 2×2 km. The 25-category USGS land-use classification scheme was adopted to provide land-cover data for the model domains. The initial and lateral boundary conditions for the outermost domain were provided by the European Center for Medium range Weather Forecast (ECMWF) numerical weather prediction (NWP) model, together with Sea-Surface Temperature (SST) data. For the rest of the physics

options, the cloud radiation scheme (Dudhia, 1989) and the five-layer soil model (Dudhia, 1996) were applied, as well as the Grell cumulus scheme (Grell, 1993) in the outermost domain (no cumulus parameterization in the inner domain). The model results were compared with sonic anemometer measurements of turbulence and routine meteorological data.

10.3 Results and Discussion

For this study, the 14 September 1994, was selected from the MEDCAPHOT-TRACE experimental campaign (Ziomas, 1998). A large set of meteorological measurements (air temperature, wind speed and direction, heat and momentum fluxes, etc.) were available for this day, as well as tethered balloon soundings, up to a height of 600 m at the NOA and Marousi stations (Batchvarova and Gryning, 1998). The surface synoptic circulation of the simulated day over the greater Athens area was characterized by the ridge from an extended anticyclone centred over northern Africa, and the synoptic wind was weak from the northern sector. These conditions favoured the development of a local weak sea-breeze circulation, which was observed only up to the city centre. In Fig. 10.1, the studied area is presented and the position of three ground stations: NOA – a downtown station located on top of a hill (107 m above sea level, asl), Peiraias – an urban station at the harbour, and Marousi – a suburban station located 13 km inland inside a grove that is surrounded by buildings of different heights.

During the day, the increase in diffusion coefficients (Fig. 10.2b) and air temperature (Fig. 10.3), calculated by the modifications in the 'dynamical' part (MRF-dyn scheme) due to the modified profile functions, is compensated by the decrease, calculated by the modifications in the 'thermal' part (MRF-ther scheme), resulting in a total decrease. The calculated decrease by the MRF-ther scheme is mainly attributed to the heat storage flux which exceeds that of the anthropogenic heat flux and acts as a sink in the thermodynamical equation at the surface layer. It should be mentioned that the MRF-urban scheme includes the modifications of both parts, plus the increase in the roughness length.

A decrease in turbulence and fluxes during the day is calculated by both modifications (Fig. 10.4). In particular, the decrease in the sensible heat flux (Fig. 10.4a, b) is related mainly to the smaller temperature gradients near the surface, produced by the combined effect of the anthropogenic heat, the heat storage, and the shadowing effects of buildings. The decrease in the friction velocity (Fig. 10.4c, d) is mainly due to the modification in the convective velocity (Dandou et al., 2005) and the reduced wind speed, because of the increased roughness length. It should be mentioned that the increase in roughness length would lead to an increase in the friction velocity, but the acceleration of the diffusion due to the enhancement of the diffusion coefficients normalizes the temperature gradients. This process pushes back the establishment of a strong instability and brings possibly the fluxes back to lower levels. The improvement is more apparent at the NOA station, where most

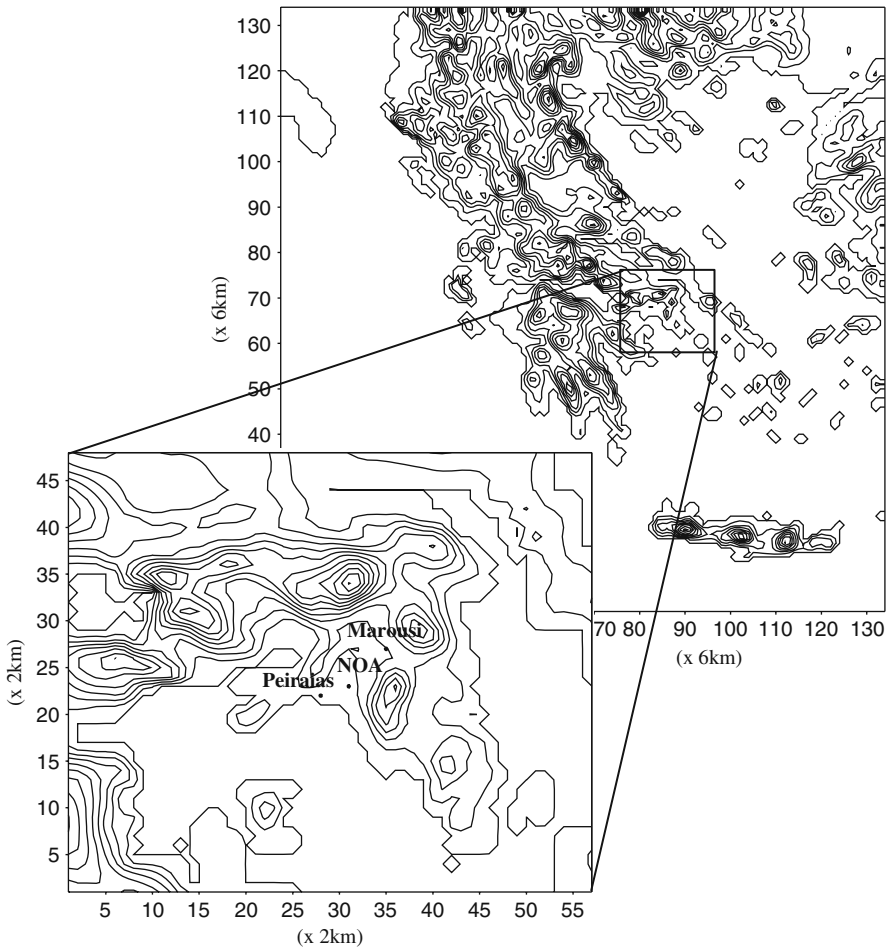

Fig. 10.1 Nested domain for modelling the Attiki peninsula and the position of three ground stations: NOA, Peiraias and Marousi. The spatial resolutions are 6 and 2 km and the topography contour lines are every 100-m interval for the Attiki peninsula and every 200-m interval for the extended area of Greece

of the area at this particular grid is characterised as urban (85%) in comparison to Marousi (52%). In addition, it should mentioned that the measurements should be regarded as indicative, since they depend closely on the station characteristics and are not representative of the whole 4 km^2 grid area.

Wind simulations were performed by the MRF-urban scheme on 15 September 1994, when the sea-breeze evolution was more intense compared to the previous day. During the day, a slowing in the sea-breeze front was found and a reasonable frictional retard concerning its penetration, as the air moved over the city of Athens, compared with both the MRF scheme (not presented) and the unrealistic 'no-city'

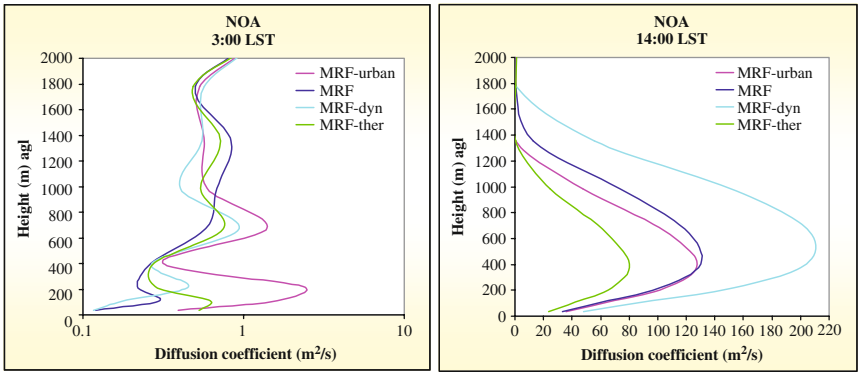

(a) (b)

Fig. 10.2 Diffusion coefficient profiles at (**a**) 03:00 of local standard time (LST) and (**b**) 14:00 LST on 14 September 1994 at the NOA stations, as calculated by the MRF, MRF-urban, -dyn and -ther schemes

MRF run (Fig. 10.5b) (Dandou, et al., 2009). The slowing is mainly attributed to the significant increase of the roughness length in the urban environment compared to the rural area. In addition, the developed urban-heat island was displaced inland 5–7 km (not presented).

During the night, the calculated total increase in temperature, diffusion coefficients, turbulence and fluxes (Figs. 10.2a, 10.3 and 10.4) is due to the increase calculated by both modifications in both parts. In particular, both the anthropogenic heat flux and the heat storage flux are released into the shallow mixing height of the atmosphere, producing temperature increase, proportional to the density of buildings and the human activity. Moreover, the modified diffusion coefficients, under stable con-

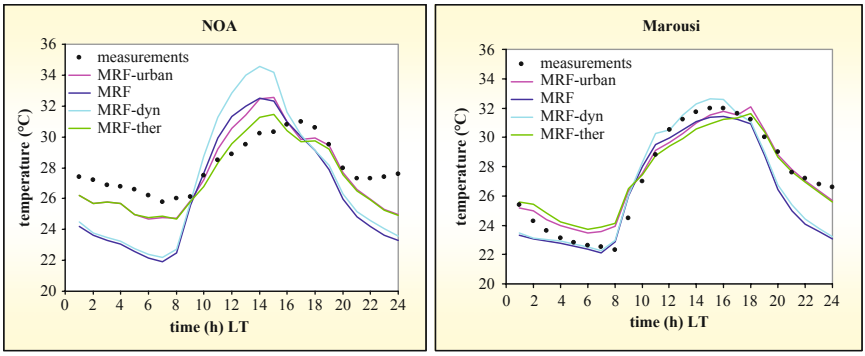

(a) (b)

Fig. 10.3 Time series (local diurnal cycle) of air temperature at 10 m agl on 14 September 1994, as calculated by the MRF, MRF-urban, -dyn and -ther schemes and measured (black circles) at the (**a**) NOA and (**b**) Marousi stations

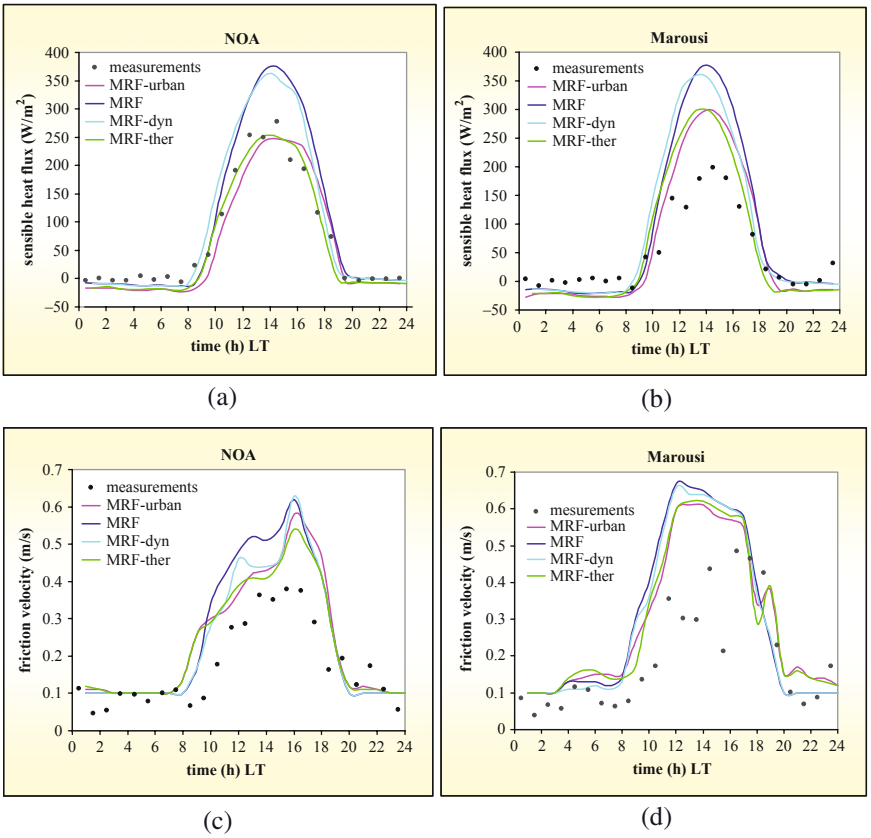

Fig. 10.4 Time series (local diurnal cycle) of sonic anemometer turbulence measurements of sensible heat flux (**a** and **b**) and friction velocity (**c** and **d**) at the NOA and Marousi sites, at 15 m agl, together with MRF, MRF-urban, -dyn and -ther modelling results on 14 September 1994

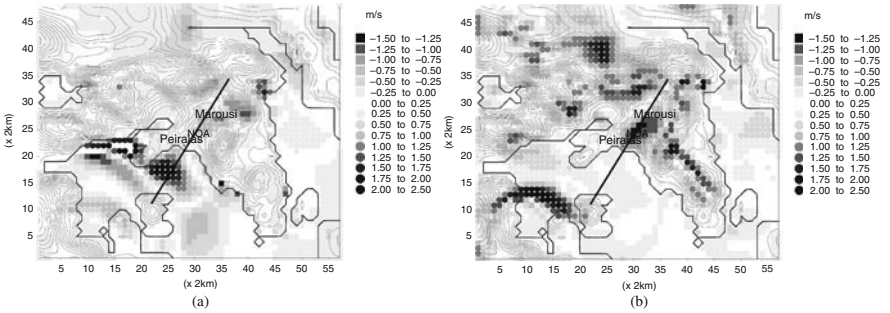

Fig. 10.5 The spatial distribution of horizontal wind speed differences in m s^{-1} (at 10 m agl) between the MRF-urban and 'no-city' run, at (**a**) 3:00 LST and (**b**) 14:00 LST on 15 September 1994

ditions (King et al., 2001), also lead to an increase in the diffusion processes at the surface layer (Fig. 10.2a). The increase in the wind speed values, calculated by the MRF-urban scheme in the lower atmosphere at the city centre, compared to the unrealistic no-city run (Fig. 10.5a), could be directly related to the influence of the urban heat island, which is more intense during the night and exceeds the expected frictional retard due to the increased roughness length.

10.4 Conclusions

Modifications, both in the 'dynamical' and 'thermal' parts, seem to play an important role and improve the model's results. In particular, the MRF-urban scheme calculated a decrease in the air temperature amplitude wave, and is in a better agreement with the measurements. During the day, the decrease in air temperature, diffusion coefficients and sensible heat flux is mainly attributed to the modifications in the 'thermal' part and, in particular, to the heat storage flux, plus the increase in the roughness length. The modifications in the 'dynamical' part are significant in the calculated decrease of the friction velocity.

The MRF-urban scheme calculated a slowing of the sea breeze front and a reasonable frictional retard concerning its penetration, during the day. This can mainly be attributed to the higher roughness of the urban canopy compared to the surrounding area. In addition, the developed urban-heat island was displaced inland. The unrealistic 'no-city' MRF run revealed the existence of other important mechanisms (e.g. sea-breeze) which coexist with urban influences, when an urban area is surrounded by complex topography.

During the night, the calculated total increase in air temperature, diffusion coefficients, turbulence and fluxes is due to the calculated increase by both 'dynamical' and 'thermal' parts. The anthropogenic heat flux and the heat storage flux are both released into the lower troposphere, producing a temperature increase which is enhanced by the increase in the diffusion processes at the surface layer due to the modified diffusion coefficients under stable conditions. The calculated increase in the wind speed, by the MRF-urban scheme, could be directly related to the influence of the urban heat island, which is more intense during the night.

Acknowledgments We are grateful to the COST Action 715 and 728 activities which actually inspired this study.

References

Akylas, E., Tsakos, Y., Tombrou, M. and Lalas D. P. 2003. Considerations on minimum friction velocity. Q. J. R. Meteorol. Soc., 129, 1929–1943.

Akylas, E. and Tombrou, M. 2005. Reconsidering and generalized interpolation between Kansas-type formulae and free convection forms. Boundary-Layer Meteorol., 115, 381–398.

Batchvarova, E. and Gryning, S.-E. 1998. Wind climatology, atmospheric turbulence and internal

boundary-layer development in Athens during the MEDCAPHOT-TRACE experiment. Atmos Environ. 32(12), 2055–2069.

Brown, M., 2000. Urban parameterizations for mesoscale meteorological models. In Mesoscale Atmospheric Dispersion, Adv, Air Pollut. Ser., vol. 9, edited by Z. Boybey, WIT Press, Boston, pp. 193–255.

Dandou, A., Tombrou, M., Akylas, E., Soulakellis, N. and Bossioli, E. 2005. Development and evaluation of an urban parameterization scheme in the Penn State/NCAR Mesoscale Model (MM5). J. Geophys. Res. 110, D10102, doi:10.1029/2004JD005192.

Dandou, A., Tombrou, M. and Soulakellis, N. 2009. The influence of the city of Athens on the evolution of the sea breeze front. Bound. Layer Meteorol., 131(1), 35–51, doi 10.1007/s10546-008-9306-x.

Dudhia, J., 1989. Numerical study of convection observed during the winter monsoon experiment using a mesoscale two-dimensional model. J. Atmos. Sci., 46, 3077–3107.

Dudhia, J., 1996. A multi-layer soil temperature model for MM5. Preprints, the 6th PSU/NCAR Meso-scale Model users, Workshop, Boulder CO, July, National Centre for Atmospheric Research, pp. 49–50.

Fan, H. and Sailor, D. J. 2005. Modeling the impacts of anthropogenic heating on the urban climate of Philadelphia: a comparison of implementations in two PBL schemes. Atmos. Environ. 39, 73–84, doi:10.1016/j.atmosenv.2004.09.031.

Grell, G. A. 1993. Prognostic evaluation of assumptions used by cumulus parameterizations. Mon. Wea. Rev. 121, 764–787.

Grell, G. A., Dudhia, J. and Stauffer, D. 1994. A description of the fifth-generation pess state/NCAR mesoscale model (MM5). NCAR technical note, NCAR/TN-398+STR, 138 pp.

Grimmond, C. S. B., Cleugh, H. A. and Oke, T. R. 1991. An objective urban heat storage model and its comparison with other schemes. Atmos. Environ., Part B, 25, 311–326.

Hong, S.-Y. and Pan, H.-L. 1996. Nonlocal Boundary-Layer vertical diffusion in a medium-range forecast model. Mon. Wea. Rev., 124, 2322–2339.

King, J. C., Connolley, W. M. and Derbyshire, S. H. 2001. Sensitivity of modeled Antarctic climate to surface and boundary-layer flux parameterizations. Q. J. R. Meteorol. Soc., 127, 779–794.

Martilli, A., Clappier, A. and Rotach, M. W. 2002. An urban surface exchange parameterization for mesoscale models. Boundary-Layer Meteorol., 194, 261–304.

Seaman, N. L. 2000. Meteorological modelling for air-quality assessments. Atmos. Environ., 34, 2231–2259.

Troen, I. and Mahrt, L. 1986. A simple model for the atmospheric Boundary-Layer: Sensitivity to surface evaporation. Boundary-Layer Meteorol., 37, 129–148.

Ziomas, I. C. 1998. The Mediterranean campaign of photochemical tracers-transport and chemical evolution (MED-CAPHOT-TRACE): An outline. Atmos. Environ., 32, 2045–2053.

Chapter 11
Urban Surface Energy Balance Models: Model Characteristics and Methodology for a Comparison Study

CSB Grimmond, Martin Best, Janet Barlow, A. J. Arnfield, J.-J. Baik, A. Baklanov, S. Belcher, M. Bruse, I. Calmet, F. Chen, P. Clark, A. Dandou, E. Erell, K. Fortuniak, R. Hamdi, M. Kanda, T. Kawai, H. Kondo, S. Krayenhoff, S. H. Lee, S.-B. Limor, A. Martilli, V. Masson, S. Miao, G. Mills, R. Moriwaki, K. Oleson, A. Porson, U. Sievers, M. Tombrou, J. Voogt, and T. Williamson

Abstract Many urban surface energy balance models now exist. These vary in complexity from simple schemes that represent the city as a concrete slab, to those which incorporate detailed representations of momentum and energy fluxes distributed within the atmospheric boundary layer. While many of these schemes have been evaluated against observations, with some models even compared with the same data sets, such evaluations have not been undertaken in a controlled manner to enable direct comparison. For other types of climate model, for instance the Project for Intercomparison of Land-Surface Parameterization Schemes (PILPS) experiments (Henderson-Sellers et al., 1993), such controlled comparisons have been shown to provide important insights into both the mechanics of the models and the physics of the real world. This paper describes the progress that has been made to date on a systematic and controlled comparison of urban surface schemes. The models to be considered, and their key attributes, are described, along with the methodology to be used for the evaluation.

11.1 Introduction

The world's population is becoming increasingly urbanised. The fraction of the global population living in cities now exceeds 50% and urban dwellers are expected to reach 6 billion people, or two-thirds of the global population, by the year 2050 (UN, 2004). On the same timescale, climate change predictions estimate an increase in global mean temperature of 0.5–1.5 °C (IPCC, 2001). Whilst predicting human induced climate change on a regional scale is still uncertain, one climate

CSB Grimmond (✉)
King's College London, London, UK
e-mail: Sue.Grimmond@kcl.ac.uk

A. Baklanov et al. (eds.), *Meteorological and Air Quality Models for Urban Areas*,
DOI 10.1007/978-3-642-00298-4_11,

phenomenon which is clearly attributable to human activity is the urban heat island (UHI). Urban areas often are several degrees warmer than the surrounding countryside, particularly at night under clear, calm conditions (Oke, 1973; Grimmond, 2007). Enhanced urban temperatures affect energy demand, air pollution concentrations and chemistry, water use, and human comfort, and have implications for human health and well being. The development of sustainable cities over the next century requires a clear understanding of how urban areas influence the local climate and increasingly, surface energy balance models are being used as tools in urban design and performance evaluation (e.g. Hacker et al., 2004). A consequence of warm surface temperatures is that air is more vigorously mixed upward, hence air pollution dispersion modelling benefits from better representation of the urban surface energy balance. Moreover, as atmospheric boundary layer motions (for heights less than 1–2 km) are very sensitive to the surface energy balance, an improved understanding of urban surface-atmosphere exchanges will better allow the impact of cities on regional scale weather systems to be determined (Taha, 1999; Bornstein and Lin, 2000).

The fundamental processes that need to be modelled are the surface-atmosphere exchanges of heat, mass and momentum at the local-scale. In cities these exchanges are altered by the materials and morphology of the urban environment, human behaviour, and the addition of anthropogenic heat flux (Q_F) to the available energy:

$$Q^* + Q_F = Q_H + Q_E + \Delta Q_S$$

where Q^* is net all wave radiation, Q_H is the turbulent sensible heat flux, Q_E is the turbulent latent heat flux and ΔQ_S is the net heat storage flux associated with heating/cooling of this mass (gas, liquids, and solids).

Recently there has been a rapid increase in the number of land-atmosphere exchange models that explicitly parameterize urban surfaces (see reviews of Brown, 2001; Best, 2006; Masson, 2006; Martilli, 2007; Lee and Park, 2008). These have been developed with the aim of predicting temperatures at different spatial scales, guiding more energy efficient design and construction, and improving air quality, meteorological and regional climate forecasting. The models differ significantly in the exchanges they explicitly consider and in the approach taken to modelling each flux. Applications and evaluations illustrate that the inclusion of even simple urban surface parameterizations leads to improved temperature predictions (e.g. Taha, 1999). However, while evaluations of individual models have been undertaken, there has been no systematic evaluation addressing questions such as:

- Do the models produce physically realistic simulations of urban heat exchange?
- How complex do parameterizations of heat exchange need to be to simulate physically realistic fluxes and temperatures?
- What are the costs (processing time, data requirements) versus the benefits (improvements in model prediction) between different types of models?

- And, in terms of observational studies, are we measuring the correct variables at the appropriate spatial and temporal scales to evaluate models?

Here we outline a methodology to undertake a comprehensive and controlled evaluation of a range of urban surface energy balance schemes using a staged methodology and carefully released evaluation data. The overall aim of the project is to gain insight into the strengths and weaknesses of different classes of urban models, with particular focus on the level of complexity (physical understanding, data requirements, spatial detail and temporal resolution) relevant for different applications. The purpose of this initial paper is two-fold: first, to describe the characteristics of the urban models to be compared; and second, to outline the methodology to be used in the overall study. Structured model evaluations such as this have inherent value in identifying deficiencies in a community's modelling capabilities (see for example, the outcomes of PILPS, Henderson-Sellers et al., 1993) and in supporting the design of field experiments to collect key data for model runs and evaluations.

11.2 Urban Surface Energy Balance Models

A wide range of approaches have been adopted to represent the surface energy balance in urban areas. Here we present a broad list of urban surface energy balance models (Table 11.1) for which each is given a code or acronym used hereafter to describe it. Where multiple versions of the models exist, they are differentiated.

11.2.1 Model Outputs

To be included in this comparison, a model must be able to predict the surface energy balance fluxes representative of the local (or neighbourhood) scale. Many of the models are also capable of calculating additional terms, typically air and surface temperatures and wind speed, and providing more detailed flux information, for example by facet, and these are recorded in Table 11.2. Notable differences between models relate to whether the canyon is assumed to have an orientation and thus, sunlit or shaded walls at appropriate times of the day (e.g. CLMU, CAT, SUNBEEM), or if the model is without orientation so that only one 'wall' is resolved and considered representative of the integrated urban domain (e.g. TEB). In the latter case, there are three distinct built facets: wall, roof, and road. Obviously, the issue of sunlit or shaded facets also relates to roads (the floor of the canyon). The most detailed models can calculate the spatial variability along facets (e.g. TUF3D). As an aside, it should be noted that there are other models (e.g. CFD models) that simulate within-canyon variations in more detail, although such micro-scale variations are not the focus of this work.

Table 11.1 Urban surface energy balance models. Acronyms, model names and publications with key details

CODE	Model name	Reference with details of model
BEP02*	Building Effect Parameterization	Martilli et al. (2002)
BEP05	Building Effect Parameterization	Hamdi (2005); Hamdi and Schayes (2007)
CAT*	Canyon Air Temperature	Erell and Williamson (2006)
CLMU*	Community Land Model – Urban	Oleson et al. (2008a, b)
ENVImet*	*Envi*ronmental Meteorology Model	Bruse and Fleer (1998)
GCTTC*	Green Cluster Thermal Time Constant model	Shashua-Bar and Hoffman (2002, 2004)
HIM	Heat Island Model	Saitoh et al. (1996)
HIRLAM-U*	Urbanised version of DMI-HIRLAM model	Baklanov et al. (2006, 2008); Mahura et al. (2006); Zilitinkevich et al. (2006)
LUMPS*	Local-scale Urban Meteorological Parameterization Scheme	Grimmond and Oke (2002); Offerle et al. (2003)
MM5u*	Penn State/NCAR Mesoscale Model model, where urban modifications have been incorporated	Dandou et al. (2005)
MOSES1T*	Met. Office Surface Exchange Scheme 1 Tile	Best (2005); Essery et al. (2003)
MOSES2T*	Met. Office Surface Exchange Scheme 2 Tile	Best et al. (2006); Essery et al. (2003)
MOUSES*	Met Office Urban Surface Exchange Scheme	Harman et al. (2004a, b)
MUCM*	Multi-layer Urban Canopy Model	Kondo et al. (2005); Kondo and Liu (1998)
MUKLIMO*	Microscale Urban Climate Model	Sievers (1995)
NSLUCM	Noah land surface model/Single-layer Urban Canopy Model	Kusaka et al. (2001); Chen et al. (2004)
PTEBU	Photovoltaic Town Energy Balance for an Urban Canopy	Tian et al. (2007)
R-AUSSSM	Revised Architecture-Urban-Soil-Simultaneous Simulation Model	Tanimoto et al. (2004)
RUM*	Reading Urban Model	Harman and Belcher (2006)
SEBM	Surface Energy Balance Model	Tso et al. (1991)
SHIM	Surface Heat Island Model	Johnson et al. (1991)
SLUCM	Simple Single-layer Urban Canopy Model	Kusaka et al. (2001)
SM2U*	Soil Model for Submesoscales, Urbanized Version	Dupont and Mestayer (2006); Dupont et al. (2006)
SUEB*	Slab Urban Energy Balance Model	Fortuniak et al. (2004, 2005)
SUMM*	Simple Urban Energy Balance Model for Meso-Scale Simulation	Kanda et al. (2005a, b)
SUNBEEM	Simple Urban Neighbourhood Boundary Energy Exchange Model	Arnfield (2000)
TEB*	Town Energy Balance	Masson (2000); Masson et al. (2002); Lemonsu et al. (2004)
TEB07*	Town Energy Balance 07	Hamdi and Masson (2008)
TUF2D*	Temperatures of Urban Facets in 2D	Krayenhoff and Voogt (2007)

Table 11.1 (continued)

CODE	Model name	Reference with details of model
TUF3D*	Temperature of Urban Facets in 3D	Krayenhoff and Voogt (2007)
UCLM*	Urban Canopy Layer Model	Mills (1997)
UCM	Urban Canyon Model	Sakakibara (1996)
UEB	Urban Energy Balance	Montávez et al. (2000)
UHSM	Urban Heat Storage Model	Bonacquisti et al. (2006)
VUCM*	Vegetated Urban Canopy Model	Lee and Park (2008)

*indicates confirmed participant in comparison project.

11.2.2 Representation of the Urban Environment

There are a number of different ways to model the urban surface to predict local scale energy balance fluxes. First, there is the issue of whether the surface consists of purely built surfaces or whether vegetation is also taken into account (Table 11.3). Generally, there are two different methods to incorporate vegetation: (1) it is treated as a separate surface (referred to here as 'tiles') that does not interact with other surface types until the first layer of the meso-scale model (e.g. TEB, MOSES); or (2) it is embedded into the urban area so that it affects, and is affected by, the built environment (e.g. CLMU, SUNBEEM, LUMPS) (referred to here as 'integrated'). Some models have both capabilities (Table 11.3). Vegetation is modelled using separate vegetation models that have been well tested, such as in the PILPS comparisons, in extensively vegetated areas (Yang and Dickinson, 1995; Shao and Henderson-Sellers, 1996; Qu et al., 1998; Schlosser et al., 2000; Henderson-Sellers et al., 2003; Irranejad et al., 2003) and resistance schemes that have been developed for urban areas (e.g. Arnfield, 2000; using Grimmond and Oke, 1991).

Second, is the issue of how the built environment is modelled. As indicated in Sect. 11.2.1, a wide range of variables is modelled (resulting in outputs). Alternatively models can be described in terms of their representation of the surface: either slab, single layer, or multi-layer (Table 11.4). *Slab models* (e.g. Best, 2005) represent the urban area in terms of a surface (e.g. concrete) with appropriate thermal characteristics. *Single layer models* represent a city as a layer of buildings with the overall surface heat exchange being the sum of exchanges on individual surfaces. This allows for more realistic representations of radiative trapping and turbulent exchange (Masson, 2000; Kusaka et al., 2001; Harman et al., 2004a). *Multi layer models* use a similar approach to single layer models, but model energy exchanges at multiple levels within the canopy, thereby allowing for varying building heights (e.g. BEP, TUF3D). Single and multi-layer models also differ in their spatial representation of the urban morphology, modelling one temperature and set of energy exchanges per facet versus multiple temperatures and energy exchanges per facet (the latter).

Table 11.2 Model outputs in addition to the local-scale fluxes. Net all-wave radiation (Q^* – W m^{-2}); Sensible heat flux (Q_H W m^{-2}); Latent heat flux (Q_E – W m^{-2}); Storage heat flux (ΔQ_S – W m^{-2}); Air temperature (T_a K/C), Surface temperature (T_s K/C), Wind speed (WS m s^{-1}). Ud indicates user dependent; typ. – typically; P – partial. See text for further explanation and Table 11.1 for key to model codes

		Canyon							Facet							Facet with orientation							
CODE	Time step	Q^*	Q_H	Q_E	Q_S	T_a	T_s	WS	Q^*	Q_H	Q_E	Q_S	T_a	T_s	WS	Q^*	Q_H	Q_E	Q_S	T_a	T_s	WS	
BEP02	Ud	Y	Y	N	Y	Y	Y	Y	Y	Y	N	Y	Y	Y	Y	Y	Y	N	Y	N	Y	N	
BEP05	Ud	Y	Y	N	Y	Y	Y	Y	Y	Y	N	Y	N	Y	N	N	N	N	N	N	N	N	
CAT	1 h	N	Y	Y	N	Y	N	N	Y	Y	Y	Y	N	Y	Y	Y	Y	Y	Y	N	Y	Y	
CLMU	1200–3600 s	Y	Y	Y	Y	Y	N	Y	Y	Y	Y	Y	N	Y	N	N	N	N	N	N	N	N	
ENVImet	typ. 2–10 s	Y	Y	Y	Y	Y	Y	Y	Y	Y	Y	Y	Y	Y	Y	Y	Y	Y	Y	Y	Y	Y	
GCTTC	24 h	Y	Y	Y	Y	Y	Y	N	Y	Y	Y	Y	N	Y	N	Y	Y	Y	Y	N	Y	N	
HIRLAM-U	Ud, typ. 300 s	N	N	N	N	N	N	Y	N	N	N	N	N	N	Y	N	N	N	N	N	N	N	
LUMPS	1 h	N	N	N	N	N	N	N	N	N	N	N	N	N	N	N	N	N	N	N	N	N	
MM5u	Ud	N	N	N	N	N	N	N	N	N	N	N	N	N	N	N	N	N	N	N	N	N	
MOSES1T	Ud	N	N	N	N	N	N	N	N	N	N	N	N	N	N	N	N	N	N	N	N	N	
MOSES2T	Ud	Y	Y	Y	Y	N	Y	N	N	N	N	N	N	N	N	N	N	N	N	N	N	N	
MUCM	10–120 s	Y	Y	Y	Y	Y	Y	Y	Y	Y	Y	Y	Y	Y	P	p	p	p	p	N	p	N	
MUKLIMO	Ud, typ. 3 h	N	N	N	N	Y	N	Y	N	N	N	N	N	N	N	N	N	N	N	N	N	N	
NSLUCM	Us (few minutes to 3600 s)	Y	Y	Y	Y	Y	Y	Y	Y	Y	Y	Y	N	Y	N	p	p	p	p	N	p	N	
SM2U	Ud, typ. 300 s	Y	Y	Y	Y	N	Y	N	N	N	N	N	N	N	N	N	N	N	N	N	N	N	
MOUSES	Ud	Y	Y	Y	Y	N	Y	Y	N	N	N	N	N	N	N	N	N	N	N	N	N	N	
SUEB	1 s	N	N	N	N	N	N	N	N	N	N	N	N	N	N	N	N	N	N	N	N	N	
SUMM	Ud	Y	Y	Y	Y	N	Y	N	Y	Y	Y	Y	N	Y	N	Y	Y	Y	Y	N	Y	N	
SUNBEEM	U d	Y	Y	Y	N	Y	Y	Y	Y	Y	Y	N	Y	Y	Y	Y	Y	Y	Y	N	Y	Y	
TEB	60–900 s, typ. 300 s	Y	Y	Y	Y	Y	N	Y	Y	Y	Y	Y	N	Y	N	N	N	N	N	N	N	N	
TEB07	Ud	Y	Y	Y	Y	Y	N	Y	Y	Y	Y	Y	N	Y	N	N	N	N	N	N	N	N	
TUF2D, TUF3D	Variable (typ. 10–100 s)	Y	Y	N	Y	Y	Y	Y	Y	Y	N	Y	Y	Y	Y	Y	Y	N	Y	Y	Y	Y	
UCLM	1 h	Y	Y	Y	Y	Y	Y	Y	Y	Y	Y	Y	Y	Y	Y	Y	Y	Y	Y	Y	Y	Y	
VUCM	Ud	Y	Y	Y	Y	Y	N	Y	Y	Y	Y	Y	N	Y	N	N	N	N	N	N	N	N	

Table 11.3 Approach to vegetation modelling. See text for further explanation and Table 11.1 for key to model codes

Approach	Model
Canopy layer at the ground, leaves in the atmosphere	MUKLIMO
Integrated	CAT, LUMPS, ENVImet, GCTTC, MUCM, SUES, SUNBEEM
Integrated (separately included)	VUCM
Integrated or separate tile	CLMU, SM2U
None	TUF2D, TUF3D, SUEB, UCLM
Separate tile	BEP02, BEP05, HIRLAM-U, NSLUCM, MM5u, MOSES1T, MOSES2T, MOUSES, TEB, TEB07, SUMM

Table 11.5 provides a summary of the features of the urban surface that are actually resolved by the models; for example, whether the canyon is a whole unit or if walls and roofs are separate facets. Also included is whether each of these elements has a specific orientation and whether they can be sunlit and shaded. Some models assume an infinitely long canyon with no orientation and therefore only one wall needs to be modelled (e.g. TEB); others have infinitely long canyons that run in two cardinal directions each with varying sunlit and shaded wall areas through the day (and at different times of year). To date, the intersection of such canyons has received less attention (except in SUNBEEM) although it will be included in some way when the site attributes are calculated and used in the model descriptions (see Sect. 11.2.4).

Table 11.4 Categorisation of models in terms of slab, single layer, or multiple layer. See text for further explanation and Table 11.1 for key to model codes

Slab	Single layer	Multiple layer
MOSES1T	AUSSSM	BEP02
MOSES2T	CAT	BEP05
SUEB	CLMU	ENVImet
SM2U	GCTTC	MUCM
	HIRLAM-U (+ analytical profile in canopy)	MUKLIMO (ground)
	LUMPS	R-AUSSSM
	MOUSES	SUEB
	MUKLIMO (walls, roof, canopy)	SUMM
	NSLUCM	SUNBEEM
	RUM	TEB07
	SLUCM	TUF2D, TUF3D
	SUES	UCLM
	SUNBEEM	
	TEB	
	VUCM	

Table 11.5 Levels modelled and features resolved in each model. Y – yes, N – no P – partial. See text for further explanation and Table 11.1 for key to model codes

	Levels			Features resolved							
							Walls			Road	
Model	Within canyon	Above canyon	Canyon top	Canyons	Turbulence within canyon	Roof	Walls	Sunlit/Shaded	Orientation	Road	Sunlit/Shaded
BEP02	Y	Y	Y	Y	Y	Y	Y	Y	Y	Y	Y
BEP05	Y	Y	Y	Y	Y	Y	Y	Y	Y	Y	N
CAT	Y	N	N	Y	N	N	Y	Y	Y		Y
CLMU	Y	N	N	N, C1	N	Y	Y	Y	N		N
ENVImet	Y	Y	Y	Y	Y	Y	Y	Y	Y	Y	Y
GCTTC	N	N	N	Y	Y	Y	Y	Y	Y		N
HIRLAM-U	P	Y	P	P	P, C2	P	N	N	N	P	N
LUMPS	N	Y	N	N	N	N	N	N	N	N	N
MM5u	N	N	N	N	N, C2	N	N	N	N		N
MOSES1T	N	N	N	N	N	N	N	N	N	N	N
MOSES2T	N	N	N	Y	N	Y	N	N	N		N
MOUSES	N	N	N	Y	Y	Y	N	N	N	N	N
MUCM	Y	Y	Y	Y	P	Y	Y	P	N	Y	P
MUKLIMO	Y	Y	Y	Y	N	Y	Y	N	N	Y	N
NSLUCM	Y	N	N	C1	N				Y		
SM2U	N	N	Y	P	N	Y	P	P	Y	P	P
SUEB	N	N	N	N	N	N	N	N	N	N	N
SUMM	N	Y	N	Y	N	Y			Y		
SUNBEEM	Y	P	Y	Y	N	Y	Y	Y	Y	Y	Y
TEB	Y	N	N	N	N	Y	Y	N	N	Y	N
TEB07	Y	Y	Y	Y	Y	Y	Y	N	N	Y	N
TUF2D, UF3D	Y	Y	Y	Y	N	Y	Y	Y	Y	Y	Y
UCLM	Y	N	Y	Y	Y				Y		
VUCM	Y	N	N	N	N				N		

C1 pervious and impervious canyon floor; C2 turbulence is resolved in the surface layer in total.

11.2.3 Model Inputs

Inputs consist of three general types: (1) the parameters to describe the site; (2) the variables required to drive the model; and (3) the initial conditions required to initiate the model runs. Obviously, the first set of information is needed in any type of model run, so there is no difference between a typical run and an offline model evaluation run. For the second set of data, for a normal online run, would be the meso- (or larger-) scale model with data 'passed down' to the surface scheme to force it. These data are therefore updated at each time step. The third set of input, initial conditions, are explicitly related to the surface scheme rather than to wider models of which these schemes may be a part. For some models and some variables these may be the same as (2) but for others there are additional requirements.

The complexity of urban areas demand a large number of model parameters; here they are sub-divided into two groups: the built environment (Table 11.6) and urban vegetation (Table 11.7). In terms of the morphometric characteristics of the built form, inputs vary greatly depending on whether basic information is used (e.g. height and width) from which the required parameters are calculated (e.g. canyon aspect ratio, sky view factor), or if 'higher' level parameters are inputs. This can give the impression that there are larger differences in the model inputs than there really are. Other parameters of the built environment relate to the nature of the materials used and include parameters that are concerned with radiative transfer (e.g. albedo, emissivity) and conductive characteristics. These characteristics may be specified in different ways relative to urban form; for example, relative to mass (specific heat capacity) or volume (volumetric heat capacity). Alternatively, materials may be specified and model 'look-up' tables used to assign the appropriate parameters. The details of the tiled-models that draw on vegetation schemes are not summarised in Table 11.7 because they are extensively evaluated (see Sect. 11.2.2). Typically, the vegetation characteristics are assigned by using a default number of classes (e.g. 11 in SM2U, 5 in MOSES).

Anthropogenic heat flux is dealt with in a wide variety of ways. For example, some schemes capture this flux by specifying fixed internal temperatures and traffic counts (Table 11.6), which provides temporal dynamics to the flux estimates. Other models require the flux to be provided as a direct input (e.g. GCTTC, CAT).

The variables that are used to drive the models are listed in Table 11.8 . These relate to wind, temperature, humidity, radiation, and soil characteristics and as noted above, some models also require the anthropogenic heat flux to be directly supplied as an input. From the nature of the inputs, it is evident that a wide variety of approaches is used, for example, to determine the radiative forcing. Some models calculate radiation, others take the short and long wave radiative fluxes as a direct input, while others add further detail by differentiating between direct and diffuse components (e.g. MUCM, CLMU, VUCM, CAT, SUNBEEM).

The final set of inputs relates to the initial conditions. The information required about temperature profiles within a building or the soil may be the most significant for some of the models. Such data are typically difficult to obtain. One consequence

Table 11.6 Parameters related to the 'built environment' (Y – yes; N – No). See text for further explanation and Table 11.1 for key to model codes

Model	λ_p	λ_f	ψ	F	A_w	A_O	z_r	$\mathbf{z_f}$	z_B	z_{or}	W_B	D_B	Fl_D	S L/W/ d/N	LAA	Traf	T_{intW}	T_{intR}	T_i	T_{DS}	Mat	HT	MT	ε_{fac}	α_{fac}	α	LL	τ	z_{ofac}
BEP02	N	N	N	N	N	N	N	N	Y	N	Y	Y	Y	Y	Y	N	N	N	Y	Y	N	K,Cp		Y	Y	N	Y	N	Y
BEP05	N	N	N	V	N	N	N	N	Y	N	Y	Y	Y	YL/d/N	N	N	N	N	Y	Y	Y	K, Cp	N	Y	Y	N	N	N	Y
CAT	N	N	Y	N	N	N	Y	Y	Y	N	N	N	N	N	Y	N	N	N	N	N	Y	N	N	Y	Y	Y	Y	N	N
CLMU	Y	N	N	RVRCp	N	N	Y	Y	Y	N	N	Y	N	N	N	Y,C5	N	N	Y	Y	N	C_R, K, VHC	Y	Y	Y	N	Y	N	N
HIRLAMU	Y	Y	N	RVRC	N	N	N	N	Y	Y	N	N	N	N	Y	N	N	N	N	Y	Y	C_R, K		N	N	Y	Y	N	N
ENVImet	N	N	Y	Y	N	N	N	N	N	N	N	N	N	N	N	N	N	N	N	N	N	N		N	N	N	N	N	N
LUMPS	Y	N	N	RVRC	N	N	N	N	N	N	N	N	N	N	N	N	N	N	N	N	N	N	N	N	N	Y	N	N	N
GCTTC	Y	Y	Y	RVRCt	Y	Y	N	N	Y	Y	Y	N	N	Y	Y	Y, C1	N	N	N	N	Y	CR, Cp K, VHC		Y	Y	Y	Y	N	N
MM5u	N	N	N	RVRC	N	N	N	N	N	Y	N	N	N	N	N	N	N	N	N	Y	Y	C_R, K		N	N	Y	Y	N	N
MOSES1T	N	N	N	RV	N	N	N	Y	N	N	N	N	N	N	N	N	N	N	N	Y	N	C_R K,VHC		N	N	Y	Y	N	N
MOSES2T	Y	Y	N	RVRC	N	N	N	Y	Y	N	N	N	N	N	N	N	N	N	N	Y	N	C_R K,VHC		Y	Y	Y	Y	N	Y
MOUSES	Y	Y	N	RVRC	N	N	N	Y	Y	N	N	N	N	N	N	N	N	N	N	Y	N	C_R K,VHC		Y	Y	Y	Y	N	N
MUCM	Y	Y	Y	RVRCt	Y	Y	N	N	Y	N	Y	Y	Y	N	N	N	Y	Y	Y	Y	Y	C_R,K Cp, VHC, κ	Y	Y	Y	Y	Y	Y	Y
MUKLIMO	Y	Y	Y	RV	N	N	N	Y	N	Y	N	N	N	N	N	N	Y	Y	N	N	N	C_R,K Cp		N	N	N	Y	N	Y
NSLUCM	Y	Y	Y	RVRC	N	N	Y	Y	Y	Y	Y	Y	N	Y	N	Y	Y	Y	Y	Y	Y	C_R K,VHC	N	Y	Y	N	Y	N	Y
SM2U	Y	N	N	RVRC	N	N	N	Y	Y	Y	N	N	N	N	Y	Y, C2	Y	Y	Y	Y	Y, C3	C_R K,VHC	Y	Y	Y	N	Y	N	Y
SUEB	N	N	N	N	N	N	N	N	N	N	N	N	N	N	N	N	N	N	N	Y	N	C_R K, VHC, κ		N	N	Y	Y	N	Y
SUMM	Y	Y		RVRCt	N	N	Y	Y	Y	N	N	N	N	N	Y	N	N	N	N	Y	N	C_R, K, C, VHC	Y	Y	Y	N	Y	N	N
SUNBEEM	N	N	N	N	N	N	Y	Y	Y	N	Y	Y	N	Y	Y	N	Y	Y	N	Y	N	C_R, K, VHC	Y	Y	Y	N	Y	Y, C6	N
TEB	Y	Y	N	RVRCt	Y	N	Y	Y	Y	Y	N	N	N	N	N	Y, C2	N	N	Y	Y	Y	C_R K, VHC	Y	Y	Y	N	Y	N	Y

Table 11.6 (continued)

Model	λp	λ_f	ψ	F	A_w	A_O	z_r	z_f	z_B	z_{or}	W_B	D_B	Fl_D	S L/W/ d/N	LAA	Traf	T_{intW}	T_{intR}	T_i	T_{DS}	Mat	HT	MT	ε_{fac}	α_{fac}	α	LL	τ	z_{ofac}
TEB07	Y	Y	N	RV	N	N	N	Y	Y	Y	N	N	N	N	N	Y,C2	N	N	Y	Y	Y	C_R K, VHC	Y	Y	Y	N	Y	N	Y
TUF2D, TUF3D	Y	Y	N	N	N	N	N	Y	Y	N	N	N	N	d/N	Y	N	N	N	Y	Y	Y	VHC, K	Y	Y	Y	N	Y	N	Y
UCLM	Y	Y	Y	N	Y	Y	Y	Y	Y	N	Y	Y	N	Y	N	N	Y	Y	Y	Y	Y	C_R,K Cp, VHC	Y	Y	Y	Y	Y	N	Y
VUCM	Y	N	N	RVRC	Y	Y	Y	Y	Y	N	Y	Y	N	N	N	N	N	N	N	Y	Y	C_R K,VHC	Y	Y	Y	N	Y	N	Y

λ_p – building (roof) plan area ratio; λ_f – building frontal area ratio; ψ – Sky view factors (wall, ground);
F – areal fractions of RVRCt/p – road/vegetated/roof/canyon/typical/three surfaces on each facet (e.g., window/pervious canyon floor) A_w – Areas of wall;
A_O – Area open ground; z_r – Reference height; z_f – Height of forcing; z_B – Building height; z_{or} – Orographic height;
W_B – Average building width; D_B – Averaged building separation; Fl_D – Floor density distribution of the buildings in vertical direction; S L/W/d/N – Street length/width/direction/number of street directions; LAA – Long axis azimuth of the site; Traf – Traffic Vehicles
T_{intW} – Temperature inside buildings behind wall; T_{intR} – Temperature inside buildings behind roof; T_i – Room temperature; T_{DS} – Deep soil/road temperature; Mat – Materials (look-up table);
HT – heat transfer; CR – Heat capacity for soil, roofs or walls; K – Thermal conductivity of soil, wall or roof materials; Cp – Specific heat; VHC – Volumetric heat capacity of wall, street, roof materials; – Thermal diffusivity of ground/wall /road;
MT – material thickness by layers; α – Albedo; ε_{fac} – emissivity by facet; LL – Latitude and Longitude; τ – Turbidity; z_{ofac} – Roughness length of each facet.
C1 N/hr crossing the street.
C2 Sensible and latent heat fluxes due to traffic (W m^{-2}).
C3 Additional requirements: soil composition (%), pavement infiltration capacity (m s^{-1}), amount of impervious surface connected to draining network (%), Vegetation, roof, pavement max. water storage (mm).
C5 Sensible heat flux due to traffic W m^{-2}.
C6 Turbidity specified indirectly by choice of solar radiation model parameters.

Table 11.7 Vegetation related parameters (Y – yes included; N – no)

Model	LAI_{CV}	g_w	Veg	z_{CV}	α_{CV}	τ_{cv}	C_V
BEP02	N	N	N	N	N	N	N
BEP05	N	N	Y	N	Y	N	Y
CAT	N	N	N	N	N	N	N
CLMU	N	N	N	N	N	N	N
ENVImet	LAD	N	Y, 2t	N	N	N	N
GCTTC	N	N	Y	Y	Y, C1	Y, C1	N
HIRLAM-U	LAD	N	Y	N	Y	N	N
LUMPS	N	N	N	N	N	N	N
MM5u	N	N	Y	N	Y	N	N
MOSES1T	Y	N	Y, 5t	Y	N	N	N
MOSES2T	Y	N	Y, 5t	Y	N	N	N
MOUSES	Y	N	Y, 5t	Y	N	N	N
MUCM	N	Y	N	N	Y	N	N
MUKLIMO	y	Y	N	Y	Y	Y	N
NSLUCM	Y	Y	Y	N	Y	N	N
SM2U	Y	N	Y, 11t	Y	Y	N	Y
SUEB	N	N	N	N	N	N	N
SUMM	N	N	N	Y	Y	N	N
SUNBEEM	N	Y	N	N	Y,C2	N	Y
TEB	Y	N	Y, 3t	N	Y	N	N
TEB07	Y	N	Y	N	Y	N	N
TUF2D, TUF3D	N	N	N	N	N	N	N
UCLM	N	N	N	N	N	N	N
VUCM	Y	N	N	Y	Y	N	Y

LAI_{CV} – LAI of canyon vegetation; LAD leaf area density g_w – Water vapor conductance of plant canopy; Veg – Vegetation species (2t [C3/C4 vegetation],3t,5t,11t number of types); z_{CV} – Canyon vegetation height; α_{cv} –Albedo of canopy leaves; τ_{cv} – Canopy solar transmissivity; C_V – Heat capacity of vegetation.

C1 requires vegetation coverage (net of sunny spots), as a percentage of the total ground area
C2 also canopy emissivity.

is that for some models a long initialization period (spin-up) time is needed to ensure that the temperature profiles are stable and representative of conditions.

11.2.4 Methods of Calculation

Here the methods used by the different urban schemes to calculate the various fluxes are considered. Complete information is provided in the original papers. The analysis here is cursory; as the project proceeds, a more complete analysis will be undertaken.

In the model simulations, the incoming radiative fluxes will be prescribed, so the critical issue is how the outgoing radiative fluxes are determined. The major differences relate to the number of reflections the models assume and the degree of detail in assigning the surface characteristic parameters (Table 11.9). The simplest

Table 11.8 Required model input variables. (init- initial condition only) (Y – yes included; N – not included)

	Wind			Temperature				Radiation										Soil			
Code	WS	WD	TKE	T_s	T_a	Tpot	Humidity	K↓	$K\downarrow_D$	$K\downarrow_S$	L↓	CC	Z	Cp	P	ρ	R	T profile	θ	T_{water}	Q_F
BEP02	Y	Y	Y	N	N	Y		Y	N	N	Y	N	N	N	N	N	N	N	N	N	N
BEP05	Y	Y	Y	N	N	Y	U4	Y	N	N	Y	N	N	N	Y	N	N	N	N	N	N
CAT	Y	Y	N	N	Y	N	RH	Y	Y	N	N	Y	Y	N	Y	N	Y	N	N	N	Y
CLMU	Y	N	N	Y,r,w,R,S, Init	Y	N	U2	Y	Y/N	Y/N	Y	N	N	N	Y	N	Y	Yinit	Yinit	N	N
ENVImet	Y	Y	N	Y	Y	N	U1	N	Y/N	N	N	N	N	N	N	N	N	Yinit	Yinit	Y	N
GCTTC	Y	Y	N	Y, w,g,r	Y	N	Tw	Y	Y	Y	Y	Y	Y	N	N	N	N	N	N	N	Y
HIRLAM-U	Y	Y	N	N N	Init	Y	RH, e_a	N	N	N	N	Init	N	N	Y	N	N	N	N	Y	Y
LUMPS	N	N	N		Y	N	N	Y	N	N	N	N	N	N	Y	N	Y	N	N	N	N
MM5u	Y	N	N	N	Y	N	RH	N	N	N	N	N	N	N	N	N	N	N	N	Y	Y
MOSES1T	Y	Y	N	Y,U	Y	N	U2	Y	N	N	Y	N	N	N	Y	N	Y	Y	Y	N	N
MOSES2T	Y	Y	N	Y,r,U	Y	N	U2	Y	N	N	Y	N	N	N	Y	N	Y	Y	Y	N	N
MOUSES	Y	Y	N	Y, r,U	Y	N	U2	Y	Y	Y	Y	N	Y	N	Y	N	Y	Y	Y	N	N
MUCM	Y	N	N	N	N	Y	U1	Y	Y	Y	Y	Y	Y	Y	N	Y	N	Y	N	N	Y
MUKLIMO	Y	N	N	N	Y	N	U2	N	N	N	N	Y	Y	N	N	N	N	N	N	N	N
NSLUCM	Y	N	N	Y, w,g,r,s	Y	Y	SH	Y	Y	Y	Y	N	Y	N	Y	Y	Y	Y	Y	Y	Y
SM2U	Y	Y	N	Y, r,w,R,s,V	Y	N	U2	Y/N	Y/N	Y/N	Y/N	N	N	N	Y	N	Y	N	Y	Y	Y
SUEB	Y	N	N	Y, U	Y	Y	SH	Y	N	N	Y	N	N	Y	N	Y	N	Y	Y	N	N
SUMM	Y	Y/N	N	Y, r,R,w init	Y	N	Y	Y	Y/N	Y/N	Y	N	N	Y	N	Y	N	N	N	N	N
SUNBEEM	Y	Y	N	N	Y	N	e_a	Y	Y	Y	Y	Y	N	N	Y	N	N	N	N	N	N
TEB	Y	N	N	Y,r,w,R,s,V	Y	N	U2/U3	Y	Y	Y	Y	N	N	N	Y	Y	Y	Yinit	Yinit	N	Y(traf)
TEB07	Y	N	N	N	Y	N	U2/U3	Y	Y	Y	Y	N	N	N	Y	N	Y	Yinit	Yinit	N	Y(traf)

Table 11.8 (continued)

	Wind			Temperature				Radiation										Soil			
Code	WS	WD	TKE	T_s	T_a	Tpot	Humidity	K↓	$K\downarrow_D$	$K\downarrow_S$	L↓	CC	Z	Cp	P	ρ	R	T profile	θ	T_{water}	Q_F
TUF2D, TUF3D	Y	Y	N	N	Y	N	e_a	Y/N	N	N	Y/N	N	N	N	Y	N	N	N	N	N	N
UCLM	Y	Y	N	N	Y	N	e_a	N	N	N	N	Y	N	Y	Y	Y	N	N	N	N	N
VUCM	Y	N	N	Y r,w,R,s,V	Y	N	U2	N	Y	Y	Y	N	N	N	Y	Y	Y	Y	Y	N	Y

Wind related: WD – Wind direction (degrees); WS – Wind speed (m s^{-1}), TKE – Turbulent kinetic energy (m^2 s^2);
Temperature related: Tpot – Potential temperature (K); Ta – Air temperature (T_s) – Temperature of the surface w walls, g ground and r roof, R road, s soil, V vegetation; U urban slab, Init – initial condition;
Humidity: T_w – Wet Bulb T (C); e_a – Water vapour pressure (hPa); RH – Relative humidity (%); SH – Specific humidity (units U1: g kg^{-1}, U2: kg kg^{-1} U3: kg m^{-3}, U4: g m^{-3});
Radiation: K↓ – incoming shortwave radiation; S – direct radiation; D – diffuse radiation; L↓ – incoming longwave radiation; CC – cloud cover; Z – Solar zenith angle; C_p – specific heat; P – Atmospheric pressure (hPa); ρ – Air Density (kg m^3); R – Precipitation (kg m^2 s^{-1});
Soil: Tprofile – temperature profile; θ – Soil moisture content; T_{water} – Water temperature (K/C);
Q_F – Anthropogenic heat flux (W m^{-2}).

Table 11.9 Methods used to model outgoing shortwave and long wave radiation

Model	Number of reflections	Albedo	L↑
BEP02	multiple	canyon	Result of multiple reflections in the canyon, from walls and canyon floors at each grid level
BEP05	multiple	canyon	Result of multiple reflections in the canyon
CAT	one	by facet	By facet, with one emission and one reflection among facets
CLMU	multiple	by facet	By facet with multiple reflections and one emission
ENVImet	one	by facet	From energy balance of all facets
GCTTC	multiple	by facet	Prescribed
HIRLAM-U	one	bulk/town	Fast broadband schemes for solar and termal radiation (Savijärvi, 1990). emissivity function and Stefan-Boltmann law, STRACO scheme for clouds, water vapour (Sass, 2001)
LUMPS	one	bulk	Prata (1996)
MM5u	one	bulk/town	Stefan-Boltmann law, plus parameterization schemes for the clouds and water vapour (e.g. Stephens, 1978; Garand, 1983)
MOSES1T	one	bulk	Prescribed bulk emissivity
MOSES2T	one	canyon, roof	Prescribed emissivity values for canyon and roof
MOUSES	multiple	bulk/effective	Effective emissivity by multiple reflections
MUCM	two	by facet	
MUKLIMO			From energy balance of all facets
NSLUCM	one	by facet	One reflection
SM2U	infinite	bulk/effective	Effective emissivity
SUEB	one	bulk/town	By emissivity
SUMM	multiple	facet	Result of multiple reflections
SUNBEEM	multiple	by facet	By facet with multiple reflection
TEB	infinite	canyon, roof	Result of two reflections in the canyon
TEB07	infinite	canyon, roof	Result of two reflections in the canyon
TUF2D, TUF3D	multiple (min 2)	patches/facet	Multiple reflection (minimum 2) between patches (and emission by patches initially)
UCLM	two	facet	Emitted longwave radiation computed for each facet (no reflections) using energy budget.
VUCM	three	canyon, roof	One reflection

models use a single assigned bulk value (e.g. albedo) and have just one reflection (e.g. LUMPS). Thus they do not account for the different material characteristics in urban area as do CLMU and TEB, for example.

As already noted there are a wide range of approaches to account for the anthropogenic heat flux (Table 11.10). Currently this is the flux for which the least sophisticated approaches are adopted. The term most typically is prescribed although some, but not all, components may be calculated (e.g. fixed or mobile sources) in

Table 11.10 Methods used to calculate anthropogenic heat flux (Q_F)

Model	Anthropogenic heat flux methods
BEP02, BEP05, SUNBEEM	Partially accounted for by imposing a fixed temp at the building interior
CAT	Prescribed, adjusted for diurnal variations
CLMU	Prescribed traffic fluxes, parameterized waste heat fluxes from heating/ air conditioning
ENVImet	From heat transfer equations through walls
HIRLAM-U	Calculated (offline) as a temporal & spatial function of available parameters by 4 methods (emission, night light, land-use, population) (Baklanov et al., 2005)
GCTTC	Prescribed per vehicle (for vehicles only)
MM5u, NSLUCM	Calculated (offline) as a temporal & spatial function of the anthropogenic emissions
MOSES2T, MOSES1T, MOUSES, SUEB	Not modelled itself but possible to be included for calculation of turbulent fluxes
MUCM	Modelled by Kikegawa et al. Offline
MUKLIMO	Heat fluxes through the walls and roofs computed with fixed temp at the buildings interior
TEB, TEB07 TUF2D, TUF3D	Domestic heating computed
UCLM	Not directly included. Heat can be added to building interior.
VUCM, SM2U	Prescribed bulk value

some models. This flux is most significant in the wintertime when the additional energy from human sources is most important relative to the net all wave radiation. That said, in many urban areas energy use is becoming increasingly significant in the summer due to air conditioning usage (Watson et al., 1997). Anthropogenic heat flux may only be significant in areas with very high flux densities (e.g. Tokyo, Ichinose et al., 1999). At key times of the day and night, and specifically at transitions between them, this flux could become more significant.

The turbulent sensible heat fluxes are typically modelled using some form of resistance scheme (Table 11.11). Differences depend on the degree of detail of the surface to be modelled; i.e. a bulk surface resistance or a resistance network accounting for differences between surfaces. Varying approaches are taken for these resistances, ranging, for example, from those based on the Penman-Monteith equation (e.g. LUMPS) to resistance networks that take into account changes in stability and the orientation of the surface that is shedding the heat (e.g. TUF3D). Correspondingly, a number of different resistance schemes are used (e.g. Rowley, 1930; Clarke, 1985; Zilitinkevich, 1995; Guilloteau, 1998; Harman et al., 2004b). The methods used to determine the stability functions are important because they feedback and impact on the outgoing longwave radiation. Many of the methods assume that Monin-Obukhov similarity holds, but this may not be applicable within the urban canyon (Roth, 2000). However, given the lack of well-tested alternatives, this may be the most appropriate set of assumptions.

Table 11.11 Methods to calculate turbulent sensible heat flux (Q_H)

Model	Turbulent sensible heat flux methods
BEP02, BEP05, SUNBEEM	For walls based on Clarke (1985)
CAT	Resistance between canyon surfaces and air based on Hagishima and Tanimoto (2003); at canyon top depends on stability, using empirical parameterization
CLMU	Resistance network accounting for differences between surfaces
ENVImet	From turbulence model (wall function) and surface energy balance
GCTTC	Calculated for each surface based on the attenuated radiation by the CTTC factor
LUMPS	deBruin and Holtslag (1982) modified Penman Monteith modified for urban areas (Grimmond and Oke, 2002)
HIRLAM-U, MM5u	Parametric formulation based on the specific heat capacity for moist air, the density of the atmosphere, the surface friction velocity and the surface temperature scale
MOSES2T, MOSES1T	Standard resistance, based upon MO similarity theory
MOUSES	Resistance network based on Harman et al. (2004)
MUCM	MO or Jurges
MUKLIMO	From surface energy balances at the soil, walls and roofs using MO laws
NSLUCM	MO based on Louis (1979) and Jurge's formulation, and calculated from each surface
SM2U	MO Resistance (Guilloteau, 1998; Zilitinkevich, 1995)
SUEB	MO similarity Louis (1979) modified by Mascart et al. (1995)
SUMM	Resistance (top-down method, Kanda et al., 2005)
TEB, TEB07	Resistance
TUF2D, TUF3D	Resistances based on flat-plate heat transfer coefficients (vertical patches) and based on MO similarity (horizontal patches)
UCLM	Exchange based on canyon air and surface temperature difference, wind speed and prescribed heat transfer coefficient.
VUCM	Parametric formulation

The storage heat flux methods involve, amongst others, empirically-based approaches such as objective hysteresis model (OHM)(e.g. MM5u, LUMPS, HIRLAM-U, CAT) and thermal diffusion approaches (Table 11.12). Models use varying numbers of layers to represent substrate materials, and as noted in the model inputs, materials are described in a wide variety of ways with implications for how the heat storage term can be calculated.

The methods used to calculate drag include roughness length approaches and distributed drag within the atmosphere (Table 11.13). Those that distribute the drag within the canopy might be expected to require more computational time and have greater data needs to describe the urban morphology.

A wide range of approaches are used to calculate the latent heat fluxes reflecting a range of possible representations of vegetated and/or wet surfaces. Some models assume that the urban area is dry and therefore ignore the latent heat flux completely; others have wet built surfaces but no vegetation; and some include vegetation as either a separate tile or as integrated (Table 11.3, 11.7, and 11.14). As with the

Table 11.12 Methods used to calculate storage heat flux (ΔQ_s)

Model	Storage heat flux methods
BEP02	Total storage heat flux is the sum of the storage heat flux of roofs, walls, and road. For each surface the storage comes from the energy budget that is solved
CAT, HIRLAM-U, MM5u, LUMPS	OHM scheme (Grimmond et al., 1991)
ENVImet	Soil 1D model, fully resolved, walls/building system no storage term
GCTTC	Residual from radiation after allowing for sensible and latent heat.
MUCM	Finite difference
MUKLIMO	Walls and roofs have a heat capacity
NSLUCM	Multi-layer thermal diffusion within wall/roof/road
SM2U	Budget + Conduction + Force restore
SUMM	Multi-layer thermal diffusion within walls/roof/road
SUEB	As Q_G in urban slab (solution of multi layer thermal diffusion equation)
SUNBEEM	1D finite difference solution of heat conduction equation for each facet
BEP05,TEB, TEB07, CLMU, BEP05, TUF2D, TUF3D, MOSES2T, MOSES1T, VUCM, MOUSES	Diffusion
UCLM	Model calculates substrate heat exchange and changes substrate temperatures accordingly.

Table 11.13 Methods used to calculate drag

Model	Drag
BEP02, BEP05, TEB07	Drag distributed within the atmosphere
CAT, GCTTC, TEB	Not included
CLMU, LUMPS, MM5u TUF2D, TUF3D, UCLM, VUCM MOSES1T, MOSES2T, SUEB	Prescribed Roughness length
ENVImet	3D Navier Stokes equation fully solved
HIRLAM-U	Roughness length with stability dependence Zilitinkevich et al. (2006)
MOUSES	Roughness length with MacDonald et al. (1998)
MUCM	Drag distributed within the atmosphere
MUKLIMO	Solving 3D Navier Stokes equation with roughness lengths at all material surfaces
NSLUCM	Exponential wind profile
SM2U	Roughness length Bottema (1995), Raupach (1994, 1995), Guilloteau (1998), MacDonald et al. (1998)
SUNBEEM	Roughness length

Table 11.14 Methods used to calculate latent heat flux (Q_E) and soil moisture

Model	Latent heat flux method	Soil moisture method
BEP02	Not included	Not included
CAT	Resistances based on the Penman-Monteith equation (Grimmond and Oke, 2002)	Not included
CLMU	Resistance network accounting for differences between surfaces	Layers
GCTTC	Evapotranspiration per 1 m^2 of vegetated coverage estimated empirically Shashua-Bar and Hoffman (2002) method	Not included
HIRLAM-U	Bulk method over each subgrid-scale surface type and tile method for flux aggregation	Force-restore, 2 soil layers + forest canopy, ISBA scheme (Noilhan and Planton, 1989)
LUMPS	deBruin and Holtslag (1982) modified Penman Monteith	Not included
ENVImet	Soil hydrological model, at Surface Halstead parameter calculated, Vegetation Photosynthesis/ Transpiration model	Prognostic 1-d multilayer model
NSLUCM	Using land-surface model for latent heat fluxes from natural surfaces, and bulk/slab model for evaporation from anthropogenic surfaces	Prognostic multi-layer soil model for natural surfaces and one-layer slab model for athropogenic surface
MUCM	Conductance based on Shulze et al. (1994)	Not included
MM5u	Parametric formulation based on the heat of vaporization, the available moisture, the molecular diffusivity, the depth of the molecular layer and the specific humidity at the surface and the lowest model level	Five-Layer Soil Model (Dudhia, 1996)
MOSES1T MOSES2T	Standard resistance based upon MO similarity theory	Prognostic 1-d multilayer model
MUKLIMO	Resistance law within the canopy, MO from there to the atmosphere	Prognostic 1-d multilayer model
SM2U	Resistance (Noilhan and Planton, 1989)	Force-restore, 2 layers + reservoir
MOUSES	Resistance	Prognostic 1D multilayer model
TEB	Resistance	Bucket
TEB07		Bucket
TUF2D, TUF3D	Not included	Not included
BEP05	Penman-Monteith formulation (Monteith, 1981)	Force-restore
SUEB	Resistances based on Best (1998)	Not included
SUMM	Resistance	Not included
SUNBEEM	Penman-Monteith formulation (Monteith, 1981)	No explicit soil moisture. Thermal properties for vegetated canyon floor may reflect soil moisture
UCLM	Not included	Not included
VUCM	Parametric formulation	Layers

calculation of the turbulent sensible heat flux, the methods for calculating the latent heat flux typically involve some form of resistance scheme whereas some prescribe a value based on areal extent of vegetation (e.g. GCTTC).

11.3 Methodology for the Model Comparison

The methodology to be adopted follows that used in PILPS, the Project for Intercomparison of Land-Surface Parameterization Schemes (Henderson-Sellers et al., 1993). This involves four stages. The models are all run offline so the forcing data are provided for the 'top' of the model and so there is no feedback to larger scale conditions within the modelling domain. The smallest time unit of analysis will be hourly and the spatial unit will be an area that is representative of the local scale (equivalent to one grid point in a meso-scale model). Initially participants will be provided with very limited information about the chosen site(s), only being given the forcing variables. In subsequent runs, more information will be provided to ensure that a controlled experiment is achieved. By undertaking this staged approach it should be possible to establish the required accuracy for each of the model parameters by comparing the quality of the simulation at each stage. This methodology is endorsed by the GEWEX Global Land Atmosphere System Study (GLASS) panel, which coordinates the PILPS experiments (A. Pitman, personal communication, 2006). More specifically the steps are:

1) *Forcing data only*: The models are run with no prior knowledge of the urban surface (i.e. each group determines their own default values for all of their parameters); only the main forcing data will be supplied, e.g. winds, temperature, solar radiation.
2) *Add urban morphology*: This involves releasing morphological information to the modellers, e.g. building density, mean building height, vegetation fraction. These data are more readily available on a global basis.
3) *Add urban fabric properties*: Details of building materials are then given, such as thermal properties, surface cover fraction and albedo. This information is specific to each city and is not generally known on a global basis. Reliance on these types of data makes a scheme such as this difficult for global applications.
4) *Add evaluation data*: At the final stage, the evaluation dataset is released to allow optimisation of model parameters for best fit to observations. At this stage, modelling groups will also return information on their optimised parameters as well as the standard outputs. The methods used by individual groups to determine what they regard as their optimized parameter set will be also gathered.

The model evaluations will involve statistical analysis of the *performance of the models relative to the observations*. The observations will be for one site and will consist of a range of data that varies seasonally. This assessment will be conducted flux-by-flux (radiative, turbulent sensible and latent heat fluxes) and will consist

of an hour-by-hour evaluation along with comparisons over longer (daily, monthly, seasonal, annual) time periods. The statistics used will include a range of metrics (mean, standard deviation, probability distribution function, linear regression, root mean square error (systematic, unsystematic), index of agreement, mean absolute error, mean bias error, correlation coefficient, coefficient of determination, etc.). Each provides insight into different aspects of model performance.

The analysis will also assess the ability of each model to simulate known urban climatological phenomena. It is now well documented that the energy exchange processes in cities (relative to a rural area) are modified by the presence of buildings and other anthropogenic structures in the following key ways:

- urban areas reflect less shortwave radiation, due to trapping and multiple reflections between buildings (Arnfield, 1982)
- materials used in urban areas have high thermal heat capacity, i.e. there is 'storage heat flux' into the buildings by day (Grimmond and Oke, 1999a; Offerle et al., 2005) and significant release at night
- the surface area is increased, which combined with materials of a high heat capacity, means that more heat is absorbed and emitted (Harman et al., 2004b)
- the morphology of buildings affects flow, and thus determines the rate of exchange of heat with the air above (Barlow and Belcher, 2002; Barlow et al., 2004)
- buildings and traffic generate additional anthropogenic sources of heat (Grimmond, 1992; Sailor and Lu, 2004; Offerle et al., 2005)
- evaporative cooling is decreased due to reduction in vegetation cover; thus the latent heat flux may be relatively small (Grimmond and Oke, 1991; Grimmond and Oke, 1999b)
- positive sensible heat fluxes are more probable at night in highly built up areas (Grimmond and Oke, 2002)

Many of the models under consideration also predict variables beyond the surface energy balance terms. It is often these variables that are of specific interest in many applications. For example, air temperature and humidity are reported as part of a weather forecast but are also of interest for health and air quality applications. Similarly, atmospheric stability and wind speed are of interest in pollution dispersion applications.

By staging the comparison and considering model performance individually and across groups of models defined in terms of key attributes, we will aim to address the following four key questions:

1) *What are the main physical processes that need to be resolved to simulate realistically, urban energy balance exchanges?* This will be addressed by grouping models in terms of the processes that they represent, to determine whether models which represent certain processes produce significantly better results. By staging the comparisons so that the experiment finishes with the optimisation of the parameters for each model, it will be possible to determine

whether the optimized parameters actually represent the processes they are meant to, by assessing whether the parameters are within physically reasonable bounds.

2) *How complex does a model need to be in order to produce a realistic simulation of urban fluxes and temperatures?* More complex models tend to be more difficult to implement and require greater computational resources. By comparing the performance of models grouped in terms of complexity, it will be possible to determine the model complexity required to accurately represent known (observed) urban climatic features.
3) *Which input parameter information is required by an urban model to perform realistically?* An array of parameters, particularly related to the urban surface, is used in model simulations; specifically information on surface materials, building heights and shapes, distribution of heat sources, etc. Clearly, it is impossible to incorporate into a model, or even to collect data, on all aspects of the urban surface. Therefore guidance is needed to balance the complexity (and availability) of the input parameters with the veracity of the models output. To assess this, the models will be run in stages, with increasingly accurate parameter information provided at each stage. By assessing the quality of the simulations for each group at each stage, it will be possible to determine: the minimum number of parameters required for a realistic simulation; what these parameters are, and how accurately they need to be known.
4) *What are the main research priorities for future observational campaigns within urban areas?* By answering the third question, it will also be possible to determine whether the essential parameters are being measured in observational studies of cities, and whether techniques for determining these parameters actually exist. This will enable advice to be given to the measurement community in terms of prioritising future observational research campaigns and to determine the routine measurements to be assimilated into forecast or air quality models.

11.4 Conclusions

Given the broad range of applications in which urban surface energy balance schemes are being used (e.g. simulations of the UHI, evaluation of different building/development strategies, air quality modelling, regional weather forecasting) and the potential range of applications, a more systematic evaluation of existing models and areas of weakness is needed. This project will contribute to developing the science for a sustainable future, as urban land use increases globally and as increasing populations become exposed to microclimates with undoubted anthropogenic influences.

Acknowledgments We wish to thank the UK Met Office, Vasilis Pappas (KCL), Rob Mullen (KCL), Robert Ewen (KCL), Professor Andy Pitman (Macquarie University) and Dr Catherine Souch (RGS-IBG) for their contributions to this project to date.

References

Arnfield, A.J.: Estimation of diffuse irradiance on sloping, obstructed surfaces – an error analysis. Archives for Meteorology Geophysics and Bioclimatology Series B-Theoretical and Applied Climatology, 30, 303–320, 1982.

Arnfield, A.J.: A simple model of urban canyon energy budget and its validation, Phys. Geog., 21, 305–326, 2000.

Baklanov, A., Mahura, A., Nielsen, N.W. and Petersen, C.: Approaches for urbanization of DMI-HIRLAM NWP model. HIRLAM Newsletter 49, pp. 61–75, 2006.

Baklanov, A., Mestayer, P.G., Clappier, A., Zilitinkevich, S., Joffre, S., Mahura, A. and Nielsen, N.W.: Towards improving the simulation of meteorological fields in urban areas through updated/advanced surface fluxes description, Atmos. Chem. Phys., 8, 523–543, 2008.

Barlow, J.F. and Belcher, S.E.: A wind tunnel model for quantifying fluxes in the urban boundary layer, Bound.-Layer Meteorol., 104, 131–150, 2002.

Barlow, J.F., Harman, I.N. and Belcher, S.E.: Scalar fluxes from urban street canyons, Part I: Laboratory simulation, Bound.-Layer Meteorol., 113, 369–385, 2004.

Best, M.J., Grimmond, C.S.B. and Villani, M.G.: Evaluation of the urban tile in MOSES using surface energy balance observations, Bound.-Layer Meteorol., 118, 503–525, 2006.

Best, M.J.: Representing urban areas within operational numerical weather prediction models, Bound.-Layer Meteorol., 114, 91–109, 2005.

Best, M.J.: Progress towards better weather forecasts for city dwellers: from short range to climate change, Theo. Appl. Clim., 84, 47–55, 2006.

Bonacquisti, V., Casale, G.R., Palmieri, S. and Siani, A.M.: A canopy layer model and its application to Rome, Sci. Total Environ., 364, 1–13, 2006.

Bornstein, R. and Lin, Q.L.: Urban heat islands and summertime convective thunderstorms in Atlanta: three case studies, Atmos. Environ., 34, 507–516, 2000.

Bottema, M. Aerodynamic roughness parameters for homogeneous building groups. Part I: Theory, Document SUB-MESO # 18, Ecole Centrale de Nantes, 40 pp., 1995.

Brown, M.J.: Urban parameterizations for mesoscale meteorological models. In Z. Boybeyi (ed.), Mesoscale Atmospheric Dispersion, Computational Mechanics, 2001.

Bruse, M. and Fleer, H.: Simulating surface–plant–air interactions inside urban environments with a three dimensional numerical model, Environ. Modelling Software, 13, 373–384, 1998.

Clarke, J.A.: Energy Simulation in Building Design, Adam Hilger, Bristol, 362 pp., 1985.

Dandou, A., Tombrou, M., Akylas, E., Soulakellis, N. and Bossioli, E.: Development and evaluation of an urban parameterization scheme in the Penn State/NCAR Mesoscale model (MM5), J. Geophys. Res., 110, D10102, 2005.

de Bruin, H.A.R. and Holtslag, A.A.M.: A simple parameterization of surface fluxes of sensible and latent heat during daytime compared with the Penman–Monteith concept. J. Appl. Meteor., 21, 1610–1621, 1982.

Dudhia, J.: 'A multi-layer soil temperature model for MM5', Preprints, *The Sixth PSU/NCAR Mesoscale Model Users', Workshop*, 22–24 July 1996, Boulder, Colorado, 49–50, 1996.

Dupont, S. and Mestayer, P.G.: Parameterisation of the urban energy budget with the submesoscale soil model, J. Appl. Meteorol. Climatol., 45, 1744–1765, 2005.

Dupont, S., Mestayer, P.G., Guilloteau, E., Berthier, E. and Andrieu, H.: Parameterisation of the urban water budget with the submesoscale soil model, J. Appl. Meteorol. Climatol., 45, 624–648, 2006.

Erell, E. and Williamson, T.: Simulating air temperature in an urban street canyon in all weather conditions using measured data from a reference meteorological station, Int. J. Climatol. 26, 1671–1694, 2006.

Essery, R.L.H., Best, M.J., Betts, R.A., Cox, P.M. and Taylor, C.M.: Explicit representation of subgrid heterogeneity in a GCM land surface scheme, J. Hydrometeorol., 4, 530–543, 2003.

Fortuniak, K., Offerle, B. and Grimmond, C.S.B.: Slab surface energy balance scheme and its application to parameterisation of the energy fluxes on urban areas, NATO ASI, Kiev, Ukraine, 4-15.05 2004, 82–83, [www.met.rdg.ac.uk/urb_met/NATO_ASI/talks.html] 2004.

Fortuniak, K., Offerle, B. and Grimmond, C.S.B.: Application of a slab surface energy balance model to determine surface parameters for urban areas, Lund eRep. Phys. Geog., 5, 90–91, [www.nateko.lu.se/Elibrary/LeRPG/LeRPG5Article.pdf] 2005.

Garand, L.: Some improvements and complements to the infrared emissivity algorithm including a parameterization of the absorption in the continuum region, *J. Atmos. Sci*., 40, 230–244, 1983.

Grimmond, C.S.B.: The suburban energy balance: Methodological considerations and results for a mid-latitude west coast city under winter and spring conditions, Int. J Climatol., 12, 481–497, 1992.

Grimmond, C.S.B., Cleugh, H.A. and Oke, T.R.: An objective urban heat storage model and its comparison with other schemes. *Atmos. Environ.*, 25B, 311–326, 1991.

Grimmond, C.S.B. and Oke, T.R.: An evaporation-interception model for urban areas, Water Resour. Res., 27, 1739–1755, 1991.

Grimmond, C.S.B. and Oke, T.R.: Heat storage in urban areas: observations and evaluation of a simple model, J. Appl. Meteorol., 38, 922–940, 1999a.

Grimmond, C.S.B. and Oke, T.R.: Rates of evaporation in urban areas, International Association of Hydrological Sciences Publication, 259, 235–243, 1999b.

Grimmond, C.S.B. and Oke, T.R.: Turbulent heat fluxes in urban areas: Observations and local-scale urban meteorological parameterization scheme (LUMPS), J. Appl. Meteorol., 41, 792–810, 2002.

Grimmond, C.S.B.: Urbanization and global environmental change: Local effects of urban warming, Geograph. J., 173, 83–88, 2007.

Guilloteau, E.: Optimized computation of transfer coefficients in surface layer with different momentum and heat roughness length, Bound. Layer Meteorol., 87, 147–160, 1998.

Hacker, J.N., Holmes, M.J., Belcher, S.E. and Davies, G.: Climate change and the internal environment of buildings: A designers guide, TM36, pp. 52. Chartered Inst. Building Services Eng. and Royal Inst. British Architects. ISBN: 190328750, 2004.

Hagishima, A. and Tanimoto, J.: Field measurements for estimating the convective heat transfer coefficient at building surfaces, Build. Environ., 38, 873–881, 2003.

Hamdi, R.: Numerical study of the atmospheric boundary layer over urban areas: validations for the cities of Basel and Marseilles, PhD thesis, 34/2005 Catholic university of Louvain, Belgium, 2005.

Hamdi, R. and Schayes, G.: Validation of the Martilli's urban boundary layer scheme with measurements from two mid-lattitude European cities, Atmos. Chem. Phys., 7, 4513–4526, 2007.

Hamdi, R. and Masson, V.: Inclusion of a drag approach in the Town Energy Balance (TEB) scheme: offline 1-D evaluation in a street canyon, J. Appl. Meteor. Clim., 47, 2627–2644, 2008.

Harman, I.N., Barlow, J.F. and Belcher, S.E.: Scalar fluxes from urban street canyons, Part II: Model, Bound.-Layer Meteorol., 113, 387–410, 2004b.

Harman, I.N., Best, M.J. and Belcher, S.E.: Radiative exchange in an urban street canyon, Bound.-Layer Meteorol., 110, 301–316, 2004a.

Harman, I.N., Belcher, S.E.: The surface energy balance and boundary layer over urban street canyons, Q. J. The Royal Meteorological Society, 132(621), 2749–2768, 2006.

Henderson-Sellers, A., Yang, Z.L. and Dickinson, R.E.: The project for intercomparison of land-surface parameterization schemes, Bull. AMS, 74, 1335–1349, 1993.

Henderson-Sellers, A., Irannejad, P., McGuffie, K., and Pitman, A.: Predicting land-surface climates-better skill or moving targets? Geophys. Res. Lett., 30, 14, 1777, doi:10.1029/2003GL017387, 2003.

Ichinose, T., Shimodozono, K. and Hanaki, K.: Impact of anthropogenic heat on urban climate in Tokyo. Atmos. Environ., 33, 3897–3909, 1999.

IPCC: Third Assessment Report: Climate Change 2001, ed. Watson, R.T. and core writing team, IPCC, Geneva, Switzerland, pp. 184, 2001.

Irranejad, P., Henderson-Sellers, A., Sharmeen, S.: Importance of land-surface parameterization for latent heat simulation in global atmospheric models, Geophys. Res. Lett., 30, 17, 1904, doi:10.1029/2003/GL018044, 2003.

Johnson, G.T., Oke, T.R., Lyons, T.J., Steyn, D.G., Watson, I.D., Voogt, J.A.: Simulation of surface urban heat islands under ideal conditions at night. 1. Theory and tests against field data, Bound.-Layer Meteorol., 56(3), 275–294, 1991.

Kanda, M., Kawai, T., Kanega, M., Moriwaki, R., Narita, K. and Hagishima, A.: A simple energy balance model for regular building arrays, Bound.-Layer Meteorol., 116, 423–443, 2005a.

Kanda, M., Kawai, T., Nakagawa, K.: A simple theoretical radiation scheme for regular building arrays. Bound.-Layer Meteorol., 114, 71–90, 2005b.

Kondo, H. and Liu, F.H.: A study on the urban thermal environment obtained through a one-dimensional urban canopy model, J. Jpn. Soc. Atmos. Environ., 33, 179–192, 1998 (in Japanese).

Kondo, H., Genchi, Y., Kikegawa, Y., Ohashi, Y., Yoshikado, H. and Komiyama, H.: Development of a multi-layer urban canopy model for the analysis of energy consumption in a big city: Structure of the urban canopy model and its basic performance. Bound.-Layer Meteorol., 116, 395–421, 2005.

Krayenhoff, E.S., Voogt, J.A.: A microscale three-dimensional urban energy balance model for studying surface temperatures, Bound.-Layer Meteorol., 123, 433–461, 2007.

Kusaka, H., Kondo, H., Kikegawa, Y. and Kimura, F.: A simple single-layer urban canopy model for atmospheric models: comparison with multi-layer and slab models, Bound.-Layer Meteorol., 101, 329–358, 2001.

Lee, S.-H. and Park, S.-U.: A vegetated urban canopy model for meteorological and environmental modelling, Bound.-Layer Meteorol., 126, 73–102, 2008.

Lemonsu, A., Grimmond, C.S.B. and Masson, V.: Modelling the surface energy balance of an old Mediterranean city core, J. Appl. Meteorol., 43, 312–327, 2004.

Macdonald, R.W., Griffith, R.F., Hall, D.J.: An improved method for estimation of surface roughness of obstacle arrays, Atmos. Environ., 32, 1857–1864, 1998.

Mahura, A., Baklanov, A., Petersen, C., Sattler, K., Amstrup, B. and Nielsen, N.W.: ISBA scheme performance in high resolution modelling for low winds conditions. HIRLAM Newsletter, 49, 22–35, 2006.

Martilli, A.: Current research and future challenges in urban mesoscale modelling, Int. J. Climatol., 27, 1909–1918, 2007.

Martilli, A., Clappier, A. and Rotach, M.W.: An urban surface exchange parameterisation for mesoscale models, Bound.-Layer Meteorol., 104, 261–304, 2002.

Masson, V.: A physically-based scheme for the urban energy budget in atmospheric models, Bound.-Layer Meteorol., 41, 1011–1026, 2000.

Masson, V.: Urban surface modeling and the meso-scale impact of cities, Theor. Appl. Climatol., 84, 35–45, 2006.

Masson, V., Grimmond, C.S.B. and Oke, T.R.: Evaluation of the Town Energy Balance (TEB) scheme with direct measurements from dry districts in two cities, J. Appl. Meteorol., 41, 1011–1026, 2002.

Mills, G.: An urban canopy-layer climate model, Theor. Appl. Climatol., 57, 229–244, 1997.

Montávez, J.P., Jiménez, J.I. and Sarsa, A.: A monte carlo model of the nocturnal surface temperatures in urban canyons, Bound.-Layer Meteorol., 96, 433–452, 2000.

Monteith, J.L.: Evaporation and surface temperature, Q. J. Roy. Meteor. Soc. 107, 1–27, 1981.

Noilhan, J. and Planton, S.: A simple parameterization of land-surface processes for numerical meteorological models, Mon. Wea. Rev., 117, 536–549, 1989.

Offerle, B., Grimmond, C.S.B. and Oke, T.R.: Parameterization of net all-wave radiation for urban areas, J. Appl. Meteorol., 42, 1157–1173, 2003.

Offerle, B., Grimmond, C.S.B. and Fortuniak, K.: Heat storage and anthropogenic heat flux in relation to the energy balance of a central European city centre, Int. J. Climatol., 25, 1405–1419, 2006.

Oke, T.R.: City size and urban heat island, Atmos. Environ., 7, 769–779, 1973.

Oleson, K.W., Bonan, G.B., Feddema, J. and Vertenstein, M.: An urban parameterization for a global climate model: 2. Sensitivity to input parameters and the simulated heat island in offline simulations, J. Appl. Meteorol. Climatol., 47, 1061–1076, 2008a.

Oleson. K.W., Bonan, G.B., Feddema, J., Vertenstein, M. and Grimmond, C.S.B.: An urban parameterization for a global climate model: 1. Formulation & evaluation, J. Appl. Meteorol. Climatol., 47, 1038–1060, 2008b.

Qu, W.,. Henderson-Sellers, A., Pitman, A., Chen, T.H., Abramopoulos, F., Boone, A., Chang, S., Chen, F., Dai, Y., Dickinson, R.E., Dumenil, L., Ek, M., Gedney, N., Gusev, Y.M., Kim, J., Koster, R., Kowalczyk, E.A., Lean, J., Lettenmaier, D., Liang, X., Mahfouf, J.-F., Mengelkamp, H.-T., Mitchell, K., Nasonova, O.N., Noilhan, J., Robock, A., Rosenzweig, C., Schaake, J., Schlosser, C.A., Schulz, J.-P., Shmakin, A.B., Verseghy, D.L., Wetzel, P., Wood, E.F., Yang, Z.-L., Zeng, Q.: Sensitivity of latent heat flux from PILPS land-surface schemes to perturbations of surface air temperature, J. Atmos. Sci., 55, 1909–1926, 1998.

Raupach, M.R.: Simplified expressions for vegetation roughness length and zero-plane displacement, Bound. Layer Meteorol., 71, 211–216, 1994.

Raupach, M.R.: Corrigenda, Bound. Layer Meteorol., 76, 303–304, 1995.

Roth, M.: Review of atmospheric turbulence over cities, Q. J. Roy. Meteorol. Soc., 126, 941–990, 2000.

Rowley, F.B., Algren, A.B. and Blackshaw, J.L.: Surface conductances as affected by air velocity, temperature and character of surface. ASHRAE Trans., 36, 429–446, 1930.

Savijärvi, H.: Fast radiation parameterization schemes for mesoscale and short-range forecast models, J. Appl. Meteorol., 29, 437–447, 1990.

Sailor, D.J. and Lu, L.A.: top-down methodology for developing diurnal and seasonal anthropogenic heating profiles for urban areas. Atmos. Environ., 38, 2737–2748, 2004.

Saitoh, T.S., Shimada, T. and Hoshi, H.: Modeling and simulation of the Tokyo urban heat island, Atmos. Environ., 30, 3431–3442, 1996.

Sakakibara, Y.: A numerical study of the effect of urban geometry upon the surface energy budget, Atmos. Environ., 30, 487–496, 1996.

Schlosser, C.A., Slater, A.G., Robock, A., Pitman, A., Vinnikov, K.Y., Henderson-Sellers, A., Speranskaya, N.A. and Mitchell, K.: PILPS 2(D) Contributers: Simulations of a Boreal Grassland Hydrology at Valdai, Russia: PILPS Phase 2(d), Mon. Wea. Rev., 128, 301–321, 2000.

Shao, Y. and Henderson-Sellers, A.: Modeling soil moisture : a project for intercomparison of land surface parameterization schemes Phase 2(b), JGR, 101, 7227–7250, 1996.

Shashua-Bar, L. and Hoffman, M.E.: The Green CTTC model for predicting the air temperature in small urban wooded sites, Build. Environ., 37, 1279–1288, 2002.

Shashua-Bar, L. and Hoffman, M.E.: Quantitative evaluation of passive cooling of the UCL microclimate in hot regions in summer, Build. Environ., 39, 1087–1099, 2004.

Sievers, U.: Verallgemeinerung der Stromfunktionsmethode auf drei Dimensionen, Meteorol. Zeitschrift, N.F. 4, 3–15, 1995.

Stephens, G.L.: Radiation profiles in extended water clouds. II: Parameterization schemes, J. Atmos. Sci., 35, 2123–2132, 1978.

Taha, H.: Modifying a mesoscale meteorological model to better incorporate urban heat storage: A bulk parameterization approach, J. Appl. Meteorol., 38, 466–473, 1999.

Tanimoto, J., Hagishima, A. and Chimklai, P.: An approach for coupled simulation of building thermal effects and urban climatology, Energy Build., 36, 781–793, 2004.

Tian, W., Wang, Y., Xie, Y., Wu, D., Zhu, L. and Ren, J.: Effect of building integrated photovoltaics on microclimate of urban canopy layer, Build. Environ., 42, 1891–1901, 2007.

Tso, C.P., Chan, B.K. and Hashim, M.A.: Analytical solutions to the near-neutral atmospheric surface energy balance with and without heat storage for urban climatological studies, J. Appl. Meteorol., 30, 413–424, 1991.

UN: http://www.un.org/esa/population/publications/wup2003/2003Highlights.pdf. accessed 10/27/2004.

Watson, R.T., Zinyowera, M.C. and Moss, R.H.: The Regional Impacts of Climate Change An Assessment of Vulnerability, http://www.grida.no/climate/ipcc/regional/index.htm [last accessed 8 Aug 2007] 1997.

Yang, Z.-L. and Dickinson, R.E.: Preliminary study of spin-up processes in land surface models with the first stage data of Project for Intercomparison of Land Surface Parameterization Schemes Phase 1(a), JGR, 100, 16553–16578, 1995.

Zilitinkevich, S.S.: Non-local turbulent transport: pollution dispersion aspects of coherent structure of convective flows. In: H. Power, N. Moussiopoulos, and C.A. Brebbia (eds.), Air pollution III – Volume I. Air pollution theory and simulation, Computational Mechanics Publications, Southampton, Boston, 53–60, 1995.

Zilitinkevich, S.S., Baklanov, A.A., Mammarella, I. and Joffre, S.M.: The effect of stratification on the surface resistance for very rough vegetated and urban surfaces. In: 6th International Conference on Urban Climate, June 12–16, Goteborg, Sweden, ISBN-10:91-613-9000-1, pp. 415–418, 2006 (submitted to Bound.-Layer Meteorol.).

Chapter 12
Measuring Meteorology in Urban Areas – Some Progress and Many Problems

Sven-Erik Gryning and Ekaterina Batchvarova

Abstract Examples of the use of remote sensing with relevance for the urban boundary layer are presented as an inspiration for future observational studies in urban areas. The examples, involve the measurement of: the vertical wind profile and horizontal variability of the mean wind speed over a forest; and the depth of the marine boundary layer. Research radio-soundings are an indispensable tool in observational campaigns.

12.1 Introduction

The temporal and spatial variability of meteorological measurements inside the boundary layer constitute major obstacles in the interpretation of the observations. In numerical models properties are averaged over the grid cells; however, grid cells usually cover several types of terrain. Turbulence and wind interact in a non-linear way to changes in the underlying surface (Batchvarova et al., 2001), consequently even over seemingly homogeneous terrain variations in the turbulence can be considerable. Despite these fundamental difficulties in the interpretation of measurements, the thrust of experimental research in the field of boundary layer meteorology has been fuelled by point measurements.

Following Batchvarova and Gryning (2006) Fig. 12.1 shows a schematic sketch of a slice of an urban area with indication of the scales and their regimes. It looks complicated but nevertheless constitutes a considerable simplification. The roughness sub-layer (Fig. 12.1) is complicated as the turbulence varies in space and time in an erratic manner. The dispersive stress, being the transport of momentum by spatial fluctuations, is considerable and is expected to be larger when the roughness elements have non-uniform sizes. It increases towards the ground which can be

S.-E. Gryning (✉)
Risø National Laboratory/DTU, Roskilde, Denmark
e-mail: sven-erik.gryning@risoe.dk

A. Baklanov et al. (eds.), *Meteorological and Air Quality Models for Urban Areas*,
DOI 10.1007/978-3-642-00298-4_12,

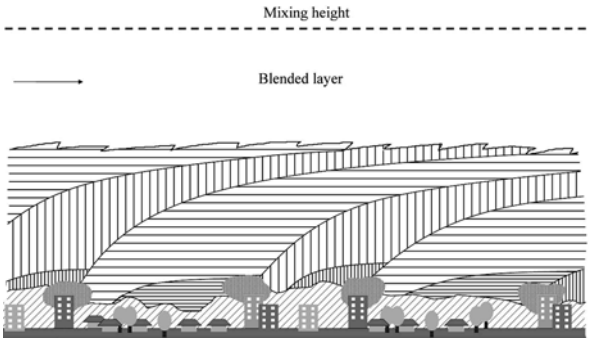

Fig. 12.1 Schematics of the boundary layer structure over an urban area. The vertical and horizontal patterns represent the underlying surface of the neighbourhoods of tall and low buildings, respectively. Broad spaced patterns represent the urban internal boundary layers where advection processes are important. Fine spaced patterns show the inertial sublayers that are in equilibrium with the underlying surface and where Monin-Obukhov scaling applies. The forward slash pattern represents the roughness sublayer that is highly inhomogeneous both in its vertical and horizontal structure. The dotted pattern represents adjustment zones between neighbourhoods with large accelerations and shear in the flow near the top of the canopy. Above the height where the internal boundary layers are intermixed the effects of the individual neighbourhoods cannot be distinguished any more – the so-called blended layer

taken as a dynamical definition of the depth of the roughness sub-layer. Thus point measurements in urban areas can be problematic.

The height of the roughness sub-layer is generally considered to be 3–5 times the building height (Fig. 12.2). In many experimental campaigns the meteorological masts in urban areas are placed on top of buildings reaching rarely beyond one or two building heights so are typically within the roughness sub-layer. Interpretation of the measurements therefore, should be done in the framework of roughness sublayer considerations, as surface layer theory as Monin-Obukhov similarity is not applicable (see also Feddersen, B., 2005).

Fig. 12.2 **(a)** Mast in the BUBBLE experiment (Rotach et al., 2004) where measurements represent the roughness sub-layer. **(b)** Copenhagen experiment (Gryning and Lyck, 1984) where the measurements were performed above the roughness sub-layer

In the hope to serve as inspiration for future measurements in urban areas some results from a campaign over a forest using wind LiDAR are presented. There are many similarities in the structure of the turbulence and wind field over a forest and an urban area, but it should be noted that inside the forest canopy and street canyons the conditions are very different. The forest campaign took place in 85 year old beech forest on the island of Zealand (Denmark). The area is flat. The beech trees are on the average 25 m tall with scattered stands of conifers. The displacement height is 20.6 m and the roughness length 1.8 m (Dellwik and Jensen, 2005).

A wind LiDAR was installed on a mast 40 m above ground and 15 m above the trees. It consists of a focused continuous wave laser beam scanning conically at an angle of ≈30°. The instrument measures the Doppler-shift of the light backscatter signal which comes from particles in the atmosphere, and this is then transformed into a horizontal and vertical wind velocity. Figure 12.3 shows an example of a half hourly averaged wind profile above the forest. It can be seen that the wind profile is smooth with an indication of a jump at ≈90 m.

The corresponding wind direction is shown in Fig. 12.4. Over the main part of the profile except at the lowest level, a weak clockwise turning (veering) can be observed in accordance with the Ekman spiral. The turning over the whole layer is about 3.5° which is about the same as the uncertainty for wind direction measurements by wind vanes. It should be noted that the above wind direction profile could not have been detected in measurements from a tall mast equipped with a dense profile of wind vanes.

More interesting, however, are the results when the wind LiDAR was shooting horizontally over the forest, in this case in a range between 20 and 60 m from the LiDAR, 15 m above the 25 m tall trees. Two examples are shown averaged over half an hour for high and low wind speed conditions (Fig. 12.5). A considerable variability in the mean wind speed in a range of only 40 m can be observed, ranging from 9.3 to 10.6 m s^{-1} for the high and from 1.5 to 2.1 m s^{-1} for the low wind speed case. Similar plots from the campaign show a comparable

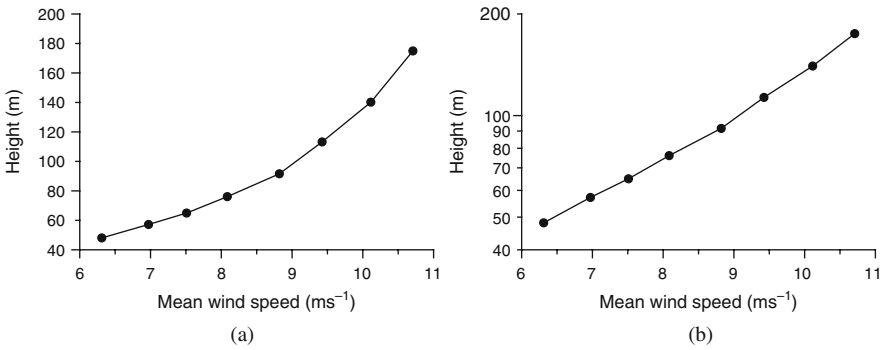

Fig. 12.3 Wind profile (m s^{-1}) above a 25 m high forest as a function of height on the **(a)** linear and **(b)** logarithmic scales

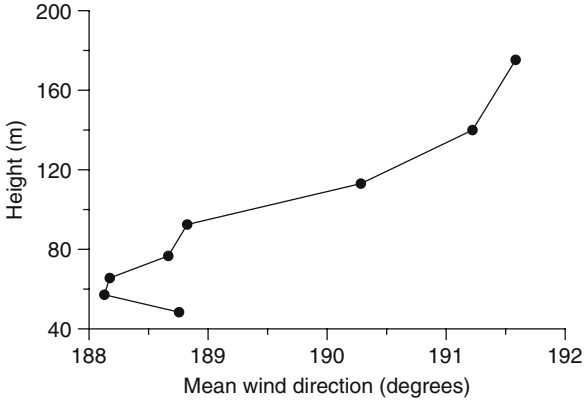

Fig. 12.4 Mean wind direction above a 25 m high forest

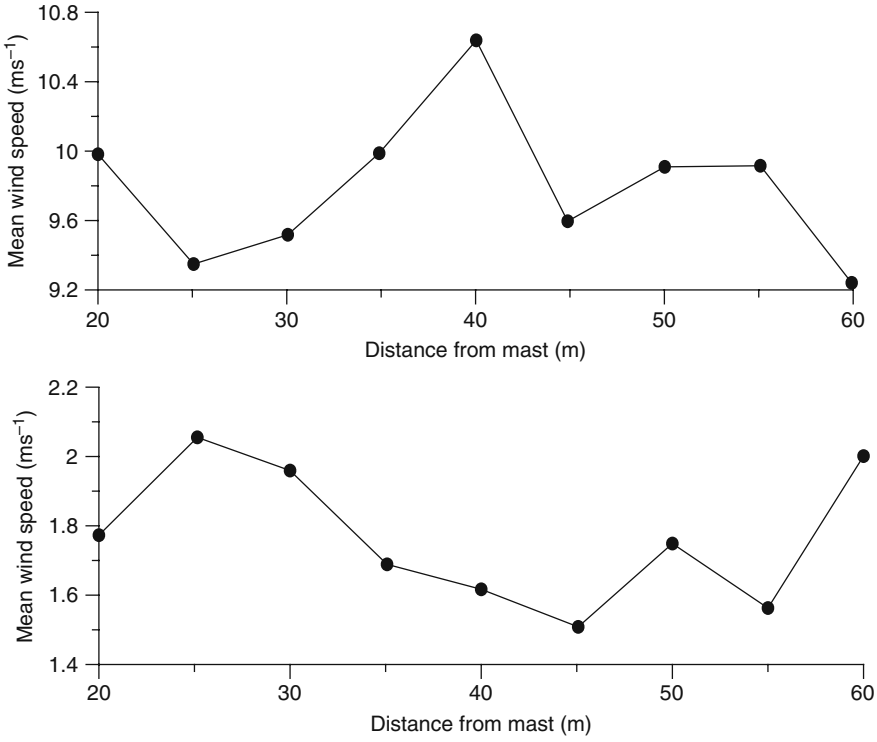

Fig. 12.5 Horizontal variability of the mean wind speed at 40 m above the ground in a 25 m high forest: high wind conditions (*upper panel*) and low wind conditions (*lower panel*)

variability in the spatial wind field and without a systematic horizontal pattern. It would be very interesting in a similar way to study the vertical wind profile and horizontal variability of the wind over the roofs of buildings in an urban area.

12.2 The Height of the Boundary Layer

The best way to estimate the height of the boundary layer is from profiles of turbulence, momentum and heat flux, but this is generally not possible because meteorological masts do not reach far enough into the boundary layer except under special conditions. The height of the boundary layer is a parameter that despite its obvious importance (Gryning et al., 1987) is often unfairly treated or even neglected in experimental campaigns. This also holds for campaigns in urban areas. Nevertheless it is an important meteorological parameter in the urban context because the behaviour and characteristics of the urban boundary layer are quite different from the usual perception over rural terrain, the main difference being the rarity of stable conditions in a wide range of urban settlements.

The use of a remote sensing for routine measurements of the boundary layer height is an interesting challenge. The ceilometer is a new not yet fully explored instrument for boundary layer depth measurements. It is an inexpensive and sturdy instrument originally developed for routine cloud height observations, consisting of a vertically pointing laser and a receiver in the same location. It determines profiles by measuring the time required for a pulse of light to be scattered back from the particles in the air. Since the instrument will note any returns, it is possible to determine particle profiles by looking at the whole pattern of returned energy. This has been developed in research and could be applied for operational purposes. Assuming that particles within the boundary layer originate from the ground and that the particle concentration above the boundary layer is comparatively small, the height of the boundary layer can be determined from particle profiles measures by a ceilometer.

In the Galathea expedition (http://www.galathea.nu/) a ceilometer was used successfully to determine the depth of the marine boundary layer (Fig. 12.6). The measurements were performed in the up welling zone west of Namibia. It can be seen that the marine boundary layer is shallow, having a depth of about 200 m. Part of the time atmospheric waves form on the top of the boundary layer. Obviously the sea-spray is confined to the boundary layer and does not penetrate up into the free atmosphere, constituting near ideal conditions for measurements of the depth of the boundary layer by use of a ceilometer. The traditional way of measuring the boundary layer height (Fig. 12.6c,d,e) is to look for jumps in the profiles from radiosoundings; especially in the potential temperature, but also humidity and wind speed and direction, and the variability of the wind direction. In the radiosoundings performed outside Namibia the top of the boundary layer is made known by 15 K increase of

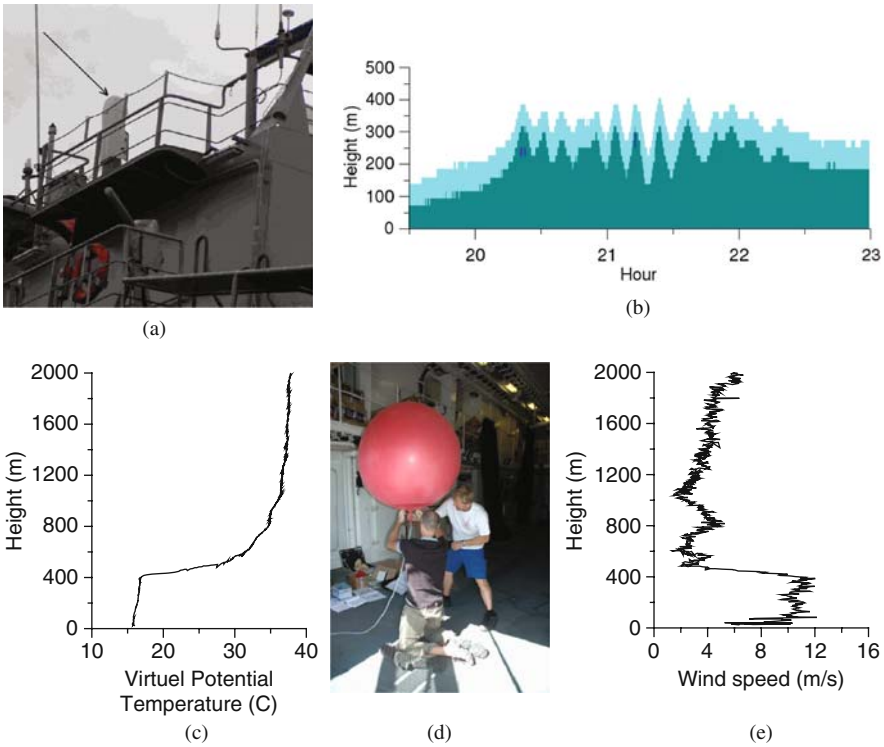

Fig. 12.6 **(a)** Ceilometer (*arrow*) mounted on the research ship Galathea; **(b)** An example of boundary layer structure measured by the ceilometer during the Galathea expedition. The darker is the colour the higher is the particle concentration. **(c, e)** Radiosonde profiles taken with **(d)** during the same event

potential temperature and a simultaneous decrease of the wind speed from 11 to 3 m s^{-1}, ideal conditions for the formation of waves (Fig. 12.6).

12.3 Conclusions

Examples of the use of remote sensing with relevance to the urban areas are presented. The technique offers possibility to measure the horizontal variability of the mean wind in the roughness sub-layer over an urban area as well as the wind profile at a specific location. These can add valuable insight into the structure of the urban boundary layer. The use of remote sensing to estimate the depth of the marine boundary layer has proven to be very successful. Radiosounding is still an indispensable tool in boundary layer research adding valuable information not available from other instruments.

Acknowledgments The authors thank Ebba Dellwik for the figures from the forest campaign. The work is related to activities of the authors within COST-728, COST-732, and COST-735.

References

Batchvarova, E., Gryning, S.E.: Progress in urban dispersion studies. Theor. Appl. Climatol. 84, 57–67, 2006.

Batchvarova, E., Gryning, S.-E., Hasager, C.B.: Regional fluxes of momentum and sensible heat over a sub-arctic landscape during late winter. Boundary-Layer Meteorol. 99, 489–507, 2001.

Dellwik, E., Jensen, N.O.: Flux-profile relationships over a fetch limited beech forest. Boundary-Layer Meteorol. 115, 179–204, 2005.

Feddersen, B.: Wind tunnel modelling of turbulence and dispersion above tall and highly dense urban roughness. Diss., Naturwissenschaften, Eidgenössische Technische Hochschule ETH Zürich, Nr. 15934, 2005.

Gryning, S.E., Lyck, E.: Atmospheric dispersion from elevated sources in an urban area: Comparison between tracer experiments and model calculations. J. Climate Appl. Meteorol. 23, 651–660, 1984.

Gryning, S.-E., Holtslag, A.A.M., Irwin, J.S., Sivertsen, B.: Applied dispersion modelling based on meteorological scaling parameters. Atmos. Environ. 21, 79–89, 1987.

Rotach, M.W., Gryning, S.E., Batchvarova, E., Christen, A., Vogt, R.: Pollutant dispersion close to an urban surface – the BUBBLE tracer experiment. Meteorol. Atmos. Phys. 87, 39–56, 2004.

Chapter 13
Derivation of Vertical Wind and Turbulence Profiles, the Mixing-Layer Height, and the Vertical Turbulent Exchange Coefficient from Sodar and Ceilometer Soundings in Urban Measurement Campaigns

Stefan Emeis

Abstract Vertical profiles of the mean wind speed, the variance of the vertical wind component, and the turbulence intensity from sodar measurements over urban areas are presented. These profiles show typical urban features due to the increased roughness and the increased heat storage of the urban surface. The mixing layer height derived from combined sodar and ceilometer measurements is shown. Vertical profiles of the turbulent viscosity (or vertical turbulent exchange coefficient) are analysed from sodar data. All these data can serve in the evaluation and verification of results from regional numerical weather prediction and climate models.

13.1 Introduction

The urban heat island (UHI) is an important meteorological feature of large cities. It influences the ventilation, the air quality, and the climate inside the built-up areas as well as the interaction of the urban environment with its surroundings (Crutzen, 2004). Long-term in-situ measurements of vertical profiles and turbulent fluxes within the UHI several hundreds of metres above ground are not possible. Therefore, models (Batchvarova and Gryning, 2006) and ground-based remote sensing (Grimmond, 2006) must fill this gap. Remote sensing data will be the basis for evaluation and verification of the model results. Long-term remote sensing measurement campaigns have been made so far over only very few cities. Wind and turbulence profiles for Hanover, Linz (Austria), and Moscow (Russia) are shown in Emeis (2004a), Emeis et al. (2007a), and Lokoshchenko et al. (2007). Mixing layer height (MLH) statistics for Moscow and Hanover are available in Lokoshchenko (2002) and Emeis and Türk (2004). MLH has important implications for urban air quality (Emeis and Schäfer, 2006; Schäfer et al., 2006; Piringer et al., 2007).

S. Emeis (✉)
Institute for Meteorology and Climate Research, Atmospheric Environmental Research (IMK-IFU), Forschungszentrum Karlsruhe GmbH, Garmisch-Partenkirchen, Germany
e-mail: stefan.emeis@imk.fzk.de

A. Baklanov et al. (eds.), *Meteorological and Air Quality Models for Urban Areas*,
DOI 10.1007/978-3-642-00298-4_13,

Remote measurements of turbulent viscosity are only available for complex rural terrain (Campistron et al., 1991; Emeis, 2004b; Kouznetsov et al., 2007) and not for urban areas. However the ability of remote sensing of turbulent viscosity is closely related to the ability of remote sensing of vertical turbulent fluxes (see e.g. Engelbart et al., 2007).

Here typical results for profiles, MLH, and turbulent viscosity from optical and acoustic ground-based remote sensing from some of the above mentioned studies and further measurements made in Budapest (Hungary) and Paris (France) are presented.

13.2 Results

13.2.1 Profiles and Diurnal Variation of Mean Wind Speed

Monthly mean wind speed profiles have been measured by a sodar over Hanover (Germany) (Emeis, 2004a), Budapest (Hungary) (Fig. 13.1), and at Charles de Gaulle airport near Paris (France) (Fig. 13.2). A typical feature of all these profiles is the strong vertical wind speed shear in the first hundreds of metres above ground due to the large surface roughness of cities.

The diurnal variation of wind speed at several heights above ground (Emeis, 2004a; Fig. 13.1a) is also derived from this dataset. The usual nocturnal decrease of wind speed near the ground (at about from 50 to 100 m height) is missing or, at least, considerably reduced over cities because a higher nocturnal level of turbulence. This turbulence is due to the larger surface roughness, and the reduced thermal stability is due to the larger heat storage of cities.

13.2.2 Profiles and Diurnal Variation of the Variance of the Vertical Wind Component

Mean vertical profiles of the variance of the vertical wind component over Hanover, Budapest (Fig. 13.3), and Paris (Fig. 13.4) have been derived from sodar measurements. The square of this variance describes one part of the turbulent kinetic energy (TKE) contained in the air. If the turbulence is isotropic it describes just one third of TKE. A typical feature in the urban boundary layer (UBL) is the increase of this variance with height even at night time in a layer which is several hundred metres deep. For the lower 100 m this indicates that the UBL often has a very unstable thermal stratification. Above this near-surface layer the increase of the variance continues, especially in spring and summer, due to the frequent occurrence of low-level jets which produce mechanical turbulence through the large wind speed shear underneath of them. The nocturnal production of mechanical turbulence had been

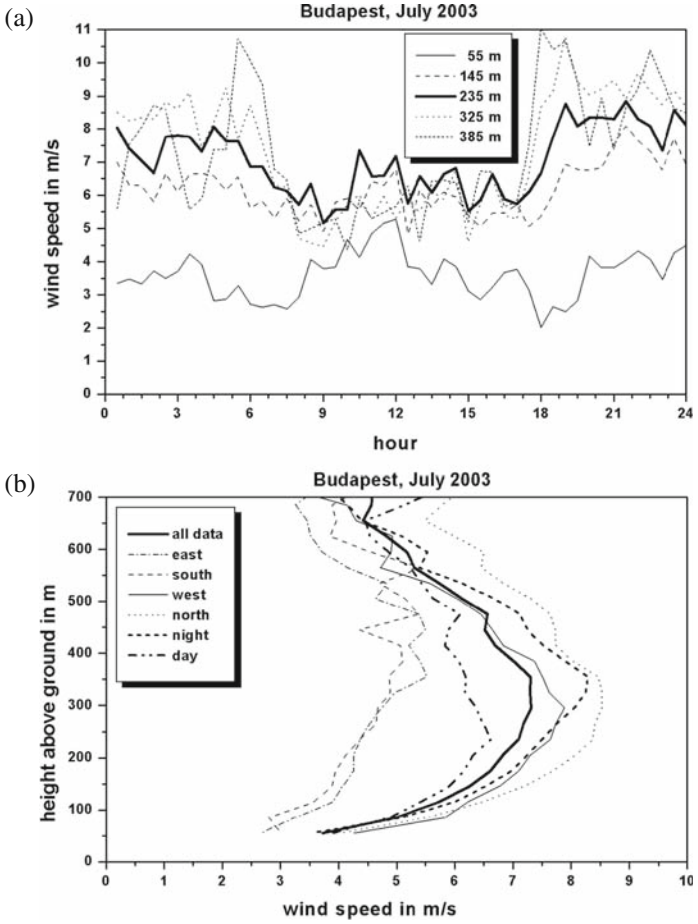

Fig. 13.1 Monthly mean wind speed over Budapest in July 2003: **(a)** diurnal variation and **(b)** vertical profiles

proven for the first time from sodar measurements by Reitebuch et al. (2000). This turbulence is essential for urban air quality because it mixes ozone and other air pollutants downward from the residual layer (Sect. 13.2.3, Fig. 13.5) into the nocturnal surface layer. The nocturnal increase of near-surface ozone concentrations is documented in Reitebuch et al. (2000) and Alföldy et al. (2007). This special feature of the vertically increasing variance is an example for the interaction of the UBL, which is coined by enhanced turbulence, with a typical nocturnal phenomenon of the rural boundary layer, the low-level jet.

From Fig. 13.4 it is clearly visible that the variance of the vertical wind component of air coming from built-up areas is considerably larger than in air coming from rural areas. The diurnal variation of the variance of the vertical wind component

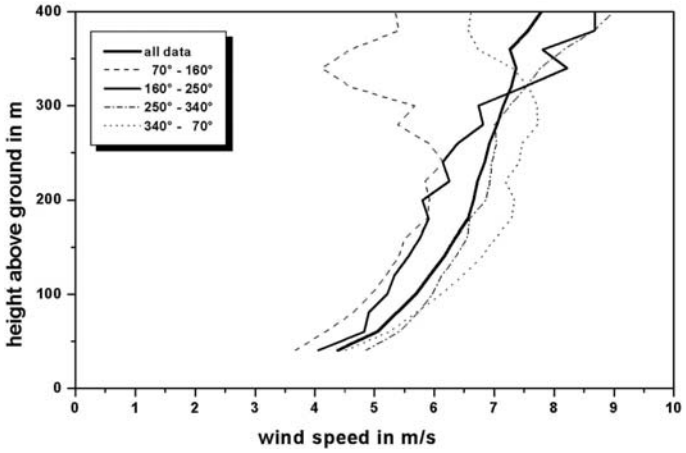

Fig. 13.2 Wind profiles measured by sodar at CDG airport. Winds from the sector 160–250° (*thin full line*) are from built-up areas (airport infrastructure) only, winds from 340–70° (*dotted line*) are from rural areas only

from sodar measurements is shown in Fig. 13.3a. The nocturnal level of this variance is considerably higher than over rural terrain.

13.2.3 Stratification of the Urban Boundary Layer and Mixing-Layer Height

The combined use of acoustic (sodar) and optical (ceilometer, i.e. a mini-lidar) remote sensing allows analysing the diurnal variation of the vertical structure of the entire UBL and the MLH over Budapest (Fig. 13.5). The lidar easily reaches heights of 3000 m and more while the maximum vertical range for the sodar is only 1300 m. Figure 13.5 shows for four summer days the diurnal variation in the occurrence of the nocturnal stable boundary layer (SBL), the daytime convective boundary layer (CBL), and the residual layer (RL) which is left aloft after the formation of a new stable layer near the ground in the evening. It is this residual layer where for example ozone survives during the night until it is mixed downward again on the next morning when the new CBL grows.

Long-term measurements like in Hanover allow statistical evaluations of MLH (Fig. 13.6). The MLH is an important parameter which determines and limits the dilution of freshly emitted pollutants. The mean diurnal variation of MLH shows a clear annual variation. The variation is largest in spring and summer months and nearly vanishes in late autumn. Details of the MLH estimation from remote sensing data are given in Emeis and Türk (2004), Emeis et al. (2007b) and Emeis et al. (2008). Recommendations from the COST-715 Action with respect to MLH are documented in Piringer et al. (2007).

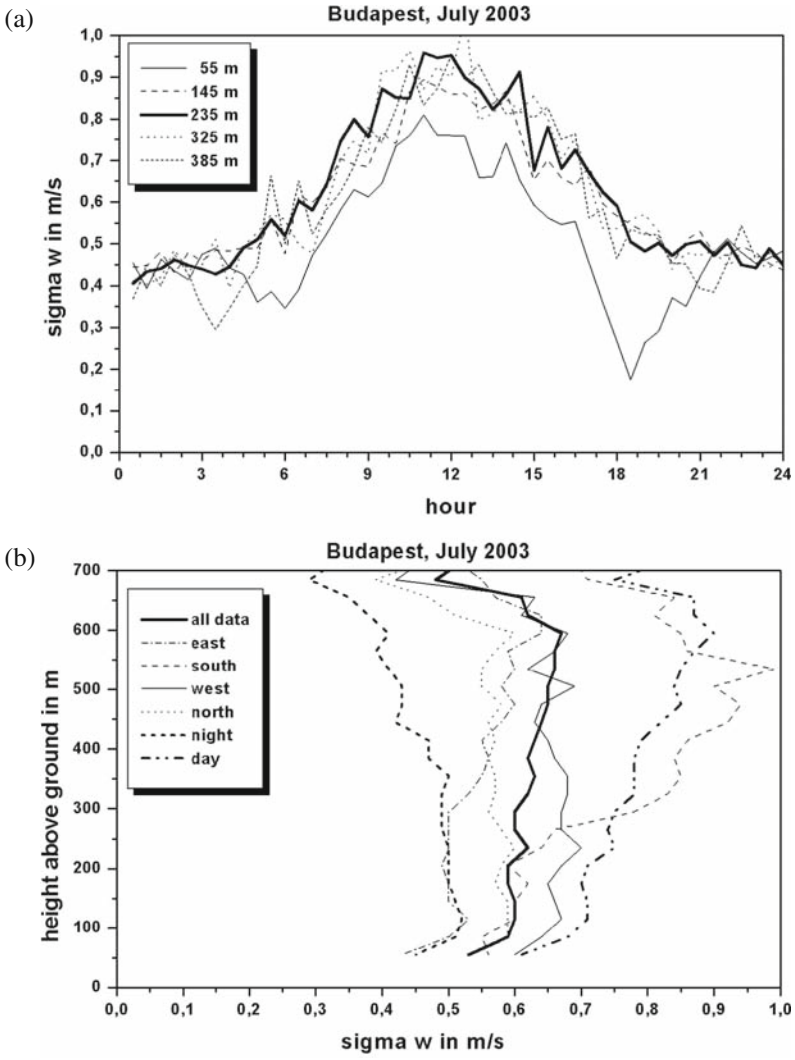

Fig. 13.3 Variance of vertical wind component over Budapest **(a)** diurnal cycle and **(b)** with height

13.2.4 Turbulent Viscosity

An important variable in turbulence parameterizations for mesoscale numerical models is the vertical turbulent exchange coefficient. This quantity is identical to the turbulent viscosity of the atmosphere. An attempt to derive the vertical profile of the vertical turbulent exchange coefficient from sodar measurements is displayed in Fig. 13.7. Theoretically, the turbulent viscosity could be derived from the ratio of the vertical turbulent momentum flux and the mean vertical wind speed gradient.

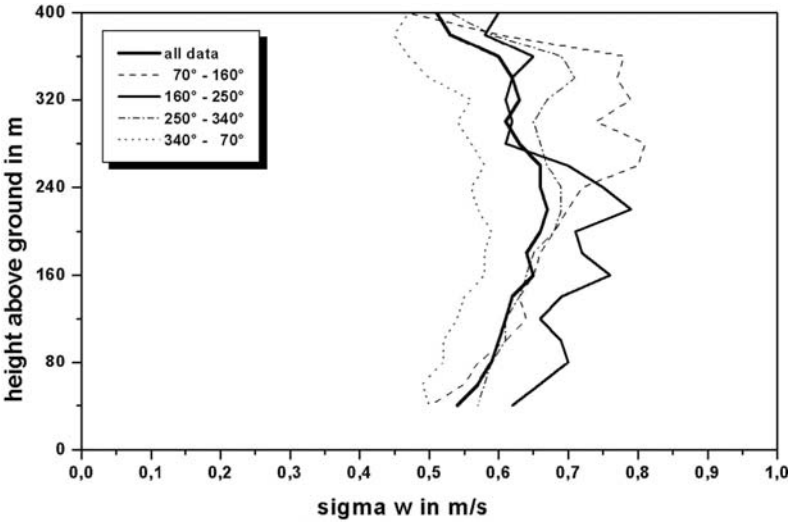

Fig. 13.4 Variance of the vertical wind component over Paris CDG airport. Winds from the sector 160–250° (*thin full line*) are from built-up areas (airport infrastructure), winds from 340–70° (*dotted line*) are from rural areas only

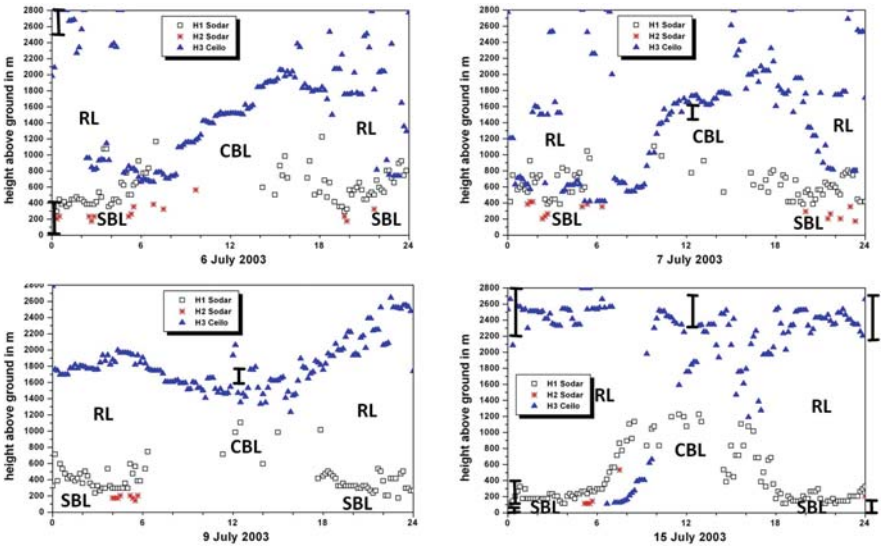

Fig. 13.5 Vertical structure of the entire boundary layer over Budapest on typical summer days from simultaneous measurements with a sodar (*open squares and asterisks*) and a ceilometer (*triangles*) from Emeis and Schäfer (2006) RL denotes "residual layer", SBL "stable boundary layer" and CBL "convective boundary layer"

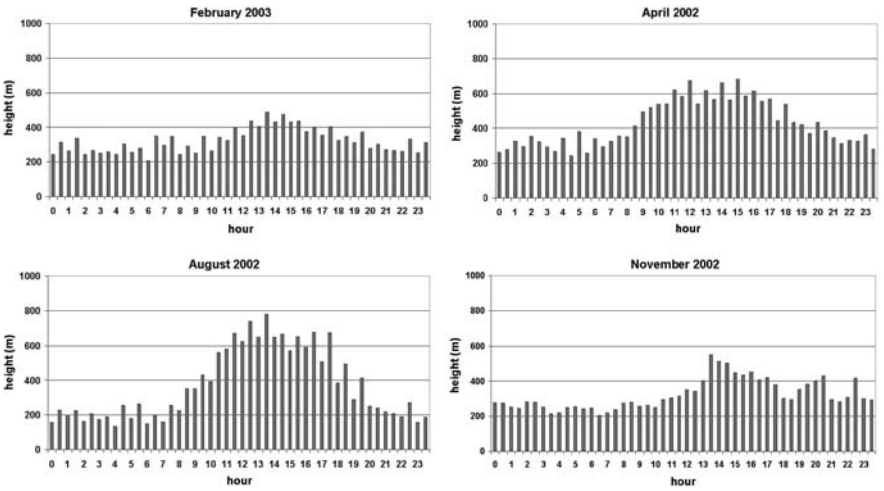

Fig. 13.6 Mean diurnal variation of mixing layer height over Hannover for four months from sodar data (from Emeis and Türk, 2004)

Only the latter quantity is directly available from sodar measurements. For the profiles shown in Fig. 13.7 the vertical turbulent momentum flux has been assumed to be proportional to the variance of the vertical wind component. Details of the determination of the turbulent viscosity are given in Emeis (2004b).

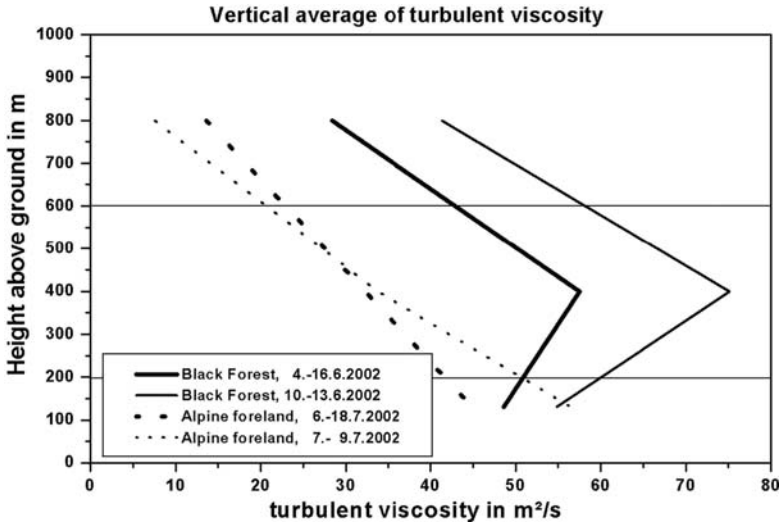

Fig. 13.7 Estimated vertical profiles of the vertical turbulent exchange coefficient over level and highly complex terrain from sodar measurements (from Emeis, 2004b)

13.3 Conclusions and Outlook

The paper has shown that ground-based acoustic remote sounding with a sodar can give detailed information on the vertical profiles of wind and turbulence in the urban boundary layer (UBL). Together with optical remote sensing from a celiometer, the height of the mixing layer can be determined. From long-term measurement campaigns with these instruments characteristic and important features of UBL have been documented. Especially the turbulence profiles show, partly in interaction with the surrounding rural boundary layer, significant peculiarities. Therefore, these existing remote sensing data from UBLs form an important data set for the evaluation and verification of numerical simulations for UBL. They can also help to formulate proper parameterizations for an urbanization of the models.

Ground-based remote sensing is presently still a developing subject. The application of radio-acoustic sounding systems (RASS) can bring measurements of vertical temperature profiles (Emeis et al. 2009). A comparison of simultaneous measurements with a sodar, a ceilometer, and a RASS can be found in Emeis et al. (2004). Currently under development are measurement and data evaluation strategies to measure turbulent fluxes by remote sensing (Engelbart et al., 2007 and Kouznetsov et al., 2007). A rather new line of development is the measurement of boundary layer winds with optical remotes sensing (Emeis et al., 2007c).

References

Alföldy, B., J. Osán, Z. Tóth, S. Török, A. Harbusch, C. Jahn, S. Emeis, K. Schäfer, 2007: Aerosol optical depth, aerosol composition and air pollution during summer and winter conditions in Budapest. Sci. Total Environ., 383, 141–163. DOI: 10.1016/j.scitotenv.2007.04.037.

Batchvarova, E., S.-E. Gryning, 2006: Progress in urban dispersion studies. Theor. Appl. Climatol., 84, 57–67.

Campistron, B., A.W. Huggins, A.B. Long, 1991: Investigations of a winter mountain storm in Utah. Part III: Single-Doppler radar measurements of turbulence. J. Atmos. Sci. 48, 1306–1318.

Crutzen, P.J., 2004: New Directions: The growing urban heat and pollution "island" effect – impact on chemistry and climate. Atmos. Environ., 38, 3539–3540.

Emeis, S., 2004a: Vertical wind profiles over an urban area. Meteorol. Z., 13, 353–359. DOI: 10.1127/0941-2948/2004/0013-0353.

Emeis, S., 2004b: Parameterization of turbulent viscosity over orography. Meteorol. Z., 13, 33–38. DOI: 10.1127/0941-2948/2004/0013-0033.

Emeis, S., K. Schäfer, 2006: Remote sensing methods to investigate boundary-layer structures relevant to air pollution in cities. Bound-Layer. Meteorol., 121, 377–385. DOI: 10.1007/s10546-006-9068-2.

Emeis, S., M. Türk, 2004: Frequency distributions of the mixing height over an urban area from SODAR data. Meteorol. Z., 13, 361–367. DOI: 10.1127/0941-2948/2004/0013-0361.

Emeis, S., Chr. Münkel, S. Vogt, W.J. Müller, K. Schäfer, 2004: Atmospheric boundary-layer structure from simultaneous SODAR, RASS, and ceilometer measurements. Atmos. Environ., 38, 273–286. DOI: 10.1016/j.atmosenv.2003.09.054.

Emeis, S., K. Baumann-Stanzer, M. Piringer, M. Kallistratova, R. Kouznetsov, V. Yushkov, 2007a: Wind and turbulence in the urban boundary layer – analysis from acoustic remote sensing data and fit to analytical relations. Meteorol. Z., 16, 393–406, DOI: 10.1127/0941-2948/2007/0217.

Emeis, S., C. Jahn, C. Münkel, C. Münsterer, K. Schäfer, 2007b: Multiple atmospheric layering and mixing-layer height in the Inn valley observed by remote sensing. Meteorol. Z., 16, 415–424, DOI: 10.1127/0941-2948/2007/0203.

Emeis, S., M. Harris, R.M. Banta, 2007c: Boundary-layer anemometry by optical remote sensing for wind energy applications. Meteorol. Z., 16, 337–347. DOI: 10.1127/0941-2948/2007/0225.

Emeis, S., Schäfer K., and Münkel C., 2008: Surface-based remote sensing of the mixing-layer height – a review. Meteorol Z., 17, 621–630. DOI: 10.1127/0941-2948/2008/0312.

Emeis, S., Schäfer K., and Münkel C., 2009: Observation of the structure of the urban boundary layer with different ceilometers and validation by RASS data. Meteorol. Z., 18, 149–154. DOI: 10.1127/0941-2948/2009/0365.

Engelbart, D., M. Kallistratova, R. Kouznetsov, 2007: Determination of the Turbulent Fluxes of Heat and Momentum in the ABL by Ground-Based Remote-Sensing Techniques (a Review). Meteorol. Z., 16, 325–335. DOI: 10.1127/0941-2948/2007/0224

Grimmond, C.S.B., 2006: Progress in measuring and observing the urban atmosphere. Theor. Appl. Climatol., 84, 3–22.

Kouznetsov, R., V. Kramar, M. Kallistratova, 2007: The vertical structure of turbulent momentum flux in the lower part of the atmospheric boundary layer. Meteorol. Z., 16, 367–373. DOI: 10.1127/0941-2948/2007/0205.

Lokoshchenko, M., 2002: Long-term sodar observations in Moscow and a new approach to potential mixing determination by Radiosonde data. J. Atmos. Oceanic Technol. 19, 1151–1162.

Lokoshchenko, M., V.G. Perepelkin, N.V. Semenova, 2007: Standard deviation of the wind vertical component and its dynamics in Moscow by the sodar data. Meteorol. Z., 16, 407–418. DOI: 10.1127/0941-2948/2007/0209.

Piringer, M., S. Joffre, A. Baklanov, A. Christen, M. Deserti, K. De Ridder, S. Emeis, P. Mestayer, M. Tombrou, D. Middleton, K. Baumann-Stanzer, A. Dandou, A. Karppinen, J. Burzynski, 2007: The surface energy balance and the mixing height in urban areas – activities and recommendations of COST-Action 715. Bound.-Layer Meteorol., 124, 3–24. DOI: 10.1007/s10546-007-9170-0.

Reitebuch, O., A. Straßburger, S. Emeis, W. Kuttler, 2000: Nocturnal secondary ozone concentration maxima analysed by SODAR observations and surface measurements. Atmos. Environ., 34, 4315–4329. DOI: 10.1016/S1352-2310(00)00185-0.

Schäfer, K., S. Emeis, H. Hoffmann, C. Jahn, 2006: Influence of mixing layer height upon air pollution in urban and sub-urban areas. Meteorol. Z., 15, 647–658. DOI: 10.1127/0941-2948/2006/0164.

Chapter 14
Verification and Case Studies for Urban Effects in HIRLAM Numerical Weather Forecasting

Alexander Mahura, Alexander Baklanov, Claus Petersen, Niels W. Nielsen, and Bjarne Amstrup

Abstract In our study, the performance of the DMI HIgh Resolution Limited Area Models (HIRLAM)-U01/I01 research models (1.4 km horizontal resolution) with simple (urban roughness and anthropogenic heat flux) and complex (building effects parameterizations) urbanization were tested and verified. The simulations of the DMI-HIRLAM-U01/I01 without (i.e. the control run) and with the urbanized modules were performed in a short-term mode, i.e. for days with different meteorological conditions (such as typical and low winds), and in a long-term mode on a monthly basis. The comparison of the DMI-HIRLAM urbanized vs. control runs during the same period was performed. Detailed analyses of spatial and temporal variability of simulated conditions such as the wind characteristics, temperature and relative humidity over the metropolitan area of Copenhagen and surroundings were then completed. The diurnal variability of meteorological and derived characteristics over these urban areas was investigated. The verification of these characteristics was performed for selected urban/suburban stations located in the Copenhagen area.

14.1 Introduction

In urban areas, in contrast with rural areas, the boundary layer is more complex, and hence, requires special treatment. The surface energy balance is the major equation used in many models to evaluate thermodynamical and dynamical patterns above the ground surface. This includes storage, sensible, and latent heat fluxes (plus anthropogenic heat flux). Often in these areas the meteorological network is sparse and measurements do not reflect the characteristic meteorological state of the urban terrain (Piringer et al., 2002). Moreover, the fluxes are rarely directly measured at such sites. Observational studies (in North American cities, during summer time) (Grimmond and Oke, 1995) on evaluation of local-scale surface heat fluxes

A. Mahura (✉)
Danish Meteorological Institute, DMI, Lyngbyvej 100, DK-2100, Copenhagen
e-mail: ama@dmi.dk

A. Baklanov et al. (eds.), *Meteorological and Air Quality Models for Urban Areas*,
DOI 10.1007/978-3-642-00298-4_14,

variability have shown that, in general, these have magnitudes and diurnal behaviour similar to rural areas, but within the city itself there are differences between districts of the city.

The goal of our study is to evaluate effects of urbanization of a numerical weather prediction (NWP) model on simulating meteorological fields for specific cases and overall model performance over the urbanized areas. The specific objectives include: (1) perform short- and long-term simulations of meteorological fields using NWP model in two modes: control vs. urbanized runs; (2) evaluate effects of urbanization on temporal-spatial structure and variability of simulated meteorological fields; and (3) estimate the diurnal cycle and the differences between control and urbanized runs for meteorological variables such as air temperature, wind, and relative humidity.

14.2 Methodology

14.2.1 DMI-HIRLAM NWP Modelling and Meteorological Data

The DMI performs daily forecasts of meteorological fields employing the High Resolution Limited Area Model (HIRLAM) model (Unden et al., 2002). The present DMI weather forecasting system (Yang et al., 2005) is based on HIRLAM 7. Since summer of 2004, it consists of two nested models: DMI-HIRLAM-T15 and -S05 (Fig. 14.1a) as well as running also on specific testing and research domains (such -Q05, -L15, -M15 – not shown) covering different regions of the Northern Hemisphere. Previously several nested DMI-HIRLAM models called -G, -N, -E, and -D were run operationally with horizontal resolutions of 0.45, 0.15, 0.15, and 0.05º, respectively (Sass et al., 2002).

The models T15 and S05 are identical, except for the horizontal resolution (15 vs. 5 km) and geographical boundaries of domains. Both versions have 40 verti-

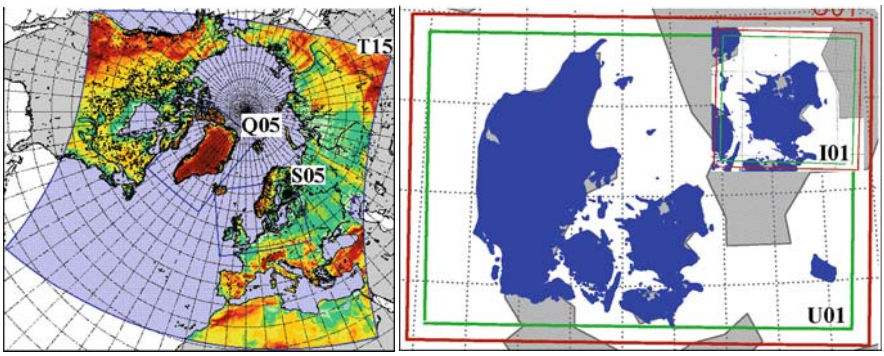

Fig. 14.1 DMI-HIRLAM-NWP modelling domains **(a)** operational -T15 and -S05 and **(b)** research -U01 and -I01

cal layers. The lateral boundary values are received from ECMWF every 6 h. The system is run on NEC-SX6 DMI supercomputer, and the produced model output files are archived on the mass storage system. The current operational DMI forecasting model includes the digital filtering initialization, semi-Lagrangian advection scheme, and a set of physical parameterizations such as Savijaervi radiation, STRACO condensation, CBR turbulence scheme, and ISBA land surface scheme.

Several specific tests and verification of the DMI-HIRLAM-U01/I01 models (Fig. 14.1b) for high resolution (Mahura et al., 2005) and urbanization (Baklanov et al., 2006b; Mahura et al., 2006) were conducted within the FUMAPEX project (Baklanov et al., 2005, 2006a). For these models the preparation of land-use classification based on CORINE dataset (CORINE, 2000) and climate generation files had a resolution of 1.4 km. These on-going research activities are part of the DMI-Enviro-HIRLAM model developments and tests (Mahura et al., 2008).

14.2.2 Approach Based on Improved Urban Roughness and Anthropogenic Fluxes

The simple NWP urbanisation includes modifications of the Interaction Soil Biosphere Atmosphere (ISBA) land surface scheme based on the original proposed by Noilhan and Planton (1989) and updated and used by the DMI-HIRLAM model. The changes include modifications of the urban roughness, anthropogenic heat flux and albedo parameters in grid cells of modelling domains where the urban class is present. The urban roughness changes by up to 2 m when the urban class becomes 100% of a grid-cell. The anthropogenic heat flux is modified similarly, with a maximum value which ranges from 10 to 200 Wm^{-2}. Albedo for the summer varies by factor of two (0.2–0.4) relative to the winter because of snow coverage. This approach is the cheapest way to simulate in operational forecast applications and NWP models with low vertical resolution (i.e. the first computational vertical level is higher than 20 m).

In our study, the urban related modifications of the ISBA land surface scheme are evaluated. Over the grid cells of the modelling domain where, at least, a small fraction of urban related class was presented, the roughness was modified to reflect the urban area presence. The anthropogenic heat fluxes were also added for the same grid cells. A combined contribution of these two features into the formation of airflow over the urban areas was incorporated into the land surface scheme of the model, where the model domain covers the entire territory of Denmark.

14.2.3 Building Effect Parameterization

The Building Effect Parameterization (BEP) module includes the urban sub-layer parameterisation based on the drag term in the main equations suggested by Martilli et al. (2002) with modifications for implementation into NWP models and several further improvements (Hamdi and Shayes, 2007). The aim of the urban sub-layer

parameterisation is to simulate the effect of buildings on meso-scale atmospheric flow. It takes into account the main characteristics of the urban environment: (i) vertical and horizontal surfaces (wall, canyon floor and roofs), (ii) shadowing and radiative trapping effects of the buildings, (iii) anthropogenic heat fluxes through the buildings wall and roof. In this parameterisation, the city is represented as a combination of several urban classes. Each class is characterised by an array of buildings of the same width located at the same distance from each other (canyon width), but with different heights (with a probability of particular heights). To simplify the formulation we assume that the length of the street canyons is equal to the horizontal grid size. The vertical urban structure is defined on a numerical grid.

In our study, the BEP urban module was used to simulate the effects of buildings on atmospheric urban flow taking into account a set of main characteristics of the urban environment. Copenhagen is represented as a combination of several urban classes. Each class is characterized by an array of buildings of the same width located at the same distance from each other, but with different heights.

14.3 Results and Discussions: Sensitivity Tests and Verification for Copenhagen Metropolitan Areas

The DMI-HIRLAM research models -U01 and -I01 (1.4 km resolution) were run for the Copenhagen metropolitan area and surroundings (Fig. 14.1a). Independent runs were performed for several specific cases and in a long-term mode. These included: (1) control run with no modifications in the ISBA surface scheme; and (2) modified urbanised runs including (a) urban roughness and anthropogenic heat fluxes modifications, and (b) building effect parameterization module.

The outputs for specific dates (+24 hour forecast) were evaluated for the Copenhagen metropolitan area. The meteorological fields' simulations were driven using boundary conditions of the DMI-HIRLAM-S05 model. These conditions were used as input for simulation of meteorological fields for the urbanized high resolution model. The diurnal cycle of meteorological variables and difference fields (2D) for wind velocity (at 10 m), humidity and temperature (at 2 m), pressure as well as fluxes were analyzed comparing outputs of the control run relative to the urbanized runs.

14.3.1 Modified Urban Roughness and Anthropogenic Fluxes

Incorporating actual urban roughness and anthropogenic heat flux values modified the structure of the surface layer wind and temperature fields over the urban and suburban areas (Fig. 14.2). During daytime, the wind velocities became lower. With roughness increased up to 2 m, this effect became more visible for suburban areas. At night, this effect is smaller. The average differences in velocities can be up to 3 m s^{-1}. For temperature, the urban roughness effect did not contribute significantly compared with wind. The differences also became well pronounced over the

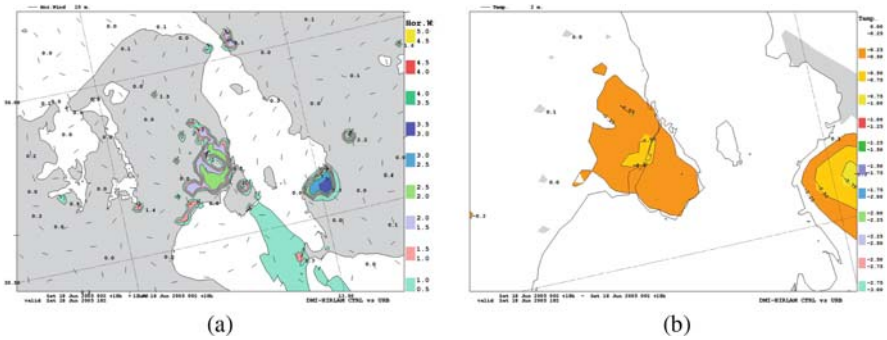

Fig. 14.2 Sensitivity tests to urban features with the DMI-HIRLAM high resolution model are shown as the difference fields (runs without vs. with modifications, i.e. urban roughness and anthropogenic heat flux) for the **(a)** 10 m wind velocity and **(b)** 2 m temperature over the Copenhagen and Malmö metropolitan areas on 18 Jun 2005, 18 UTC (See also Colour Plate 13 on page 177)

Malmo (Sweden) urban area even reaching a higher value. Anthropogenic heat flux increased the temperature above the urban cells with higher values at night and in evening hours and a minimum at noon. For both urbanised areas, this increase is, on average, up to 1–1.5 ºC but with a large variance.

The diurnal variability of wind direction was modelled in all runs with practically no differences between the control and modified runs. When only anthropogenic heat flux is included the wind velocity between 07-19 UTC is closer to the observed local maximum compared with urban roughness run. Combining roughness and anthropogenic heat flux should provide better results. For temperature, when the anthropogenic heat flux is included, the fit to observational data is better for urban compared with suburban stations. Moreover, additional inclusion of a storage heat flux (using for example, the objective hysteresis model Grimmond et al., 1991) can allow adjustments in the time shift of the temperature field observed on a diurnal cycle, and especially during the transitional morning and evening periods.

It is important to remark that, in comparison with the original (non-urbanised) model, the computational time for this urbanised version of the model is almost the same this variant of the urban parameterisations in NWP models is computationally very cheap.

14.3.2 Modified Urban Building Effects

The difference plots for wind velocity at 10 m and air temperature at 2 m (on example of forecasts on 1st August 2004 at 06 UTC) are shown in Fig. 14.3 for both types of urbanization.

For wind velocity, the effect of BEP urbanization is also well pronounced over the metropolitan area showing a maximum of 1.5 m s^{-1}in the morning, although it has a smaller extension of the area where it is observed compared with anthropogenic heat plus roughness urbanization. Throughout the day, the highest differences in

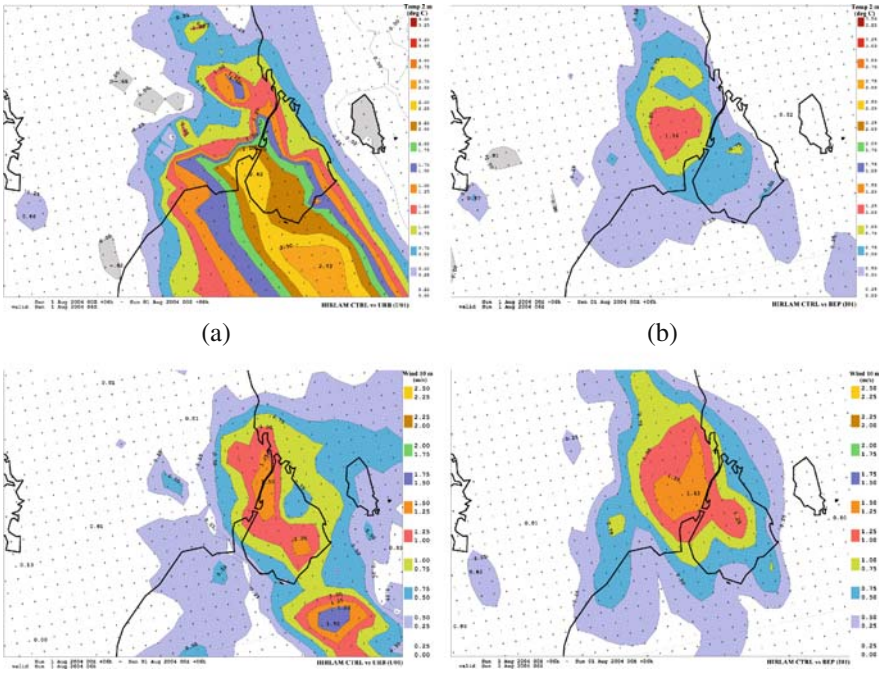

Fig. 14.3 Difference plots (between outputs of the DMI-HIRLAM control and urbanized runs using **(a,c)** R+AHF - anthropogenic heat flux and rouhgness and **(b,d)** BEP modifications of the ISBA land-surface scheme) for the **(a,b)** air temperature at 2 m and **(c,d)** wind velocity at 10 m on 1st August 2004 at 06 UTC (See also Colour Plate 14 on page 177)

wind velocities reached a maximum of more than 3.5 m s^{-1} during daytime and depending on the dominant wind direction. The wind velocity difference is the lowest (less than 0.1 m s^{-1}) during the evening and night hours. For temperature, this "urban pattern" is also well defined, but similarly has small area coverage too. The highest difference is 1.3 ºC in the morning. It varies through the day reaching a minimum during late evening hours. Such behaviour might be related to BEP where more attention is given to the dynamical than the thermal, because the anthropogenic heat flux contribution is not included (except for building wall heat transfer).

14.3.3 Overall Urbanized NWP Performance

Evaluation of the HIRLAM NWP models (two resolutions) has been conducted through analysis of meteorological parameters for the diurnal variations of the average air temperature, wind velocity, and relative humidity. This evaluation was performed also with a focus on only on six urban/suburban meteorological stations of the Copenhagen metropolitan area. As an example, the diurnal variability for 00 UTC forecasts for the relative humidity and wind velocity at 10 m is shown in

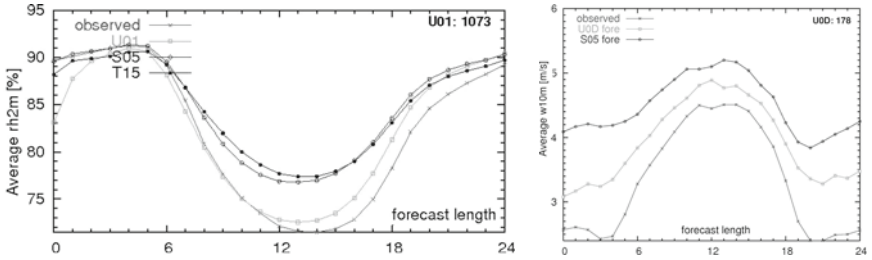

(a) (b)

Fig. 14.4 Diurnal variability for 00 UTC forecasts for the average **(a)** relative humidity at 2 m and **(b)** wind velocity at 10 m for the **(a)** all and **(b)** six urban/suburban Danish stations during July 2004 as a function of the forecast length based on the DMI–HIRLAM–T15/S05 and –U01+urb model runs vs. observations

Fig. 14.4. As seen the urbanized U01 model has good predictive skills compared with two other models (S05 and T15) of lower resolution. In general, the air temperature is well predicted during morning and evening hours. The wind velocity is overpredicted, but it is of the higher accuracy compared with other models. Analysis of the diurnal variability for the relative humidity showed comparable results for all models during night and evening hours, but the urbanized version has a better predictability during daytime.

14.4 Conclusions

The urbanization of DMI-HIRLAM model with modified roughness, anthropogenic heat fluxes and building effects allowed the modelling of effects over urbanized areas. On average, the differences between NWP control vs. urbanized runs over the Copenhagen metropolitan area and surroundings the following was found:

- For typical wind conditions, the differences for: (1) wind at 10 m is less than 0.5 m s^{-1} (with a maximum up to 1.5, at midday); (2) air temperature at 2 m is less than 0.25 ºC (with a maximum up to 0.5 ºC, at night time); and (3) relative humidity is a few percent (with a maximum up to 5%, at midday).
- For low wind conditions, the differences for: (1) wind at 10 m is more than 1 m/s (with a maximum up to 3 m s^{-1}, at night time); (2) air temperature at 2 m is more than 0.5 ºC (with a maximum up to 1.5 ºC, at night time); (3) relative humidity is a few percent (with a maximum up to 7%, at midday).

The long-term runs with the DMI-HIRLAM-U01/I01 high resolution urbanized models showed a slight improvement in overall NWP model performance, but this improvement is more significant over the urban areas.

Evaluation of urbanized DMI-HIRLAM model urbanized with SM2U module is needed at longer time periods. In particular, the analyses of simulated fluxes (served as input into the NWP model), urban module performance, CPU usage, and other capabilities are planned.

Acknowledgments We are grateful to the COST Action 728 which actually influenced the carrying out of this study. In this study the DMI facilities of NEC SX6 had been used for simulations. Thanks for advice to the DMI EDB Computer Support Department. This research is done within the frameworks of the DMI-Enviro-HIRLAM project activities.

References

Baklanov, A., Mestayer, P., Clappier, A., Zilitinkevich, S., Joffre, S., Mahura, A., Nielsen, N.W. **2005**: On the parameterization of the urban atmospheric sublayer in meteorological models. *Atmospheric Chemistry and Physics Discussions*, 5, 12119–12176.

Baklanov, A., Mahura, A., Nielsen, N.W., Petersen, C. **2006a**: Approaches for urbanization of DMI-HIRLAM NWP model. *HIRLAM Newsletter* 49, pp. 61–75.

Baklanov, A., Mahura, A., Petersen, C., Sattler, K., Nielsen, N.W. **2006b**: Effects of urbanized areas for NWP DMI-HIrlam high resolution model operational runs. *Journal of Computational Technologies*, 11, 157–167.

CORINE, **2000**: CORINE Land Cover Dataset 2000. European Environmental Agency. http://dataservice.eea.eu.int/dataservice/

Grimmond, C.S.B., Oke, T.R. **1995**: Comparison of heat fluxes from summertime observations in the suburbs of four North American cities. *Journal of Applied Meteorology*, 34, 873–889.

Grimmond, C.S.B., Cleugh, H.A., Oke, T.R. **1991**: An objective urban heat storage model and its comparison with other schemes. *Atmospheric Environment*, 25B, 311–326.

Hamdi, M., Schayes, G. **2007**: Validation of the Martilli's urban boundary layer scheme with measurements from two mid-latitude European cities. *Atmospheric Chemistry and Physics*, 7, 4513–4526.

Mahura, A., Baklanov, A., Petersen, C., Sattler, K., Amstrup, B., Nielsen, N.W. **2006**: ISBA Scheme Performance in High Resolution Modelling for Low Winds Conditions. *HIRLAM Newsletter* 49, pp. 22–35.

Mahura, A., Petersen, C., Baklanov, A., Korsholm, U.S., Amstrup, B., Sattler, K. **2008**: Verification of long-term DMI-HIRLAM NWP modelling runs using urbanization and building effect parametrization modules. *HIRLAM NewsLetters*, 53, 50–60.

Mahura, A., Sattler, K., Petersen, C., Amstrup, B., Baklanov, A. **2005**: DMI-HIRLAM Modelling with High Resolution Setup and Simulations for Areas of Denmark. *DMI Tech. Report* 05-12, 45 p.

Martilli, A., Clappier, A., Rotach, M.W. **2002**: An urban surface exchange parameterisation for mesoscale models. *Boundary-Layer Meteorology*, 104, 261–304.

Noilhan, J., Planton, S., **1989**: A Simple Parameterization of Land Surface Processes for Meteorological Models', *Monthly Weather Review*, 117, 536–549.

Piringer, M., Grimmond, C.S.B., Joffre, S.M., Mestayer, P., Middleton, D.R., Rotach, M.W., Baklanov, A., De Ridder, K., Ferreira, J., Guilloteau, E., Karppinen, A., Martilli, A., Masson, V., Tombrou, M. **2002**: Investigating the Surface Energy Balance in Urban Areas – Recent Advances and Future Needs. *Water, Air and Soil Pollution: Focus,* 2, 1–16.

Sass, B., Nielsen, N.W., Jørgensen, J.U., Amstrup, B., Kmit, M., Mogensen, K.S. **2002**: The operational DMI-HIRLAM system – 2002-version. *DMI Technical Report* 02-05, 60 p.

Unden, P., Rontu, L., Järvinen, H., Lynch, P., Calvo, J., Cats, G., Cuhart, J., Eerola, K. etc. **2002**: HIRLAM-5 Scientific Documentation. December 2002, *HIRLAM-5 Project Report,* SMHI.

Yang, X., Petersen, C., Amstrup, B., Andersen, B., Feddersen, H., Kmit, M., Korsholm, U., Lindberg, K., Mogensen, K., Sass, B., Sattler, K., Nielsen, W. **2005**: The MDI-HIRLAM upgrade in June 2004. *DMI Technical Report*, 05-09, 35 p.

Chapter 15
Model Urbanization Strategy: Summaries, Recommendations and Requirements

Alexander Baklanov, Jason Ching, CSB Grimmond, and Alberto Martilli

15.1 Introduction

The urban canopy (UC), the layer of the atmosphere between the ground and the top of the highest buildings, is the region where people live and human activities take place. Because of this importance (e.g., human health, preservation of buildings) significant efforts have been dedicated to its investigation. Such studies shed light on the high complexity of atmospheric circulations in the UC, primarily because of the presence of obstacles (buildings) large enough to strongly modify air flow and the thermal exchanges between these surfaces and the atmosphere. The high level of heterogeneity of the UC has been a challenge for atmospheric modeling in urban areas, even for mesoscale models with a typical resolution of the order of 1 km; the basic characteristics of the perturbations induced by the obstacles still remaining unresolved at this model resolution. Over the last decade, with the increase of computational processing power, several mesoscale modeling systems, each with different urban canopy parameterization (UCP) schemes, have been developed and applied with the primary aim of representing the subgrid effects of urban surfaces on their mean variables.

15.2 "Fitness-for-Purpose" Guidance

UCP schemes used in models cover a wide spectrum ranging, from simple ones with a limited number of parameters, such as basic roughness and scale length for thermal or density stability, to multi-parameter sets that include vertical profile descriptions of building and vegetation size and shape. As their level of detail increases, the computational demands for running such models also increase. We note that there are no existing rules governing the appropriate levels of detail and specificity of UCPs that a model must have. However, it is of practical importance

A. Baklanov (✉)
Danish Meteorological Institute, Copenhagen, Denmark,
e-mail: alb@dmi.dk

A. Baklanov et al. (eds.), *Meteorological and Air Quality Models for Urban Areas*,
DOI 10.1007/978-3-642-00298-4_15,

to achieve a balance between the level of detail and precision desired to describe the urban boundary layer with the computational costs and availability of commensurate descriptive data to run such models. This leads to a practical guideline that the choice of level of descriptive complexity of these UCPs be based both on "fitness-for-purpose" and the appropriate grid resolution of the requisite application. Here we list and highlight the requirements of five common applications.

(1) *Air quality exposure studies* to assess the impact of atmospheric pollutants on human health. Model concentration outputs are needed that accurately characterize pollution "hot spots" or gradients at a sufficiently fine grid resolution commensurate to the extent in which significant exposure impacts occur.
(2) *Urban climatology studies and development of strategies for mitigating the intensity of heat islands.* Information is needed to estimate human comfort and stress based on air temperature, relative humidity, and solar radiation. Model parameterization schemes need information about physical attributes of the underlying surface (buildings and vegetation), such as albedo, soil moisture, building material's thermal conductivity, and capacity as well as anthropogenic sources of heating.
(3) *Emergency response and predicting for site locations where toxic gases have been released*. Needs improved methods and modeling of urban-scale transport and building and street canyon resolved dispersion and inverse modeling approaches for determining release location.
(4) *Advanced air quality and weather forecasting* to improve on the predicted future state of the atmosphere (clouds, rain, air, temperature, winds, etc.) and to inform and provide guidance to the public on adverse air quality conditions.
(5) *Urban planning* to evaluate local climate and air quality impacts caused by urban developments and three-dimensional (3D) urban morphological structures.

Air quality exposure, urban climatology, emergency response, and urban planning models need detailed resolution of UC features, whereas weather and air quality forecasts are more focused on estimating the gross vertical exchange of heat, momentum, and pollution between the top of the canopy and the atmosphere. Case studies supporting air quality assessments, urban climatology, and urban planning studies are not relatively constrained by large computer demands to achieve their target accuracy and precision estimates; whereas weather forecasting and emergency response model applications must, for practical reasons, scale down the details of their UC descriptions to achieve the required rapid output response times.

At some point, it will be necessary to perform evaluation of models based on their fitness for purpose. Depending on the type of application, the ranking of atmospheric variables by their roles or importance may be useful for operational model evaluation purposes (see Table 15.1). This exercise is somewhat subjective as the atmospheric variables are interconnected in some way. For example, wind speed and direction is considered more important for air quality and dispersion applications than for urban climatology studies as those variables control pollutant transport. However, the role of wind is of indirect importance because it affects the magnitude

Table 15.1 Ranking of importance of variables by (example) application

Application versus importance	Air quality	Urban climatology	Emergency response	Weather forecasting	Urban planning
Wind speed	Very important	Important	Very important	Important above the canopy	Very important
Wind direction	Very important	Important	Very important	Important above the canopy	Very important
Temperature (and Humidity)	Important	Very, very important	Important	Very important (2-m temperature)	Very important
Pollutant concentration	Very, very important		Very important		Very important
Turbulent Fluxes	Very important	Very important		Very important (at the top of the canopy)	Very important

of heat exchange between surfaces (walls, roofs, and streets) and the atmosphere, thus impacting urban microclimates.

Additional criteria are needed for a robust evaluation based on fitness of purpose concepts. For example, whereas predicted pollutant concentration is a crucial variable for air quality studies, it will be important, in some applications, to focus on different statistical measures. For example, when considering averaging time, one should be clear whether the focus is on the averaging period, on the peak or the number of hours above a certain threshold, or on some other discriminator. Similarly, it would be useful to set objectives based on the degree of precision needed (e.g., Is it sufficient to have a modeled wind speed within 1 m s^{-1} of measurements for air quality simulations?). Thus, practical targets to be reached in terms of level of precision of outputs for the UCP implemented into models would be established for the models' intended use at the outset of the evaluation.

15.3 Strategy to Urbanize Different Types of Models

Current types of UC schemes available for model implementation are reviewed in this section, in the context of their application requirements. Given different modeling objectives, there are several types of UC schemes and associated atmospheric models available. They can be separated into three primary categories:

(1) single-layer and slab/bulk-type UC schemes,
(2) multilayer UC schemes, and
(3) obstacle-resolved microscale models.

The first two categories are sufficiently simple (in their grid-averaged representation of urban morphological features as parameters) to be coupled into classical numerical atmospheric models. The third corresponds to computational fluid dynamic (CFD)-type explicit building-scale resolved models.

The simplest approaches, which include the traditional Reynold's averaging scheme (using roughness and displacement length), are single-layer schemes that link the UC effects to the atmospheric boundary layer through the model's lowest layer. In these methods, the urban scheme is implemented through parameterization of each grid's radiative and turbulent flux values. Moreover, details regarding drag aspects typically are addressed through various ad hoc approaches. For example, simple analytical wind profile formulations for applications inside the canopy typically are introduced. Removing this limitation requires implementation of urban schemes with multi-layers in which the flux quantities interact with the atmospheric variable (Martilli et al., 2002; Dupont et al., 2004). This approach requires additional terms in the prognostic equations of the atmospheric models (e.g., drag term in momentum equations, heating term in temperature equations, production term in turbulent kinetic energy equations). Such models require the addition of layers from the surface to the top of the highest urban feature, thus representing the morphological features as functions of height for each grid. This allows the schemes to model the interactions between air and the urban environment at several heights. Thus, it is possible to simulate the in-canopy flows with greater precision than in single-layer models. However, additional prognostic equations and vertical model levels are required for this type of implementation. Consequently, whereas the effects of surface features are better represented, the computation burden is increased because of the increased integration time step and treatment of additional modeling details. This additional burden presents a limit in the use of multilayer canopy models in NWP forecasting. Clearly, as seen in Fig. 15.1, care must be taken at the outset to understand and balance the need for greater precision obtainable with full canopy details and model turnaround time.

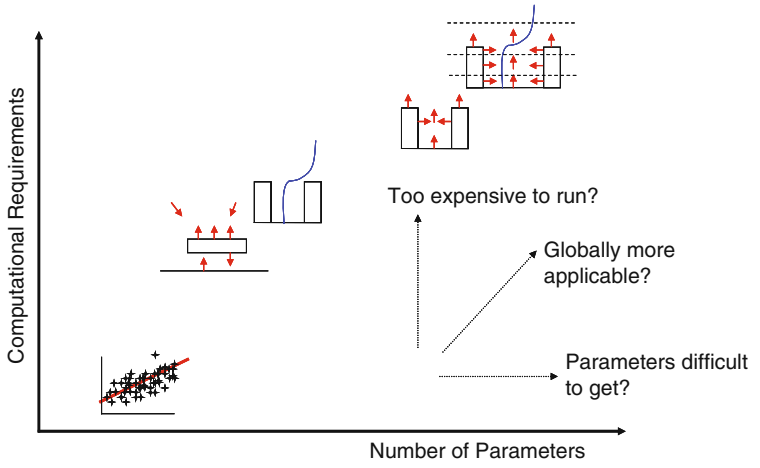

Fig. 15.1 Schematic diagramme depicting computational requirement increases with the inclusion of increased levels of UCP sophistication in UC models (from workshop presentation by Grimmond et al. (Chapter 11) of this volume)

15.4 Overview of Major Applications

15.4.1 Numerical Weather Prediction and Meso-Meteorological Models

The simplest approach for meteorological models is to modify the existing non-urban approaches (e.g., the Monin-Obukhov similarity theory, MOST) for urban areas by introducing different values to represent each grid's effective roughness lengths, displacement height and components and parameters of heating, including the anthropogenic heat flux, heat storage capacity, albedo, and emissivity for each urban land use class. Operational forecasts for urban areas using models with increasingly more sophisticated urban schemes will require significant advancements in computer power.

Beginning with Brown and Williams (1998), who included urban effects in their turbulence closure scheme, methods with increasing levels of sophistication have been introduced into today's mesoscale models. Masson (2000) included a detailed canyon energy balance scheme into the surface energy balance, whereas Martilli et al. (2002) and Dupont et al. (2004) included the effects from canyon walls, roofs, and streets in each prognostic planetary boundary layer (PBL) equation. A similar, but less complex urbanization scheme that shows promise toward capturing fine-scale urban weather phenomena, was a single-layer scheme developed by Kusaka and Kimura (2004a, b). With these advances came the requirement for detailed urban morphological data (i.e., on the scale of a few meters), including land use and land cover, surface roughness, building geometric and thermal characteristics, and anthropogenic heat fluxes (Chapter 1 of this volume). Thus, depending on fit-for-purpose analyses for specific urban applications, the next level of sophistication in NWP models may be through implementation of advanced single-layer UCP schemes. This approach is a relatively inexpensive and practical means of improving on the modified MOST approach.

15.4.2 Urban Air Pollution and Emergency Response Models

Urban and regional-scale atmospheric pollution models, can operate in either a *prognostic mode*, or in post event analysis i.e., *retrospective mode*. Each mode has priorities and requirements that do not necessarily overlap. In prognostic mode, air quality forecasts are produced using meteorological information from NWP forecasts. The retrospective mode is used in air quality simulations necessary to conducting regulatory impact and cost-benefit analyses, developing source control strategies, and performing human exposure assessments. Such simulations require the highest precision and accuracy possible based on the most complete and highly detailed meteorological simulations for specific meteorological scenarios of interest, typically those for which air quality is poorest. For retrospective assessments, the precision and accuracy of the meteorological simulation is more important than timeliness.

For air quality forecasts, the sophistication of UCP schemes in NWP models is governed by operational requirements. To obtain products, that will help with guidance in reducing poor air quality in street canyons, from forecast mode, may require special ad hoc urban meteorological post processing. However, for applications such as emission control strategies, where vertical profiles of the meteorological and turbulent characteristics are needed in great detail, similar post-processing might not be sufficient.

Studies to assess air pollution health effects are an important objective that may be satisfied best with retrospective approaches. Population exposure modeling will require highly detailed multi-pollutant and multi-scale air quality models, as well as high-resolution urban morphology, population distribution, and human activities databases (Baklanov et al., 2007). For these and similar applications, the emphasis will be on implementing urban schemes at a grid resolution that can provide the appropriate transport and turbulence details within the UC.

The fitness-for-purpose analysis also governs the choice of local-scale emergency preparedness modeling for accidental biological, chemical, or nuclear releases, and moreover, is clearly one of scale. For direct response and for operational purposes where timeliness is important urban meteorological observations and/or forecast products coupled with dispersion models are appropriate. For planning and assessment purposes and for the near-sources region, obstacle-resolved modeling approaches (e.g., CFD modeling) may be required. Such approaches will require careful linkage to outputs of urban-scale models, and both will require basic building and vegetation descriptions. Ideally, specific urban feature effects that should be incorporated into this type of application will include the following:

- Impact of urban surfaces on pollutant deposition (e.g., vertical walls, building materials and structure, vegetation)
- Information regarding chemical transformation such as lifetime of chemical species (e.g., inside street canyons), heterogeneity of solar radiation (street shadows, albedo, and emissivity), and specific aerosol dynamics in street canyons (e.g., resuspension processes)
- Very detailed, high-resolution data on the mobile emission of pollutants
- Indoor–outdoor pollutant exchange information

15.4.3 Multiscale Atmospheric Environment Modeling

Air quality in urban areas is influenced by local pollutant emission sources as well as transport of species on regional and global scales. In turn, transport of air pollutants from urban areas will impact on regional and global scale air quality. Current atmospheric-chemical-transport (ACT) models apply model nesting approaches as a means for treating the up- and down-scaling to account for this multi-scale dimension (Moussiopoulos, 1995; Fernando et al., 2001; Baklanov, 2007).

For down-scaling, a chain of urban models of different scales with sub-domain nests using finer grid sizes is applied. A common approach is to use outputs of large-scale models as boundary condition inputs to domains employing smaller grids successively from global to urban and street scales. It is well recognized that transport and transformation are nonlinear in scale (especially for reactive and rapidly deposited species), and parameters controlling atmospheric processes are typically grid-size dependent. Usually, the microscale (street canyon) models are obstacle-resolving and consider the detailed geometry of the buildings and UC, whereas the up-scaled city-scale (sub-meso) or mesoscale models consider parameterizations of urban effects or statistical descriptions of the urban building geometry. FUMAPEX (Baklanov, 2006) is an example of model down-scaling with integration of urban meteorology, air pollution, and population exposure modeling. Downscaling from regional (or global) meteorological models to the urban-scale meteorological models, with statistically parameterized building effects, and further downscaling to microscale obstacle-resolved, CFD-type models was included in the methodology.

Likewise, methods are needed for regional- and global-scale models to properly account for downwind transport of pollutant species from urban sources in regional- and global-scale contexts. This is because the modeled composition by species is grid-size dependent. Thus, for global and climate change models, the mesoscale model can provide a proper pollutant species accounting from biogenic and urban sources ranging from small urban areas to megacities to regional and global scales. It serves investigations of the evolution of pollutants from large urban plumes (e.g., Sarrat et al., 2006) or from major industrial and power-generation point sources. Such plumes are subgrid phenomena for the regional-global models that have the highest resolution (between 10- and 100-km grid sizes) in the focus areas. Therefore, urban-scale models can provide appropriate composition mix for the regional-global model. Currently, to understand the impact of aerosols and gas-phase compounds emitted from local/urban sources on regional and global scales, at least three scales of the integrated atmosphere-chemistry-aerosol and general circulation models are being considered: (1) local, (2) regional, and (3) global. Note that two-way nesting approaches are ideal for situations in which the scale effects in both directions (from the mesoscale on the microscale and from the microscale on the mesoscale) are important. However, such approaches are difficult to implement.

15.4.4 Urban Pollution and Climate Integrated Modeling

Integrated air quality modeling systems are tools that help in understanding impacts from aerosols and gas-phase compounds emitted from urban sources on the urban, regional, and global climate. The integration of urbanized NWP and ACT models is a strategic approach to providing the science-based tools for assessments of urban air quality and population exposure in the context of global to regional to urban transport and climate change. This is reasonable because meteorology governs the transport and transformations of anthropogenic and biogenic pollutants, drives urban air quality and emergency preparedness models; meteorological and

pollution components have complex and combined effects on human health (e.g., hot spots, heat stresses); and pollutants, especially urban aerosols, influence climate forcing and meteorological events (precipitation, thunderstorms, etc.). The online integration of mesoscale meteorological models and atmospheric aerosol and chemical transport models enables the utilization of all meteorological 3D fields in ACT models at each time step and the consideration of feedback among air pollution (e.g., urban aerosols), meteorological processes, and climate forcing (e.g., WRF-Chem: Grell et al., 2005; Enviro-HIRLAM: Baklanov et al., 2008).

Chemical species in the atmosphere, such as CO_2 and ozone act as greenhouse gases to influence weather and atmospheric processes. Aerosols such as sea salt, dust, primary and secondary particles of anthropogenic and natural origin are also airborne and contribute to atmospheric processes in a complex manner. Some aerosol components (black carbon, iron, aluminum, and polycyclic and nitrated aromatic compounds) warm the air by absorbing solar and thermal-infrared radiation, whereas others (water, sulphate, nitrate, and most organic compounds) cool the air by backscattering incidental short-wave radiation into space. The effects of urban aerosols and other chemical species on meteorological parameters have many different pathways (direct, indirect, semi-direct effects, etc.) that these online, coupled modeling systems are capable of addressing.

15.5 Database and Evaluation Aspects of Urbanized Models

It is evident that there are a large range of applications that involve an urban focus. Moreover, given the wide range of model complexities, operational and data input requirements, and diverse applications, we find that there is no "one-size-fits-all" modeling approach that addresses the wide range of modeling objectives. Thus, for urban applications, the fitness-for-purpose concept is a relevant and important consideration. In this survey, we have identified a number of considerations; some of the major ones are outlined below.

15.5.1 Database Requirements

Models of urban areas will be required to provide reliable predictions at fine 3D resolution of turbulent exchanges, air flow and thermodynamic characteristics. To meet these requirements, parameterizations are being developed and implemented with varying degrees of detail in terms of features and sophistication relative to the actual features of individual cities. One limitation to the degree of complexity in the model parameterizations is the availability of appropriate morphology information. For operational needs, the requirements are fulfilled using specifications associated with limited numbers of urban land use categories, each with specified surface properties such as roughness, displacement lengths, albedo, moisture availability, and thermal properties. For research and development applications, models that can

capture more detailed effects of urban morphological features and underlying surfaces and building materials, at increasingly higher spatial resolutions, employ more explicit and highly detailed sets of 3D canopy parameters and within-grid land use classes.

A common requirement for environmental models is the description of the underlying surface layer. Technological advancements allow increasingly sophisticated definitions of land cover characteristics (e.g., shape files with high resolution [~1 m] definition of buildings and vegetation). Data of this type are now becoming routinely available for many urban areas of the world with the information technology available to facilitate dissemination. In the United States, a pilot project is underway to serve as a community-based technology enabler of such data; this or comparable systems can be developed to handle the needs on an international basis (Chapter 1 of this volume). A community-based system should decrease administrative barriers and increase international collaborative efforts to advance modeling tools.

15.5.2 Evaluation

Once the target variables and degree of precision needed for the application purpose are identified (Table 15.1), it is necessary to determine whether the parameterizations are capable of reaching these targets. Several techniques are available.

- *Real scale measurements.* As measurements are taken in a real city, a model should be able to reproduce them; however, very often it is difficult to have enough measurements, and, where measurements are taken, its representativeness of the gridded fields must be ascertained. The model computes the equivalent of a spatial average over the grid cell (usually a few kilometers or, at best, several hundreds of meters). Outputs from models that introduce vertical resolution within the UC and capture the effects of urban building and vegetation features are virtual fields, and the task of evaluating such outputs is challenging. Model-predicted vertical profiles of variables in the canopy reflect the aggregated influence of all the canopy features as virtual elements within the grid. In reality, such features take up finite volumes, and building-induced flows are subgrid features. Thus, any single or set of measurements will not provide a representation of the gridded fields but will, more or less, be under the influence of the nearest buildings or obstacles. This is a design feature that has yet to be resolved in developing field measurement strategies to evaluate predictions of within-canopy fields.

  Future guidance may come from insights gained using coupled UC models and building-resolved flows, both of which are driven by the same set of building datasets. Currently, evaluations performed above the canopy layer (blending layer) should not be subject to this conceptual difficulty, but, in and of itself, it does not provide the requisite within-canopy evaluation.
- *Remote sensing data.* A variety of satellite platforms do now provide data on surface variables and for urban areas. In particular, skin temperature is considered a

very important variable because it exerts a strong control on boundary layer processes and the intensity of the heat island. Such data would be very useful toward diagnostic evaluation of urban model predictions. Of course, care is required to address scale issues of observation and models. There are some critical assumptions in the derivation of the remotely sensed variables (e.g., emissivities, mixed pixels). The comparison also is biased to conditions that the remotely sensed data are operational (e.g., clear sky conditions for surface temperature, time of overpass).

Also, because models have varying treatments for handling subgrid land use and coverage, some of the resulting differences between observed and modeled skin temperature may be result, in part, from these treatments.

- *Scale-model measurements.* Wind tunnels have the advantage that external conditions can be controlled and are repeatable, but are limited by certain conditions (e.g., Reynolds number may be a factor of 100 less than in the real world; no concurrent radiative moisture forcing; typically treats only neutral stratification cases). Numerical models allow for a wide range of conditions with real meteorological forcing to be compared (Chapter 5 of this volume). To date these models remain simple in morphology and arrangement.
- *CFD (large eddy simulation [LES] or Reynolds-averaged Navier-Stokes [RANS]) models.* Such building resolving models can be run over a limited part of a city to investigate flow properties to be used in UCP. Using CFD models, it is possible to derive the spatial averages required for UCP (Chapter 2 of this volume; Chapter 4 of this volume). CFD-RANS lacks the accuracy for some complex configurations. CFD-LES is more accurate but much more expensive in CPU time, which, thereby, limits its use.
- *Operational testing.* Real-scale routine data from weather networks are used for evaluation, most typically for weather forecasts (e.g., Chapter 3 of this volume).

15.6 Potential Community Activities

There is a wide range of activities that are needed to support the recent improvements to the state of urbanization of models. These fall into a variety of categories. To date, a systematic evaluation of urban land surface schemes has not taken place as it has for vegetated environments. The model comparison outlined in Grimmond et al. (Chapter 11 of this volume) takes some initial steps to address this. As they note, it is anticipated that there will be need for further observations. There is a clear need for both intensive and extensive observational data sets to allow the wide range of variables to be evaluated over a wide range of synoptic conditions. The development of urban testbeds and urban atmospheric observatories (e.g., Helsinki, Shanghai, London, Paris, Hanover, Phoenix, Oklahoma City, Houston, New York City, and Washington, DC) and long-term urban campaigns (e.g., CAPITOUL, BUBBLE) enable these issues to be addressed. For example, studies evaluating the Martilli scheme (Martilli et al., 2002) show that it is able to reproduce the generation of the urban heat island effect and to represent correctly most of the behavior

of the fluxes over Basel and Marseilles city centers (Hamdi and Schayes, 2005). There is a continuing need for modelers and observers to communicate. As models are used for a variety of purposes, there is a need for increasing the range of variables observed to ensure as complete a range of evaluation as possible. This may mean having testbeds and observatories with different objectives and dataset richness.

There is a wide range of processes and variables that need to be evaluated over a broad spectrum of conditions (meteorological, morphological, geographical setting, etc.). For example, a deeper understanding of urban PBL dynamics requires development of long-term urban testbeds in a variety of geographic regions (e.g., inland, coastal, complex terrain) and in many climate regimes, with a variety of urban core types (e.g., deep versus shallow, homogeneous versus heterogeneous).

The conceptual issue of evaluation of model prediction of the flow within the canopy is not satisfactorily resolved at this time, and a framework to address this is needed. Ideal urban testbeds would include quasi-permanent mesoscale networks, with surface, canyon, rooftop, and PBL meteorological and air quality observations. These real-time, quality-assured data would be used for real-time urban-scale weather and air quality forecasts, as well as for emergency response actions after releases of air toxins (with an indoor-outdoor linkage) and for climate change impact studies.

In addition, the testbeds should be able to accommodate intensive short-term field observational studies that could involve turbulent flux and pollutant tracer measurements. Problems also exist in the evaluation of microscale CFD meteorological model results by use of field study or canyon wind tunnel observations (e.g., wind tunnel wall effects, the isolated nature of wind tunnel urban domains, the periodic LES and CFD lateral boundary conditions). When comparisons are done with these limitations in mind (e.g., only compare model results with wind tunnel results over urban centers), however, they show good agreement among the methods.

Obviously, with increasing evaluation, there will be enhanced development of the models. It is also clear that, within the chain of needs between meteorological forcing and applications, there is a range of new developments needed (see Sect. 15.3).

Finally, user friendly and multifaceted urban databases and enabling technology are critical and core capabilities for advancing urban modeling and boundary layer research. We see the National Urban Database and Access Portal Tool as a research and development resource toward future improved UCP descriptions and scientific bases for advanced urban modeling applications. With careful thought to its implementation, the concept of this prototype system is extensible on an international basis. For such an enterprise, we suggest several guiding principles be adopted. First, that this type of database be open and community-wide and available both universally and in as an unrestricted form as possible. Second, that both protocols and mechanisms should be established for its maintenance, upgrading, updating, and archiving. Further, issues of availability and sources of high-resolution data sets will need to be addressed.

Disclaimer: *The research presented here by one of its authors (Ching) was performed under the Memorandum of Understanding between U.S. EPA and the U.S.*

Department of Commerce's National Oceanic and Atmospheric Administration (NOAA) and under agreement number DW13921548. This work constitutes a contribution to the NOAA Air Quality Program. Although this manuscript has been reviewed by EPA and NOAA and approved for publication, it does not necessarily reflect their policies or views.

References

Baklanov, A., 2006: Overview of the European project FUMAPEX. *Atmos. Chem. Phys.*, 6, 2005–2015, www.atmos-chem-phys.net/6/2005/2006/

Baklanov, A., 2007: Urban air flow researches for air pollution, emergency preparedness and urban weather prediction. Chapter 9 in: Flow and transport processes with complex obstructions: Applications to cities vegetative canopies and industry. Eds. Ye. A. Gayev and J.C.R. Hunt, Springer, 311–357.

Baklanov, A., O. Hänninen, L.H. Slørdal, J. Kukkonen, N. Bjergene, B. Fay, S. Finardi, S.C. Hoe, M. Jantunen, A. Karppinen, A. Rasmussen, A. Skouloudis, R.S. Sokhi, J.H. Sørensen, and V. Ødegaard, 2007: Integrated systems for forecasting urban meteorology, air pollution and population exposure. *Atmos. Chem. Phys.*, 7, 855–874.

Baklanov, A., U. Korsholm, A. Mahura, C. Petersen, and A. Gross, 2008: ENVIRO-HIRLAM: on-line coupled modelling of urban meteorology and air pollution. *Adv. Sci. Res.*, 2, 41–46.

Brown, M. and M. Williams, 1998: An urban canopy parameterization for mesoscale meteorological models. AMS 2nd Urban Environment Symposium, Albuquerque, NM.

Dupont, S., T.L. Otte, and J.K.S. Ching, 2004: Simulation of meteorological fields within and above urban and rural canopies with a mesoscale model (MM5) *Bound.-Layer Meteor.*, 2004, 113, 111–158.

Fernando, H.J.S., S.M. Lee, J. Anderson, M. Princevac, E. Pardyjak, and S. Grossman-Clarke, 2001: Urban fluid mechanics: air circulation and contaminant dispersion in cities. *J Environ. Fluid. Mech.* 1(1), 107–164.

Grell, G.A., S.E. Peckham, R. Schmitz, S.A. McKeen, G. Frost, W.C. Skamarock, and B. Eder, 2005: Fully coupled "online" chemistry within the WRF model. *Atmos. Environ.*, 39(37), 6957–6975.

Hamdi, R. and G. Schayes, 2005: Validation of the Martilli urban boundary layer scheme with measurements from two mid-latitude European cities. *Atmos Chem. Phys. Discuss*., 5, 4257–4289. www.atmos-chem-phys.org/acpd/5/4257/ SRef-ID: 1680-7375/acpd/2005-5-4257, European Geosciences Union.

Kusaka, H. and F. Kimura, 2004a: Coupling a single-layer urban canopy model with a simple atmospheric model: Impact on urban heat island simulation for an idealized case. *J. Meteor. Soc. Japan*, 82, 67–80.

Kusaka, H. and F. Kimura, 2004b: Thermal effects of urban canyon structure on the nocturnal heat island: numerical experiment using a mesoscale model coupled with an urban canopy model. *J. Appl. Meteorol.*, 43, 1899–1910.

Martilli, A., A. Clappier, and M.W. Rotach, 2002: An urban surface exchange parameterization for mesoscale models. *Bound.-Layer Meteorol.,* 104, 261–304.

Masson, V., 2000: A physically-based scheme for the urban energy budget in atmospheric models. *Bound.-Layer Meteorol.*, 98, 357–397.

Moussiopoulos, N., 1995: The EUMAC Zooming Model, a tool for local-to-regional air quality studies. *Meteorol. Atmos. Phys.*, 57, 115–133.

Sarrat, C., A. Lemonsu, V. Masson, G. Guedalia, 2006: Impact of urban heat island on regional atmospheric pollution. *Atmos. Environ.*, 40, 1743–1758.

Appendix 1
Program of the COST 728 Workshop on Model Urbanization Strategy, UK Met Office, Exeter, UK, 3–4 May 2007

Green Island Conference Room 2

Thursday 3 May

9:00–9:30	Registration at Met Office reception and collection of badges
9:30–9:40	Welcome from Met Office, ***Maria Athanassiadou***
9:40–10:00	Introduction into Workshop Aims and Overview of results from the ICUC-06 'Model urbanisation' Roundtable, ***Alexander Baklanov***

Urban Morphology and Databases

10:00–10:20	Rationale and current activities on urban morphology and databases, ***Jason Ching***
10:20–10:40	Vertical profiles of the variance of the vertical wind component and turbulence intensities from sodar measurements from urban measurement campaigns, ***Stefan Emeis***
10:40–11:00	The present setup for the urban experiment in Bonn, Germany, ***Dirk Schüttemeyer****, C. Simmer, A. F. Moene, O. Hartogensis*
11:00–11:30	**Coffee Break**

Parametrisations of Urban Canopy

11:30–11:50	Meteorological measurements in urban area, ***Sven-Erik Gryning*** *and* ***Ekaterina Batchvarova***
11:50–12:10	A parametrization for sub-grid emission variability, ***Stefano Galmarini***

A. Baklanov et al. (eds.), *Meteorological and Air Quality Models for Urban Areas*,
DOI 10.1007/978-3-642-00298-4_BM2,

12:10–12:30	The effect of stratification on the aerodynamic roughness length, *Sergej Zilitinkevich, I. Mammarella,* ***A. A. Baklanov***, *S. M. Joffre*
12:30–14:00	**Lunch**
14:00–14:20	How to use CFD (RANS or LES) models for urban parameterizations, ***Alberto Martilli***
14:20–14:40	Turbulence statistics from DNS and LES – implications for urban canopy models, ***Omduth Coceal***
14:40–15:00	Evolution and Performance of the Urban Scheme of the Unified Model, ***Aurore Porson****, Peter Clark, Martin Best, Stephen Belcher*
15:00–15:20	Urban soil-canopy-atmosphere exchanges at submesoscales : learning from model development, validation, and coupling with LES, ***Patrice Mestayer*** *and Isabelle Calmet*
15:20–16:00	**Coffee Break**

Verification and Case Studies/Experiments

16:00–16:20	Performance of different sub-grid-scale surface flux parametrizations for urban and rural areas, ***Sylvia Bohnenstengel***
16:20–16:40	Sensitivity tests in the dynamical and thermal part of the MRF-urban PBL scheme in the MM5 model, ***Aggeliki Dandou*** *and* ***Maria Tombrou***

Friday 4 May

9:30–9:50	FUMAPEX experience of model urbanisation, ***Alexander Baklanov***
9:50–10:10	CAPITOUL experiment: first experimental results and parameterization, ***Valery Masson***
10:10–10:30	Verification and Case Studies for Urban Effects in HIRLAM Numerical Weather Forecasting, *A. Mahura,* ***Alexander Baklanov***, *C. Petersen, N. W. Nielsen, B. Amstrup*
10:30–10:50	Progress on an urban surface energy balance model comparison study, ***CSB Grimmond****, M. Best, J. Barlow*
10:50–11:20	**Coffee Break**

Strategy for Urbanization of Different Types of Models

11:20–11:40	Urban models in Japan/CDF approach and scale model experiment, ***Manabu Kanda***
11:40–12:00	Advancing the multi-scale urban modelling in the community mesoscale WRF model: current status and future plan, ***Fei Chen***
12:00–12:20	Urbanization of US meso-scale models, ***Bob Bornstein***
12:20–14:00	**Lunch**

Discussions/Round table to build a joint strategy, recommendations and requirements

Plans for WG on 'Model urbanization strategy' and web-portal for information exchange

Appendix 2
List of Workshop Participants

Participant	Institute
Dr. Maria Athanassiadou	Atmospheric Dispersion Group, Met Office, FitzRoy Road, Exeter, EX1 3 PB Tel.: +44 (0) 1392 886096; Fax: +44 (0) 1392 885681 E-mail: maria.athanassiadou@metoffice.gov.uk http://www.metoffice.gov.uk
Prof. Alexander Baklanov	Research Department, Danish Meteorological Institute (DMI) Lyngbyvej 100, DK-2100 Copenhagen, Denmark Tel.: +45 39157441; Fax: +45 39157460 E-mail: alb@dmi.dk; Web: http://dmi.dk
Dr. Ekaterina Batchvarova	National Istitute of Meteorology and Hydrology 66 Tzarigradsko Chausse, BG-1784 SOFIA E-mail: ekaterina.batchvarova@meteo.bg
Sylvia Bohnenstengel	Max Planck Institute, Hamburg, Germany, Bundesstrasse 53, 20146 Hamburg Tel.: 004940438285590; Fax: 004940438285452 E-mail: sylvia.bohnenstengel@zmaw.de
Prof. Bob Bornstein	Department of Meteorology, One Washington Square San Jose State University, San Jose, CA 95192 USA E-mail: pblmodel@hotmail.com
Prof. Fei Chen	NCAR/RAL, P.O. Box 3000, Boulder, CO 80307 Tel.: 303-497-8454; Fax: 303-497-8401 E-mail: feichen@ucar.edu http://www.rap.ucar.edu/projects/land
Dr. Jason Ching	Atmospheric Modeling and Analysis Division, NERL/ORD/USEPA E-mail: Ching.Jason@epamail.epa.gov
Dr. Peter Clark	Met Office Joint Centre for Mesoscale Meteorology (JCMM), Meteorology Building University of Reading P.O. Box 243, Earley Gate Reading Berkshire RG6 6BB United Kingdom Tel.: +44 (0)118 378 6523; Fax: +44 (0)118 378 8791 E-mail: peter.clark@metoffice.gov.uk http://www.metoffice.gov.uk

Dr. Omduth Coceal	NCAS-Weather, Department of Meteorology, University of Reading, P.O. Box 243, Reading RG6 6BB, UK Tel.: 44 (0)118 378 6979; Fax: 44 (0)118 378 8905 E-mail: o.coceal@reading.ac.uk Web: www.met.rdg.ac.uk/∼sws97oc
Aggeliki Dandou	University of Athens, Greece, Department of Physics Division of Applied Physics Tel.: +30 210 72 76 837; Fax: +30 210 72 95 281 E-mail: antant@phys.uoa.gr
Dr. Stefan Emeis	Institut für Meteorologie und Klimaforschung – Atmosphärische Umweltforschung – Forschungszentrum Karlsruhe GmbH, Kreuzeckbahnstr. 19, 82467 Garmisch-Partenkirchen Tel.: +49 (0)8821 183 240; Fax: +49 (0)8821 73 5 73 E-mail: stefan.emeis@imk.fzk.de
Dr. Stefano Galmarini	Tp 441, Joint Research Center, 21020, Ispra, Tel.: +39 0332 785382; Fax: +39 0332 785466 http://rem.jrc.cec.eu.int/∼galmarin/ E-mail: stefano.galmarini@jrc.it
Prof. CSB Grimmond	Environmental Monitoring and Modelling Group, Department of Geography, King's College London, The Strand, London WC2R 2LS, United Kingdom Tel.: 44 20 7848 2275; Fax: 44 20 7848 2287 E-mail: Sue.Grimmond@kcl.ac.uk http://www.kcl.ac.uk/ip/suegrimmond/
PhD & Dr. scient. Sven-Erik Gryning	Wind Energy Department, Risø National Laboratory,Technical University of Denmark, DK 4000-Roskilde, Denmark Tel.: +45 46775005; Fax: +45 46775970 E-mail: sven-erik.gryning@risoe.dk
Prof. Manabu Kanda	Dept. of International Development Eng., Tokyo Institute of Technology, Ookayama 2-12-1, Meguro-ku,152-8552 Tokyo, Japan Tel.: +81-3-5734-2768; Fax: +81-3-5734-2768 E-mail: kanda.m.aa@m.titech.ac.jp
Dr. Christopher Kiley	Joint Science and Technology Office for Chemical and Biological Defense 571-642-6793; 8211 Terminal Road, Suite 1000; Lorton, VA 22079-1421 E-mail: christopher.kiley_contractor@dtra.mil
Dr. Alberto Martilli	CIEMAT, Madrid, Spain E-mail: alberto.martilli@ciemat.es
Dr. Valery Masson	CNRM/GMME/TURBAU, 42 av Coriolis, 31057 Toulouse, France Tel.: (+33) 5 61 07 94 64; Fax: (+33) 5 61 07 96 26 E-mail: valery.masson@meteo.fr
Dr. Patrice Mestayer	Institut de Recherche Sciences et Techniques de la Ville (FR CNRS 2488), Laboratoire de Mecanique des Fluides (UMR CNRS 6598); Ecole Centrale de Nantes, B.P. 92101, F-44321 NANTES Cedex 3, France Tel.: +33 (0)240 37 16 78; Fax: +33 (0)240 37 25 56 http://www.ec-nantes.fr/ –> LMF –> DAH

Dr. Aurore Porson	Department of Meteorology, University of Reading, UK E-mail: a.n.f.porson@reading.ac.uk
Dr. Dirk Schüttemeyer	Meteorological Institute, University of Bonn, Germany E-mail: schuettemeyer@googlemail.com
Dr. Paul Skomorowski	Department Environmental Meteorology, Central Institute for Meteorology and Geodynamics – ZAMG, Hohe Warte 38 A-1190 Vienna, Austria Tel.: +43 1 36026 – 2405; Fax: +43 1 36026 – 74 E-mail: paul.skomorowski@zamg.ac.at
Dr. Maria Tombrou	Dept. of Applied Physics, University Campus, Zografou, Athens GR 157 84, GREECE E-mail: mtombrou@phys.uoa.gr
Heather Thompson	E-mail: HLW459@bham.ac.uk

Colour Plate

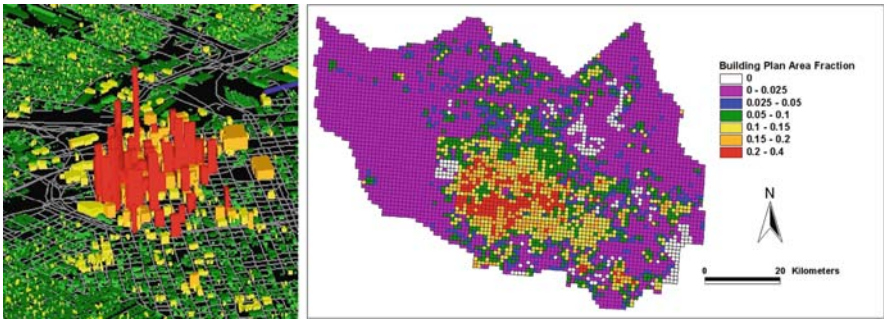

(a) (b)

Plate 1 **(a)** 3D building data derived from airborne lidar platform for 1 × 1 km section of downtown Houston. **(b)** Building plan area density, an example of a UCP for Harris County (Houston Metropolitan area) (cf. Table 1.1) (See also Figure 1.1 on page 4)

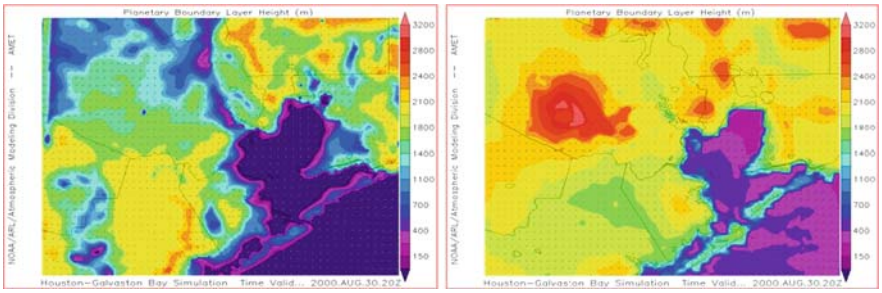

(a) (b)

Plate 2 Simulations of mixed layer heights size for 2100 GMT on August 30, 2000 using MM5 with **(a)** UCP and **(b)** standard version of MM5 at 1 km grid (See also Figure 1.2 on page 7)

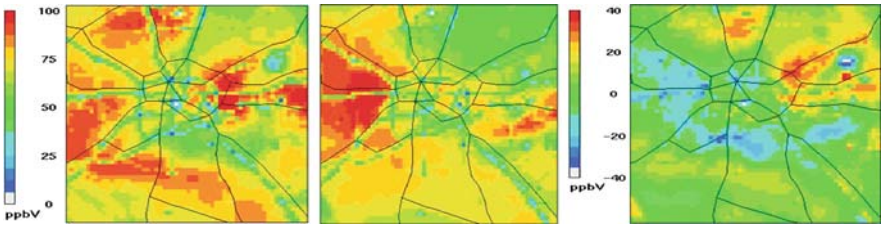

(a) (b) (c)

Plate 3 Simulations of surface ozone using CMAQ driven by UCP **(a)** and No-UCP **(b)** versions of MM5 (see Fig. 1.2) and **(c)** differences between simulations (at 2100 GMT on August 30, 2000) (See also Figure 1.3 on page 8)

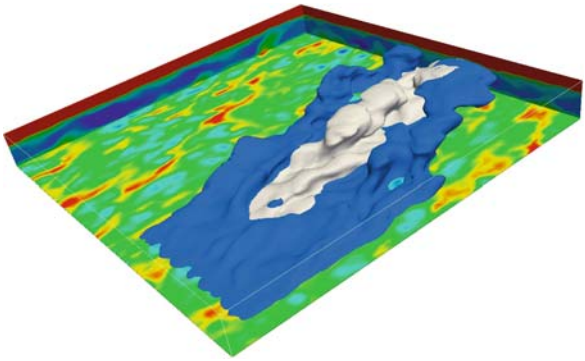

Plate 4 Instantaneous contour plot of the concentration fields for the two emission scenarios (64% in *blue* and 16% in *grey*) after two hours of simulation and with a threshold of 0.1 ppb. The potential temperature is also shown as coloured surfaces (See also Figure 2.2 on page 14)

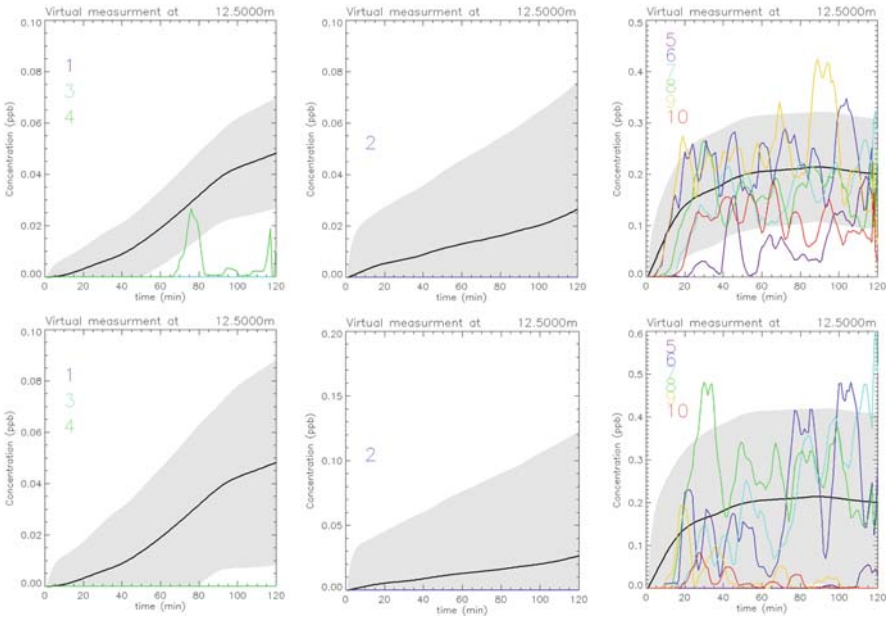

Plate 5 Time profiles of the instantaneous concentrations sampled at 12.5 m and at the 10 locations (Fig. 2.4). The *thick black lines* show the average concentration obtained by the FVM model. The *shading* is the variance calculated with the new formulation. (*Upper*) 64% Emission Surface/Grid-Cell Surface case. (*Lower*) 16% Emission Surface/Grid-Cell Surface scenario (See also Figure 2.5 on page 16)

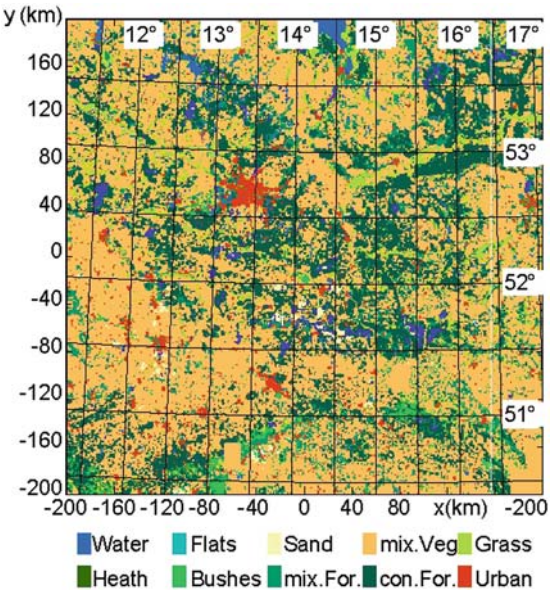

Plate 6 Land use in the model domain (See also Figure 3.1 on page 23)

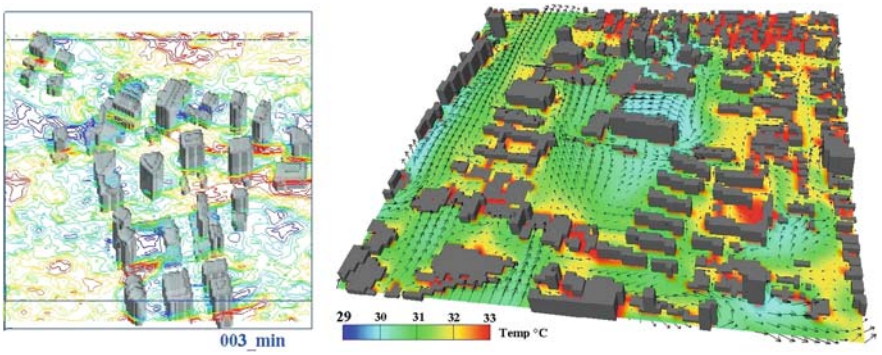

Plate 7 Examples of CFD application to realistic urban geometries. **(a)** Contour map of instantaneous surface wind in Sinjuku (from Kanda, 2006c), and **(b)** contour map of instantaneous surface temperature field and surface wind vector at a coastal area in Tokyo (from Ashie et al., 2005). The area is 500 m × 500 m for **(a)** and **(b)** (See also Figure 5.1 on page 41)

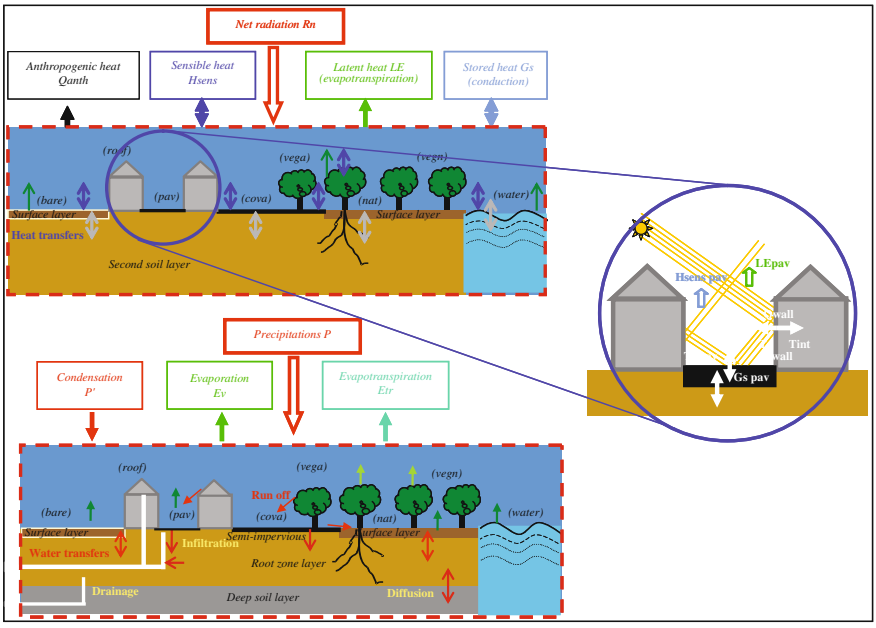

Plate 8 Schematic representation of SM2U: the *upper box* shows the processes modelled in the energy budget part, with a zoom on the in-street radiation and heat storage processes due to building walls; the *lower box* shows the modelled water transfer processes. The *black brackets* indicate the different possible tiles within one grid mesh. Precipitation is a model input while the net radiation is computed by the model from the incoming global and atmospheric radiation inputs (See also Figure 6.1 on page 48)

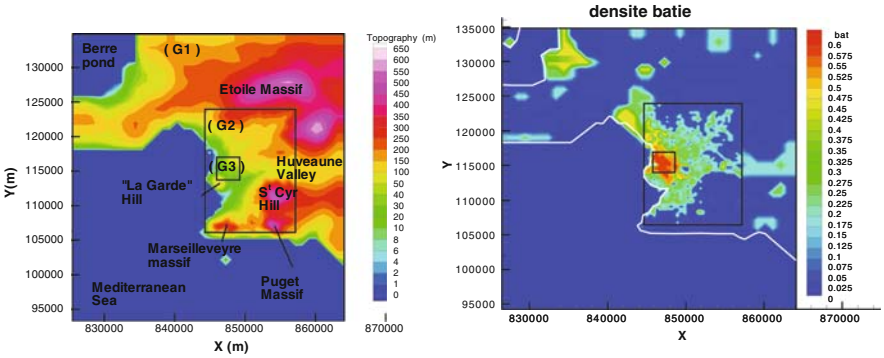

(a) (b)

Plate 9 Marseille area (**a**) topography and (**b**) building density. Black rectangles indicate the three computational grid limits, G1 (990 m mesh), G2 (330 m) over the urban area and G3 (110 m) over the city centre (See also Figure 6.8 on page 54)

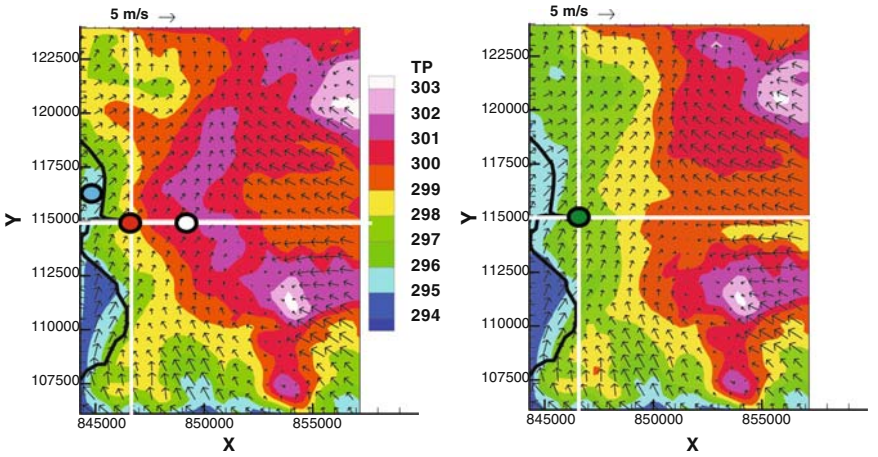

(a) (b)

Plate 10 City influence on the low level fields: (**a**) potential temperature (colours) and wind (vectors) at 1300 UTC (June 25, 2001) at 7.5 m above ground level (G2 domain), actual situation; (**b**) alternate simulation without the city (see text) – the white lines indicate the positions of Fig. 6.10 vertical cross-sections and the numbers indicate those of Fig. 6.11 vertical profiles (See also Figure 6.9 on page 55)

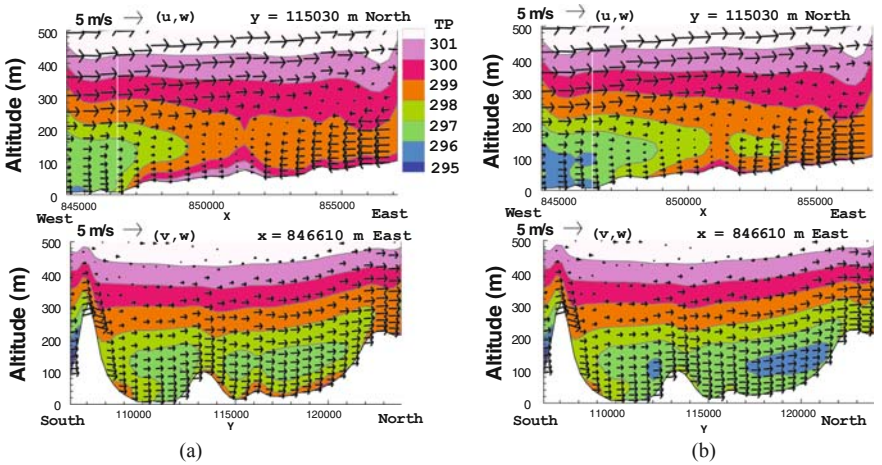

Plate 11 (**a**) Vertical W-E (*top*) and S-N (*bottom*) cross-sections of the atmospheric boundary layer potential temperature and wind fields – same situation as Fig. 6.9, actual situation; (**b**) alternate simulation without the city. The white lines indicate the position of Fig. 6.11 city centre vertical profiles (2 and 4) (See also Figure 6.10 on page 55)

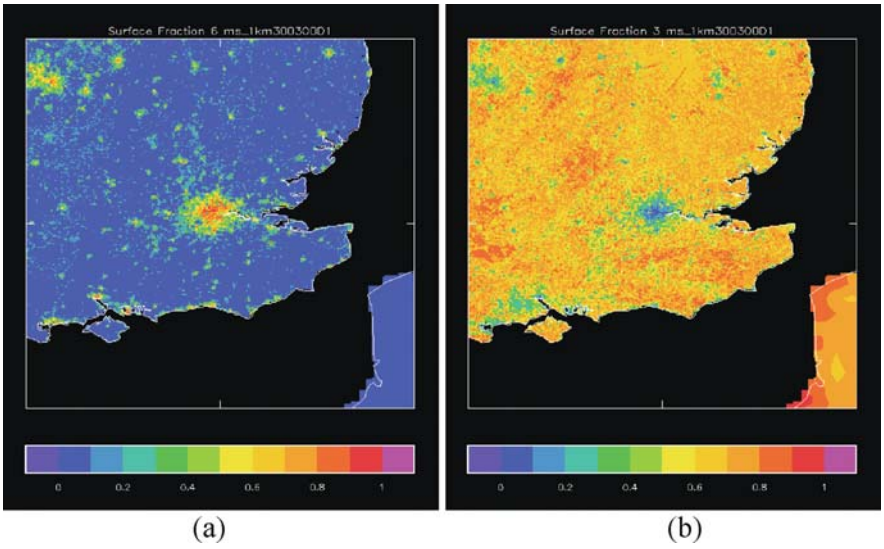

Plate 12 Land-use fraction at 1 km resolution over SE England (centred on London) derived from CEH data **(a)** urban **(b)** C3 grass (i.e. grass and crops) (See also Figure 9.1 on page 79)

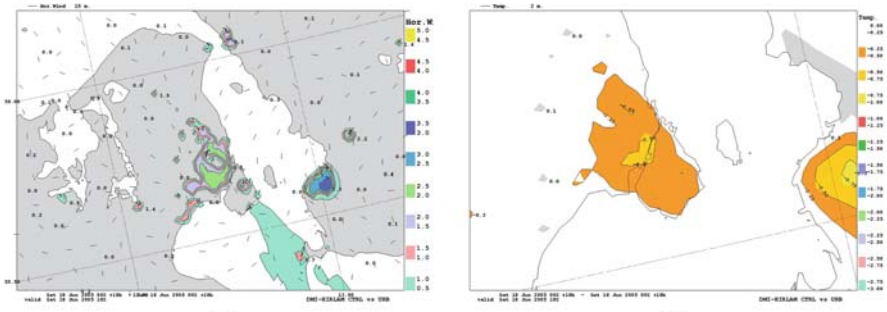

(a) (b)

Plate 13 Sensitivity tests to urban features with the DMI-HIRLAM high resolution model are shown as the difference fields (runs without vs. with modifications, i.e. urban roughness and anthropogenic heat flux) for the **(a)** 10 m wind velocity and **(b)** 2 m temperature over the Copenhagen and Malmö metropolitan areas on 18 Jun 2005, 18 UTC (See also Figure 14.2 on page 147)

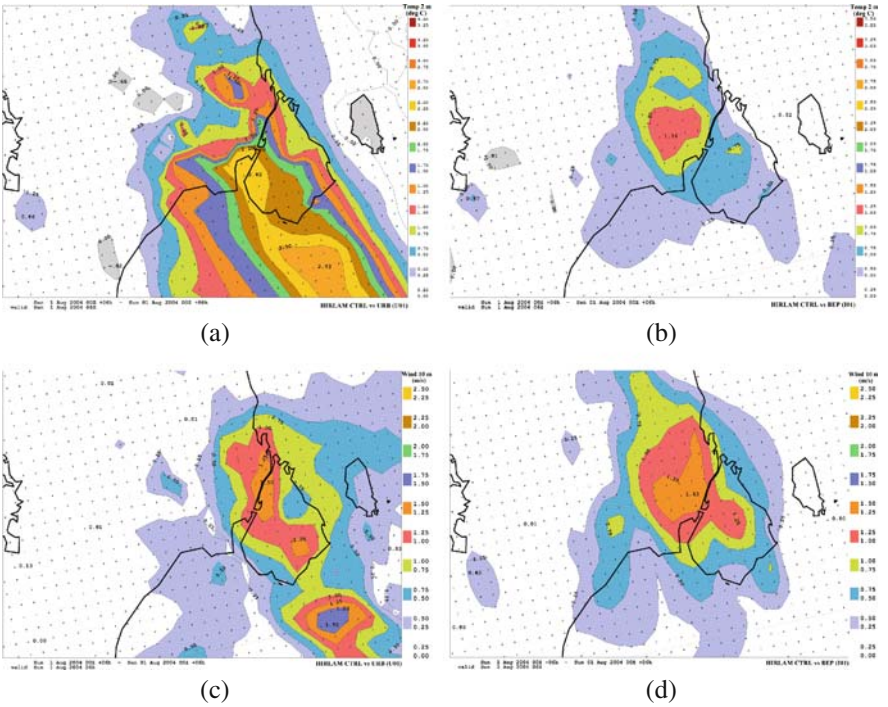

(a) (b)

(c) (d)

Plate 14 Difference plots (between outputs of the DMI-HIRLAM control and urbanized runs using **(a,c)** R+AHF - anthropogenic heat flux and rouhgness and **(b,d)** BEP modifications of the ISBA land-surface scheme) for the **(a,b)** air temperature at 2 m and **(c,d)** wind velocity at 10 m on 1st August 2004 at 06 UTC (See also Figure 14.3 on page 148)

Index

A
Aerodynamic roughness, 59–66
Airborne LiDARsystem, 6
Air pollution, 60, 65, 69, 70, 98, 155–156, 157, 158
Air pollution health effects, 156
Air quality forecast, 69, 155, 156, 161
Air quality modeling systems, 157
Albedo, 49, 53, 71, 72, 73, 79, 84, 85, 88, 105, 107, 108, 111, 145, 152, 155, 156, 158
Anthropogenic heat flux, 70, 71, 72, 75, 79, 89, 91, 93, 98, 105, 110, 111, 112, 143, 145, 146, 147, 148, 149, 155
Application
  for advanced air quality and weather forecasting, 152, 153
  for air quality, 7, 98, 117, 118, 152, 153
  for emergency, 152, 153
  for urban climatology and development of strategies for mitigation, 152, 153
  for urban planning, 152, 153
Application - ranking of importance, 153
Approach to vegetation modeling, 103
Atmospheric boundary layer (ABL), 14, 47, 51, 56, 60, 87, 88
Atmospheric chemical transport (ACT) model, 156, 157, 158
Averaging operator, 32, 33, 34

B
Basel urban boundary layer experiment (BUBBLE), 64, 73, 126, 160
Blending height approach, 22, 78
Bowen ratio, 21, 22
Building effect parameterization (BEP), 72, 73, 74, 75, 100, 101, 145–146, 147, 148
Building UCPs, 5
Built environment, 101, 105, 106
Buoyancy, 17, 18, 62

C
Canopy exchanges, 47
Canopy morphology descriptors, 51
Canopy UCPs, 5
Categorisation of models in terms of slab, single layer or multi-layer, 103
Ceilometer, 129, 130, 133–140
Characteristics of the urban environment, 146
Chemical, biological and nuclear (CBN), 6
Climate and air pollution modeling, 60
Climate change, 97, 157, 161
Coastal city, 47, 52
Community multiscale air quality (CMAQ) modeling system, 7, 8
Community system, 3, 4, 159
Comprehensive outdoor scale mode (COSMO), 39, 42–44
Computational fluid dynamics (CFD), 31–37, 40
Computational processing unit (CPU), 32, 34, 160
Convective atmospheric boundary layer, 11, 12
Convective boundary layer (CBL), 13, 88, 136, 138
Courant Friedrich Levy condition, 32
CPU time, 32, 34, 160

D
Database, 3–8, 51, 69, 156, 158–160, 161
Digital elevation model (DEM), 6
Digital terrain model (DTM), 6
Dispersive flux, 40
Dispersive stress, 34, 35, 36, 125
Displacement height, 5, 61, 64, 71, 72, 127, 155
Dissipation, 17, 18
Drainage, 48, 49, 53, 79
  network, 49, 51, 53, 107
Dry convective boundary layer, 13

E
Eddy viscosity, 61, 62, 63
Effective roughness and flux, 69
Effect of stratification, 59–66
Emergency models, 70
Emergency preparedness, 156, 157
Emergency response, 152, 153, 155, 161
Emissions, 5, 6, 11, 12, 17, 21, 70, 112
  variance parameterization, 15
Emissivity, 49, 53, 85, 105, 107, 108, 111, 155, 156
Energy budget, 5, 47, 48, 49, 51, 52, 73, 87, 111, 114
Ensemble approach, 32
ESCOMPTE, 49, 50, 52, 73
European center for medium range weather forecast (ECMWF), 88, 145
Evaluation data, 99, 116
Evapotranspiration, 48, 50, 115

F
Field campaign, 34, 75
Field data, 41, 43
Field experiment, 43, 99
Finite volume model (FVM), 13, 14, 16, 71, 72, 74
Flat canopy approach, 49, 50, 56
FLUENT, 35
Flux aggregation method, 21, 22, 23, 25
Force-restore method, 81
Friction velocity, 22, 24, 59, 89, 92, 93, 113
FUMAPEX, 52, 69–75, 145, 157

G
Geometry of buildings, 72
German weather service (DWD), 21, 22, 24, 71, 74

H
Heat storage, 40, 42, 43, 48, 49, 50, 71, 72, 88, 89, 91, 93, 98, 101, 113, 133, 134, 155
  capacity, 50, 105, 107, 108, 113, 114, 117
  flux, 13, 21, 22, 23, 49, 50, 51, 52, 53, 71, 73, 75, 79, 82, 89, 91, 92, 93, 98, 102, 105, 107, 110, 111, 112, 113, 114, 115, 116, 117, 129, 143, 145, 146, 147, 148, 155
  net, 98
Height of the boundary layer, 129–130
High resolution, 3–8, 14, 15, 34, 47, 71, 88, 143, 144, 145, 146, 147, 149, 156, 159, 161
  building data, 4, 6, 159
  urban data, 3–8, 161
  urban morphological features, 3, 153, 159
High resolution limited area model (HIRLAM), 52, 71, 72, 73, 74, 100, 102, 103, 104, 106, 108, 109, 111, 112, 113, 114, 115, 143–150, 158
Hit rate, 21, 24, 25, 26, 35
Homeland security infrastructure program (HSIP), 6
Hydrostatic stability, 59, 65
Hysteresis, objective hysteresis model (OHM), 88, 113, 147

I
Interaction soil biosphere atmosphere (ISBA) land surface scheme, 47, 58, 115, 145, 146, 148
Interaction soil biosphere atmosphere (ISBA) model, 47, 48, 115, 145, 146, 148
Internal boundary layer, 70

K
Karmann constant, 24, 59, 61

L
Land atmosphere exchange models, 98
Land use, 3, 6, 7, 21, 23, 24, 51, 69, 71, 72, 78, 79, 88, 112, 118, 145, 155, 158, 160
  class, 23, 24, 71, 72, 88, 145, 155, 159
  classification, 88, 145
  cover, 88
  database, 69
Large eddy simulations (LES), 11, 12, 13, 14, 15, 17, 34, 35, 40, 41, 43, 47–56, 160, 161, 164
Large turbulent eddy, 40
Latent heat flux, 21, 22, 23, 26, 48, 49, 51, 52, 75, 98, 102, 107, 113, 115, 116, 117, 143
Levels modeled and features resolved, 105
Lidar derived building data, 4
Linear, areal, and point sources, 12

M
Material radiative and thermodynamic properties, 51
Medium range forecast (MRF), 87–93, 164
Meso-meteorological models, 75, 155
Meso-scale atmospheric models, 146
MEsoscale TRAnsport and Stream (METRAS), 24, 26
Mesoscale weather forecast systems, 39
Meteorological air quality and human exposure modeling systems, 3

Methods
used to calculate anthropogenic heat flux, 112
used to calculate drag, 113, 114
used to calculate latent heat flux and soil moisture, 115
used to calculate storage heat flux, 114
used to calculate turbulent sensible heat flux, 115
used to model outgoing shortwave and long-wave radiation, 111
Microscale airflow, 34
Mixed layer simulations, 7
Mixing layer height (MLH), 113–140
MM5, 4, 5, 6, 7, 8, 52, 71, 73, 74, 87–93, 100, 102, 103, 104, 106, 108, 109, 111, 112, 113, 114
Model urbanization, 151–162
Momentum and energy fluxes, 97
Monin-Obukhov, 40, 60, 62, 71, 77, 112, 126, 155
length scale, 62
Monin-Obukhov similarity theory (MOST), 40, 71, 77, 78, 155
Morphology of the urban environment, 98
MRF urban scheme, 87, 90, 93
Multi-faceted approach, 85
Multi-layer models, 101

N
National Urban Database with Access Portal Tool (NUDAPT), 3, 4, 5, 6, 7, 8, 161
Navier-Stokes equations, 11, 34
NCAR, 52, 87, 88, 100, 167
Neutrally stratified boundary layer, 59
Neutral stratification, 63, 160
Nuclear Accident ModEl (NAME), 78
Nudging approach, 24
Numerical weather forecasting, 60, 143–150
Numerical weather prediction (NWP), 69, 77, 88, 113, 144, 155

O
Observation study, 99, 118, 125, 143, 161
Operational testing, 160

P
Parameter averaging, 21, 22, 25, 26, 27
Parameterization of surface fluxes, 21
Penn State / NCAR Mesoscale model (MM5), 87, 88, 100
Planetary boundary layer (PBL), 87–93, 88, 155, 161
Portal technology, 3, 4
Probability density function, 33
Prognostic equation for variance of pollutant concentration, 17–18
Project for intercomparison of land-surface parameterization scheme (PILPS), 97, 99, 101, 116

R
Radiation balance, 71, 85
Real scale measurements, 159
Remote sensing data, 133, 136, 159
Residual layer (RL), 135, 136, 138
Reynolds-averaged Navier-Stokes (RANS), 13, 14, 15, 17, 34, 35, 40, 160
Reynolds decomposition / stress, 33
Richardson number, 65
Rough-concrete approach, 85
Roughness
approach, 86
elements, 41, 59, 60, 62, 125
layer, 60, 61, 62, 63
layer eddy viscosity, 62, 63
length, 5, 23, 42, 49, 59–66, 71, 73, 79, 82, 83, 88, 89, 91, 93, 107, 113, 114, 127, 155
length for heat, 42, 73, 82, 83
sub-layer, 125, 126, 130
Roughness sub-layer (RSL), 41, 125, 126, 130

S
Scale decomposition, 11
Scale-model measurements, 160
Sea
breeze, 54, 87, 88, 89, 90, 93
surface temperature (SST), 88
Sensible heat flux, 13, 22, 48, 49, 50, 51, 52
Sensible heat flux, 98, 116
Sensible heat / latent heat / storage heat flux, 102
Sensitivitystudies, 3, 4, 7, 47
Shadowing and radiation trapping, 49
Single layer models, 101
Sky-view factor, 85
Slab models, 101
Sodar and ceilometer soundings / measurements, 133–140
Soil model for sub-mesoscale urban version (SM2-U), 47, 73, 74, 75
Spatial averaging, 33, 35
Stable boundary layer (SBL), 136, 138
Stable stratification, 22, 60, 61, 63, 64, 65
Stratification, 22, 59–66, 134, 136–137, 160
Street canyon, 40, 52, 70, 85, 127, 146, 152, 156, 157

Strongly unstable stratification, 63
Sub-grid
scale concentration variance, 12
scale parameterization, 23, 25
scale processes, 11
scale surface fluxes, 21, 22, 23, 24, 27
Surface
energy budget, 5, 47, 49
exchange scheme, 77, 78, 100
fluxes, 21, 22, 23, 24, 27, 48, 77, 78, 79, 85
geometry, 39, 42, 43, 44
properties, 22, 158
radiative and thermodynamic properties, 51
stress and flux of heat and momentum, 88
Surface energy balance, 41, 42, 43, 51, 79, 80, 82, 85, 88, 97–118, 143, 155

T
Thermal canopy, 79–84
Tiled approach, 78
Tiling approach, 48, 49
Turbulent coefficient, 17
Turbulent flow, 59
Turbulent kinetic energy (TKE), 17, 69, 88, 110, 134, 154
Turbulent latent heat flux, 51, 98
Turbulent sensible heat flux, 49, 51, 98, 112, 113, 116
Turbulent transport, 18, 24
Turbulent velocity scale, 61
Turbulent viscosity, 133, 134, 137–139
Two-tile approach, 85
Typical urban surface cover mode, 49

U
Unified Model (UM), 77–86
Unstable stratification, 22, 61, 63, 64
Urban air pollution, 155–156
Urban air quality, 3, 69, 70, 133, 135, 157
Urban air quality information and forecasting system (UAQIFS), 70
Urban areas, 3, 8, 11, 21, 26, 31, 33, 34, 39, 69, 70, 71, 72, 73, 77, 79, 80, 81, 82, 85, 87, 98, 99, 101, 105, 112, 113, 117, 118, 125–130, 133, 134, 143, 145, 146, 149, 151, 155, 156, 157, 158, 159
Urban boundary layer (UBL), 35, 64, 70, 125, 129, 130, 134, 136–137, 140, 152
Urban canopy layer, 40, 72, 101
Urban canopy models, 39, 40, 75
Urban canopy parameterization (UCP), 4, 5, 6, 7, 8, 31–37, 32, 151, 152, 153, 154, 155, 156, 160, 161
Urban canopy parameterization (UCP) scheme, 151
Urban canopy parameters (UCP), 3, 4, 5, 6
Urban canopy (UC), 3, 4, 5, 6, 7, 31–37, 39, 40, 63, 64, 71, 72, 73, 75, 77, 93, 100, 101, 151
Urban climate, 41, 42–44, 70, 87, 100
Urban climatology, 47, 152, 153
Urban effect on low wind conditions, 128
Urban effect on typical wind conditions, 149
Urban fabric properties, 116
Urban features can influence, 70
Urban flux, 71, 77, 118
Urban fluxes and sub-layer parameterization, 71–73
Urban geometry, 21, 84
Urban heat flux, 26, 72, 129
Urban heat island effect, 160
Urban heat island (UHI), 26, 40, 70, 81, 88, 91, 93, 98, 133, 160
Urban heat storage, 40, 88, 101
Urbanization, 48, 71–73, 79, 81, 85, 87, 140, 143, 144, 145, 147, 149, 151–162
Urbanization of the model, 140
Urbanization of relevant sub-models and processes, 71
Urbanized areas, 47, 144, 149
Urban land use categories, 158
Urban land use class, 71, 155
Urban measurement campaigns, 133–140, 163
Urban meteorology, 3–8, 40, 41, 69, 70, 157
Urban modeling, 161
Urban morphology, 101, 113, 116, 156
Urban parameterization, 34, 36
Urban roughness, 69, 71, 143, 145, 146, 147
Urban and rural areas, 21–27
Urban scale weather forecast, 70
Urban-soil-canopy-atmosphere exchange, 47–56
Urban and sub-urban environments, 11
Urban surface energy balance, 88, 97–118
Urban surface energy balance models / schemes, 97–118
Urban surface energy budget, 49
Urban surface energy fluxes, 41
Urban surface schemes, 97
Urban surface sub-layer (USL), 74
Urban tile, 78, 79
Urban vegetation, 105

United States Environmental Protection Agency (US EPA), 3, 8, 52
User community, 4, 8

V
Vegetation UCPs, 5
Velocity gradient, 61
Vertical flux of momentum, 35, 60
Vertical turbulent exchange coefficient, 133–140
Vertical turbulent flux of buoyancy, 62
Vertical turbulent length scale, 60
Vertical wind and turbulence profiles, 133–140

W
Water budget, 48, 50, 56, 73
Well-mixed convective boundary layer, 88
Wind LiDAR, 127
Wind tunnel experiment / study, 24
WRF, 4, 8, 52, 158